ÉCOLE DE TECHNOLOGIE SUPÉRIEURE
UNIVERSITÉ DU QUÉBEC

MANUSCRIPT-BASED THESIS PRESENTED TO
L'ÉCOLE DE TECHNOLOGIE SUPÉRIEURE

IN PARTIAL FULFILLMENT OF THE REQUIREMENTS
FOR THE DEGREE OF DOCTOR OF PHILOSOPHY
Ph.D.

BY
Jie CHEN

IMPROVEMENTS OF STATISTICAL DOWNSCALING METHODS AND EVALUATION OF THEIR CONTRIBUTIONS TO THE UNCERTAINTY OF HYDROLOGIC IMPACTS IN A CHANGING CLIMATE

MONTREAL, JULY 28 2011

BOARD OF EXAMINERS

THIS THESIS HAS BEEN EVALUATED

BY THE FOLLOWING BOARD OF EXAMINERS

Mr. François Brissette, Eng., Ph.D., Thesis Supervisor
Département de génie de la construction à l'École de technologie supérieure

Mr. Maarouf Saad, Eng., Ph.D., President of the Board of Examiners
Doyen des études à l'École de technologie supérieure

Mr. Robert Leconte, Eng., Ph.D., Jury Membre
Département de génie de civil à l'Université de Sherbrooke

Mr. Jean-Sébastien Dubé , Eng., Ph.D., Jury Membre
Département de génie de la construction à l'École de technologie supérieure

Mr. Van-Thanh-Van Nguyen, , Eng., Ph.D., External Examiner
Departement of Civil Engineering and Applied Mechanics, McGill University

THIS THESIS WAS PRESENTED AND DEFENDED

BEFORE A BOARD OF EXAMINERS AND PUBLIC

JUNE 20 2011

AT ÉCOLE DE TECHNOLOGIE SUPÉRIEURE

FOREWARD

This PhD thesis was written between September 2008 and March 2011, under the supervision of Professor François Brissette at the École de technologie supérieure, Université du Québec. The main objective was to couple climate models and statistical downscaling methods for quantifying the hydrologic impacts of climate change for a Canadian river basin (Quebec Province). It is a part of the project "Impact of climate change in Canadian River Basins and adaptation strategies for the hydropower industry", supported by the Natural Science and Engineering Research Council of Canada (NSERC), Hydro-Québec, Manitoba Hydro and the Ouranos Consortium on Regional Climatology and Adaptation Climate Change. This research focused on approaches to generate climate projections that could be used for impact studies, with an emphasis on hydrology.

This PhD thesis is structured by means of articles. Eight articles were published in or submitted to scientific journals with peer review. The PhD student is the first author and the thesis supervisor is the main co-author for all the articles. These articles are presented in Chapters 1-8, comprising the main body of the thesis. Additional results are presented in the appendix. An "Introduction" section presents the research background, the main scientific problems and the objectives, as well as a general methodology. A literature review follows. A brief conclusion drawn from the articles and some recommendations for further research are presented following the articles. The bibliography at the end of the thesis contains all the references used in the course of completing this thesis.

ACKNOWLEDGEMENTS

I am grateful for all the support I have received whilst researching and writing this PhD thesis. It would not have been possible without help from so many people in so many ways.

It is difficult to overstate my gratitude to my PhD supervisor, Prof. François Brissette, for his supervision, advice and key scientific insights guiding me to complete this thesis. You are a fabulous advisor: sharp, cheery, perceptive, and mindful of the things that truly matter. Whenever I lost track on how to proceed, you offered helpful advice. With your enthusiasm, inspiration, and patient efforts to explain things clearly and simply, you helped to make research fun. Throughout my research and thesis-writing periods, you provided encouragement, sound advice, good company, and lots of good ideas. I would have been lost without your counsel. On the other hand, you have encouraged me to pursue my own side-projects, allowing me to expand my horizons. You have also given me a number of opportunities to attend international conferences and meet interdisciplinary scientists. Moreover, as an international student whose first language is much different from French, having studied at a French-language university with very little French background was a difficult task. You showed extreme patience and encouraged me to overcome every problem. I feel very privileged and lucky to have had such an excellent supervisor. I would like to offer my sincere appreciation to you. I am also very grateful to Prof. Robert Leconte for giving me valuable advice on my research and the guidance to avoid getting lost in my explorations. You made numerous suggestions on how to improve my research and this thesis and without your input many issues would not have been identified.

I would like to thank the jury members who evaluated my thesis: Prof. Maarouf Saad (École de technologie supérieure), Prof. Robert Leconte (Université de Sherbrooke), Prof. Jean-Sébastien Dubé (École de technologie supérieure) and Prof. Van-Thanh-Van Nguyen (McGill University). Your suggestions made a significant contribution to my thesis. Your comments were relevant, constructive and clear and reflect the fact that there is always room for improvement.

Thanks are due to all the scientists at Hydro-Quebec and at the Ouranos Consortium who participated in their own way in this project: Marie Minville, Blaise Gauvin St-Denis, Anne Frigon and Patrice Constanza. Studies in climate change are multi-disciplinary; your expertise was indispensable. A special thanks to Marie Minville for giving me her program for Bias Correction of climate data. I also thank Profs Peter Rasmussen and Trish Stadnyk and their students at the University of Manitoba for giving me suggestions for my research project.

I am grateful to the secretaries and librarians at the École de technologie supérieure, Université du Québec, for assisting me in many different ways. Without your help, I could not have completed my PhD studies so smoothly.

My colleagues who have graduated and those who remain at the DRAME lab ensured I was constantly engaged and entertained along the way. Annie Poulin, Yan Zhao, Josée Beauchamp, Chloé Alassimone, Mélanie Trudel, Anne-Sophie Pruvost, Richard Arsenault, Pascal Côté, Didier Haguma, Jonathan Roy, Antonin Coladon, Sébastien Tilmant, and Jean-Stephane Malo -- you are all so nice. I am very happy to work with you guys. Thank you all. Especially, thank you Annie for the simulation of HYDROTEL.

I would like to also thank my Master supervisors Prof. Wenzhao Liu and Prof. Xunchang Zhang. Although I graduated several years ago, you still consistently supported me and gave me good suggestions for my PhD studies.

Importantly, I wish to thank my parents, my sister, my brother-in-law, my niece and my girlfriend. Despite the geographical distance, you were always nearby. My shadow and my light, you encouraged, supported, understood, and loved me at every moment, and I am intellectually indebted to your ideas and our conversations. This thesis is dedicated to you.

I thank the following organizations for providing financial support for this project: the Natural Science and Engineering Research Council of Canada (NSERC), Hydro-Québec,

Manitoba Hydro and the Ouranos Consortium on Regional Climatology and Adaptation Climate Change. I also appreciate the funding support from the Quebec Fund for Research on Nature and Technology (FQRNT).

Outside of the lab, plenty of friends kept me sane and happy in Montreal. I am very happy to know you guys in this gorgeous city. Thank you very much. I also thank my friends in China and in other countries. Even though we could not see each other frequently, you are always beside me.

Finally, many, many thanks to all the people who made this thesis possible -- those who are mentioned above and those who are not. May life will be sweet with all of you! Thank you very much again!!

IMPROVEMENTS OF STATISTICAL DOWNSCALING METHODS AND EVALUATION OF THEIR CONTRIBUTIONS TO THE UNCERTAINTY OF HYDROLOGIC IMPACTS IN A CHANGING CLIMATE

Jie CHEN

ABSTRACT

The most important impacts of climate change will likely be linked to water resources. Hydropower companies throughout the world increasingly realize that they must deal with future climate change. To evaluate future impacts, realistic climate projections that encompass the uncertainty linked to climate change are needed. Given the relatively large biases of General Circulation Model (GCM) outputs, particularly for precipitation and to a lesser extent for temperatures at the regional scale, it is necessary to perform some post-processing to improve these global-scale models for hydrologic and water resource management studies. The two most commonly used approaches, dynamical and statistical downscaling, each have significant advantages and drawbacks. It is not a simple task to select one over the other.

This work aims at coupling global and regional climate models and statistical downscaling into a new hybrid method by merging stochastic weather generators with climate models that quantify the hydrological impacts of climate change for a Canadian river basin. The performances of stochastic weather generators were first improved. A statistical downscaling method combining attributes of both stochastic weather generator and change factor (CF) methods was then developed. Several aspects of statistical downscaling were also evaluated. Moreover, global uncertainty and the downscaling uncertainty were outlined in quantifying the hydrological impacts of climate change.

A spectral correction method and integration scheme resulted in a weather generator that can accurately produce the low-frequency variability of precipitation and temperatures, as well as the auto- and cross-correlations of and between maximum and minimum temperature (Tmax and Tmin).

A large number of atmospheric predictors were used to assess the ability of statistical methods to downscale precipitation to the station scale. The downscaling of daily precipitation occurrence was mostly unsuccessful with both linear regression methods and using discriminant analysis, even though the latter was much better. Explained variances were very low for regression-based downscaling of precipitation, although results were consistently improved as the climate model resolution was made progressively finer. Even when going to the 15-km resolution Canadian Reginal Climate Model (CRCM), the predictors still explained less than 50% of the total site precipitation variance. Despite the added complexity, the weather typing approach was not much better at downscaling precipitation than the approaches without classification.

The weather generator was used as a downscaling tool to downscale outputs of the CRCM (45km scale) to catchment scale. Its performance was further compared with the CF method for quantifying the hydrological impacts of climate change. Both downscaling methods suggested increases in annual and seasonal discharges for the 2025-2084 period. The weather generator-based method predicts more increase in spring (AMJ) discharge, as well as smaller increases in summer-autumn (JASON) and winter (DJFM) discharges than the CF method. Moreover, both methods indicated increases in mean annual and seasonal low flows, while there are considerable differences between their predictions.

All downscaling methods including dynamical and statistical approaches suggested general increases in winter discharge (November - April) and decreases in summer discharge for the 2071-2099 horizon. Winter flows would be especially large for regression-based methods, which also predicted the largest temperature increases in autumn and winter. Peak discharges would appear earlier for all downscaling methods, but their timing varies according to the downscaling method.

A GCM was consistently a major uncertainty contributor when quantifying the hydrological impacts of climate change. However, other sources of uncertainty such as the choice of downscaling method and natural variability, as represented by GCM ensemble runs, also had a comparable and even larger uncertainty affect depending on the criteria. For example, the downscaling method was the largest source of uncertainty with respect to spring discharge magnitude, annual low flow and peak discharge; while GCM initial conditions (which were a member of the ensemble runs) dominated the uncertainty for the time to peak discharge and the time to the end of flood. Uncertainties linked to greenhouse gase emission scenarios (GGES) and hydrological model structure also played an important role in hydrological predictions, but these were somewhat less than those related to GCMs and the downscaling method. Uncertainties due to the hydrological model parameters had less impact than those of the other five sources.

Overall, combining Regional Climate Models (RCMs) and statistical downscaling in a unified approach appeared to have significant advantages in quantifying the hydrological impacts of climate change. Any management and adaptation of water resource systems should consider the effects of future climate change, as well as all sources of uncertainty.

Key words: climate change, hydrology, weather generator, downscaling, climate model, uncertainty

IMPROVEMENTS OF STATISTICAL DOWNSCALING METHODS AND EVALUATION OF THEIR CONTRIBUTIONS TO THE UNCERTAINTY OF HYDROLOGIC IMPACTS IN A CHANGING CLIMATE

Jie CHEN

RÉSUMÉ

Les plus importants impacts dus aux changements climatiques seront vraisemblablement liées aux ressources en eau. Les producteurs d'hydroélectricité réalisent maintenant qu'ils doivent tenir compte de ces changements. Pour évaluer adéquatement les impacts futurs, il existe un besoin pour des projections climatiques réalistes qui encadrent l'incertitude liée aux changements climatiques. Compte tenu des biais liés aux simulations des modèles climatiques, et ce particulièrement pour les précipitations, il est nécessaire de traiter les sorties de ces modèles pour les besoins d'études d'impacts en hydrologie ou en gestion des ressources hydriques. Les deux approches couramment utilisées à cet effet (approches de mise à l'échelle dynamique et statistique) ont chacune leurs avantages et inconvénients, et il est difficile de les départager.

Ce travail vise à coupler les sorties de modèles climatiques globaux et régionaux avec une approche statistique de mise à l'échelle basée sur un générateur stochastique de climat, et de quantifier les impacts hydrologiques des changements climatiques sur deux bassins versants québécois (Manicouagan 5 et Ceizur). La performance d'un générateur stochastique de climat fut d'abord améliorée et une approche hybride combinant le générateur de climat et la méthode de mise à l'échelle 'des deltas' a été développée. L'incertitude liée au choix d'une méthode de mise à l'échelle a été quantifiée dans le cas d'études hydrologiques.

Une approche de correction spectrale et un schéma intégré pour la génération des températures a résulté en un générateur de climat capable de reproduire la variabilité interannuelle des précipitations et températures, de même que l'autocorrélation et les corrélations croisées des températures maximales et minimales.

Le générateur de climat ainsi amélioré a été utilisé comme outil de mise à l'échelle sur deux bassins versants, et a été comparé à la méthode des deltas pour la quantification des impacts de changements climatiques. Les deux méthodes suggèrent des augmentations de débits annuels et saisonniers pour la période 2025-2084. L'approche du générateur stochastique suggère toutefois des augmentations de débits plus grandes au printemps et plus faibles l'été.

Un grand nombre de prédicteurs atmosphériques a été utilisé pour valider l'habileté des approches de régressions linéaires, couramment utilisées. La mise à l'échelle de l'occurrence des précipitations a résulté en un faible taux de succès. Le pourcentage de variance expliqué pour la mise à l'échelle des quantités de précipitation est très bas, et ce pour l'ensemble des stations testées et modèles climatiques utilisés. Bien que globalement médiocre, la performance de ces approches augmente avec l'augmentation de la résolution des modèles

climatiques utilisées (300km, 45km, 15km). Une étape additionnelle de classification en types de climat n'a pas amélioré la performance de manière significative.

Toutes les méthodes de mise à l'échelle utilisées/développées dans le cadre de cette étude prévoient une augmentation des débits hivernaux et une diminution des débits d'été pour la période 2071-2099. L'augmentation des débits hivernaux est particulièrement grande pour les méthodes basées sur les régressions linéaires, qui prédisent aussi les plus grandes augmentations de température pour l'automne et l'été. La pointe de crue printanière est devancée pour toutes les méthodes testées mais les résultats varient en fonction de la méthode.

Les modèles climatiques contribuent à l'incertitude globale du changement climatique de façon majeure peu importe le critère utilisé. Toutefois, d'autres sources d'incertitude telles que les approches de mise à l'échelle et la variabilité naturelle (telle que représenté par les simulations d'ensemble des modèles climatiques) peuvent contribuer à l'incertitude globale de manière similaire (et même plus) dépendant du critère choisi. Par exemple, le choix d'une méthode de mise à l'échelle est la principale source d'incertitude pour la pointe de la crue printanière et les débits d'étiage, alors que la variabilité naturelle domine l'incertitude pour les dates d'occurrence de la crue printanière et de la fin de la crue. L'incertitude liée au scénario d'émission et au modèle hydrologique est aussi importante, mais moins que les sources mentionnées ci-haut. L'incertitude liée au choix de paramètres du modèle hydrologique était la moins importante pour tous les critères choisis.

De façon globale, la combinaison de méthodes dynamique et statistique de mise à l'échelle présente des avantages dans la quantification des impacts hydrologiques du changement climatique, notamment dans la détermination de l'incertitude future.

Mots clés: changement climatique, hydrologie, générateur de climat, mise à l'échelle, modèle climatique, incertitude

TABLE OF CONTENTS

LIST OF TABLES

LIST OF FIGURES

LIST OF ABBREVIATION AND ACRONYMS

AMO	Atlantic Multidecadal Oscillation
BC	Bias correction
CCCMA-CGCM3	Canadian general circulation model of Canadian Centre for Climatemodelling and analysis, version 3
CF	Change factor
CLIGEN	Climate generator
CRCM	Canadian Regional Climate Model
CSIRO	General circulation model of the Australian Commonwealth Scientific and Research Organization
DA	Discriminant Analysis
DASR	Discriminant Analysis for downscaling precipitation occurrence and Step-wise Regression method for downscaling precipitation amounts
EA	East Atlantic Pattern
EA/WR	East Atlantic / West Russia Pattern
ENSO	El Niño-Southern Oscillation
EP/NP	East Pacific / North Pacific Pattern
FFT	Fast Fourier Transforms
GFDL-CM2.0	General circulation model of Geophysical Fluid Dynamics Laboratory, United States, version 2.0
GGES	Greenhouse Gase Emission Scenario
HMETS	Hydrological Model École de technologie supérieure
HSAMI	A lumped conceptual rainfall-runoff model developed by Hydro-Québec

HYDROTEL	A spatially-distributed and physically-based Hydrological model developed by a research team from the Institut National de la Recherche Scientifique in Quebec City, Canada
MIROC3.2-Medres	Model for Interdisciplinary Research on Climate, Japan, version 3.2
MPI-ECHAM5	General circulation model of Max Planck Institute for Meteorology, Germany, version 5
MPP	Mean monthly precipitation
MRI-CGCM2.3	General circulation model of Meteorological Research Institute, version 2.3
NAO	North Atlantic Oscillation
NCEP	National Center for Environmental Prediction
P01	Transition probability of precipitation occurrence of a wet day following a dry day
P11	Transition probability of precipitation occurrence of a wet day following a wet day
PCA	Principle component analysis
PDF	Probability density function
PDO	Pacific Decadal Oscillation
PI	Unconditional probability of daily precipitation occurrence
PNA	Pacific / North American Pattern
RCM	Regional Climate Model
SCA	Scandinavia Pattern
SD	Statistical downscaling
SDSM	Statistical downscaling model
SLP	Sea Level Pressure
SST	Sea Surface Temperature

Tmax	Maximum air temperature
Tmin	Minimum air temperature
WeaGETS	Weather Generator École de technologie supérieure
WG	Weather generator
WGEN	Weather generator developed by Richardson (1981)
WP	West Pacific Pattern

INTRODUCTION

The average surface air temperature of Earth rose more than 0.7 °C (1.3°F) over the last century. Significantly, it has spiked dramatically in recent years, reaching a new high in 1998 (Henson, 2008). This warming has disrupted the climate system and water cycle process. Whitfield and Cannon (2000) showed that reductions in summer flows, increases in winter precipitation and earlier spring flows were observed in Quebec, Canada. The Intergovernmental Panel on Climate Change (IPCC, 2007) stated that global mean temperature will likely increase between 1.8-4.0 °C by the end of this century. The larger increase in temperature will have further discernible impacts on continental water resources (IPCC, 2007, Srikanthan and McMahon, 2001; Xu and Singh, 2004). Small changes in precipitation frequency and/or quantity can result in distinct effects on the mean annual discharge for a watershed (Risbey and Entekhabi, 1996; Whitfield and Cannon, 2000; Muzik, 2001). Changes in catchment hydrology will then affect the performance and management of water systems, since hydropower generation is modulated by water resources. Hydropower companies throughout the world increasingly realize that they must deal with climate change. In Canada alone, hydropower is a multi-billion dollar industry, especially for the Province of Quebec, which was the world's fourth largest producer of hydropower with 7% of the international production (Quebec Government, 2004). Moreover, the increasing occurrence of more intense climate events like very severe storms may also increase environmental stresses. In this context, water resource management will face even more challenges. Management will need to be adjusted based not only on the natural variability of past climate but also in relation to future climate changes, because the climate observations in recent decades no longer fall within the variability of past climate due to the increase of greenhouse gas emissions (IPCC, 2007).

To better evaluate the impacts of future climate change will require the development of high quality climate projections and the best possible estimation of uncertainty. Even through General Circulation Models (GCMs) were developed to predict future climate, their spatial and temporal resolutions are too coarse to assess the catchment and site-specific impacts of

climate change (Leavesley, 1994; Hostetler, 1994). Therefore, for impact studies it is necessary to perform some post-processing to improve upon these global-scale models. This post-processing is called downscaling and it addresses the scale difference between global models and the local scale at which impact studies are generally conducted. There are two widely used downscaling techniques: dynamic downscaling and statistical downscaling. Dynamic downscaling is developed based on dynamic formulations using the initial and time-dependent lateral boundary conditions of GCMs to achieve a higher spatial resolution by nesting Regional Climate Models (RCMs) (Caya and Laprise, 1999). The spatial resolution of an RCM is much improved over that of a GCM, but it is still too coarse for small or medium-size watersheds and site-specific impact studies. Moreover, RCMs are only available for limited regions, due to their large computational cost (Solman and Nunez, 1999). To address these problems, statistical downscaling methods have been proposed. Statistical downscaling involves linking the states of some variables representing a large scale (GCM or RCM grid scale, predictors) and the states of some variables representing a much smaller scale (catchment or site scale, predictands). A range of statistical downscaling approaches have been developed, and can be classified into three categories: transfer function, weather typing and weather generator (Kidson and Thompson, 1998; Mearns et al., 1999a, b; Murphy, 1999; Wilby et al., 2000). The main strengths of statistical downscaling over dynamic downscaling are the low computational cost and the relative ease of application. Thus, it is often used as a complementary technique to downscale GCM outputs. However, statistical downscaling approaches also have drawbacks. For example, the probable lack of a stable relationship between predictors and predictands in the transfer function method, as well as in the weather typing scheme (Chen et al., 2011a). In addition, the adjustment of transition probabilities of precipitation occurrence, such as a wet day following a wet day (P11) and a wet day following a dry day (P01) is still a challenge for the weather generator based method.

Over the past decade, stochastic weather generators were widely used in climate change studies as a downscaling tool. Daily stochastic weather generators such as Weather GENerator (WGEN; Richardson, 1981; Richardson and Wright, 1984), CLImate GENerator

(CLIGEN; Nicks et al., 1995) and Weather Generator Ecole de Technologie Superieure (WeaGETS; Chen et al., 2011b) can rapidly produce multiple-year outputs at a daily time scale, which can be used to quantify the impacts of climate change (Wilks, 1992, 1999a; Pruski and Nearing, 2002; Zhang et al., 2004, Zhang, 2005; Zhang and Liu, 2005) , especially for extreme climate events. This is achieved by perturbing the parameters of the weather generator according to the relative changes projected by a climate model. One significant problem with current stochastic weather generators is the underestimation of the monthly and inter-annual variances, because they do not take into account the low-frequency component of climate variability (Buishand, 1978; Johnson et al., 1996; Wilks, 1989, 1999b; Gregory et al., 1993; Katz and Parlange, 1993, 1998; Hansen and Mavromatis, 2001).

Since each downscaling method has its unique advantages and drawbacks, it is not a trivial task to select one over the other. This work aims at combining climate models and statistical downscaling in a new hybrid method by merging stochastic weather generator with climate models for quantifying the hydrologic impacts in a changed climate. To proceed along these lines, weather generators were first improved in their capacity to generate precipitation, maximum temperature (Tmax) and minimum temperature (Tmin). Several aspects of statistical downscaling were then evaluated, as well as the global uncertainty involved in quantifying the hydrological impacts of climate change. This thesis also looks at the uncertainty associated with the choice of a downscaling method.

This thesis consists of five parts: an introduction, literature review, main body, general conclusions and recommendations. The introduction covers the background and scientific problem and outlines the objectives. The methodology and structure of the thesis are also summarized in the introduction. The literature review presents relevant scientific articles published on stochastic weather generators and statistical downscaling. Hydrological modeling in climate change studies and the uncertainty of hydrological impact studies under climate change are also described in the literature review. The main body of the thesis consists of eight published or submitted research articles. These are presented in chapters 1 to 8. General conclusions are summarized after the presentation of the main body. Finally, the

limitations of this research and recommendations for further studies are described. The appendices contain additional unpublished results.

The eight articles presented in Chapters 1-8 can be divided into five sections: 1: stochastic weather generator improvements (Chapters 1-3); 2: statistical downscaling (Chapters 4-5); 3: downscaling of weather generator parameters (Chapter 6); 4: downscaling uncertainty (Chapter 7); and 5: global uncertainty of hydrologic impacts (Chapter 8). The links between the chapters and the flow chart of this research are presented in Figure 0.1.

Section 1: Stochastic weather generator improvements (Articles 1-3):

Since the reliability of downscaled projections depends on the performance of the weather generator, the first step involved improvements to weather generators. These are presented separately in three articles (Chapters 1-3 in this thesis). (1) A spectral correction method is presented to deal with the low-frequency problem for precipitation. The power spectra were computed using Fast Fourier Transforms (FFT). Low-frequency variability was modeled based on the observed power spectra of monthly and annual precipitations. Generation of synthetic monthly and yearly time series was achieved by assigning random phases for each spectral component. The link to daily parameters was established through linear functions. (2) Two widely used weather generators (WGEN and CLIGEN) were integrated into a hybrid method to solve the correlation problems for Tmax and Tmin. The above-mentioned spectral correction method was further applied to correct the inter-annual variability for Tmax and Tmin. (3) A stochastic weather generator incorporating the aforementioned improvements was developed and made available to the scientific community as an open source code. First-order and higher-order (second and third-orders) Markov chains were used to produce precipitation occurrence. Two distributions (exponential and gamma) were provided to generate precipitation amount. The conditional and unconditional schemes derived from CLIGEN and WGEN were made available to simulate Tmax and Tmin.

Section 2: Statistical downscaling (Articles 4-5):

Precipitation, a critical element of hydrology studies that is also much more difficult to downscale than temperature, was the only variable evaluated in this section. Several aspects

of the statistical downscaling of precipitation were examined, and are presented by two articles (Chapters 4-5 in this thesis). The first (Chapter 4) includes the following aspects: (a) downscaling of precipitation using a statistical downscaling model (SDSM), (b) downscaling of precipitation occurrence using a discriminant analysis based model, and downscaling of precipitation amount using a stepwise linear regression method (DASR), (c) evaluation of the improvement in statistical downscaling using RCM variables as predictors over GCM, based on an SDSM-like model, and (d) an assessment of the efficiency of the weather typing approach in downscaling precipitation. The second (Chapter 5) evaluates the reliability of the regression-based method in downscaling precipitation for North America. The precipitation occurrence and amount were downscaled by a discriminant analysis-based model and a stepwise linear regression approach, respectively. The percentages of correct wet and dry day classifications and the percentages of explained variance for both calibration and validation were used as criteria to assess the reliability of statistical downscaling across North-America.

Section 3: Downscaling of weather generator parameters (Article 6):

This section presents a new hybrid statistical downscaling method combining the attributes of both stochastic weather generator and change factor (CF) methods, using RCM-projected precipitation and temperatures as predictors. The parameters of the weather generator were modified to take into account variations projected by a climate model. These variations were based on the CF approach. For example, take the probability of precipitation occurrence P01. For various reasons, the P01 obtained from climate model data would not match the P01 measured at a station. Thus, similarly to the CF method, the difference between the P01 obtained from climate models in present and future climates was applied to the observed data. The same method was also applied to the probability of precipitation occurrence, P11, to monthly mean precipitation and monthly Tmax and Tmin. The variance of monthly precipitation, Tmax and Tmin were adjusted using a proportional method. The hydrological impacts of climate change were then quantified based on the simulation of a hydrological model for a Canadian river basin (Quebec Province) for the 2025-2084s period (centered by 30-year moving averages from 2011-2099).

The downscaling of weather generator parameters using atmospheric circulation indices, GCM and RCM variables as predictors was also investigated. Since weak corrections were obtained between atmospheric circulation indices and four precipitation parameters (P01, P11, unconditional probability of daily precipitation occurrence and seasonal precipitation), as well as between GCM (RCM) predictors and precipitation parameters, this downscaling experiment was unsuccessful. Thus, there was no article written for this work. The correlations between atmospheric circulation indices and precipitation parameters calculated for 16 stations dispersed across North America, as well as correlations between GCM (RCM) predictors and precipitation parameters are presented in appendix A to give a reference for further studies.

Section 4: Downscaling uncertainty (Article 7):

The uncertainty of six downscaling methods was investigated in the context of quantifying the hydrological impacts of climate change for a Canadian river basin (Quebec province). These methods regrouped dynamical and statistical approaches, including the CF method, the bias correction method and the above-mentioned weather generator-based approach. Future (2070-2099) hydrological regimes simulated with a hydrological model were compared to the reference period (1970-1999) using the average hydrograph, annual and seasonal mean discharge and peak discharge as criteria.

Section 5: Global uncertainty of hydrologic impacts (Article 8):

This section considered global uncertainty by combining results from an ensemble of six GCMs, two greenhouse gas emission scenarios (GGES), five GCM initial conditions, four downscaling techniques, three hydrological model structures and ten sets of hydrological model parameters. Each climate projection was equally weighted to predict the hydrology on a Canadian river basin (Quebec Province) for the 2081-2100 horizon. Future (2081-2100) hydrological regimes simulated with three hydrological models were compared to the reference period (1971-1990) using mean annual discharge, mean seasonal discharge, annual low flow (95%), peak discharge, time to the beginning of flood, time to peak discharge and time to the end of flood as criteria.

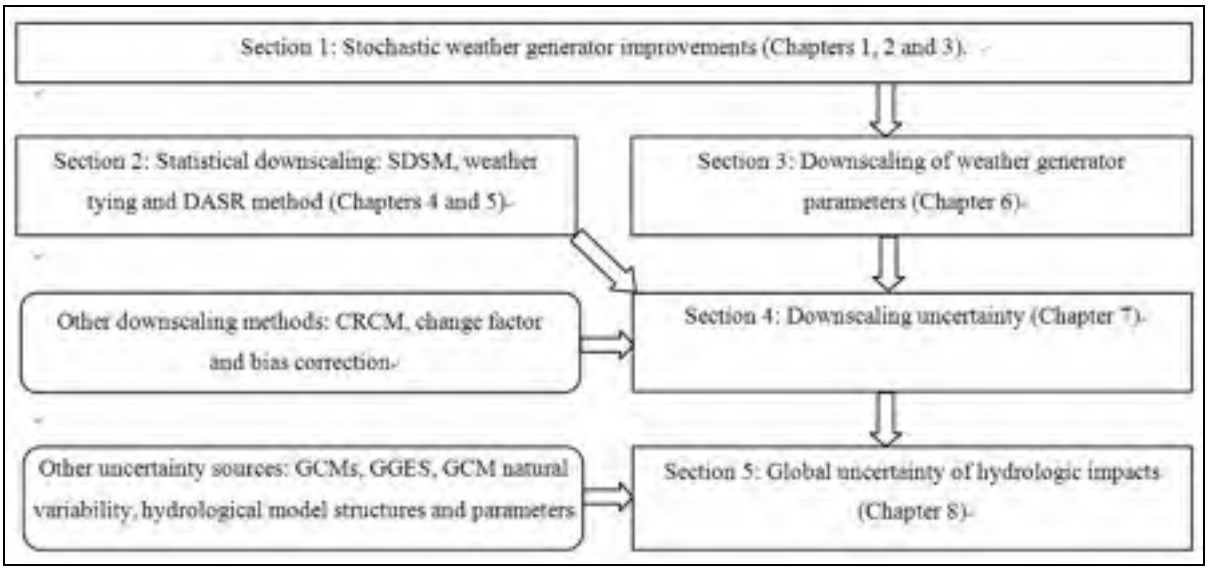

Figure 0. 1 Flow chart of this work.

LITERATURE REVIEW

This session first introduces the research progress of stochastic weather generators in producing daily precipitation and temperature. Then, dynamical and statistical downscaling are summarized, especially a range of statistical downscaling including transfer function, weather generator and weather typing approaches are highlighted. The hydrological modeling in climate change studies and global uncertainty of hydrological impacts studies are briefly described next.

1) Stochastic weather generators

With the growing use of physically based response models like hydrological and agricultural models, there is frequently a requirement of weather generators to generate long climate series as inputs of those models to simulate the long term effects of climate variability. The generated climate series are expected to be statistically similar to those of the actual data. The most appealing property of weather generators is that they provide a complete record for any desired period of time. Moreover, they are able to generate daily weather data for ungauged areas through interpolating model parameters from adjacent gauged sites (Baffaut et al., 1996). Recently, weather generators have been used as downscaling tools to produce multiple-year climate change scenarios at daily time scale for assessing the impacts of climate change (Semenov & Barrow, 1997; Wilks, 1992, 1999a; Pruski and Nearing, 2002; Zhang et al., 2004; Zhang, 2005; Zhang and Liu, 2005; Minville et al., 2008). Over last three decades, several stochastic weather generators have been developed, such as Weather Generator (WGEN) (Richardson, 1981; Richardson and Wright, 1984), USCLIMATE (Hanson et al., 1994), Climate Generator (CLIGEN) (Nicks et al., 1995), Climate Generator (ClimGen) (Stockle et al., 1999) and Long Ashton Research Station-Weather Generator (LARS-WG) (Semenov and Barrow, 2002).

1.1) Precipitation models

Most weather generators separately deal with the precipitation occurrence and intensity processes. The precipitation occurrence is separated into two weather states: wet and dry.

The daily precipitation intensity process involves the simulation of nonzero precipitation amounts.

1.1.1) Precipitation occurrence models

Models of rainfall occurrence include two main types which are based on Markov chains and alternative renewal process.

The simplest and widely used statistical model for simulating daily precipitation occurrence is the first order, two-state Markov model (Katz, 1977; Richardson, 1981; Wilks, 1989, 1992; Nicks et al., 1995), which can be defined in terms of two transition probabilities, a wet day following a dry day (P01) and a wet day following a wet day (P01):

$$P01 = \Pr\{\text{precipitation on day t} \mid \text{no precipitation on day t-1}\} \quad (1a)$$

$$P11 = \Pr\{\text{precipitation on day t} \mid \text{precipitation on day t-1}\} \quad (1b)$$

Since precipitation either occurs or does not on a given day, the two complementary transition probabilities are P00 = 1-P01 and P10 = 1-P11. The first-order Markov model is adequate for generating wet spells (Wilks, 1999b; Zhang and Garbrecht, 2003; Chen et al., 2009). However, it underestimates the long dry spell in some regions (Buishand, 1978; Guttorp, 1995; Racsko et al., 1991; Semenov and Porter, 1995; Wilks, 1999b; Chen et al., 2009).

A generalization of first-order Markov model is to consider higher-order Markov model like second- and third-order (Chin, 1977; Gates and Tong, 1976; Wilks, 1999b). If a deficiency of first-order Markov model in simulating the precipitation occurrence is the underestimation of long dry spells, the higher-order models may have positive effects. However, one problem of higher-order Markov model used in climate change studies is that too many parameters require to be determined. Due to first-order model adequately simulates the wet spells, Stern and Coe (1984) and Wilks (1999b) suggested using hybrid order Markov chains, which use

first-order Markov model for wet spells, but allow higher-order model for dry sequences. Thus, the requirement of determined parameters is significant decreased from 2^k to $k+1$, where k is the order of Markov model. Wilks (1999b) examined different precipitation occurrence models including first-, second-, third- and hybrid order Markov models, Negative Binomial and Mixed Geometric distributions in reproducing wet and dry spell lengths. The results showed that every precipitation occurrence model reasonably well represented the wet spells. However, all Markov model underestimated the longest dry spells, but high-order Markov models performed better than first-order model, and spell-length models were better than Markov model.

In the alternating renewal process, the precipitation time series is considered as a sequence of alternating wet and dry spells of varying length, rather than simulating precipitation occurrence day by day. Different distributions may then be used to fit the wet and dry spells independently. Those distributions normally include the logarithmic series (Green, 1964), truncated negative binomial distribution (Buishand, 1978), truncated geometric distribution (Roldan and Woolhiser, 1982) and semi-empirical distribution (Semenov and Barrow, 2002). Foufoula-Georgiou and Lettenmaier (1987) used a Markov renewal model for simulating precipitation occurrences, where the time between precipitation occurrences was sampled from two different geometric distributions and the transition from one distribution to the other was governed by a Markov chain. Smith (1987) introduced a family of models termed Markov-Bernoulli processes consisting of a sequence of Bernoulli trials with randomized success probabilities described by a first-order, two-state Markov chain to generate precipitation occurrences. Semenov and Barrow (2002) used the semi-empirical distributions for the lengths of wet and dry day spells in LARS-WG. The generated lengths derived from the semi-empirical distribution which fitted by observed series. The results showed that every single series from the observed data was well reproduced by semi-empirical distributions. The comparison of LARS-WG with WGEN demonstrated that semi-empirical distribution is better than first order Markov model (Semenov et al., 1998). However, the ability of the alternating renewal process method depends on the parameter estimation, thus, a long

observed time series (normally more than 25 years) is needed. Moreover, it is susceptible to poor parameter estimates in arid regions (Roldan and Woolhiser, 1982).

1.1.2) Precipitation intensity models

The other important process of stochastic weather generator is the generation of daily precipitation intensity on wet days. A number of models have been proposed to generate daily precipitation intensity given the occurrence of a wet day. The simplest one is the exponential distribution (Todorovic and Woolhiser, 1974; Richardson, 1981) which has a probability density function given by

$$f(x) = \lambda e^{-\lambda x} \tag{2}$$

where x is daily precipitation intensity and λ is the distribution parameter (equal to the inverse of the mean).

The Weibull probability distribution was also used to simulate the daily precipitation intensity (Stockle et al., 1999; Kevin et al., 2005). For a wet day the precipitation amount is generated by

$$f(x) = \frac{\alpha}{\beta^{\alpha}} x^{\alpha-1} e^{-(x/\beta)^{\alpha}} \tag{3}$$

where α and β are the two distribution parameters.

One other widely used distribution is two-parameter Gamma distribution (Jones et al., 1972; Goodspeed and Pierrehumbert, 1975; Coe and Stern, 1982; Richardson and Wright, 1984; Woolhiser and Roldan, 1982), the probability density function for this distribution is

$$f(x) = \frac{(x/\beta)^{\alpha-1} \exp[-x/\beta]}{\beta \Gamma(\alpha)} \tag{4}$$

where α and β are the two distribution parameters, and Γ(α) indicates the gamma function evaluated at α.

The mixed Exponential distribution was also used in some researches (Woolhiser and Pegram, 1979; Woolhiser and Roldan, 1982, 1986), with a probability density function of

$$f(x) = \frac{\alpha}{\beta_1}\exp(\frac{-x}{\beta_1}) + \frac{1-\alpha}{\beta_2}\exp(\frac{-x}{\beta_2}) \tag{5}$$

This distribution is a probability mixture of two one-parameter exponential distributions. The parameter α is the mixing probability, which determines the weights given to the two exponential distributions with scale parameters β_1 and β_2.

A three-parameter skewed normal distribution was also used to generate the daily precipitation intensity (Nicks and Lane, 1989, Nicks et al., 1995).

$$\lambda = \frac{6}{g}\left\{\left[\frac{g}{2}\left(\frac{x-\mu}{s}\right)+1\right]^{1/3} - 1\right\} + \frac{g}{6} \tag{6}$$

where, λ is standard normal deviate; μ, s and g are the mean, standard deviation and skew coefficient of daily precipitation intensity, respectively.

Besides distributions describe above, a truncated power of normal distribution (Bardossy and Plate, 1992; Hutchinson et al., 1993), kappa distribution (Chapman, 1994, 1998) and semi-empirical distribution (Semenov and Barrow, 2002) were also used to simulate the daily precipitation intensity.

Numerous studies were conducted to evaluate, compare and improve the ability of weather generators in simulating the daily precipitation intensity (Johnson et al., 1996; Headrick and Wilson, 1997; Semenov et al., 1998; Wilks, 1999b; Zhang and Garbrecht, 2003; Kevin et al.,

2005; Elshamy et al., 2006; Zhang et al., 2007; Kou et al., 2007; Chen et al., 2008; Chen et al., 2009). Chapman (1994, 1998) compared five models including the exponential, gamma, kappa, mixed exponential and skewed normal distributions in simulating daily precipitation intensity. The results showed that the best one is the skewed normal distribution, followed by mixed exponential, kappa and gamma distributions, and the worst is the exponential distribution. Wilks (1999b) compared the ability of independent and identically gamma distribution, common-α gamma distribution and mixed exponential distribution. The results demonstrated that mixed exponential distribution was the best one, next was the common-α gamma distribution and then the identically gamma distribution. Those comparisons indicate that more complex distributions may be more capable in simulating daily precipitation intensity, although most of them are satisfactory in producing the means of daily, monthly and annual precipitation amounts. However, weather generators less well reproduce extreme precipitation events (Buishand, 1978; Guttorp, 1995; Racsko et al., 1991; Semenov and Porter, 1995), because most of these distributions are not "heavy tailed". Wilks (1999b) examined the ability of the identically gamma distribution, common-α gamma and mixed exponential distributions in reproducing the observed extremes (largest daily precipitation in each month) of precipitation amount and demonstrated that the common-α gamma distribution is better than identically gamma distribution, and the mixed exponential distribution was the best one in matching the observed extremes. However, the distribution of extreme precipitation can vary quite drastically on a regional basis and it is difficult to find a distribution that is suitable for all climate zones.

The other problem with weather generators is that they underestimate low-frequency variance (Buishand, 1978; Johnson et al., 1996; Wilks, 1989, 1999b; Gregory et al., 1993; Katz and Parlange, 1993, 1998; Hansen and Mavromatis, 2001), because they do not take into account the low-frequency component of climate variability.

The low-frequency variability of precipitation depends on the daily precipitation occurrence and intensity processes. Wilks (1999b) compared a diverse range of precipitation occurrence and intensity models in preserving low-frequency variability. The results demonstrated that

none of models and combinations achieved complete recovery of the observed variance in monthly total precipitation, although increasingly complex component models did succeed in reducing the overdispersion between the synthetic and observed variability. This was unsatisfactory because although the complexity of the models was increased, it still did not take into account the low-frequency component of climate variability. These simple stationary models (whose statistics do not change from month to month and from year to year) cannot fully reproduce the variability of a nonstationary climate, which therefore makes the introduction of some degree of nonstationarity into these models appropriate.

Hansen and Mavromatis (2001) attempted to improve inter-annual variability characteristics by perturbing monthly parameters using a low-frequency stochastic model, and evaluated the effectiveness of the low-frequency component on low-frequency variability of the generated monthly climate at 25 locations in the continental USA. The results indicated that for monthly precipitation, the low-frequency correction reduced total error and eliminated negative bias of inter-annual variability, and reduced the number of station-months with significant differences between observed and generated inter-annual variability, but it over-represented the variability of precipitation frequency.

Dubrovsky et al. (2004) applied the monthly generator (based on a first-order linear autoregressive model) to fit the low-frequency variability based on the daily WGEN-like weather generator, Met & Roll. The results demonstrated that conditioning the daily generator on a monthly generator has the most positive effect, especially on the output of a hydrological model, and the variability of the monthly streamflow characteristics was better simulated. However, this method still could not reproduce the observed standard deviations and autocorrelations of monthly and annual precipitations exactly, because it did not specifically consider the inter-annual variability, thus indicating that schemes for correcting monthly variability have limited effect at the annual scale.

Wang and Nathan (2007) also provided a method for coupling daily and monthly time scales in the stochastic generation of rainfall series. The key feature of the method involves first

generating two similar time series, one preserving key statistical properties at a finer time scale and the other at a coarser time scale. The finer time scale series is then adjusted to make it consistent with the coarser one. This method appears to perform well in that it satisfactorily preserved some key statistical properties at daily, monthly and even yearly scales. However, it was only tested for the coefficient of variation on Australian weather data. Other statistics, such as the autocorrelation of annual precipitation, are important for some applications.

1.2) Temperature models

Generation of maximum temperature (Tmax) and minimum temperature (Tmin) are the usual main components of the weather generator and it is very important for climate change impacts studies.

Comparatively to precipitation, temperatures are much simpler to produce, since they often approximately follow a normal distribution. However, daily Tmax and Tmin are correlated with each other and this correlation varies depending on whether the day is dry or wet. Thus, the preservation of these correlations is an important criterion to assess the performance of a weather generator.

Richardson (1981, 1984) applied a first-order linear autoregressive model to generate the residual series of Tmax and Tmin in WGEN. This approach is good at reproducing the lags 0 and 1 correlations, but the lags of greater than one day could not be well preserved (Richardson, 1981). CLIGEN uses two random numbers to generate the standard normal deviate. The second number for one day is reused as the first number for the next day (Nicks et al., 1995). But this method underestimated the correlations; especially the day-to-day persistence (Zhang, 2004; Chen et al., 2008). In order to simplify the procedure, LARS-WG uses constant lag 1 auto-correlations for Tmax and Tmin and pre-set cross-correlation between them. These simplifications apparently are unable to exactly preserve the correlations, especially the long-term persistence. Moreover, the generated Tmax should be larger than Tmin on any given day in order to consistent with the real climate system. However, the Tmax and Tmin are generated independently by some models such as WGEN

and version 5.111 of CLIGEN. It results in several cases that the Tmin is larger than Tmax. Thus, a range check is imposed in some weather generators. This procedure may perturb the statistics even autocorrelation of Tmin, if there are large numbers of cases that the generated Tmin are larger than Tmax. But in the latest version of CLIGEN (version 5.22564), the Tmin is generated conditionally with the Tmax, the range check is unnecessary.

Similarly to precipitation, weather generators also underestimate the low-frequency variance of Tmax and Tmin (Dubrovsky et al., 2004) because they do not explicitly take into account aspects of low-frequency component of climate variability. Dubrovsky et al. (2004) applied the monthly generator (based on a first-order linear autoregressive model) to adjust the low-frequency variability of generated Tmax and Tmin based on a daily WGEN-like weather generator, Met & Roll. The results showed that conditioning the daily weather generator on a monthly model has positive effects. However, this method still could not accurately reproduce standard deviations and autocorrelations of observed averaged yearly temperatures, because it did not specifically consider the inter-annual variability. To date, no one has been able to correct the low-frequency variability of temperatures for weather generators. The reason may be that the correction of temperatures is more complicated than precipitation because the Tmax and Tmin are correlated to each other. Correction of one variable may perturb their cross-correlations and results in Tmin larger than Tmax on any given day.

1.3) Conclusions on stochastic weather generators

Stochastic weather generators are computer models which produce synthetic daily climate variables, such as precipitation and temperature, which statistically resemble to the observed data. They are good at generating quantities of each variable. However, they are often found to be deficient with respect to two potentially important characteristics. First of all, the low-frequency variance is distinctly underestimated, which results in an underestimation of low-frequency variability of streamflow at the revier basin. Secondly, they less well represent extreme events, especially, longest dry spells and maximum daily precipitation intensity. A few published articles were conducted to deal with the low-frequency problem like

Dubrovsky et al. (2004), Wang and Nathan (2007). However, those methods still have their drawbacks and are unable to completely solve this problem. For example, Wang and Nathan's method is arguably the best available for dealing with the low-frequency problem, but it was only tested for the coefficient of variation on Australian weather data. Other statistics, such as the autocorrelation of annual precipitation, are important for some applications. Extreme value characteristics were investigated by Wilks (1999b) through the comparison of 3 daily precipitation intensity, 8 precipitation occurrence models and their combinations. Different models have different ability, but none of models and combinations could reproduce the extreme value characteristics accurately. A well adapted "heavy tailed" frequency distributions may need to be investigated. But this is not an easy task because different regions have different precipitation characteristics; it is not easy to find a distribution that is capable for every weather condition. Moreover, precipitation occurrence model like first-order Markov chain is inadequate for simulating longest dry spells in some regions. High-order Markov models perform better, but there are more parameters needed to be determined.

2) Downscaling

Mismatches of spatial and temporal resolutions between GCM outputs and the data requirements of hydrological models are major obstacles for quantifying the hydrologic impacts of climate change. This is because GCMs generally run at a resolution of 150-300 km and regional studies require a resolution of 10-50 km or finer at a daily scale. Therefore, it is common to downscale the GCM outputs from grid scale to regional or site-specific scale using dynamical and/or statistical downscaling. However, each downscaling method has its advantages and drawbacks. A growing number of studies have been undertaken to compare statistical versus dynamical models (Kidson and Thompson, 1998; Mearns et al., 1999a, b; Murphy, 1999; Wilby et al., 2000).

2.1) Dynamical downscaling

Over the past decade, regional climate model (RCM) was developed as a downscaling tool based on the initial and time-dependent lateral boundary conditions of GCM. Because of its

higher spatial resolution, the RCM has more capabilities to capture the effects of regional details on local climate such as orographic precipitation. Presently, model grids of 50 km have become feasible and finer will likely be developed in the near future along with the increase of computer performances (Bengtsson, 1996; May and Roeckner, 2001; Déqué and Gibelin, 2002).

Duffy et al. (2003) evaluated the performances of current RCMs and concluded that nearly all quantities simulated by higher-resolution RCMs agree better with observations in terms of spatial patterns, but their performance still depends on different regions and specific variables. Moreover, their resolution is still too coarse to some practical applications such as quantifying the impacts of field agriculture or small catchment water resources under climate change. At this point, the site-specific or small catchment climate data derived from statistical downscaling may be preferred.

2.2) Statistical downscaling

As a complementary technique to RCM, a diverse range of statistical downscaling techniques have been developed. Those techniques fall in three categories: transfer function, weather generator, and weather typing (Wilby and Wigley, 1997; von Storch et al., 2000; Zhang, 2005). In reality, many downscaling studies used more than one of these techniques (Wilby and Wigley, 1997). Besides the above mentioned three types of statistical downscaling, the change factor method is a relatively straightforward and widely used method. It is conducted as the following three steps. A baseline climatology is first established using long-term climate data for the site or region of interest. Secondly, changes between present and future climates projected by GCM at grid points close to the target site are calculated usually at a monthly time scale. Thirdly, the changes suggested by GCM are simply added to (for temperature) or multiplied for (for precipitation) each day in the baseline time series. This method is computationally straightforward and easy to apply. Meanwhile, local climate change scenario is directly related to changes in the GCM output. The most significant drawback is that the temporal sequencing of wet and dry days and variance of each variable are unchanged (Diaz-Nieto and Wilby, 2005).

2.2.1) Transfer function approaches

The transfer function approach involves establishing statistical linear or nonlinear relationships between observed local climatic variables (predictands) and large-scale GCM or RCM output (predictors). The methods used to derive those relationships include multivariate linear or nonlinear regressions, principal component analysis (PCA), canonical correlation analysis (CCA), singular value decomposition (SVD), artificial neural networks (ANN), etc. Most commonly used predictors from GCM output include vorticity, airflow indices, wind velocity and direction, mean sea-level pressure, geopotential heights and relative humidity, etc (Wilby et al., 1998a; Solman and Nunez, 1999; Sailor and Li, 1999; Trigo and Palutikof, 2001). Widmanm et al. (2003) and Zhang (2005) downscaled precipitation using GCM precipitation as a predictor. The results showed that the performance of using GCM precipitation as a predictor was better than conventional methods using other predictors. However, most authors agree that predictors selected should be variables that are reasonably well-reproduced by GCM, and precipitation may not fit this criterion.

The most typical transfer function approach is done with a statistical downscaling model (SDSM) which was developed by Wilby et al. (2002a) for the rapid development of single-site, ensemble scenarios of daily weather variables. This model is good at reproducing temperatures with a explained variance normally in excess of 70%. But the explained variance of precipitation is usually less than 30% (Wilby et al., 2002a).

The main strength of the transfer function approach to future climate scenario generation is the relative ease of application. A potential obstacle is probable lack of stable relationships between predictors and predictand. For example, Wilby (1997) has shown that, even within a single circulation regime, precipitation diagnostics may vary considerably from year to year.

2.2.2) Weather generator approaches

Stochastic weather generators are able to be used as a downscaling tool to produce local climate change scenarios (Wilks, 1992; Semenov and Barrow 1997). It is achieved by perturbing their parameters according to the changes projected by GCMs.

Wilby et al. (2002b) explored the use of synoptic-scale predictor variable to downscale both high- and low-frequency variability of daily precipitation at sites across the Great Britain. The results showed that the conditionally stochastic rainfall models displayed positive effects on monthly rainfall statistics relative to the control, but still did not completely remove overdispersion. In order to better simulate the low-frequency variability, predictors that used to fit the transfer functions are needed to be further investigated. As mentioned earlier, Zhang (2005) used the transfer function approach to spatially downscale monthly GCM output from grid scale to site scale using GCM precipitation as a predictor. Subsequently, the monthly precipitation was temporally downscaled to daily time scale using CLIGEN. This method is relatively simple and can produce infinite-length time series with the same statistical properties of climate scenarios. However, it adjusts the precipitation occurrence according to its relationship with monthly precipitation. The relationship between monthly precipitation and occurrence is required for further investigation. Similarly, several other studies (Wilks, 1999a; Chen et al., 2006; Kilsby et al., 2007; Qian et al., 2005, 2010; Wilks, 2010) also downscaled precipitation with weather generators through adjusting their statistical parameters on the basis of the changes of monthly precipitation. The downscaled daily precipitation series are then generated by the weather generator using adjusted parameters. The results illustrated that the proposed method is capable of reproducing the mean of daily precipitation intensity.

Overall, the appealing property of using weather generator approach is its ability to rapidly produce ensembles of climate scenarios for studying the impacts of rare climate events. The disadvantage is that the precipitation occurrence parameters cannot be easily adjusted for a changing climate.

2.2.3) Weather typing schemes

Weather typing downscaling methods involve grouping local meteorological variables in relation to different classes of atmospheric circulation based on a given weather classification scheme (Bardossy and Plate, 1992; von Storch et al., 1993). In general, weather classification procedures include PCA (White et al., 1991; Shoof and Pryor, 2001), cluster analysis (Wilks,

1995), CCA (Gyalistras et al., 1994), fuzzy rules (Bardossy et al., 1995), ANN (Bardossy et al., 1994), analogue procedures (Martin et al., 1997; Timbal et al, 2009), Lamb Weather Types (Lamb, 1972; Jones et al., 1993; Conway and Jones, 1998), etc. Given a classification scheme, weather types are grouped. The relationships between large scale variables and local meteorological variable may then be established separately for each weather type. The analogue approach is one of weather typing schemes which involves picking the event in the past when the situation most closely resembles the day in the future. The benefits of analogue approach are that it is able to preserve the spatial correlation of predictand and is easy to apply even if predictands do not follow a normal distribution. However, only events that have occurred in the past can be modeled, thus, it is unable to study rare events under future climate change.

Shoof and Pryor (2001) downscaled precipitation and temperature based on the classification scheme of PCA. First of all, PCA was employed to reduce the number of intercorrelated variables to a smaller set of uncorrelated components. Principle component elements were then calculated for every day and used as predictors to fit linear (for temperatures) and Poisson (for precipitation) transfer functions with the local meteorological variables. The results showed that the accuracy of the downscaling models of temperature was better than that of precipitation. The precipitation models exhibited lesser predictive capabilities. This may be due to use principle component elements as predictors rather than use circulation climate variables, such as vorticity, airflow indices and wind speed.

The main advantage of weather typing schemes is that local variables are closely linked to the circulation on a large scale. It provides a greater understanding of the problems that are involved compared to other downscaling techniques. The drawbacks of this method are that the reliability depends on the stationary relationship between large scale circulation and local climate, and it requires an additional task of weather classification.

2.3) Comparison of statistical downscaling methods

Given a range of downscaling techniques, it is necessary to compare the capability and reliability of those methods.

Wilby et al (1998b) investigated the abilities of six downscaling methods including two weather generator techniques (WGEN and a method based on spell-length duration (SPEL)), two methods using vorticity as a predictor (B-Circ and C-Circ), and two variations of ANN using circulation data, and circulation plus temperature data as predictors. The validation tests showed that the WGEN and SPEL methods performed better than all other methods for the majority of diagnostics. But they were incapable to capture the low-frequency variations of rainfall. B-Circ and C-Circ methods performed well and were better than ANN, because ANN overestimated the frequency of wet days.

Widmann et al. (2003) compared three statistical downscaling methods including local rescaling, SVD and local rescaling with a dynamical correction using precipitation as a predictor. The results demonstrated that the SVD method explained over 60% of the observed monthly precipitation variability at almost locations in the studied region. The local scaling method also performed very well over the most parts of the region, but less well than the SVD method. Moreover, the local rescaling with a dynamical correction method performed almost as well as the SVD approach. This research indicated using GCM simulated precipitation as a predictor may be better than using large scale atmospheric circulation variables.

Diaz-Nieto and Wilby (2005) compared the abilities of CFs and statistical downscaling methods for assessing the impact of climate change on low flow in a river basin. The results illustrated that changes of low flow related to the statistical downscaling scenarios are generally more conservative than that arising from CFs.

Wetterhall et al. (2007) evaluated four downscaling methods including two analogue methods (one using PCA and one using gradients in the pressure field (TWS)) and two conditional-probability methods (one using classification of weather patterns (MOFRBC)

and one using SDSM). The results showed that the MOFRBC and SDSM were superior to other methods for the ranked probability scores; analogue methods were better than other methods during winter and autumn; SDSM and TWS were skillful during spring and MOFRBC during summer.

Overall, each statistical downscaling method has its advantages and drawbacks. The choice of one method over others should according to the application purposes and data availability.

2.4) Conclusions on downscaling

The present GCMs are unable to resolve important catchment-scale processes because the spatial resolutions is too coarse. Therefore, two typical downscaling techniques: dynamical and statistical downscaling, have been developed to address these scale problems. Each method has its benefits and weaknesses. For example, dynamical downscaling is more physically realistic representation of the regional climate while high computer resources demanded. Statistical downscaling is easy to apply but it seldom captures climate variability at temporal or spatial scales (Conway et al., 1996) and the relationships between predictand and predictors are not always stationary. Due to above mentioned drawbacks, the comparison of downscaling methods should be continued and new techniques are needed to be developed. First of all, downscaling of weather generator parameters based on low-frequency predictors may be good at downscaling climate variability. Moreover, downscaling GCMs or RCM output using weather typing scheme may have effects on fixing the latter drawback of statistical downscaling. Because circulation-based downscaling provides greater physical understanding of the problems that are involved due to different local weather conditions are determined by different synoptic-scale circulations. Moreover, due to the unique advantages and drawbacks of each downscaling methods result in different future climate projections, it is necessary to investigate the uncertainty related to downscaling techniques for quantifying the hydrological impacts of climate change.

3) Hydrological modeling in climate change studies

Hydrologic models provide a useful framework to investigate the relationship between the regional climate and catchment water resources (Xu, 1999). Over the last two decades, a large number of researches were reported to deal with the potential effects of climate change on water resources based on hydrologic models (Diaz-Nieto and Wilby, 2005; Wilby and Harris, 2006; Minville et al., 2008, 2009). The use of hydrological models in climate change studies ranges from using simple water-balance models to assess the annual and seasonal streamflow variation (Arnell, 1992) to using complex distributed models to evaluate the variations in surface and groundwater quantity (Running and Nemani, 1991). Based on the level of complexity, different models including empirical models (annual base), monthly water-balance models, conceptual lumped models and process-based distributed models are used depending on study purposes and model availability (Leavesley, 1994). Gleick (1986) and Xu (1999) reviewed several different modelling approaches for assessing the regional hydrologic impacts of climate change. They concluded that monthly water balance models are flexible and easy to apply over other models. But this kind of model is unable to adequately account for the characteristics of individual meteorological events. Thus, it is unable to capture the rare hydrological event such as flood. In contrast, conceptual lumped models are able to assess the magnitude and timing of the process response to climate change, while their capability depends on the number of parameters and the time period of input data. Process-based distributed models are able to simulate the spatial pattern of hydrologic response within a basin (Beven, 1989; Bathurst and O'Connell, 1992). But a large quantity of data is required to calibrate and validate the models. The choice of one model should depend on practical application purposes, model and data availability. Moreover, hydrological models are designed and calibrated for stationary conditions. But in climate change studies, they are usually applied to a climate change condition. Dietterick et al. (1999) suggested that the performance of hydrological model between colder / wetter years and hotter / dryer years was similar. Thus, the hydrological model may perform well for the future climate.

4) Uncertainty of hydrological impacts under climate change context

Given the large number of GCMs, Greenhouse Gas Emissions Scenarios (GGES) and downscaling methods available, it is becoming increasingly difficult to assess the uncertainties that result from their combination. This difficulty is further amplified when taking into account the choice of an impact model (such as a hydrological model) and its parameters, which also contribute to global uncertainty. Various sources of uncertainty have been clearly identified and it has been recognized that they should be taken into account in climate change impact studies. A failure to cover the full range of uncertainty may result in severely biased impact studies. The uncertainty cascade can be classified as follows: (1) GGES; (2) GCM structure; (3) GCM initial conditions. (4) downscaling method; (5) hydrological model structure; and (6) hydrological model parameters; Running GCMs with different initial conditions is a way to assess natural variability as perceived by the climate model. Some of these uncertainty sources may be reduced in the future (through higher resolution GCMs for example), but some causes of uncertainty will always remain. The acknowledgement and proper quantification of uncertainty is vital to facilitate a risk-based approach to decision making. As such, a appropriate framework to properly sample all sources of uncertainty is very much needed. To date, there have been several hydrological impact studies that have taken some causes of uncertainties into account, but only a rare few have investigated most of the entire cascade of uncertainties listed above.

Jenkins and Lowe (2003) studied changes in global mean rainfall from different GCMs and GGES and showed that GCM uncertainty dominates GGES uncertainty. This finding has been confirmed by several other studies. Rowell (2006) investigated the uncertainty arising from RCM formulation, and compared it with three other sources of uncertainty (GCMs, GGES and GCM initial conditions (ensemble runs)) with respect to changes in seasonal precipitation and temperature for the United Kingdom. The results showed that the uncertainty due to RCM formulation was relatively small, while GCMs consistently demonstrated a dominant role for each season. Deque et al. [2007] assessed the uncertainty of ten RCMs which are driven by 3 GCMs under two GGES (A2 and B2). Some runs have been repeated three times to take into account the internal variability. The results showed that the uncertainty introduced by the choice of the driving GCM is generally larger than the other

three sources. But the RCM uncertainty for the summer precipitation has the same magnitude as the choice of the GCM. This conclusion was proved by Fowler and Ekstrom [2009], through comparing 13 RCMs in predicting changes of seasonal precipitation extreme for 9 UK rainfall regions using a weighting scheme. The results demonstrated that the largest contribution to uncertainty in the multi-model ensembles comes from the lateral boundary conditions used by RCMs including in the ensemble. These studies investigated the uncertainty on the primary outputs of climate models (temperature and/or precipitation) rather than on river flow. Different results may be obtained when transferring climate projections to watershed streamflows, since it is a non-linear process.

Prudhomme and Davies (2009) used three GCMs, two GGES and two downscaling techniques (a statistical downscaling model (SDSM) and the RCM HadRM3) to investigate the uncertainty in river flows, and demonstrated that GCMs were the main contributors to monthly mean flow uncertainty. The downscaling of originating uncertainty was also important, but the contribution of GGES to uncertainty was negligible. Kay et al. (2009) also investigated different sources of uncertainties including five GCMs, four GGES (A1F1, A2, B1 and B2), two downscaling methods (change factor (CF) and RCM)), two hydrological models, hydrological model parameters and GCM initial conditions on the impact of climate change on flood frequency in England. With this research, each source of uncertainty was assessed individually rather than in combination with each other. The results showed that the uncertainty related to GCM structure was the largest, but other sources of uncertainty were also important, although less so than GCM uncertainty. However, Booij (2005) found that the uncertainty related to GCM initial conditions was larger than that of GCMs and RCMs.

Wilby and Harris (2006) presented a probabilistic framework for quantifying different sources of uncertainties on future low flows. They used four GCMs, two GGES, two downscaling methods (SDSM and CF), two hydrological model structures and two sets of hydrological model parameters. The results again showed that GCMs are the main contributor to global uncertainty, followed by downscaling methods. Uncertainties due to hydrological model parameters and GGES were less important. This is probably the most

thorough study so far, in terms of inclusion of the most sources of uncertainty. However, it is also not fully exhaustive. Firstly, two downscaling methods, two hydrological model structures and two sets of hydrological model parameters are likely to be insufficient to represent their uncertainty envelope. They also did not consider hydrological models with different levels of complexity and structure. The study did not consider the uncertainty due to the GCM initial conditions. Finally, since the purpose of this research was to provide a framework for assessing uncertainties in climate change impact studies, the only quantified variable was river low flows. Other hydrological variables such annual, seasonal and peak discharges may respond quite differently with respect to global uncertainty.

Overall, climate change impact studies based on a single GCM and/or downscaling method and/or impact model should be interpreted with caution. Using two carefully selected models and/or methods may also be insufficient, because the process by which climate projections become hydrologic variables is non-linear.

CHAPTER 1

A DAILY STOCHASTIC WEATHER GENERATOR FOR PRESERVING LOW-FREQUENCY OF CLIMATE VARIABILITY

Jie Chen[1], François P. Brissette[1], Robert Leconte[2]

1. Department of Construction Engineering, École de technologie supérieure, Université du Québec, 1100, rue Notre-Dame Ouest, Montréal, Québec, Canada, H3C 1K3.
2. Department of Civil Engineering, Université de Sherbrooke, 2500, boul. de l'Université, Sherbrooke, Québec, Canada, J1K 2R1

This article was published in the Journal of Hydrology in May, 2010.

1.1 Abstract

Weather generators are computer models that produce time series of meteorological data that have similar statistical properties as that of observed data. The past decade has seen a sharp and renewed increase in interest in weather generators, linked to their potential use in climate change studies. One appealing property of weather generators is their ability to rapidly produce time series of unlimited length, thus permitting impact studies of rare occurrences of meteorological variables. However, one problem with daily weather generators is that they underestimate monthly and inter-annual variances because they do not take into account the low-frequency component of climate variability. This research aims to present an approach for correcting the low-frequency variability of weather variables for weather generator and to assess its ability to reproduce key statistical parameters at the daily, monthly and yearly scales. The approach is applied to precipitation which is usually the variable displaying the largest inter-annual variability. The daily stochastic precipitation model is a Richardson-based weather generator that uses a first-order two-state Markov chain for precipitation occurrence and a gamma distribution for precipitation amounts. Low-frequency variability was modelled based on observed power spectra of monthly and annual time

series. Generation of synthetic monthly and yearly precipitation data was achieved by assigning random phases for each spectral component. This preserved the power spectra, variances and the autocorrelation functions at the monthly and annual scales. The link to daily parameters was established through linear functions. The quality of these corrections was assessed through direct and indirect validation tests, with the direct validation focusing on comparing the means, standard deviations and autocorrelations of different weather series. The results showed that standard deviations of both monthly and annual precipitations were produced almost exactly. The proposed method also preserved the autocorrelation of annual precipitation. The indirect validation involved modelling the discharge of a river basin using a hydrological model driven by different precipitation series. The results showed that the corrected weather series significantly improved the variability of simulated flow discharges at the monthly and annual scales compared to those simulated using the data generated by the standard weather generator.

Keywords: Weather generator; Precipitation; Low-frequency variability; Power Spectra.

1.2 Introduction

A stochastic weather generator is a computer algorithm that uses existing meteorological records to produce a long series of synthetic daily weather data. The statistical properties of the generated data are expected to be similar to those of the actual data for a specified site. Unlike historical weather records, which may have missing data, the weather generator output provides a complete record for any desired period of time, thus enhancing the use of continuous hydrologic models (Kevin et al., 2005). Moreover, it can be used to generate daily weather data for ungauged areas through spatial interpolation of model parameters from adjacent gauged sites (Baffaut et al., 1996). An important application of weather generators involves them serving as computationally inexpensive tools to produce multiple-year climate change scenarios at the daily time scale, which are used to assess the impact of future climate change (Semenov & Barrow, 1997; Wilks, 1992, 1999a; Pruski and Nearing, 2002; Zhang et al., 2004; Zhang, 2005; Zhang and Liu, 2005; Minville et al., 2008). Model parameters of the

weather generator can be readily manipulated to simulate arbitrary changes in mean and variance quantities for sensitivity analysis, or be deliberately modified to mimic changes in mean and variance as predicted by global climate models (GCMs) for impact assessment. Over the years, several weather generators have been developed, such as the Weather Generator (WGEN) (Richardson, 1982; Richardson and Wright, 1984), USCLIMATE (Hanson et al., 1994), Climate Generator (CLIGEN) (Nicks et al., 1995), Climate Generator (ClimGen) (Stockle et al., 1999), Long Ashton Research Station -Weather Generator (LARS-WG) (Semenov and Barrow, 2002), etc. While weather generators are good at preserving the precipitation quantity, they however underestimate low-frequency variations (e.g., Buishand, 1978; Johnson et al., 1996; Wilks, 1989,1999b; Gregory et al., 1993; Katz and Parlange, 1993, 1998; Hansen and Mavromatis, 2001; Zhang and Garbrecht, 2003; Chen et al, 2009). This underprediction results from the simplifying assumption that climate, and more specifically, the daily precipitation process, is stationary. These models do not explicitly take into account aspects of low-frequency variability such as decadal oscillations, and thus underestimate monthly and yearly variances.

The low-frequency variability of precipitation depends on the daily precipitation occurrence and intensity processes, especially the variance of the daily precipitation amounts and number of wet days. Several studies have attempted to solve this drawback with weather generators. Wilks (1999b) compared the variance of monthly precipitation generated by independent and identical (iid) Gamma distribution, Common-α Gamma distribution and Mixed Exponential distribution. The results showed that the iid Gamma distributions produced substantial overdispersion, and that the Common-a Gamma distribution brings only a slight improvement to this. By contrast, the overdispersion in wet-day variance produced by the Mixed Exponential distribution was substantially smaller, although not zero, meaning that using the Mixed Exponential distribution to represent wet-day precipitation amounts in stochastic weather models should bring about a substantial improvement in the simulation of inter-annual variability. Meanwhile, Wilks (1999b) also compared the variance of the number of wet days in each month among different precipitation occurrence models, including first-, second-, third- and hybrid-order Markov models and Negative Binomial and

Mixed Geometric distribution, as well as average percentage overdispersion of total monthly precipitation, for all combinations of precipitation occurrence models and precipitation intensity models. The results demonstrated that none of the combinations achieved complete recovery of the observed variance in monthly total precipitation, although increasingly complex component models did succeed in reducing the overdispersion - or discrepancy - between the synthetic and observed variability. This was unsatisfactory because although the complexity of the models was increased, it still did not take into account the low-frequency component of climate variability. These simple stationary models (whose statistics do not change from month to month and from year to year) cannot fully reproduce the variability of a nonstationary climate, which therefore makes the introduction of some degree of nonstationarity into these models appropriate.

Hansen and Mavromatis (2001) attempted to improve inter-annual variability characteristics by perturbing monthly parameters using a low-frequency stochastic model, and evaluated the effectiveness of the low-frequency component on low-frequency variability of the generated monthly climate at 25 locations in the continental USA. The results indicated that for monthly precipitation, the low-frequency correction reduced total error and eliminated negative bias of inter-annual variability, and reduced the number of station-months with significant differences between observed and generated inter-annual variability, but it over-represented the variability of precipitation frequency.

Dubrovsky et al. (2004) applied the monthly generator (based on a first-order autoregressive model) to fit the low-frequency variability based on the daily WGEN-like weather generator, Met & Roll. The results demonstrated that conditioning the daily generator on a monthly generator has the most positive effect, especially on the output of a hydrological model, and the variability of the monthly streamflow characteristics was better simulated. However, this method still could not reproduce the observed standard deviations and autocorrelations of monthly and annual precipitations exactly, because it did not specifically consider the inter-annual variability, thus indicating that schemes for correcting monthly variability have limited effect on the annual scale.

Wang and Nathan (2007) also provided a method for coupling daily and monthly time scales in the stochastic generation of rainfall series. The key feature of the method involves first generating two similar time series, one preserving key statistical properties at a finer time scale and the other at a coarser time scale. The finer time scale series is then adjusted to make it consistent with the coarser one. This method appears to perform well in that it satisfactorily preserved some key statistical properties at daily, monthly and even yearly scales. However, it was only tested for the coefficient of variation on Australian weather data. Other statistics, such as the autocorrelation of annual precipitation, are important for some applications.

Accordingly, this research aimed to present an approach for correcting the low-frequency variability of precipitation for the weather generator, assess its ability to reproduce key statistical parameters, and to compare it against Wang and Nathan's method.

1.3 Materials and methods

1.3.1 Introduction of a stochastic weather generator

WeaGETS (Weather Generator École de Technologie Supérieure), which is a WGEN-like three-variate (precipitation, maximum and minimum air temperature) single-site stochastic weather generator programmed in Matlab, was used as the basic stochastic weather generator in this study. This paper only focuses on precipitation generation.

The precipitation component of WeaGETS is a Markov chain for occurrence and a gamma distribution for quantity. A first-order two-state Markov chain is used to generate the occurrence of wet or dry days. The probability of precipitation on a given day is based on the wet or dry status of the previous day, which can be defined in terms of the two transition probabilities:

$$P01=\Pr\{\text{precipitation on day t} \mid \text{no precipitation on day t-1}\} \quad (1.1a)$$

$$P11=\Pr\{\text{precipitation on day t} \mid \text{precipitation on day t-1}\} \quad (1.1b)$$

Since precipitation either occurs or does not occur on a given day, the two complementary transition probabilities are P00=1-P01 and P10=1-P11.

For a predicted rain day, a two-parameter Gamma distribution is used to generate daily precipitation depth (Richardson, 1981). The probability density function for this distribution is:

$$f(x) = \frac{(x/\beta)^{\alpha-1} \exp[-x/\beta]}{\beta\Gamma(\alpha)} \tag{1.2}$$

where the variable x is the daily precipitation depth, α and β are the two distribution parameters, and $\Gamma(\alpha)$ represents the gamma function evaluated at α.

1.3.2 Correction of low-frequency variability and validations

The aim of the model is to specifically account for low-frequency variability by correcting daily precipitation at the monthly and yearly scales, using power spectra of observed time series at the same scales. The power spectra are computed using Fast Fourier Transforms (FFT). Wang and Nathan's (2007) method, which is arguably the best available for dealing with the low-frequency problem, was also programmed and used as a comparison method.

The key feature of Wang and Nathan's method is that it requires that we first generate two similar time series, one preserving key statistical properties at a finer time scale and the other at a coarser time scale. The resemblance between the two series is achieved by using the finer time scale model as a building block for the coarser time scale model, and then using the same sequence of non-exceedance probabilities for the random elements as inputs to both models. The preservation of the key statistical properties of the two series at their appropriate time scales is achieved by using different sets of estimated parameters for the two models. A coupling transformation technique introduced by Koutsoyiannis (2001, 2003) is then applied to modify the finer time scale series so that this series becomes consistent with the coarser

time scale series. This transformation technique is based on a developed generalized mathematical proposition, which ensures preservation of marginal and joint second-order statistics and of linear relationships between lower- and higher-level processes. Wang and Nathan also used a basic weather generator based on WGEN (Richardson, 1984), but with the exception that its parameters are not smoothed with Fourier harmonics. To allow for a proper comparison, WeaGETS was also used without smoothing. The smoothing process eliminates sharp parameter transitions between computing periods that may occur due to outliers (such as extreme precipitation), especially for shorter time series. In either case, the weather generator should reproduce the exact monthly targeted precipitation mean (either smoothed or raw). WeaGETS parameters are computed every two weeks.

The use of FFT is widespread in engineering and signal processing, and it stems from the concept that any discrete signal (such as yearly total precipitation over a basin) can be exactly represented by a summation of sine waves with magnitude S and phase φ. Following the FFT, each sine wave component is expressed as a complex number:

$$C = X + i * Y \qquad (i = \sqrt{-1}) \tag{1.3}$$

from which the magnitude S and phase φ can be extracted with the following equations:

$$S = |C| = \sqrt{X^2 + Y^2} \tag{1.4}$$

$$\phi = \tan^{-1}(Y / X) \tag{1.5}$$

The variance and phase of each component can be modified and returned back in complex form with the following equation, and then returned back to the time domain with an inverse FFT:

$$C = S * e^{(i*\phi)} \tag{1.6}$$

By modifying the phase of each component and reverting to the time domain, a new signal with an identical power spectrum (and variance) can be created. As such, low-frequency components (such as decadal variability) will be preserved in the new signal. This property is used to modify the daily sequences from the weather generator in order to correct for the underestimated variances at the monthly and inter-annual scales. Throughout this paper, this is referred to as the spectral correction method/approach, and it is comprised of five steps:

1) A daily precipitation series was generated by WeaGETS using parameters derived from the observed daily precipitation series. In this study, the length of the generated series was 20 times that of the observed one, which allowed a precise evaluation of the statistical parameters of the synthetic time series.

2) Monthly variability was modeled based on a power spectrum using FFT for each monthly series. The generation of a new power spectrum for monthly precipitation was achieved by assigning random phases to each spectral component and transferring back to the time domain, as discussed above. Random phases were chosen from a uniform distribution over the range $[0, 2\pi]$. Since the length of generated series was 20 times of the observed one, random phases were drawn for each 20-year simulation, and subsequently integrated together. The use of the same random phase for each 20-year simulation would have resulted in identical time series.

3) The daily precipitation series generated in step (1) was adjusted incrementally. The series of the monthly precipitation derived from the WeaGETS-generated daily series (step (1)) were adjusted to the monthly series generated in step (2), using linear functions. In this adjustment procedure, the value of the increment applied to the daily series was the same for all days within a month. No adjustment was made to the precipitation occurrence.

4) Following steps (1) to (3), the standard deviation of each monthly precipitation would be corrected exactly, but that of yearly precipitation would still be lower than the observed one, since, as discussed earlier, correcting for monthly variability has limited effect on

inter-annual variability. Therefore, in this step, an additional correction for inter-annual variability was made following the procedure outlined in steps (2) and (3). This correction is made on the data that was corrected for monthly variability, not on the original data.

5) Following step (4), the variance of yearly precipitation was corrected exactly. However, this resulted in an overestimation of the variance at the monthly scale, which was previously perfectly reproduced after step (3). This indicates that the monthly precipitation variances are affected by variability at both the monthly and annual scales. Following the correction of the inter-annual variability, an additional correction was made at the monthly scale. Thus, steps (2) to (4) were repeated in an iterative scheme in order to find the correct initial monthly corrections that would result in the best reproduction of monthly precipitation variance once the yearly correction was applied. The iterative scheme is needed because correcting at either scale influences the other (correcting at the monthly scale affects the yearly scale and vice-versa).

The quality of the corrections was assessed through direct and indirect validation tests. The direct validation tries to answer the question as to how the corrected weather series resembles the observed one. It focuses on the reproduction of characteristics representing the distribution of the variables, especially standard deviations of the monthly and yearly precipitations. In this study, the means and standard deviations of WeaGETS-generated, spectral correction and Wang and Nathan's methods corrected monthly, and yearly precipitations relative to observed data were compared. Similarly, autocorrelations of annual precipitations were also compared. Since precipitation amounts are known not to have normal distributions, instead of t- and F-tests, nonparametric Mann-Whitney and squared ranks tests (Conover, 1999) were conducted to test the equality of the means and standard deviations between observed and synthesized monthly and annual precipitation series. In addition, nonparametric Kolmogorov-Smirnov (K-S) tests, which apply to any type of distributions, were used to test the equality of the population distributions of observed versus synthesized data. All the tests were two-tailed, and a significance level of P=0.05 was used.

P=0.05 refers to a Type 1 error, and the larger the P value, the more likely it is for the two series to be similar, and vice versa. The indirect validation tries to answer the question as to whether the corrected precipitation series is applicable in a given application. In this study, the indirect validation is done by comparing the statistical properties of output characteristics from a hydrological model driven by different precipitation series generated by WeaGETS, spectral correction and Wang and Nathan's approaches. Like the direct validation, the means and standard deviations of monthly and annual discharges simulated using synthesized precipitation series were compared to those of the observed series. Nonparametric Mann-Whitney, squared ranks and K-S tests were conducted to test the equality of the mean, standard deviation and distribution for monthly and annual discharges, respectively. The frequency distributions of mean and maximum annual discharges simulated using the observed and synthesized precipitation series were also compared.

1.3.3 Hydrological model

Indirect validation was based on modeling the discharge of a river basin using the hydrological model HSAMI, which was developed by Hydro-Québec, and which has been used to forecast natural inflows for over 20 years now. It is used by Hydro-Québec for hourly and daily forecasting of natural inflows on 84 watersheds with surface areas ranging from 160 km^2 to 69195 km^2, and Hydro-Québec's total installed hydropower capacities on these basins exceed 40GW. HSAMI is a 23-parameter, lumped, conceptual, rainfall-runoff model. Two parameters account for evapotranspiration, 6 for snowmelt, 10 for vertical water movement, and 5 for horizontal water movement. Vertical flows are simulated with 4 interconnected linear reservoirs (snow on the ground, surface water, unsaturated and saturated zones). Horizontal flows are filtered through 2 hydrograms and one linear reservoir. The model takes into account snow accumulation, snowmelt, soil freezing/thawing and evapotranspiration.

The basin-averaged minimum required daily input data for the model are: minimum and maximum temperatures, and liquid and solid precipitations. Cloud cover fraction and snow water equivalent can also be used as inputs, if available. A natural inflow or discharge time

series is also needed for proper calibration/validation. For this study, ten years of data was used for model calibration (1958-1968), and 34 years for validation (1969-2002). Automatic calibration of the model was performed using the shuffled complex evolution (SCE-UA) algorithm (Duan et al., 1992). The optimal combination of parameters was chosen based on the Nash-Sutcliffe criteria for both calibration and validation runs. The chosen set of parameters yielded values of the Nash-Sutcliffe criteria of 0.67 for calibration and 0.64 for validation. The relatively low values of the Nash-Sutcliffe criteria are linked due to the absence of weather stations in the southern portion of the basin and not to the hydrological model which performs extremely well in several other similar basins in Quebec.

Since the focus of this research was on the development and demonstration of an approach for correcting low-frequency variability for the weather generator, details concerning the calibration and validation of a hydrological model are not discussed here.

1.3.4 Meteorological and hydrological data

The meteorological data, including daily precipitation, maximum and minimum air temperatures of 6 stations dispersed across Canada, were used in this study. Basic information, including average annual precipitation, longitude, latitude, elevation, and record duration for these stations is given in table 1.1. Average annual precipitation at these stations varied from 268.8 mm in Yellowknife to 1827.3 mm in Langara, which adequately represents the natural climate variability in Canada.

The indirect validation is based on 44 years (1959-2002) of discharge at the Châteauguay River Basin. This unregulated river basin is located in southwest Quebec, Canada, and covers a drainage area of 2543 km^2. The basin overlaps the Canadian and US borders (60% of the basin is in Canada and 40% in the US). The average annual river discharge of the river at the watershed outlet is 40 m^3/sec., but may exceed 1000 m^3/sec. during the spring discharge. Daily area-averaged meteorological data used to estimate parameters for the weather generator and drive the hydrological model was derived from a network of 6 stations

distributed throughout and around the catchment. The discharge was derived from one hydrometric station near the basin outlet.

Table 1.1 Location, record period, and average annual precipitation for 6 stations

Region	Station name	Latitude (°N)	Longitude (°W)	Elevation (m)	Records of daily precip	Precipitation (mm)
Queen Charlotte Islands	Langara	54.25	133.05	14	1937-2006 (70)	1827.3
Middle St. Lawrence River Basin	Dorval	45.47	73.75	36	1943-1994 (52)	953.4
Vancouver Island	Victoria	48.65	123.32	19	1941-2006 (66)	871.2
Nelson and Churchill River Basin	Churchill	58.73	94.05	29	1947-2006 (60)	439.1
Okanagan River Basin	Vernon Goldstream Ranch	50.23	119.20	482	1907-1996 (90)	413.2
Mackenzie	Yellowknife	62.47	114.43	206	1945-2002 (58)	268.8

1.4 Results

1.4.1 Direct validation

Figures 1.1a and 1.1b present the time series and power spectra of observed annual precipitation at the Victoria station. By assigning random phases to each component of the power spectrum and reverting to the time domain, a new signal (annual precipitation) with an

identical power spectrum (and variance) can be created. The annual precipitation time series created (figure 1.1c) and observed data have the same power spectrum as shown in figure 1.1d.

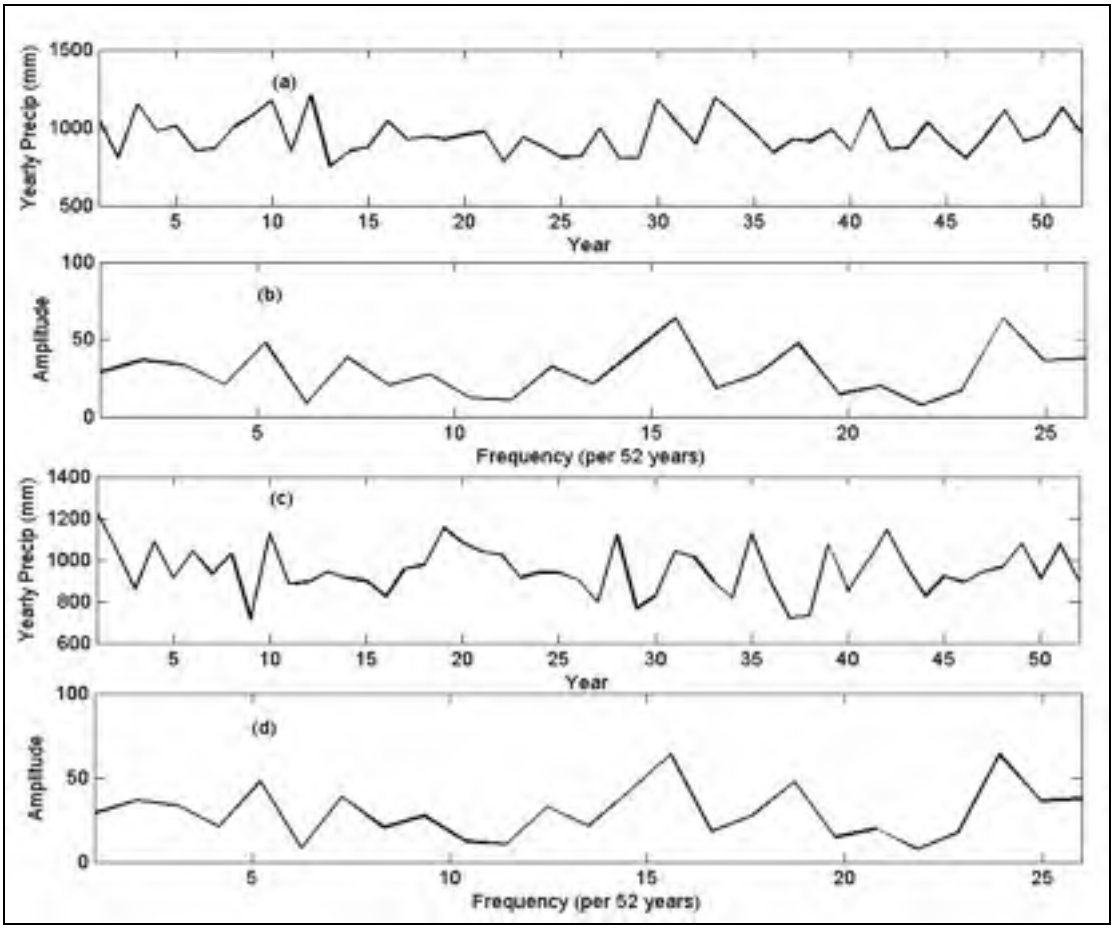

Figure 1.1 Time series ((a) and (c)) and their power spectra ((b) and (d)) of averaged annual precipitation at the Victoria station.

WeaGETS reproduced monthly and annual averaged precipitations very well (figure 1.2), and Mann-Whitney tests showed that there is no significant difference between observed and WeaGETS-generated data at the P=0.05 level (table 1.2). It indicates that the Markov chain and gamma distribution are capable of simulating the precipitation occurrence and quantity.

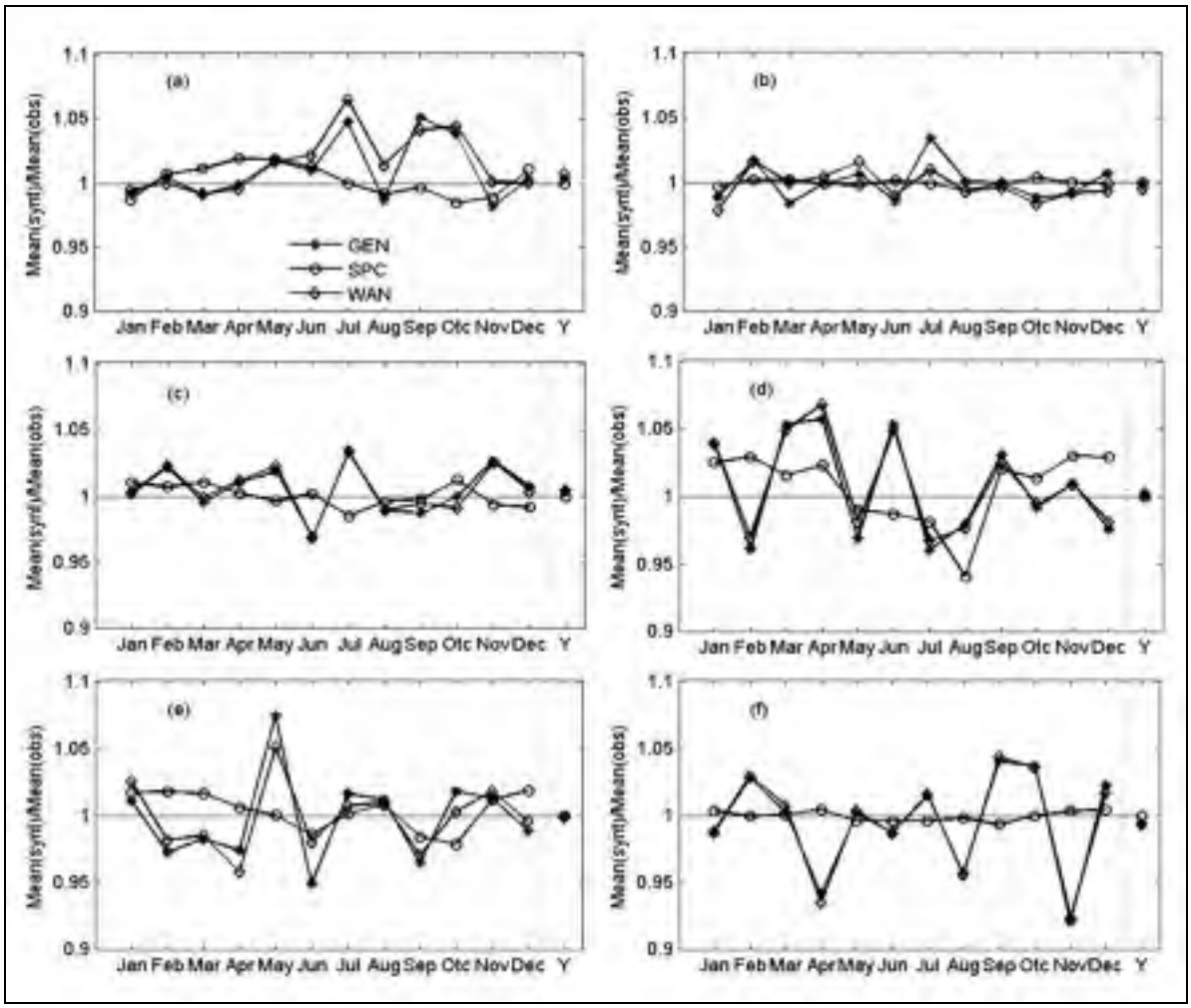

Figure 1.2 The ratios of the means of monthly and annual precipitation derived from the synthesized weather series (synt) to the means derived from the observed series (obs) for 6 stations. The synthesized precipitation series include the data generated by WeaGETS (GEN), corrected using the spectral correction approach (SPC) and Wang and Nathan's method (WAN). The stations include (a) Victoria, (b) Langara, (c) Vernon Goldstream Ranch, (d) Yellowknife, (e) Churchill, and (f) Dorval.

Wang and Nathan's method had little effect on simulating the mean of precipitation at the monthly and yearly scales (figure 1.2). All the Mann-Whitney tests between observed and corrected data were insignificant at P=0.05. Moreover, the spectral correction method also produced the mean of precipitation very well, and it was indeed better than that corrected through Wang and Nathan's method and generated by WeaGETS with precipitations

simulated almost exactly for some stations, such as the Langara and Dorval stations. All differences can be attributed to the stochastic nature of precipitation generation.

The weather generator underestimated the variability of monthly precipitation, which is represented by its standard deviation as shown in figure 1.3. The squared ranks tests further showed that standard deviations of monthly precipitations were poorly reproduced, with 22 out of 72 months for 6 stations being different at the P=0.05 level (table 1.2). However, Wang and Nathan's method performed much better at preserving the monthly variability for all months and stations. The squared ranks tests showed that standard deviations were significantly different at P=0.05 for only 1 out of 72 months. Moreover, the spectral correction approach significantly corrected the monthly standard deviations for all months and stations. It reproduced the standard deviation of observed monthly precipitation almost exactly. The squared ranks tests showed that there were no significant differences at P=0.05 for all 72 months on 6 stations.

As with the underestimation of monthly precipitation, the WeaGETS also under predicted the standard deviation of annual precipitation. The squared ranks test showed significant differences at P=0.05 for 5 out of 6 annual precipitation series. Wang and Nathan's method had some effects, but the standard deviation of annual precipitation was overestimated for some cases, such as the Victoria, Langara and Churchill stations. The squared ranks tests showed that there were significant differences at P=0.05 for 2 out of 6 stations. The spectral correction method preserved the standard deviations of annual precipitation exactly. All the squared ranks tests were insignificant at the P=0.05 level.

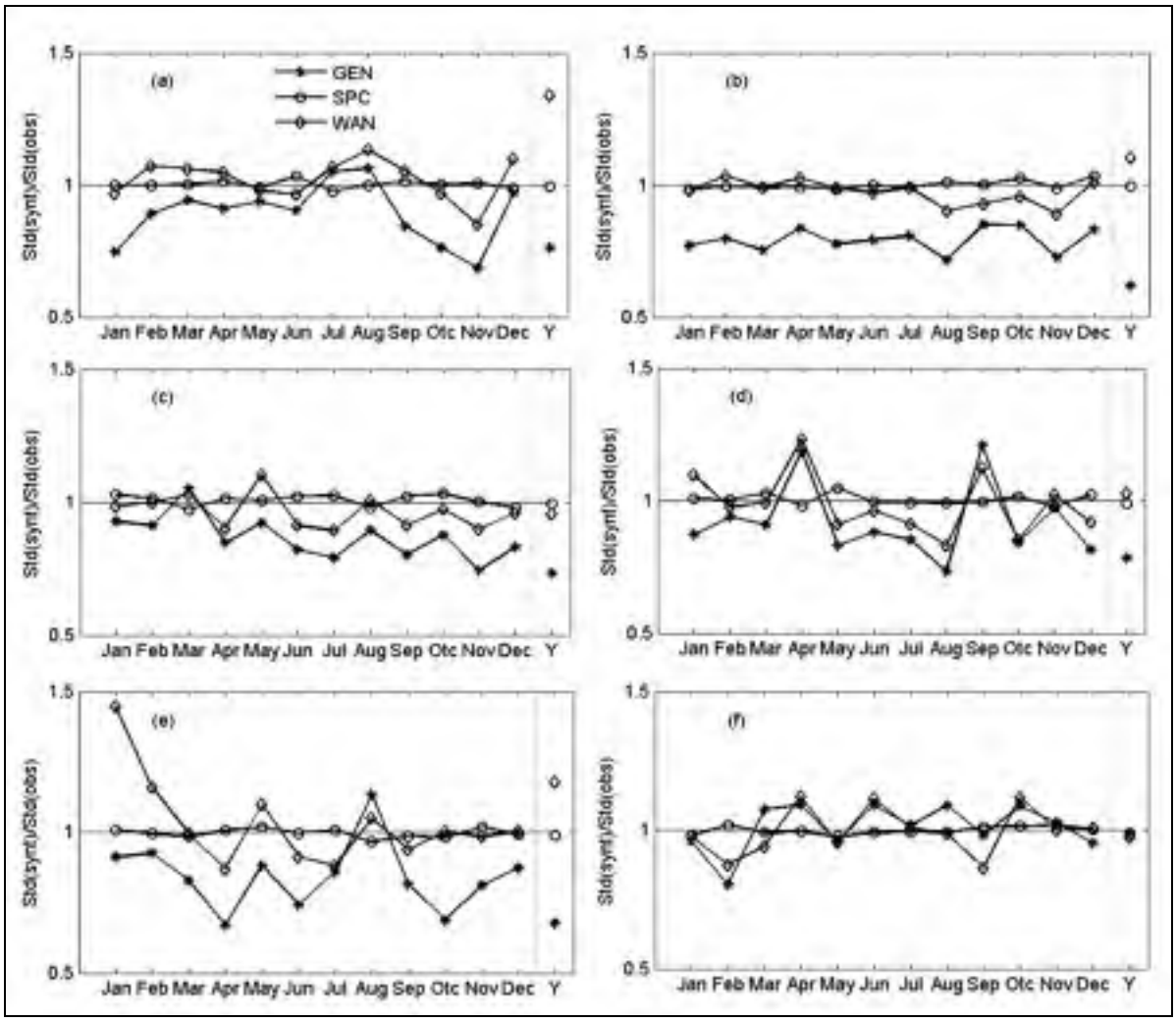

Figure 1.3 The ratios of the standard deviations of monthly and annual precipitations derived from the synthesized weather series (synt) to the standard deviations derived from the observed series (obs) for 6 stations. The synthesized precipitation series include the data generated by WeaGETS (GEN), corrected using the spectral correction (SPC) and Wang and Nathan's (WAN) methods. The stations include (a) Victoria, (b) Langara, (c) Vernon Goldstream Ranch, (d) Yellowknife, (e) Churchill, and (f) Dorval.

The WeaGETS-generated precipitation had few months which passed the K-S tests (table 1.2). Both correction approaches could improve the distribution of the monthly precipitation to some degree. The K-S tests showed that the distributions of monthly observed precipitations were statistically different for only 1 out 72 months from Wang and Nathan's method corrected data, and for no month from the spectral correction data, respectively. The

distribution of annual precipitation between WeaGETS-generated and observed data was significantly different for 2 out of 6 stations at the P=0.05 level. Both correction methods significantly improved the distributions. The K-S tests showed that there were no significant differences between the distributions of WeaGETS-generated and both corrected yearly precipitations at the P=0.05 level.

The observed annual precipitation autocorrelation functions presented in figure 1.4 display clear trends, which indicate that wetter and dryer years are not random, but rather, come in series, as was shown by the power spectra of annual precipitation series. For several hydrologic applications such as drought studies, it is important to be able to reproduce these successions of dryer/wetter years. The results for autocorrelation of precipitation at the monthly scale were similar and were not shown. WeaGETS could not preserve the autocorrelation function because it does not take into account the low-frequency component of climate variability. Although Wang and Nathan's method reproduced the standard deviations of monthly and annual precipitation well, it did not preserve the observed autocorrelation, while the spectral correction method successfully reproduced the observed autocorrelation for all 6 stations.

Table 1.2 The numbers of monthly and annual precipitation series over 72 months and 6 stations that rejected the Mann-Whitney, squared ranks and K-S tests; the synthesized data include WeaGETS-generated (GEN), spectral correction (SPC) and Wang and Nathan's methods corrected (WAN)

	Monthly			**Yearly**		
	Mann-Whitney test	**Squared ranks tests**	**K-S test**	**Mann-Whitney test**	**Squared ranks tests**	**K-S test**
GEN	0/72	22/72	4/72	0/6	5/6	2/6
SPC	0/72	0/72	1/72	0/6	0/6	0/6
WAN	0/48	1/72	0/72	0/6	2/6	0/6

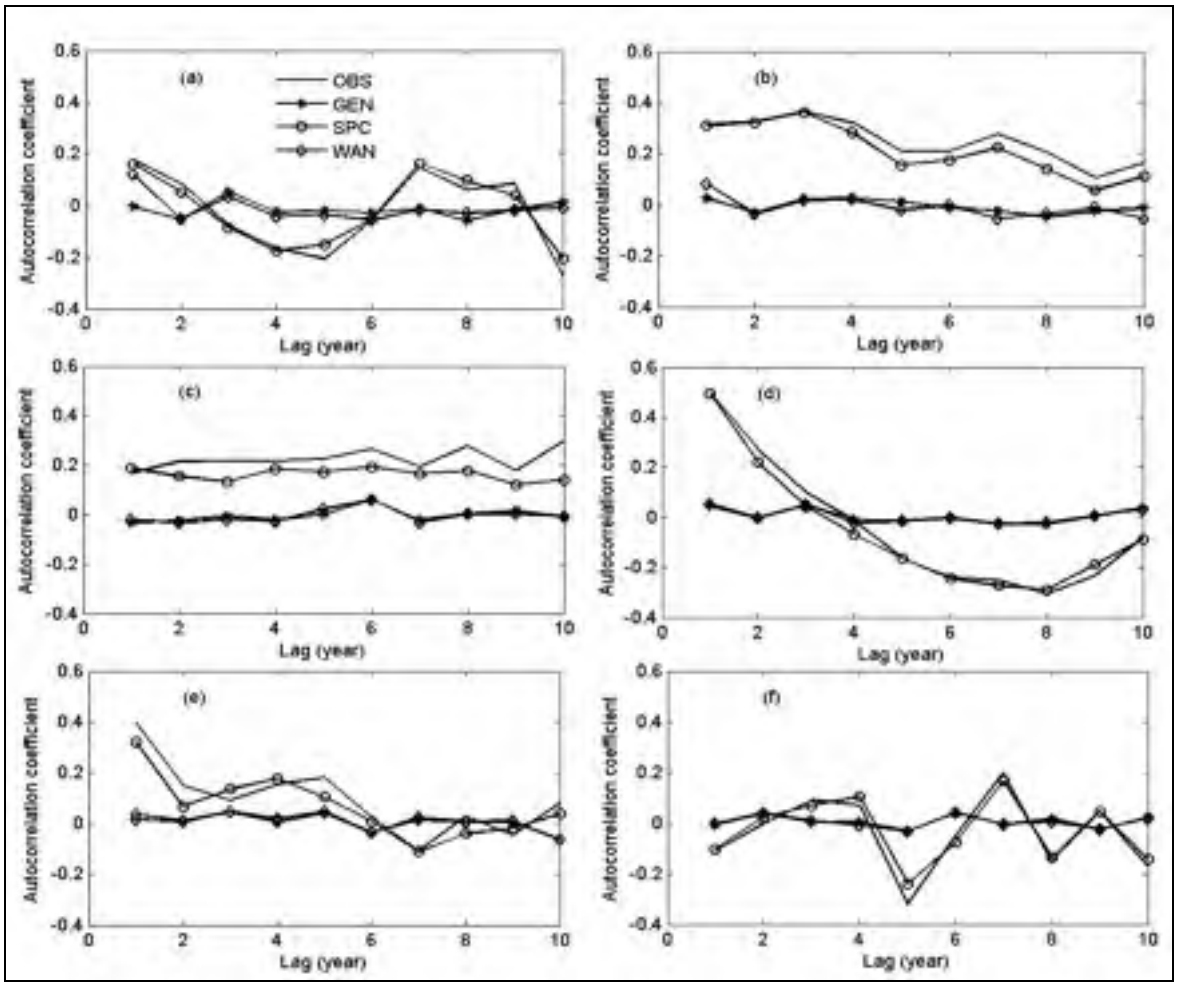

Figure 1.4 10 years lagged autocorrelation of observed (OBS), WeaGETS-generated (GEN), spectral correction (SPC) and Wang and Nathan's methods (WAN) corrected annual precipitations for 6 stations. The stations include (a) Victoria, (b) Langara, (c) Vernon Goldstream Ranch, (d) Yellowknife, (e) Churchill, and (f) Dorval.

1.4.2 Indirect validation

The indirect validation was based on modeling of the discharge of the Châteauguay River Basin using the hydrological model, HSAMI, driven by different precipitation series (observed and synthetized). In order to avoid any bias resulting from the hydrological model when comparing different methods, the control period of discharge is represented by modeled data, and not by an actual observed discharge. Further, for the control period, maximum and minimum air temperatures used to simulate the discharge were generated by

the weather generator, rather than using observed temperatures. Thus, all differences were solely attributed to the precipitation correction scheme. The hydrological model was then run with four time-series: observed, WeaGETS-generated, modified using spectral correction, and using Wang and Nathan's method.

Figure 1.5 presents the averaged hydrographs simulated with the four time series for the Châteauguay River Basin. Each synthesized weather data could properly simulate the averaged annual discharge. Moreover, not many differences existed among the discharges simulated using synthesized weather data, but the hydrographs derived from synthesized weather data were smoother because they were produced using longer time series, further indicating that the mean precipitation properties are well reproduced by the weather generator.

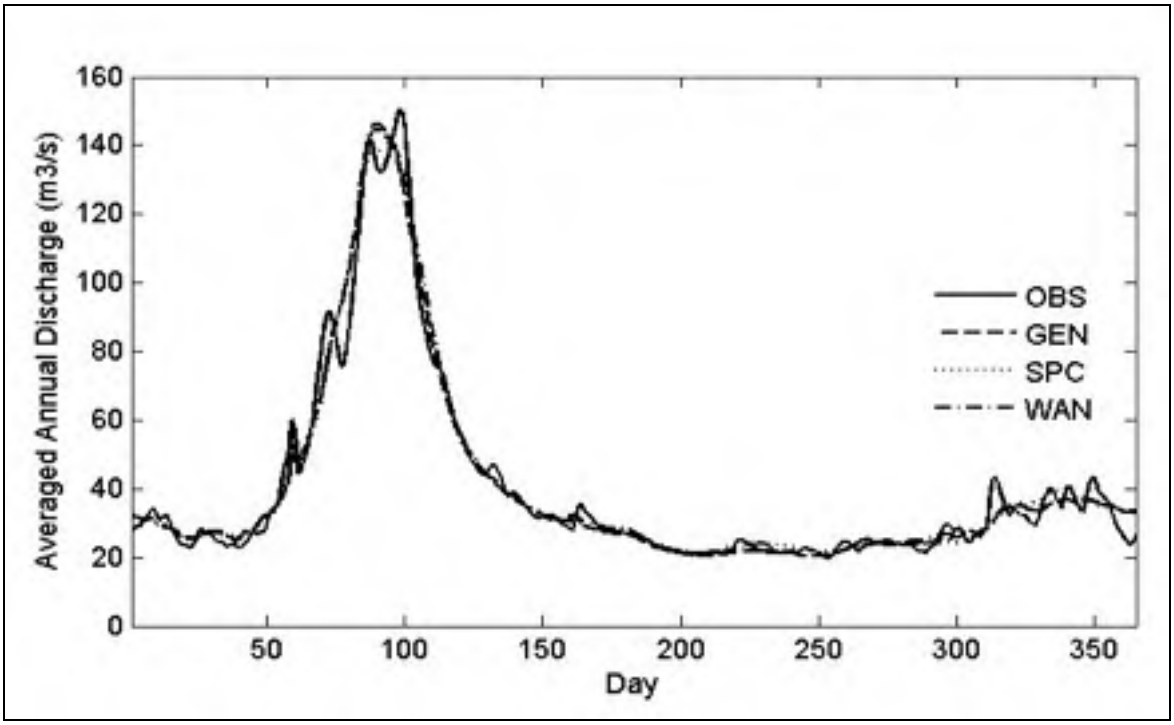

Figure 1.5 Averaged hydrographs simulated using the observed (OBS), WeaGETS-generated (GEN), and spectral correction (SPC) and Wang and Nathan's (WAN) methods corrected precipitation series for the Châteauguay river basin.

Figures 1.6a and 1.6b present the ratios of means and standard deviations of monthly and annual precipitations derived from the synthesized weather series to those derived from the observed series. The results again show that WeaGETS significantly underestimated the standard deviations of monthly and annual precipitation, while the two corrected series reproduced the standard deviations very well; indeed both corrected series reproduced the standard deviation of yearly precipitation almost exactly. The observed and synthesized weather series were used to drive the hydrologic model to simulate the discharge.

The results show that WeaGETS-generated data properly simulated the means of monthly and annual discharges although there are some fluctuations (figure 1.6c). All the Mann-Whitney tests between discharges simulated using observed and WeaGEST-generated weather series were insignificant at P=0.05 (table 1.3).

The standard deviation of discharge simulated using WeaGETS-generated data was underestimated (figure 1.6d). The squared ranks tests showed that there were significant differences at P=0.05 for 3 out of 12 months between those simulated using observed data and those simulated using WeaGETS-generated weather data. However, the standard deviation of monthly discharge simulated using the data corrected by spectral correction method was more or less improved. The squared ranks tests showed significant differences for only 1 out of 12 months at the P=0.05 level. The monthly discharges simulated using precipitation corrected by Wang and Nathan's method were also significantly improved. None of the squared ranks tests was significantly different at P=0.05 for all 12 months. Figure 1.6d shows that both correction methods result in improvement for all months, with the exception of January and February discharges, which are similar to those seen in WeaGETS-derived data. That is because the Châteauguay River Basin was covered with snow during these months, and the variability of monthly precipitation had little effect on discharges, and furthermore, discharge is also typically very low during these months. There was a significant difference between annual discharges simulated using the observed and WeaGETS-generated weather series, but the spectral correction and Wang and Nathan's

methods simulated the standard deviation of yearly discharge very well. The squared ranks tests for standard deviations were insignificant at the P=0.05 level.

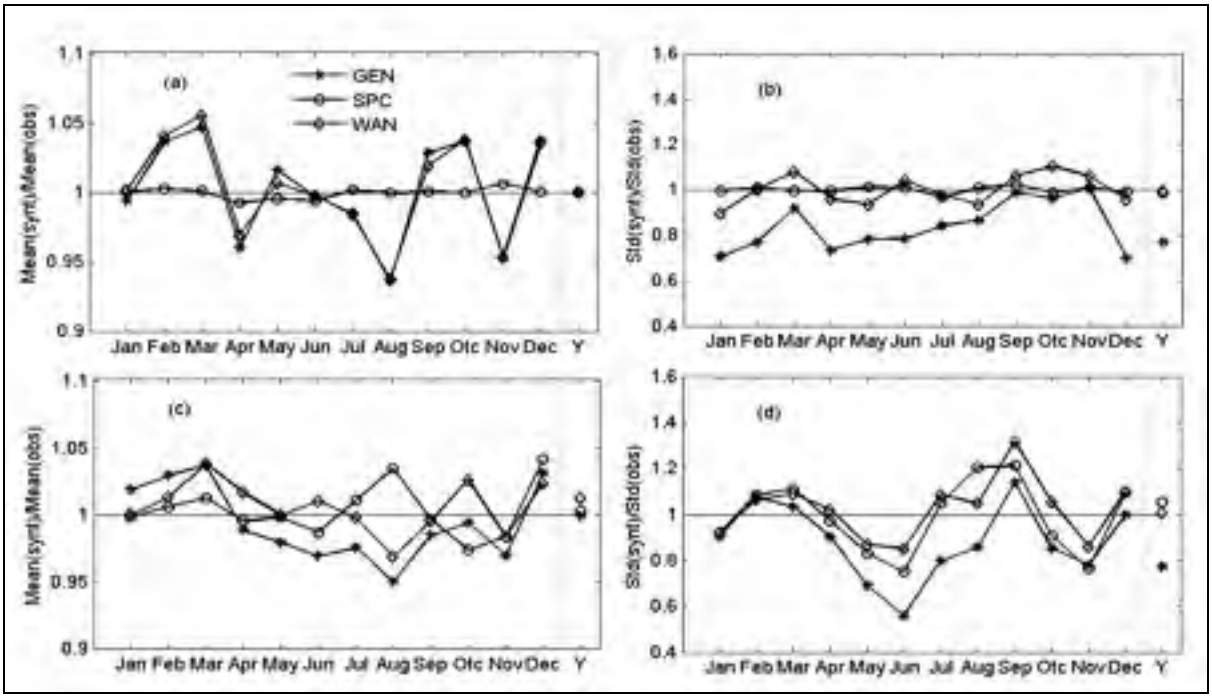

Figure 1.6 Ratios of means (a) and standard deviations (b) of monthly and annual precipitations derived from the synthesized weather series (synt) to the means and standard deviations derived from the observed series (obs); and ratios of the means (c) and standard deviations (d) of discharges simulated with the synthesized precipitation series (synt) to those simulated with the observed precipitation series (obs) at the Châteauguay River Basin; the synthesized precipitation series include WeaGETS-generated (GEN), spectral correction (SPC) and Wang and Nathan's (WAN) methods corrected data.

The K-S tests showed that distributions of discharges were not different at P=0.05 between those simulated with observed and with each synthesized weather series at the monthly and yearly scales (table 1.3).

Table 1.3 The numbers of monthly and annual discharge series over 12 months and 1 yearly series that rejected the Mann-Whitney, squared ranks and K-S tests; the synthesized data include WeaGETS-generated (GEN), spectral correction (SPC) and Wang and Nathan's (WAN) methods corrected.

	Monthly			**Yearly**		
	Mann-Whitney test	**Squared ranks tests**	**K-S test**	**Mann-Whitney test**	**Squared ranks tests**	**K-S test**
GEN	0/12	3/12	0/12	0/1	1/1	0/1
SPC	0/12	1/12	0/12	0/1	0/1	0/1
WAN	0/12	0/12	0/12	0/1	0/1	0/1

WeaGETS significantly underestimated the frequency distribution of the mean annual discharge (figure 1.7a). However, those simulated using precipitations corrected through the spectral correction and Wang and Nathan's method were significantly improved, although they were somewhat overestimated. Similarly to the simulation of averaged annual discharge, the maximum annual discharge from spring snowmelt (from February 1st to late May) simulated using WeaGETS-generated data was significantly underestimated (figure 1.7b), but was improved by the corrected weather data. However, they were still lower than the observed ones.

Similarly to the changing trends in yearly precipitation, the flood and drought years are also not random, but rather, come in a series, as shown by the autocorrelation functions of mean yearly discharge (figure 1.8). These provide the decision basis for agricultural management and hydrologic applications. However, the mean yearly discharges simulated using WeaGETS-generated precipitations and with precipitations corrected through Wang and Nathan's method could not preserve the observed autocorrelation functions. That was because the WeaGETS and Wang and Nathan's method could not reproduce the observed autocorrelation functions of averaged yearly precipitations. The spectral correction method successfully reproduced the observed autocorrelation, although not exactly.

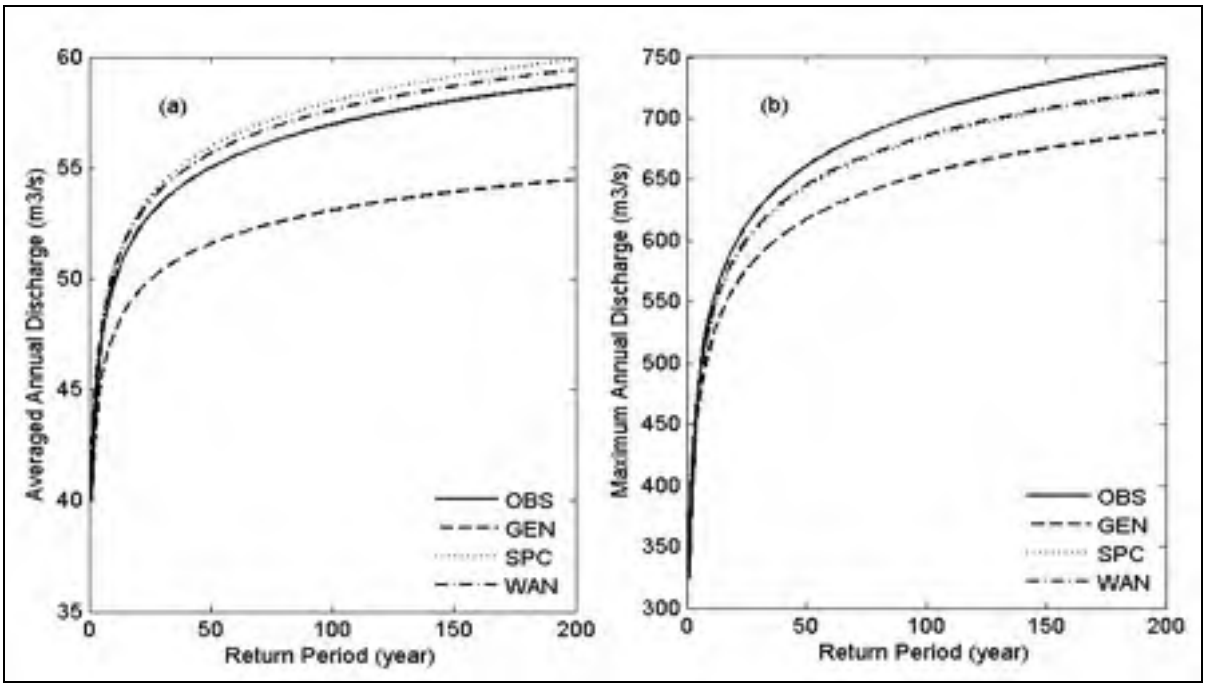

Figure 1.7 Frequencies of mean and maximum annual discharges simulated with the observed, WeaGETS-generated (GEN), and spectral correction (SPC) and Wang and Nathan's (WAN) methods corrected precipitation series.

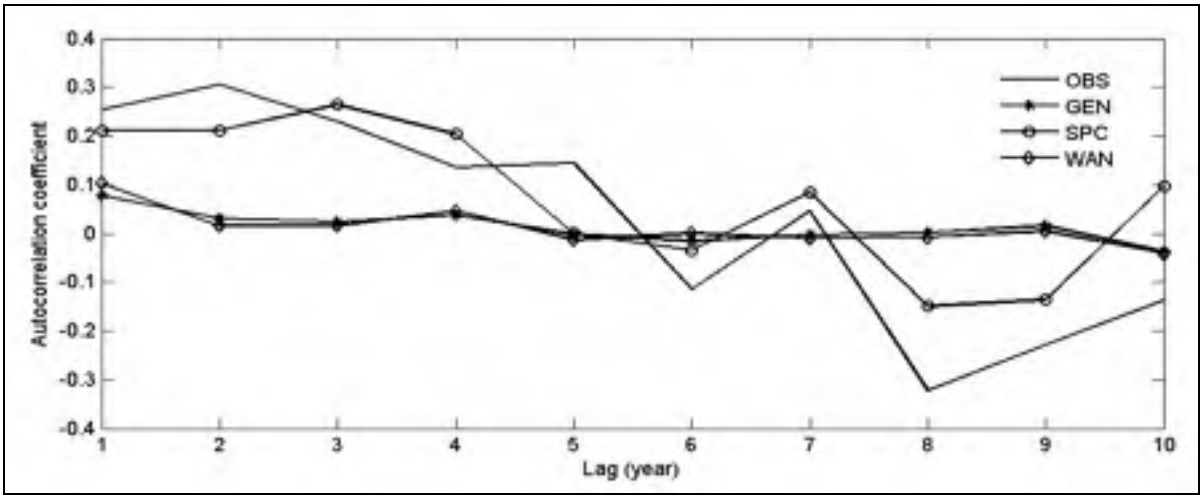

Figure 1.8 10 years lagged autocorrelation of averaged yearly discharges simulated with the observed (OBS), WeaGETS-generated (GEN), spectral correction (SPC) and Wang and Nathan's methods (WAN) corrected precipitations series.

1.5 Discussion and Conclusions

An approach based on a power spectrum for coupling time scales of stochastic time series models is presented in this research. This approach was compared with an existing method (Wang and Nathan's (2007) method) on the basis of how well the low-frequency variability of precipitation is preserved. The ability of each method to simulate the discharge of a river basin using a hydrological model was also evaluated. Low-frequency variability was first modeled using an FFT-derived power spectrum. Generation of monthly and yearly precipitation data was achieved by assigning random phases for each spectral component, which preserved the power spectrum and variances as well as the autocorrelation function. The link to daily parameters was established through linear functions, and direct and indirect validation experiments were conducted to examine the effects of those corrections. In the direct validation experiments, the statistics derived from WeaGETS-generated, spectral correction and Wang and Nathan's methods corrected precipitation series were compared with those derived from the observed series. In the indirect validation experiments, the discharge simulated by a hydrological model driven by observed and synthesized weather data were examined.

Direct validation experiments showed that the spectral correction approach reproduced the observed standard deviations of monthly and annual precipitations almost exactly. Although results were not presented, it should be noted that the standard deviation of seasonal precipitation was also significantly improved, although we did not specifically correct for it. Seasonal variance was however not as well reproduced as that of the monthly and yearly scales, which indicates that it may be useful to add the seasonal scale in the correction scheme. More importantly, the spectral correction approach could reproduce the observed autocorrelation of annual precipitation. Wang and Nathan's method also significantly improved the standard deviations of precipitation at monthly and yearly scales, but not as well, especially for annual precipitation. This is because their method only considered the variability and autocorrelation at the monthly scale, whereas the spectral correction approach considered both time scales.

The results of the indirect validation indicate that the modifications of the weather generator improved the reliability of the statistics derived from the output of the hydrological model. The precipitation series corrected through the spectral correction approach improved the statistical properties of the discharge derived from driving the hydrological model. The standard deviations of monthly and yearly discharges were better reproduced, indicating that preserving the observed low-frequency variability is very important in the simulation of discharge when used with synthetic stochastic weather series. The frequencies of mean and maximum annual discharges simulated using the spectral correction approach corrected precipitation series were also obvious improved. Wang and Nathan's method corrected precipitation series also significantly improved the simulation of discharges' variability at monthly and yearly scales compare with those simulated using WeaGETS-generated data. Moreover, the spectral correction method successfully reproduced the observed autocorrelation of averaged yearly discharge, unlike WeaGETS and Wang and Nathan's method, because the periodicities of the streamflow characteristics, i.e., timing and magnitude of peak flow and specific runoff, are related to the variation in the autocorrelation of the time-series of precipitation (Fassnacht, 2006). The spectral correction method preserved the observed autocorrelation functions of mean yearly precipitation, so it could reproduce the autocorrelation of averaged yearly discharge. This is very important in hydrologic applications. It should be noted that although the variability of monthly and yearly precipitations and autocorrelation were reproduced almost exactly by the spectral correction method, the variability of monthly discharge was not as good as that of precipitation. There may be three reasons for this. Firstly, as mentioned above, the corrections of monthly and inter-annual variability has limited effect on other time scales, and so the corrected precipitation series may still not be as good as the observed data. Secondly, the discharge was affected not only by precipitation, but also by temperatures, which control the snow melting. WeaGETS-generated temperatures were used to replace the observed ones, in order to remove any biases due to the temperature generating process. However, by doing so, another bias was introduced in which temperatures and precipitations were no longer correlated in the observed time series. Even though it seemed better to proceed as such, a new bias may however have been introduced. Thirdly, the proposed

approach keeps the precipitation occurrence process constant. Ongoing work indicates that transition probabilities also display inter-annual variability, and are partly correlated with annual precipitation. Even though the proposed spectral correction approach significantly improves the simulation of water discharge, further improvements may be required that occurrence variability be specifically taken into account. However, a relatively simple technique for adjusting the daily precipitation occurrence sequence is not immediately obvious (Wang and Nathan, 2007). Furthermore, although indirect validation is generally valid for a given impact model, location and experimental setting, further testing may be needed.

CHAPTER 2

ASSESSMENT AND IMPROVEMENT OF STOCHASTIC WEATHER GENERATORS IN SIMULATING MAXIMUM AND MINIMUM TEMPERATURES

Jie Chen[1], François P. Brissette[1], Robert Leconte[2]

1. Department of Construction Engineering, École de technologie supérieure, Université du Québec, 1100, rue Notre-Dame Street Ouest, Montréal, Québec, Canada, H3C 1K3.
2. Department of Civil Engineering, Université de Sherbrooke, 2500, boul. de l'Université, Sherbrooke, Québec, Canada, J1K 2R1

This article was submitted to the Transaction of the American Society of Agricultural and Biological Engineering in March, 2011.

2.1 Abstract

Stochastic weather generators are commonly used to generate time series of weather variables to drive agricultural and hydrologic models. One of their most appealing features is the ability to rapidly generate very long time-series for studying the impacts of rare climate events. However, they do have various problems; such as the inability to represent the inter-annual variability of the climate system, and it is difficult for them to accurately preserve the auto- and cross-correlation of maximum and minimum temperatures (Tmax and Tmin). This research aims to: (1) compare the abilities of two of the most widely-used weather generators (CLIGEN and WGEN) in generating Tmax and Tmin; (2) merge the two weather generators into a hybrid method that combines the strengths of each (referred to as the integration method); and (3) apply an approach to correct the inter-annual variability of Tmax and Tmin (referred to as the spectral correction method). The results show that CLIGEN reproduced mean daily Tmax and Tmin very well. WGEN also produced the mean daily Tmax reasonably well, but slightly underestimated the mean daily Tmin. Moreover, CLIGEN was better than WGEN at producing standard deviations of daily Tmax and Tmin. Integration and

spectral correction methods resulted in a weather generator that accurately produced mean, standard deviation and extremes of daily Tmax and Tmin. The auto- and cross-correlations of and between daily Tmax and Tmin were well reproduced and much better than those of CLIGEN- and WGEN-generated data. Moreover, the spectral correction approach successfully reproduced the observed inter-annual variability of Tmax and Tmin.

Keywords: Stochastic Weather Generator; CLIGEN; WGEN; Temperature; Climate variability

2.2 Introduction

With the growing use of physically-based response models such as hydrological and agricultural models, there has been a more frequent requirement for weather generators to generate long meteorological time series to simulate the long term effects of climate variability. Over the past three decades, several weather generators have been developed to meet this requirement, such as Weather Generator (WGEN) (Richardson, 1981; Richardson and Wright, 1984), USCLIMATE (Hanson et al., 1994), Climate Generator (CLIGEN) (Nicks et al., 1995), Climate Generator (ClimGen) (Stockle et al., 1999), and the Long Ashton Research Station-Weather Generator (LARS-WG) (Semenov and Barrow, 2002). The main reason for the development of weather generators is the ability to generate long-term synthetic daily weather data that statistically resemble the observed historical record. Weather generators can also be used to generate weather data for ungauged basins by interpolating the model parameters from adjacent gauged sites. More recently, another application of weather generators is to use them as a downscaling tool to generate climate projections at the daily time scale to quantify the impacts of future climate change (Semenov & Barrow, 1997; Wilks, 1992, 1999a; Pruski and Nearing, 2002; Zhang et al., 2004; Zhang, 2005; Zhang and Liu, 2005). This use is achieved by perturbing the weather generator parameters according to relative changes projected by a climate model (Zhang, 2005). Of all the aforementioned weather generators, WGEN and CLIGEN are arguably the ones most

widely used for simulating daily weather time series including precipitation, maximum and minimum temperatures (Tmax and Tmin) and solar radiation.

Over the past few decades, numerous studies have been conducted to evaluate, improve and compare the performance of weather generators (Qian et al., 2004; Semenov et al., 1999; Zhang and Garbrecht, 2003; Hayhoe, 2000, Chen et al., 2009). Weather generators are good at producing precipitation occurrence and quantity (Semenov et al., 1998; Chen et al., 2008, Chen et al., 2009), but have difficulties dealing with inter-annual variability. Several methods have been presented to correct this problem (Hansen and Mavromatis, 2001; Dubrovsky et al., 2004; Wang and Nathan, 2007; Chen et al., 2010). Compared to precipitation, the simulation of temperatures has been given less attention in the literature. Weather generators also significantly underestimate the monthly and annual variability of temperatures (Dubrovsky et al., 2004). Dubrovsky et al. (2004) applied a monthly generator (based on a first-order linear autoregressive model) to adjust the low-frequency variability of Tmax and Tmin based on a WGEN-like weather generator. The results demonstrated that conditioning a daily weather generator on a monthly model has positive effects. However, this model was still unable to accurately reproduce yearly variances and autocorrelations of observed temperatures because it did not specifically consider the inter-annual variability. To date, no other approaches have been proposed to correct the underestimation of monthly and annual temperature variability. One of the explanations for this lacuna is that temperatures are not considered as important as precipitation in some practical applications like hydrological studies. Another reason is that temperature correction is more difficult, because Tmax and Tmin are correlated with each other.

The preservation of the auto- and cross-correlations for and between Tmax and Tmin is an important criterion for assessing the ability of a weather generator to simulate temperatures, but very few approaches have tried to address this problem. For example, CLIGEN uses two random numbers to generate the standard normal deviate. The second number for one day is reused as the first number for the following day. This method has limited effects, however, especially for evaluating day-to-day persistence (Zhang, 2004; Chen et al., 2008). WGEN

uses a first-order linear autoregressive model to generate the residual series of Tmax and Tmin. According to this scheme, the lag 0 and lag 1 correlations are derived from the observed data and lag *k*'s correlation coefficient is given by the k^{th} power of the lag 1 correlation. This approach is thus effective at reproducing lag 0 and lag 1 correlations, but lags greater than one day are not well-preserved (Richardson, 1981).

The objectives of this work were to: (1) compare the abilities of two of the most widely-used weather generators (CLIGEN and WGEN) at generating Tmax and Tmin; (2) merge the two weather generators into a hybrid method that combines the strengths of each; and (3) apply an approach to correct the inter-annual variability of Tmax and Tmin.

2.3 Methodology

2.3.1 Stochastic weather generators

The two weather generators compared here, CLIGEN and WGEN, are arguably the ones most commonly used. They generate synthetic daily weather data using statistics derived from observed data based on a normal distribution, combined with a random number generator. Table 2.1 briefly summarizes the differences between the two weather generators at producing Tmax and Tmin. More details are presented below.

2.3.1.1 WGEN

WGEN is a four-variate (precipitation, Tmax, Tmin and solar radiation) single-site stochastic weather generator. It uses a first-order linear autoregressive model to generate Tmax and Tmin. The observed time series is first reduced to residual elements by subtracting the daily mean and dividing by the standard deviation. The means and standard deviations are conditioned on the wet or dry status (Richardson 1981). The residual series are then generated by:

$$x_{p,i}(j) = Ax_{p,i-1}(j) + B\varepsilon_{p,i}(j) \tag{2.1}$$

where $x_{p,i}(j)$ is a (2×1) matrix for day i of year p, whose elements are the residuals of Tmax (j=1) and Tmin (j=2); $\varepsilon_{p,i}(j)$ is a (2×1) matrix of independent random components that are normally distributed with a mean of zero and a variance of unity; and A and B are (2×2) matrices whose elements are defined such that the new sequences have the desired auto- and cross-correlation coefficients. The A and B matrices are determined by

$$A = M_1 M_0^{-1} \tag{2.2}$$

$$BB^T = M_0 - M_1 M_0^{-1} M_1^T \tag{2.3}$$

where the superscripts -1 and T denote the inverse and transpose of the matrix, respectively, and M_0 and M_1 are the lag 0 and lag 1 covariance matrices.

The daily values of Tmax and Tmin are found by multiplying the residuals by the standard deviation and adding the mean using the following equations.

$$T_{\max} = \mu_{\max} + \sigma_{\max} \times x_{p,i} \tag{2.4}$$

$$T_{\min} = \mu_{\min} + \sigma_{\min} \times x_{p,i} \tag{2.5}$$

Because Tmax and Tmin are generated independently using equations (2.4) and (2.5) resulting in a large number of cases where the generated Tmin is larger than Tmax on a given day. To resolve this problem, a range check is imposed, forcing Tmin to be smaller than Tmax. Tmin may be set to Tmax-1, for example. However, this has an undesirable effect on the mean and standard deviation of Tmin.

Table 2.1 Comparison of the WGEN and CLIGEN algorithms at generating maximum and minmum temperatures (Tmax and Tmin)

NO.	WGEN	CLIGEN
1	Tmax and Tmin are conditioned on wet and dry states	Tmax and Tmin are not conditioned on wet and dry states
2	The time series of observed data is reduced to a time series of residual elements. (daily basis)	Parameters are calculated for each month. (monthly basis)
3	Residual elements are analyzed to determine the auto- and cross-correlation of and between Tmax and Tmin.	Two random numbers are used to generate the standard normal deviate. The second number for one day is reused as the first number for the following day.
4	Generating residual series of Tmax and Tmin is based on a first-order linear autoregressive model. The daily values of Tmax and Tmin are found by multiplying the residuals by the standard deviation and adding the mean.	The smaller standard deviation of Tmax or Tmin is used as a base, and the other parameter is generated conditioned on the chosen parameter.
5	Tmax and Tmin are generated independently, resulting in several cases in which Tmin is larger than Tmax on a given day. A range-check scheme is imposed to force Tmin to be smaller than Tmax.	Tmin is generated conditioned on Tmax to ensure it is less than Tmax on a given day. The range check scheme is unnecessary.

2.3.1.2 CLIGEN

The CLIGEN weather generator generates daily values of Tmax, Tmin, dew point temperature, solar radiation, and wind velocity and direction, as well as precipitation-related variables such as precipitation occurrence/quantity, duration, peak storm intensity and time to

peak intensity, based on long-term monthly statistical parameters. This paper only focuses on the generation of Tmax and Tmin.

Daily Tmax and Tmin are generated using normal distributions. The long-term monthly statistical parameters, including the mean and standard deviation, are used to run CLIGEN to generate daily weather series. Specifically, the temperature with the smaller standard deviation between Tmax and Tmin is computed first, followed by the other. If the standard deviation of Tmax is larger than or equal to the standard deviation of Tmin, daily temperatures are generated by equations (2.6) and (2.7):

$$T_{\min} = \mu_{\min} + \sigma_{\min} \times \chi \tag{2.6}$$

$$T_{\max} = T_{\min} + (\mu_{\max} - \mu_{\min}) + \sqrt{{\sigma_{\max}}^2 - {\sigma_{\min}}^2} \times \chi \tag{2.7}$$

If the standard deviation of Tmax is less than that of Tmin, daily temperatures are generated by equations (2.8) and (2.9):

$$T_{\max} = \mu_{\max} + \sigma_{\max} \times \chi \tag{2.8}$$

$$T_{\min} = T_{\max} - (\mu_{\max} - \mu_{\min}) - \sqrt{{\sigma_{\min}}^2 - {\sigma_{\max}}^2} \times \chi \tag{2.9}$$

where μ is the monthly mean of the daily temperatures, σ is the standard deviation of daily temperatures, and χ is a generated standard normal deviate, which is obtained for each day using two random numbers. A Tmin generated using this scheme is always less than Tmax, which eliminates any need for the range check that must be used in WGEN to ensure that Tmin is less than Tmax.

2.3.2 Integration method

The main motivation for this work was to combine the most desirable properties of both weather generators into a hybrid method to maximize the strengths and minimize the drawbacks of each. To achieve this, WGEN is used as the basic weather generator, but instead of using equations (2.4) and (2.5), the conditional equations (2.6) – (2.9) derived from CLIGEN are used, to ensure that the Tmin is always less than the Tmax on a given day. Thus, the range check is no longer necessary. Throughout this paper, this is referred to as the integration method.

2.3.3 Correction of the inter-annual variability

An important goal of this work was to specifically correct the inter-annual variability of Tmax and Tmin using the power spectra of observed time series at the yearly scale. The power spectra are computed using Fast Fourier Transforms (FFT). This approach was proposed by Chen et al. (2010) for correcting the low-frequency variability of precipitation for weather generators.

The use of FFT is widespread in engineering and signal processing, and it stems from the concept that any discrete signal (such as yearly averaged Tmin at a station) can be exactly represented by a summation of sine waves with magnitude S and phase ϕ. Following the FFT, each sine wave component is expressed as a complex number:

$$\mathrm{C} = X + i * Y \qquad (i = \sqrt{-1}) \tag{2.10}$$

from which the magnitude S and phase ϕ can be extracted with the following equations:

$$\mathrm{S} = |C| = \sqrt{X^2 + Y^2} \tag{2.11}$$

$$\phi = \tan^{-1}(Y/X) \tag{2.12}$$

The variance and phase of each component can be modified and returned back in complex form with the following equation, and then returned back to the time domain with an inverse FFT:

$$C = S * e^{(i*\phi)} \tag{2.13}$$

By modifying the phase of each component and reverting to the time domain, a new signal with an identical power spectrum (and variance) can be created. As such, low-frequency components (such as decadal variability) will be preserved in the new signal. This property is used to modify the daily sequences from the weather generator in order to correct for the underestimated variances at the inter-annual scale. Throughout this paper, this procedure is referred to as the spectral correction method/approach, and it is comprised of three steps:

1) Daily Tmax and Tmin time series are generated by WGEN with the integration method using parameters derived from the observed daily temperature series. In this study, the length of the generated series was 20 times that of the observed one in order to precisely evaluate the statistical parameters of the synthetic time series.

2) Inter-annual variability is modeled based on a power spectrum using FFT. The generation of a new power spectrum for Tmax is achieved by assigning random phases to each spectral component and then transferring back to the time domain. To be sure not to perturb the cross-correlation between Tmax and Tmin, the random phases used to generate the power spectrum of Tmax were also used to generate that of Tmin.

3) The daily Tmax and Tmin series generated in step 1 are adjusted incrementally. The series of yearly averaged Tmax and Tmin calculated from the daily series generated in step 1 are adjusted to the yearly averaged Tmax and Tmin series generated in step 2, using linear functions.

2.3.4 Validation of each method

The diagnostics listed in table 2.2 were used to compare the observed and synthesized Tmax and Tmin. Two tailed t- and F-tests were conducted to test the equality of the mean and standard deviation between observed and synthesized Tmax and Tmin time series, respectively. A significance level of P=0.05 was used for these tests.

Table 2.2 Diagnostics for comparing each method

NO.	Diagnostics
1	Mean and standard deviation of daily Tmax and Tmin
2	Averaged yearly maximum Tmax and minimum Tmin
3	Auto- and cross-correlations of and between Tmax and Tmin
4	Autocorrelation of averaged yearly Tmax and Tmin
5	Mean and standard deviation of averaged yearly Tmax and Tmin

2.3.5 Meteorological data

Meteorological data, including daily Tmax, Tmin and precipitation for six stations dispersed across Canada, were used to drive the weather generators. To be consistent with a previous study, the chosen meteorological stations are the same ones used by Chen et al. (2010) to verify the spectral correction method for correcting low-frequency precipitation variability. Basic information, including longitude, latitude, elevation, record duration and averaged yearly Tmax and Tmin for these stations is given in table 2.3. Averaged yearly temperatures at these stations varied from -2.72°C in Churchill to 14.10°C in Victoria for Tmax, and -10.91°C in Churchill to 5.55°C in Langara for Tmin, adequately representing the natural climate variability in Canada.

Table 2.3 Location, record period, and average annual maximum and minimum temperature for six stations (Lat=latitude; Lon=longitude and Ele=elevation)

Region	Station number and name	Lat (°N)	Lon (°W)	Ele (m)	Records of daily data	Averaged yearly Tmax (°C)	Averaged yearly Tmin (°C)
Vancouver Island	(1) Victoria	48.65	123.32	19	1941-2006 (66)	14.10	5.38
Queen Charlotte Islands	(2) Langara	54.25	133.05	14	1937-2006 (70)	9.86	5.55
Okanagan River Basin	(3) Vernon Goldstream Ranch (VGR)	50.23	119.20	482	1907-1996 (90)	12.70	1.92
Mackenzie	(4) Yellow-knife	62.47	114.43	206	1945-2002 (58)	-0.57	-9.34
Nelson and Churchill River Basin	(5) Churchill	58.73	94.05	29	1947-2006 (60)	-2.72	-10.91
Middle St. Lawrence River Basin	(6) Dorval	45.47	73.75	36	1943-1994 (52)	11.08	1.59

2.4 Results

2.4.1 The relationship between averaged yearly precipitation and temperatures

One of the goals of this paper is to apply a method to correct the inter-annual variability of Tmax and Tmin for weather generators. In order to do this, correlations between averaged yearly temperatures and precipitation were looked at. If averaged yearly temperatures are

strongly correlated with precipitation, the correlation may be perturbed by correction schemes.

The correlation between averaged yearly temperatures and precipitation was tested for six stations (table 2.4). The results showed that there is no significant correlation between the averaged yearly Tmax (Tmin) and precipitation at the P=0.05 level, with the exception of the Churchill station where the correlation is nevertheless small. Therefore, it was assumed that the inter-annual variability of Tmax and Tmin can be corrected independently of precipitation.

Table 2.4 The correlation between averaged yearly Tmax (Tmin) and precipitation for six stations

Station	**Tmax vs. precipitation**		**Tmin vs. precipitation**	
	Correlation coefficient (R)	**P value**	**Correlation coefficient (R)**	**P value**
Victoria	0.120	0.338	0.191	0.125
Langara	0.207	0.085	0.207	0.058
Vernon Goldstream Ranch (VGR)	0.152	0.093	0.022	0.835
Yellowknife	0.176	0.187	0.237	0.074
Churchill	0.270	0.037	0.256	0.048
Dorval	0.183	0.193	0.126	0.374

2.4.2 Power spectra of mean yearly temperature time series

Figures 2.1a and 2.1b show the time series and power spectra of the mean yearly Tmin at the Yellowknife station. Figure 2.1b clearly shows that warmer and colder years are not randomly distributed and do display patterns associated with climate natural variability. In this case there are strong 3- and 10-year oscillations. By assigning random phases to each

component of the power spectrum and reverting to the time domain, a new signal (mean yearly Tmin) with an identical power spectrum (and thus showing the same variability) can be created. This mean yearly Tmin time series (figure 2.1c) has a power spectrum (figure 2.1d) that is almost identical to the one shown in figure 2.1b.

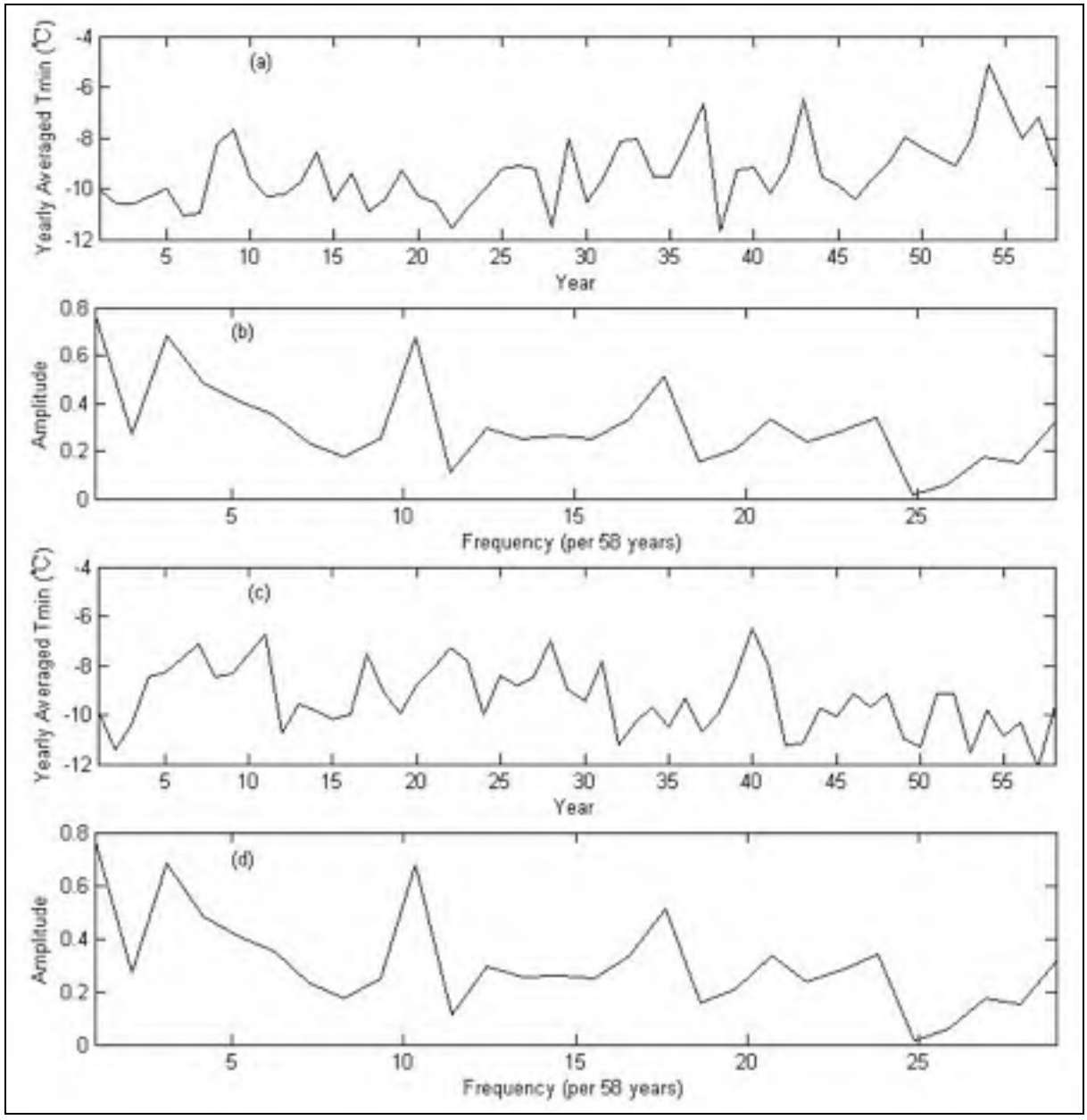

Figure 2.1 Time series ((a) and (c)) and their power spectra ((b) and (d)) of averaged yearly Tmin at the Yellowknife station.

2.4.3 Statistics of maximum and minimum temperatures

All of the methods, including CLIGEN, WGEN, integration and spectral correction approaches, reproduced the mean daily Tmax very well (table 2.5). In particular, the mean daily Tmax was exactly produced by the spectral correction method. The t-tests showed that there is no significant difference between observed and the method-generated Tmax at the P=0.05 level. WGEN somewhat underestimated the standard deviation of daily Tmax. The F-tests showed that observed and WGEN-generated Tmax are significantly different for all 6 stations. The standard deviations of CLIGEN generated-data virtually matched those from observation in all cases. All of the F-tests between observed and CLIGEN-generated data were insignificant at P=0.05. Standard deviations of daily Tmax produced by the integration and spectral correction methods were better than those generated by WGEN, but slightly worse than those generated by CLIGEN. The F-tests showed that the observed standard deviations of generated data were significantly different for the integration method (4 out of 6 stations) and for the spectral correction method (3 out of 6 stations). Looking at extremes, WGEN was the worst at preserving the averaged yearly maximum temperature with a mean absolute error (MAE) of 3.23°C. CLIGEN, integration and spectral correction methods were all better with MAEs of 1.44°C, 1.59°C and 1.60°C, respectively.

Table 2.6 shows that WGEN performed the poorest at reproducing Tmin, with MAEs of mean, standard deviation and averaged yearly minimum Tmin of 0.43°C, 0.41°C and 4.98°C, respectively. The t- and F-tests showed that the means and standard deviations of observed data were significantly different from those generated with WGEN at P = 0.05 for all stations and for 5 out of 6 stations, respectively. This is essentially because of the range check imposed in WGEN to insure that the daily Tmin is less than Tmax on any given day. CLIGEN reproduced the mean and the standard deviation of Tmin very well for all six stations. Both the integration and the spectral correction methods reproduced Tmin reasonably well, although there were significant differences for standard deviations for two and one stations out of six, respectively. For extreme Tmin, WGEN again performed less well, with an MAE of 4.98°C for the averaged yearly Tmin. CLIGEN performed the best

with an MAE of 2.82, while the integration and spectral correction had the same MAE (4.43°C).

Table 2.5 Statistics (°C) of daily Tmax by location and source
(AYMax=averaged yearly maximum)

Station	Statistic	OBS	WGEN	CLIGEN	INT	SPC
Victoria	Mean	14.10	14.09	14.10	14.10	14.10
	Std. dev	6.36	6.06*	6.36	6.25*	6.26*
	AYMax	30.75	28.05	29.85	29.55	29.51
Langara	Mean	9.86	9.86	9.86	9.87	9.86
	Std. dev	4.43	4.35*	4.43	4.39	4.43
	AYMax	20.70	19.64	20.00	19.90	19.89
Vernon Goldstream Ranch	Mean	12.70	12.72	12.70	12.68	12.70
	Std. dev	11.28	10.73*	11.28	11.04*	11.07*
	AYMax	34.81	33.22	37.45	36.43	36.46
Yellowknife	Mean	-0.57	-0.56	-0.57	-0.59	-0.57
	Std. dev	16.77	15.80*	16.76	16.55*	16.67
	AYMax	28.46	24.04	29.95	28.56	28.59
Churchill	Mean	-2.71	-2.72	-2.70	-2.76	-2.71
	Std. dev	15.46	14.47*	15.48	15.37	15.40
	AYMax	30.35	23.38	31.58	26.13	26.19
Dorval	Mean	11.08	11.07	11.08	11.05	11.08
	Std. dev	12.55	11.77*	12.54	12.35*	12.36*
	AYMax	32.79	30.15	34.50	34.40	34.43

* is different from observed time series at P = 0.05.

Table 2.6 Statistics (°C) of daily Tmin by location and source
(AYMin=averaged yearly minimum)

Station	Statistic	OBS	WGEN	CLIGEN	INT	SPC
Victoria	Mean	5.38	5.30*	5.38	5.38	5.38
	Std. dev	4.72	4.86*	4.72	4.69	4.71
	AYMin	-8.09	-8.60	-8.30	-7.11	-7.06
Langara	Mean	5.55	5.38*	5.55	5.56	5.55
	Std. dev	4.21	4.20	4.21	4.21	4.21
	AYMin	-7.90	-6.63	-6.77	-7.23	-7.25
Vernon Goldstream Ranch	Mean	1.92	1.69*	1.90	1.86	1.91
	Std. dev	8.23	8.51*	8.24	8.14*	8.18
	AYMin	-25.57	-24.66	-25.28	-21.53	-21.47
Yellowknife	Mean	-9.34	-10.27*	-9.35	-9.42	-9.34
	Std. dev	17.02	17.89*	17.01	16.97	17.01
	AYMin	-44.62	-57.34	-51.10	-54.51	-54.43
Churchill	Mean	-10.91	-11.65*	-11.00	-10.97	-10.91
	Std. dev	14.97	15.52*	14.98	15.29*	15.32*
	AYMin	-40.84	-49.86	-46.89	-49.45	-49.38
Dorval	Mean	1.59	1.17*	1.59	1.54	1.59
	Std. dev	11.74	12.34*	11.73	11.69	11.70
	AYMin	-28.87	-34.34	-31.62	-26.48	-26.43

* is different from observed time series at P = 0.05.

2.4.4 Auto- and cross-correlation of daily temperatures

Auto- and cross-correlations of and between daily Tmax and Tmin were computed for unfiltered observed and synthesized data sets. Figure 2.2 shows the results for Tmax. The observed data show a clear day-to-day persistence. WGEN predictably reproduced the observed lag 1 autocorrelation, but lags greater than one day were consistently greater than

those of the observed data with the exception of the wettest station, Langara. This indicates that WGEN may preserve the autocorrelation correctly for very wet stations. CLIGEN consistently underestimated day-to-day persistence. The integration and spectral correction methods reproduced not only the day-to-day persistence, but also the month-to-month persistence as shown by the 30-day lag results.

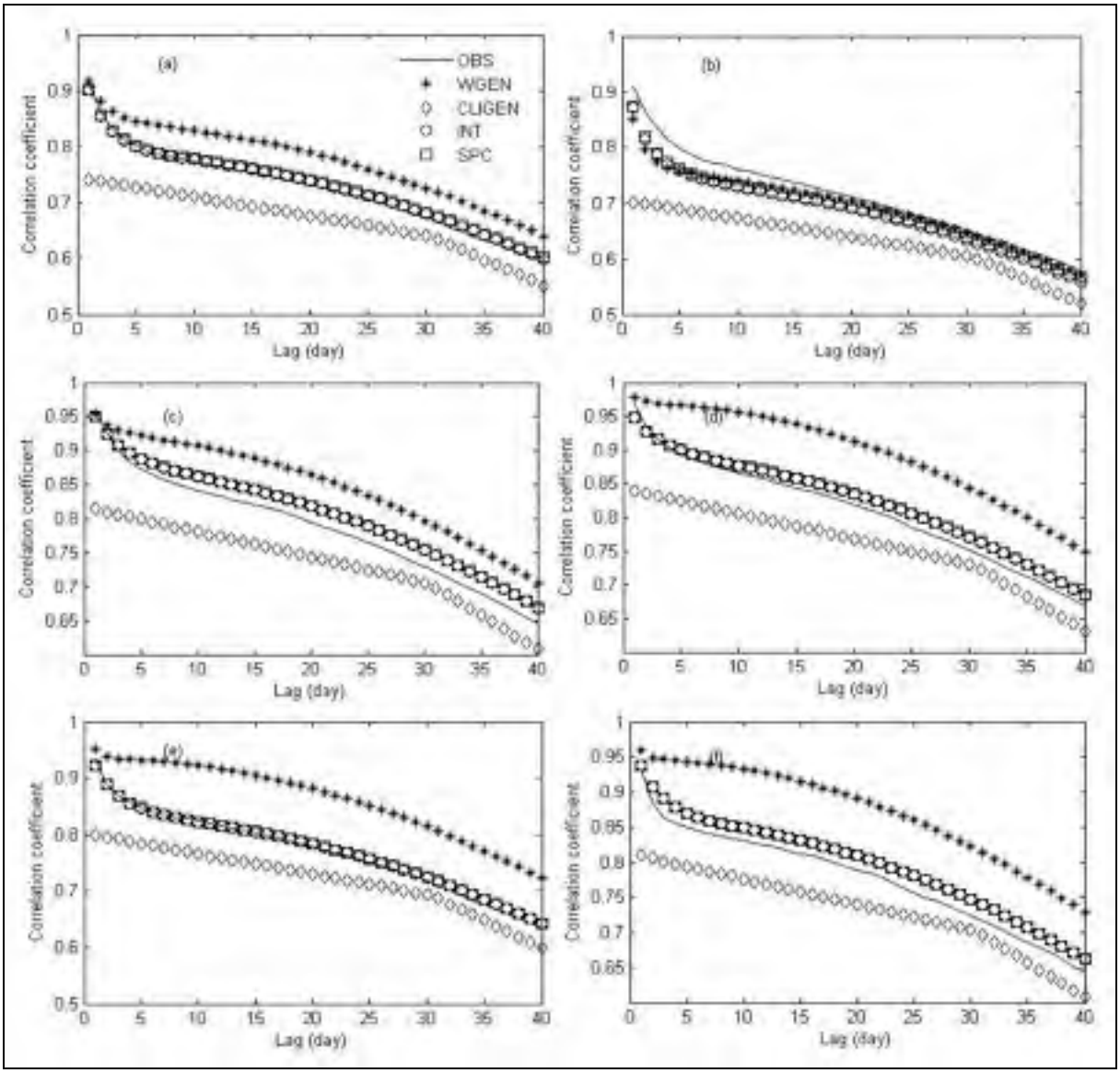

Figure 2.2 40 days of lagged autocorrelation for observed (OBS), CLIGEN-generated, WGEN-generated, integrated weather generator generated (INT) and spectral correction method corrected (SPC) daily Tmax for the 6 stations of Table 3.

Similarly to its results for Tmax, CLIGEN consistently underestimated the autocorrelation of Tmin, especially at the day-to-day persistence (figure 2.3). The other three methods worked well, although WGEN was systematically inferior to the integration and spectral correction methods. The range check imposed in WGEN has little effects on the autocorrelation of Tmin.

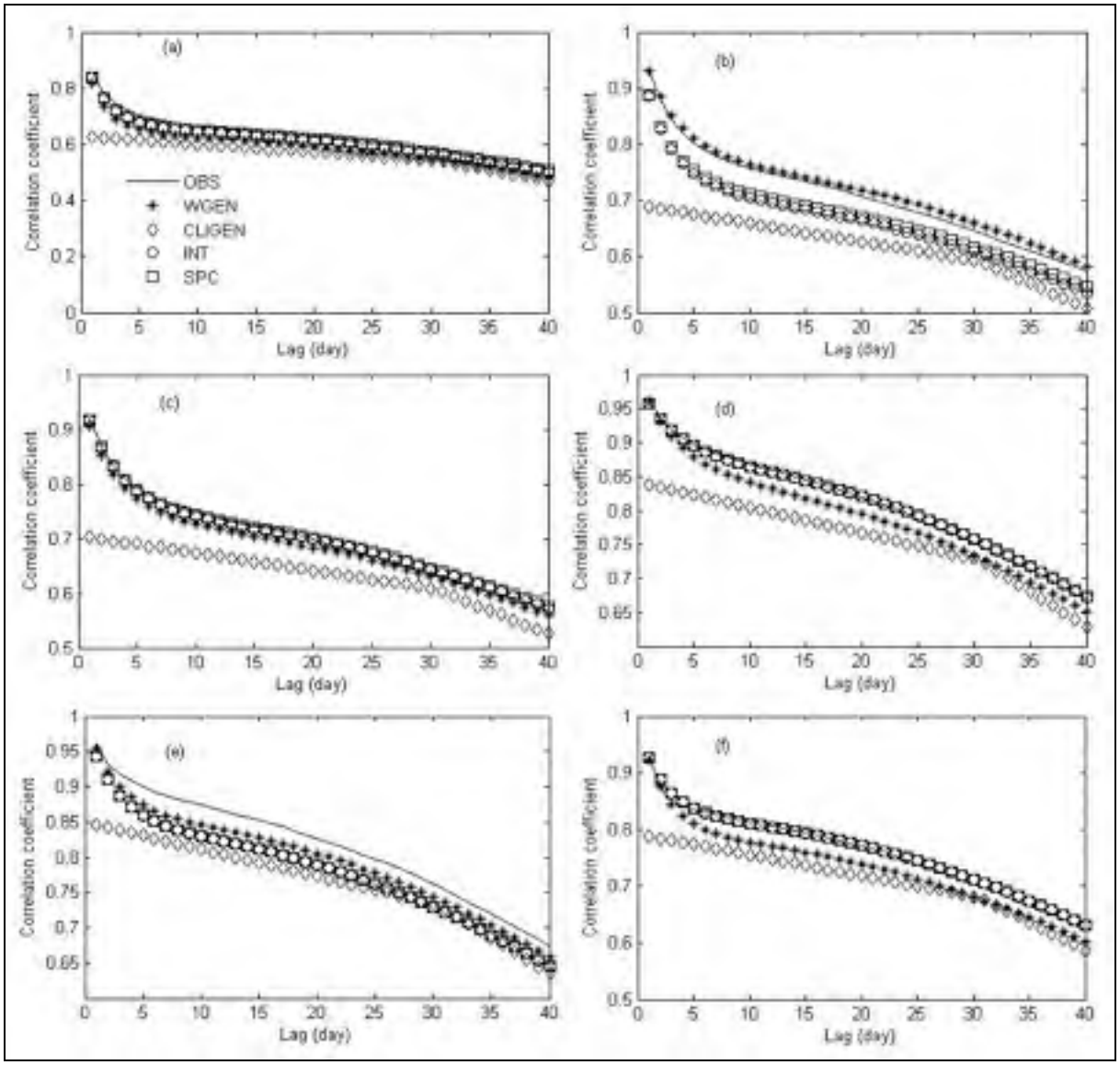

Figure 2.3 40 days of lagged autocorrelation for observed (OBS), CLIGEN-generated, WGEN-generated, integrated weather generator generated (INT) and spectral correction method corrected (SPC) daily Tmin for the 6 stations of Table 3.

Cross-correlation persistence between Tmax and Tmin is shown in figure 2.4. CLIGEN data underestimated the cross-correlations between Tmax and Tmin. Once again WGEN showed better performance than CLIGEN, while the integration and spectral correction methods were the most successful at reproducing the observed cross-correlations.

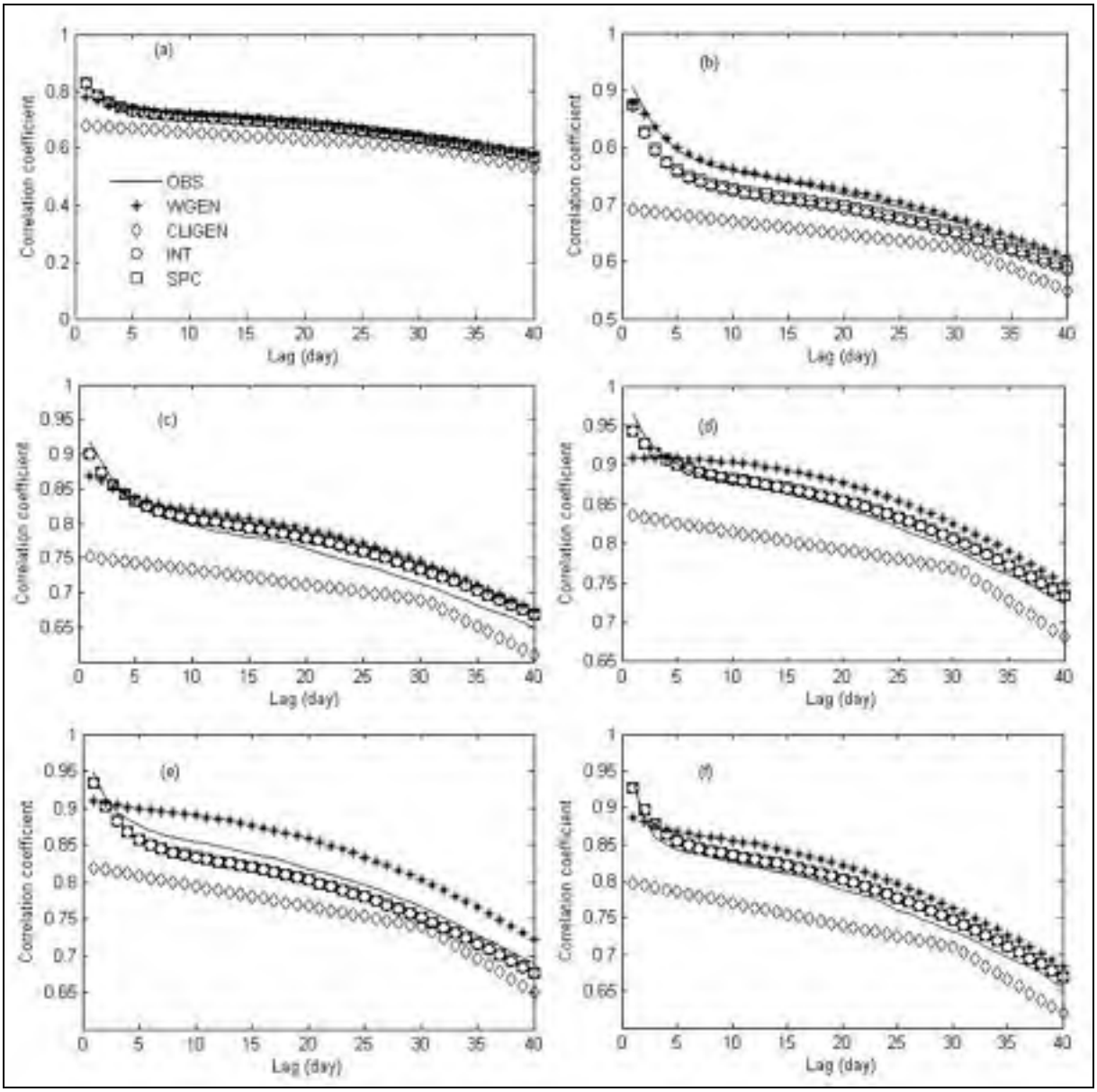

Figure 2.4 40 days of lagged cross correlation between observed (OBS), CLIGEN-generated, WGEN-generated, integrated weather generator generated (INT) and spectral correction method corrected (SPC) daily Tmax and those of daily Tmin for the 6 stations of Table 3.

2.4.5 Autocorrelation of averaged yearly temperatures

Figure 2.5 displays the autocorrelation function of the observed averaged yearly Tmin. It clearly indicates that warmer and cooler years are not random, but rather, come in series, as was shown by the power spectra of averaged yearly Tmin series (figure 2.1). Since similar results were obtained with Tmax, only the results of Tmin are shown in figure 2.5. For many applications, such as agriculture, it is important to be able to reproduce these successions of warmer/cooler years. WGEN, CLIGEN and the integrated method could not preserve the autocorrelation function for temperatures because it does not take into account the low-frequency component of climate variability. Instead, it tries to reproduce the average year, every year. The spectral correction method successfully reproduced the observed autocorrelation for all 6 stations.

2.4.6 Inter-annual variability of Tmax and Tmin

All methods reproduced the mean yearly Tmax and Tmin very well (table 2.7), with the exception of WGEN which had some problems with Tmin. The t-tests showed that mean yearly Tmins were significantly different at P=0.05 for five out of six stations. As mentioned earlier, this occurs because a range check is used with WGEN to ensure the Tmin is less than Tmax on any given day, thereby perturbing the statistics of Tmin.

CLIGEN, WGEN and the integration method underestimated the inter-annual variability of averaged yearly Tmax and Tmin, as represented by their standard deviations (table 2.8). The F-tests showed that there is a statistically significant difference between the observed data and that generated from the three methods for all 6 stations at the P=0.05 level. The integration method somewhat improved the simulation of yearly Tmax. This was because equation (2.7) was used to generate Tmax if the standard deviation of Tmax was larger than or equal to the standard deviation of Tmin. It implies that the standard deviation of Tmax was conditioned on the standard deviation of Tmin in some cases. The spectral correction method preserved the standard deviations of averaged yearly Tmax and Tmin very well for all

stations. All the F-tests between the standard deviations of observed and of the spectral correction method corrected data were insignificant at the P=0.05 level.

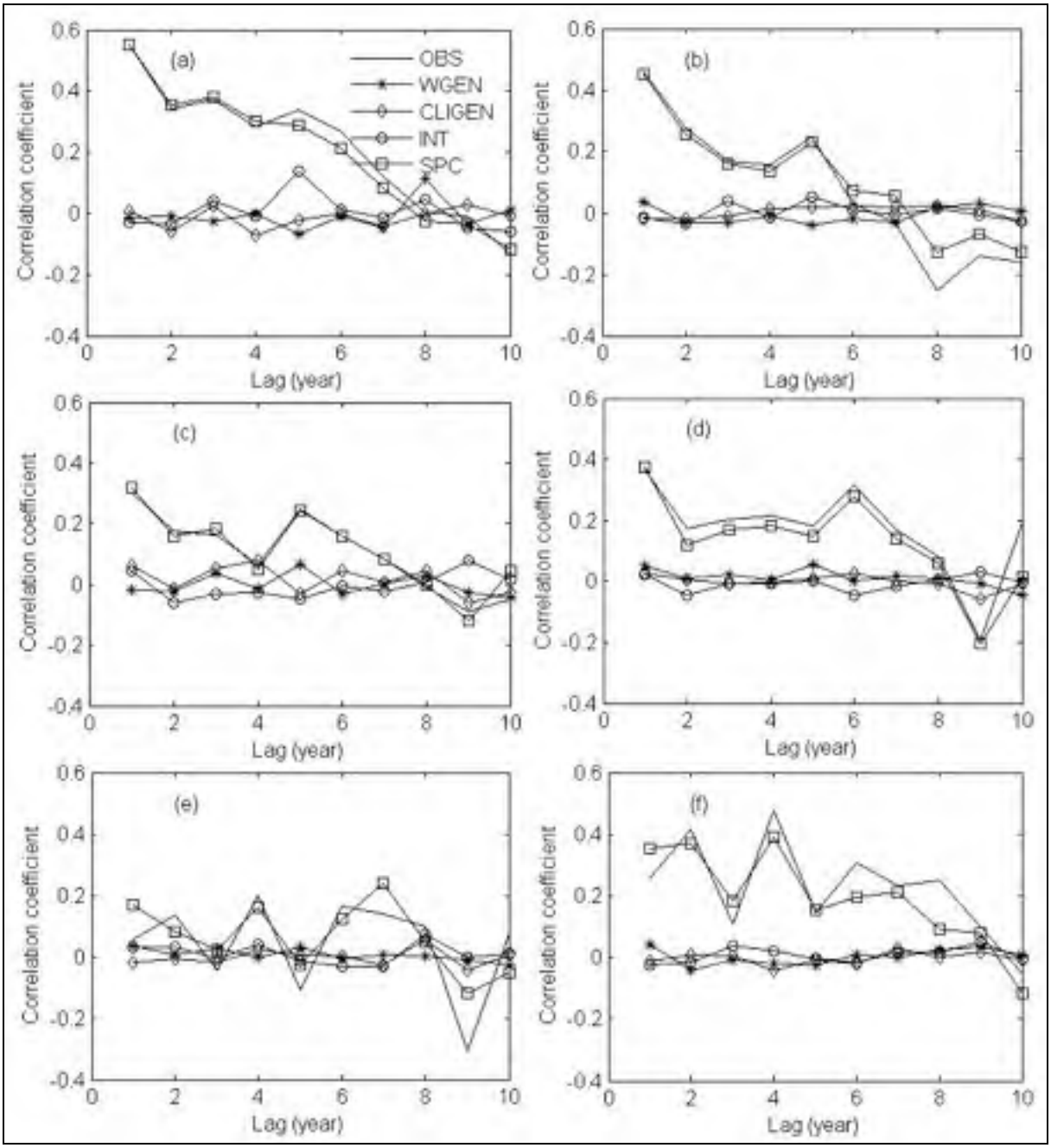

Figure 2.5 10 years of lagged autocorrelation of observed (OBS), CLIGEN-generated, WGEN-generated, integrated weather generator generated (INT) and spectral correction method corrected (SPC) averaged yearly Tmax for the 6 stations of Table 3.

Table 2.7 Means of yearly Tmax and Tmin derived from the synthesized and observed series for 6 stations. The synthesized Tmax and Tmin series include the data generated by CLIGEN, WGEN, integrated weather generator (INT), and corrected using the spectral correction method (SPC)

NO	Tmax					Tmin				
	OBS	WGEN	CLIGEN	INT	SPC	OBS	WGEN	CLIGEN	INT	SPC
1	14.10	14.09	14.10	14.10	14.10	5.38	5.30	5.38	5.39	5.38
2	9.86	9.86	9.86	9.87	9.86	5.55	5.38*	5.55	5.56	5.55
3	12.70	12.72	12.70	12.68	12.70	1.92	1.69*	1.90	1.86	1.92
4	-0.57	-0.56	-0.57	-0.59	-0.57	-9.34	-10.27*	-9.35	-9.42	-9.34
5	-2.71	-2.72	-2.70	-2.76	-2.71	-10.91	-11.65*	-11.00	-10.97	-10.91
6	11.08	11.07	11.08	11.05	11.08	1.59	1.17*	1.59	1.54	1.59

* is different from observed time series at P = 0.05.

Table 2.8 Standard deviations of yearly Tmax and Tmin derived from the synthesized and observed series for 6 stations. The synthesized precipitation series include the data generated by CLIGEN, WGEN, integrated weather generator (INT), and corrected using the spectral correction method (SPC)

NO	Tmax					Tmin				
	OBS	WGEN	CLIGEN	INT	SPC	OBS	WGEN	CLIGEN	INT	SPC
1	0.67	0.22*	0.16*	0.29*	0.67	0.59	0.27*	0.15*	0.27*	0.59
2	0.66	0.19*	0.13*	0.24*	0.65	0.72	0.26*	0.12*	0.26*	0.71
3	0.88	0.29*	0.24*	0.47*	0.88	0.95	0.55*	0.22*	0.52*	0.94
4	1.16	0.17*	0.35*	0.64*	1.13	1.35	0.98*	0.35*	0.79*	1.33
5	1.25	0.23*	0.37*	0.66*	1.21	1.18	0.70*	0.30*	0.70*	1.12
6	0.66	0.18*	0.28*	0.49*	0.64	0.82	0.65*	0.27*	0.55*	0.79

* is different from observed time series at P = 0.05.

2.5 Discussion and conclusions

Two weather generators, CLIGEN and WGEN, were compared with respect to the generation of minimum and maximum temperatures (Tmax and Tmin). Both generate Tmax and Tmin

based on a normal distribution; the main differences are that unlike WGEN, CLIGEN generates Tmax and Tmin conditioned on each other, and they use different schemes to preserve the auto- and cross-correlation of and between Tmax and Tmin. The results showed that CLIGEN reproduced the mean and standard deviation of daily Tmax and Tmin very well, and better than WGEN. This is because WGEN-independent generations of Tmax and Tmin result in a large number of cases where Tmin is larger than Tmax in a day. Any scheme forcing Tmin to be smaller than Tmax perturbs the statistics of Tmin. WGEN reproduced the observed lag 1 autocorrelation very well but its performance deteriorated rapidly for greater lags, with the exception of the wettest station -- Langara. The autocorrelation coefficients of CLIGEN-generated temperatures were consistently less than those of the observed data. The CLIGEN scheme of using two uniform random numbers for inducing additional dependency between two consecutive days is clearly inadequate, even for the lag 1 autocorrelation coefficient. Zhang (2004) and Chen et al. (2008) obtained similar results with respect to CLIGEN. WGEN proved better than CLIGEN in producing the cross-correlation between Tmax and Tmin. Neither weather generator could preserve the autocorrelation of averaged yearly Tmax and Tmin, nor preserve their inter-annual variability.

The integration and spectral correction methods resulted in weather generators that produced accurate means, standard deviations and extremes of daily Tmax and Tmin. Moreover, when compared to WGEN and CLIGEN, the integration and spectral correction schemes improved the simulations of auto- and cross-correlations for and between daily Tmax and Tmin. However, similarly to both WGEN and CLIGEN, the integration method was unable to preserve the autocorrelation function of averaged yearly Tmax and Tmin, because, as mentioned earlier, it does not take into account the low-frequency variability of climate. The spectral correction approach successfully reproduced the observed autocorrelation of averaged yearly Tmax and Tmin, and also successfully preserved the inter-annual variability of Tmax and Tmin.

Overall, coupling the integration method with the spectral correction method results in a weather generator that not only accurately preserves basic statistics including means,

standard deviations and extremes of Tmax and Tmin, but also preserves the auto- and cross-correlations for and between Tmax and Tmin. Even more importantly, this coupled method preserves the autocorrelation functions and inter-annual variability. The monthly variability was also improved along with the correction of inter-annual variability (results not shown), but it was not as good as that at the yearly scale, indicating that the scheme for correcting inter-annual variability has a limited effect at the monthly scale. Thus, it might be necessary to add monthly or seasonal variability into the correction scheme. However, this step may lead to overfitting problems, resulting in too many cases where Tmin is greater than Tmax. This paper only validated the applied methods directly, rather than linking them into practical applications. A more comprehensive assessment, including linking these methods with agricultural and hydrological models, for example, may be required in further studies.

CHAPTER 3

WEAGETS – A MATLAB-BASED DAILY SCALE WEATHER GENERATOR FOR GENERATING PRECIPITATION AND TEMPERATURE

Jie Chen[1], François P. Brissette[1], Robert Leconte[2], Annie Caron[3]

1. Department of Construction Engineering, École de technologie supérieure, Université du Québec, 1100, rue Notre-Dame Ouest, Montréal, Québec, Canada, H3C 1K3.
2. Department of Civil Engineering, Université de Sherbrooke, 2500, boul. de l'Université, Sherbrooke, Québec, Canada, J1K 2R1
3. SNC-Lavain inc., Montréal, Québec, Canada, H2Z 1Z3

This article was submitted to the Environmental Modelling & Software in February, 2011.

3.1 Abstract

Stochastic daily weather generators are often used to generate long time series of weather variables to drive hydrological and agricultural models. More recently, they have also been used as a downscaling tool for studying the impacts of climate change. This paper describes a versatile stochastic daily weather generator (WeaGETS) for producing daily precipitation, maximum and minimum temperatures (Tmax and Tmin). First, second and third-order Markov models are provided to generate precipitation occurrence, and exponential and gamma distributions are available to produce daily precipitation quantity. Precipitation generating parameters have options to be smoothed using Fourier harmonics. Two schemes (unconditional and conditional) are available to simulate Tmax and Tmin. Finally, a spectral correction approach is included to correct the well-known underestimation of monthly and inter-annual variability associated with weather generators. The Matlab freeware allows for easy modification of all routines, making it easy to add precipitation distribution or additional weather variables to simulate. The performance of this weather generator is demonstrated with respect to the generation of precipitation, Tmax and Tmin for two Canadian

meteorological stations. The results show that the widely used first-order Markov model is adequate for producing precipitation occurrence, but it underestimates the longest dry spell for dry station. The higher-order models have positive effects. The gamma distribution is consistently better than the exponential distribution at generating precipitation quantity, and the conditional scheme is better than the unconditional scheme in simulating Tmax and Tmin. WeaGETS underestimates the monthly and inter-annual variances of precipitation and temperatures. However, the spectral correction approach successfully preserves the observed low-frequency variability and autocorrelation functions of precipitation and temperatures.

Keywords: Stochastic weather generator; precipitation; temperature; Matlab

3.2 Introduction

Weather generators are computer algorithms that produce long time series of weather variables that have statistical properties comparable to those of existing records. They are also able to generate weather data at ungauged sites through the interpolation of model parameters from adjacent gauged sites (Baffult et al., 1996). Weather generators can generate weather data at various temporal scales, but the daily scale is the one that has received the most attention. Over the past decade, they have been widely used in climate change studies as a downscaling tool by perturbing their parameters to account for expected changes in precipitation and temperature (Semenov and Barrow, 1997; Wilks, 1992; Pruski and Nearing, 2002; Zhang et al., 2004; Zhang, 2005; Zhang and Liu, 2005; Kilsbyet al., 2007). The appealing property of downscaling weather generator parameters is their ability to rapidly produce ensembles of climate scenarios for studying the impacts of rare climate events. Over the past three decades, several weather generators have been developed to meet those requirements, such as WGEN (Richardson, 1981; Richardson and Wright, 1984), USCLIMATE (Hanson et al., 1994), CLIGEN (Nicks et al., 1995), ClimGen (Stockle et al., 1999) and LARS-WG (Semenov and Barrow, 2002). The generation of precipitation, maximum temperature (Tmax) and minimum temperature (Tmin) are the usual main components of these weather generators. However, these weather variables are often

generated based on different schemes, for example, daily precipitation quantity is generated using a gamma distribution in WGEN while a Pearson III distribution is used in CLIGEN. Most weather generators use a first-order Markov model to generate precipitation occurrence. This model has been shown to be adequate in temperate climates but in wet or dry areas, the use of higher-order Markov chains may be necessary (Wilks, 1999b). To circumvent this problem, LARS-WG uses empirical histograms of dry/wet series. A one-parameter exponential distribution is the simplest method used to generate daily precipitation quantity (Todorovic and Woolhiser, 1974; Richardson, 1981), but the two-parameter gamma distribution is more widely used due to its better performance. A three-parameter Person III distribution is also used to generate daily precipitation quantity in CLIGEN. Compared to precipitation, temperatures are much simpler to produce, since they often approximately follow a normal distribution. However, daily Tmax and Tmin are correlated with each other and this correlation varies depending on whether a day is dry or wet. Thus, the preservation of these correlations is an important criterion to assess the performance of a weather generator. Moreover, one problem with currently available daily weather generators is the underestimation of monthly and inter-annual variances because they do not take into account the low-frequency component of climate variability. Several methods have been presented to correct the low-frequency variability of precipitation (Hansen and Mavromatis, 2001; Dubrovsky et al., 2004; Wang and Nathan, 2007; Chen et al., 2010). The spectral correction approach of Chen et al. (2010) is arguably the best available method for dealing with the low-frequency problem.

All of the weather generators currently available only provide a single scheme to generate each climate variable, such as the first-order Markov model for precipitation occurrence and exponential or gamma distribution for wet day precipitation quantity. Users have little choice in selecting appropriate options for generating weather variables according to their specific study. Moreover, there is no scheme incorporated into weather generators to deal with their underestimation of inter-annual variability.

This paper describes a Matlab-based software package for the stochastic weather generation of precipitation and temperatures (Tmin and Tmax) for individual sites at a daily time scale. Simply by perturbing its parameters, this weather generator can also be used to evaluate the impacts of climate change. The software is named WeaGETS (Weather Generator Ecole de Technologie Supérieure). It regroups several options of other weather generators into one package, and allows for the correction of the underestimation of inter-annual variability. More importantly, users can easily tailor it to their specific needs with simple modifications.

3.3 Model description

This paper first presents the algorithm for the generation of precipitation and temperatures. Two Canadian meteorological weather stations are then selected to demonstrate the typical performance of WeaGETS. Discussion and conclusions are presented in the last section.

WeaGETS provides three options to generate precipitation occurrence, two options to produce precipitation quantity and two options to simulate Tmax and Tmin. There is also an option of smoothing the precipitation parameters with Fourier harmonics following Richardson's approach (1981), and to correct for the low-frequency variability of precipitation and temperature following the spectral correction method of Chen et al. (2010).

The basic input data include an observed weather data filename, a filename to store the subsequently generated data, a precipitation threshold value (minimum rainfall amount in 'mm' for a day to be considered wet) and the number of years of data to generate. Figure 3.1 presents the WeaGETS structure chart.

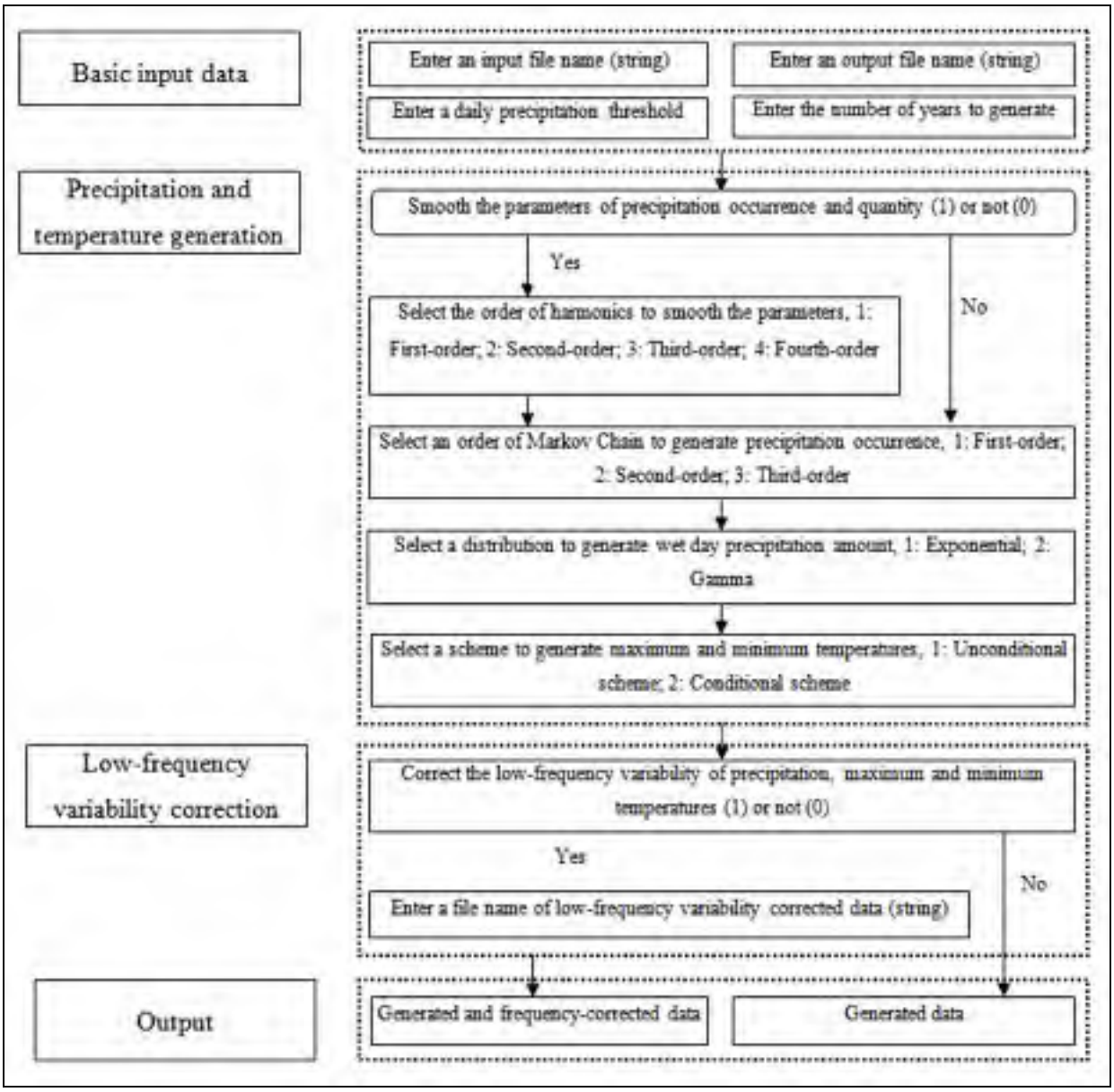

Figure 3.1 Structure chart of the WeaGETS stochastic weather generator.

3.3.1 Smoothing Scheme

The precipitation occurrence parameters include the transition probabilities of first, second and third-order Markov chains. For precipitation amounts, there is one parameter for the exponential distribution, and two parameters for the gamma distribution. These parameters are computed on a biweekly basis (26 estimations over the whole year). Because of climate

variability and the finite length of the historical records, the variation from one 2-week period to the other will not be smooth, and the true yearly distribution of the parameter value will be party hidden. The user can decide to accept sudden variations (keeping constant parameters values for the 2-week period) or to smooth the computed distribution to allow for smooth transitions of the parameters on a daily basis. In the latter case, WeaGETS will try to reproduce the precipitation characteristics of the smoothed line and not of the original observed values. In this case, generated precipitation may be slightly different than the observed precipitation. One to four Fourier harmonics can be used to smooth the yearly parameters distribution. The smoothing process eliminates sharp parameter transitions between computing periods that may occur due to outliers, especially for short time series. Figure 3.2 presents the P10 parameter smoothed by Fourier harmonics. A first-order Fourier harmonic is clearly inadequate in this case. A higher number of harmonics will better fit the data at the potential expense of reproducing trends that may not exist (as would be the case in figure 3.2d). The choice of smoothing or not, and how much smoothing is needed, is partly a philosophical debate and will depend on the experience of the modeler. In most cases, the use of two harmonics is adequate for representing seasonal trends in the precipitation-generating parameters, but this depends on local climatology.

3.3.2 Generation of precipitation occurrence

WeaGETS provides three options including first, second and third-order Markov models to produce precipitation occurrence. The first-order Markov process is the simplest and most widely used. The probability of precipitation on a given day is based on the wet or dry status of the previous day, which can be defined in terms of two transition probabilities, P01 and P11:

$$P01 = \Pr\{\text{precipitation on day t} \mid \text{no precipitation on day t-1}\} \quad (3.1a)$$

$$P11 = \Pr\{\text{precipitation on day t} \mid \text{precipitation on day t-1}\} \quad (3.1b)$$

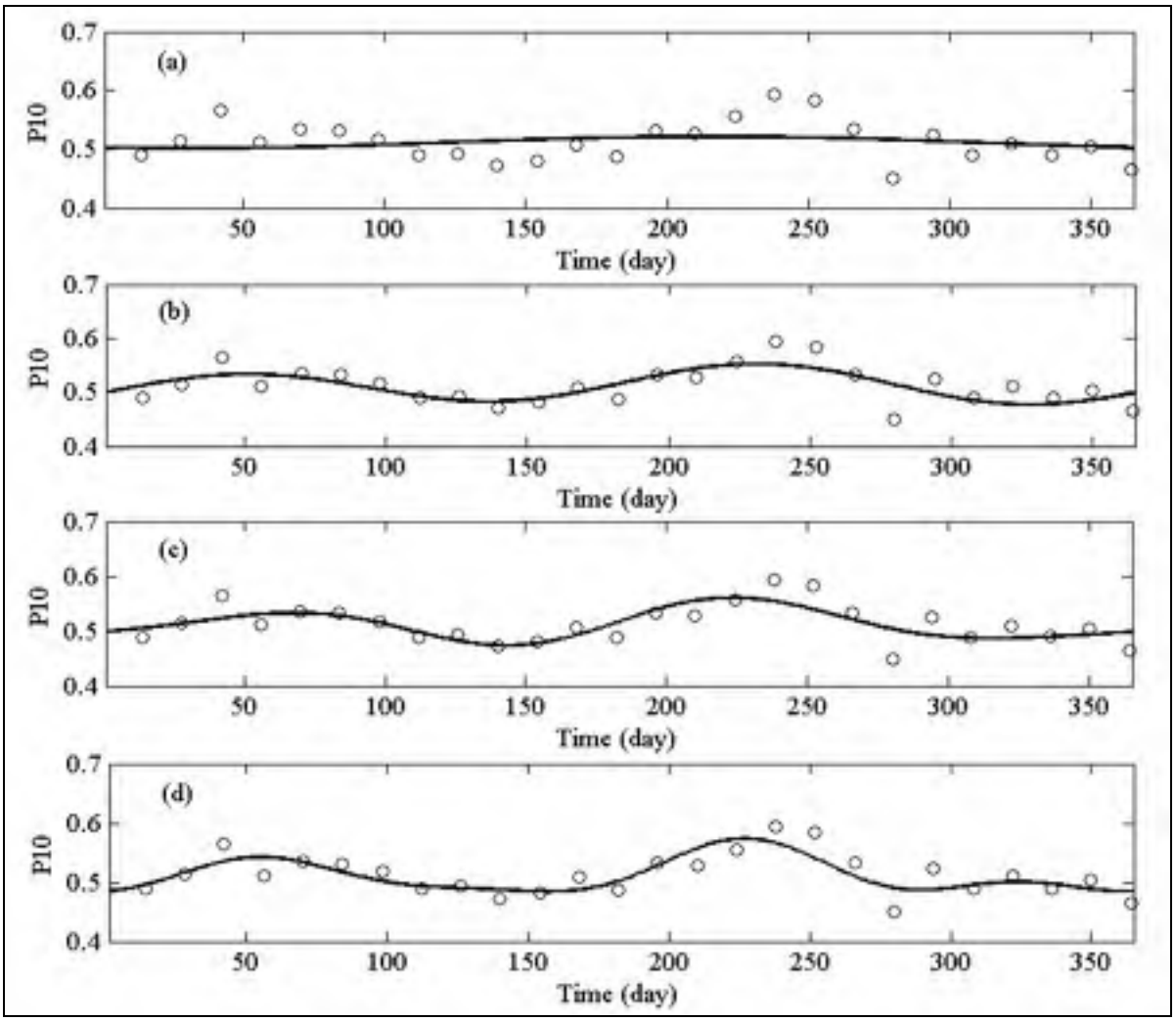

Figure 3.2 A dry day following a wet day (P10) calculated at a two-week scale and smoothed by first-order (a), second-order (b), third-order (c) and fourth-order (d) Fourier harmonics.

Since precipitation either occurs or does not occur on a given day, the two complementary transition probabilities are P00 = 1 - P01 and P10 = 1 - P11.

A generalization of the first-order Markov model is to consider higher-order Markov models such as the second and third-order models. Letting $R_t = 0$ if day t is dry, and $R_t = 1$ if day t is wet, equations (3.1a) and (3.1b) can be extended to the second and third-order Markov chains following equations (3.2) and (3.3):

$$P_{ijk} = Pr\{ R_t = k \mid R_t = j \mid R_t = i \} \tag{3.2}$$

$$P_{hijk} = Pr\{R_t = k \mid R_t = j \mid R_t = i \mid R_t = h\} \tag{3.3}$$

where h, i, j and k =0 or 1, respectively.

The number of parameters required to characterize precipitation occurrence increase exponentially with the order of Markov process. This means that two, four and eight parameters must be estimated for first, second and third-order Markov models, respectively. As mentioned earlier, first-order Markov chains may not be adequate for generating long dry or wet spells. Higher-order Markov models perform better, but more parameters must be determined. Since a minimum number of rainfall events need to be present to adequately estimate transition probabilities, second and third-order parameter estimation requires longer time series of observed precipitation. If the goal is to use WeaGETS as a downscaling tool for climate change studies, the first-order process is usually more practical because it only requires the perturbation of two parameters.

3.3.3 Generation of precipitation quantity

For a predicted rainy day, two probability distribution functions are available to produce the daily precipitation quantity. The first is the one-parameter exponential distribution, which has a probability density function given by

$$f(x) = \lambda e^{-\lambda x} \tag{3.4}$$

where x is the daily precipitation intensity and λ is the distribution parameter (equal to the inverse of the mean).

The other function is the two-parameter gamma distribution. The probability density function for this distribution is given by

$$f(x) = \frac{(x/\beta)^{\alpha-1} \exp[-x/\beta]}{\beta\Gamma(\alpha)} \tag{3.5}$$

where α and β are the two distribution parameters, and Γ(α) indicates the gamma function evaluated at α. This method is easy to compute and performs better than the exponential distribution. Therefore, it is widely used to generate daily precipitation quantity. It would be very easy to add other distribution functions, such as the mixed exponential (a three-parameter distribution) that has also been used in the literature.

3.3.4 Generation of maximum and minimum temperatures

Similarly to WGEN, the WeaGETS uses a first-order linear autoregressive model to generate Tmax and Tmin. The observed time series is first reduced to residual elements by subtracting the daily means and dividing by the standard deviations. The means and standard deviations are conditioned on the wet or dry status. The residual series are then generated by

$$\chi_{p,i}(j) = A\chi_{p,i-1}(j) + B\varepsilon_{p,i}(j) \tag{3.6}$$

where $x_{p,i}(j)$ is a (2×1) matrix for day i of year p whose elements are the residuals of Tmax (j=1) and Tmin (j=2); $\varepsilon_{p,i}(j)$ is a (2×1) matrix of independent random components that are normally distributed with a mean of zero and a variance of unity. A and B are (2×2) matrices whose elements are defined such that the new sequences have the desired auto and cross correlation coefficients. The A and B matrices are determined by

$$A = M_1 M_0^{-1} \tag{3.7}$$

$$BB^T = M_0 - M_1 M_0^{-1} M_1^T \tag{3.8}$$

where the superscripts -1 and T denote the inverse and transpose of the matrix, respectively, and M_0 and M_1 are the lag 0 and lag 1 covariance matrices.

Two options are available to generate Tmax and Tmin on top of the generated residual series. The first is derived from WGEN or version 5.111 of CLIGEN. The daily values of Tmax and Tmin are found by multiplying the residuals by the standard deviation σ and adding the mean μ (equations (3.9) and (3.10)). Throughout this paper, this option is referred to as the unconditional scheme.

$$T_{\max} = \mu_{\max} + \sigma_{\max} \times \chi_{p,i} \tag{3.9}$$

$$T_{\min} = \mu_{\min} + \sigma_{\min} \times \chi_{p,i} \tag{3.10}$$

Because Tmax and Tmin are generated independently of each other based on equations (3.9) and (3.10), there are a number of cases where Tmin is larger than Tmax. Thus, a range check is imposed to force Tmin to be less than Tmax. For example, if Tmin is greater than Tmax, Tmin is set equal to Tmax – 1.

The other option is derived from the latest version of CLIGEN (version 5.22564). The temperature with the smallest standard deviation between Tmax and Tmin is first computed, followed by the others (Chen et al. 2008). This option is referred to as the conditional scheme throughout this paper. If the standard deviation of Tmax is larger than or equal to the standard deviation of Tmin, daily temperatures are generated by equations (3.11) and (3.12):

$$T_{\min} = \mu_{\min} + \sigma_{\min} \times \chi_{p,i} \tag{3.11}$$

$$T_{\max} = T_{\min} + (\mu_{\max} - \mu_{\min}) + \sqrt{{\sigma_{\max}}^2 - {\sigma_{\min}}^2} \times \chi_{p,i} \tag{3.12}$$

If the standard deviation of Tmax is less than that of Tmin, daily temperatures are generated by equations (3.13) and (3.14):

$$T_{\max} = \mu_{\max} + \sigma_{\max} \times \chi_{p,i} \tag{3.13}$$

$$T_{\min} = T_{\max} - (\mu_{\max} - \mu_{\min}) - \sqrt{\sigma_{\min}{}^2 - \sigma_{\max}{}^2} \times \chi_{p,i} \tag{3.14}$$

Using this scheme, Tmin is always less than Tmax and no range check is necessary.

3.3.5 Correction of low-frequency variability

Weather generators underestimate the monthly and inter-annual variance, because they do not take into account the low-frequency component of climate variability. WeaGETS provides an approach to correct for this underestimation, for both precipitation and temperature.

Low-frequency variability is first modeled using a Fast Fourier Transform (FFT) based on the power spectra of the annual time series of precipitation and temperature. Generations of monthly and yearly precipitation and yearly average temperatures data are achieved by assigning random phases for each spectral component, which preserve the power spectrum and variances as well as the autocorrelation function. The link to daily parameters is established through linear functions. Throughout this paper, this is referred to as the spectral correction approach/method. The correction of monthly and inter-annual variability for precipitation follows the approach of Chen et al. (2010). Their results show that this approach performs very well in preserving the low-frequency variability of precipitation and temperatures.

3.4 Generation process

3.4.1 Input data

The input data consists of daily precipitation, Tmax and Tmin. The model does not take into account bissextile years. Any significant precipitation occurring on a February 29th should be redistributed equally on February 28th and March 1st. The maximum and minimum temperatures of a February 29th can be simply removed. Missing data should be assigned a -999 value. The input file contains the following matrices and vectors:

1) P: matrix with dimensions [*nyears**365], where *nyears* is the number of years, containing daily precipitation in mm.
2) Tmax: matrix with dimensions [*nyears* *365], where *nyears* is the number of years, containing maximum temperature in Celsius.
3) Tmin: matrix with dimensions [*nyears* *365], where *nyears* is the number of years, containing minimum temperature in Celsius.
4) yearP: vector of length [*nyears* *1] containing the years covered by the precipitation.
5) yearT: vector of length [*nyears* *1] containing the years covered by the Tmax and Tmin.

3.4.2 Output data

The output also consists of daily precipitation, Tmax and Tmin values. It contains the following matrices:

1) gP: matrix with dimensions [*gnyears**365], where *gnyears* is the number of years of generated precipitation in mm without low-frequency variability correction.
2) gTmax: matrix with dimensions [*gnyears* *365], where *gnyears* is the number of years of generated Tmax in Celsius without low-frequency variability correction.
3) gTmin: matrix with dimensions [*gnyears* *365], where *gnyears* is the number of years of generated Tmin in Celsius without low-frequency variability correction.

If the low-frequency variability correction option is chosen, another file will be produced. It also contains three matrices, named corP, corTmax and corTmin, respectively.

1) corP: matrix with dimensions [*gnyears* *365], where *gnyears* is the number of years of generated precipitation in mm with low-frequency variability correction.
2) corTmax: matrix with dimensions [*gnyears* *365], where *gnyears* is the number of years of generated Tmax in Celsius with low-frequency variability correction.
3) corTmin: matrix with dimensions [*gnyears* *365], where *gnyears* is the number of years of generated Tmin in Celsius with low-frequency variability correction.

3.4.3 Running the program

There are many subprograms in the WeaGETS package, but the user only needs to run the main program *RUN_WeaGETS.m.* All of the options will then be offered in the form of questions, presented as follows:

1) Basic input

a) Enter an input file name (string):

A name for the observed data shall be entered within single quotes, for instance, '*filename*' for the supplied file.

b) Enter an output file name (string):

A name for the generated data shall be entered within single quotes, for example '*filename_generated*'.

c) Enter a daily precipitation threshold:

Precipitation threshold is the amount of precipitation used to determine whether a given day is wet or not (0.1mm is the most commonly used value).

d) Enter the number of years to generate:

The number of years of the generated time series of precipitation and temperatures is entered here.

2) Precipitation and temperature generation

a) Smooth the parameters of precipitation occurrence and quantity (1) or do not smooth (0).

b) If option 1 is selected, enter the number of harmonics to be used (between 1 and 4).

c) Select an order of Markov Chain to generate precipitation occurrence, 1: First-order; 2: Second-order; 3: Third-order.

d) Select a distribution to generate wet day precipitation amount: 1: Exponential or 2: Gamma.
e) Select a scheme to generate Tmax and Tmin: 1: Unconditional or 2: Conditional.

3) Low-frequency variability correction

a) Correct the low-frequency variability of precipitation, Tmax and Tmin (1) or do not correct (0).

   If option 1 is selected, a filename containing the corrected data will need to be entered.

Once weather generation is completed, the first year of generated data without and with the low-frequency variability correction will be plotted.

3.5 An illustration of model performance

Two Canadian meteorological stations are used to illustrate the performance of WeaGETS. The basic information, including average annual precipitation, Tmax and Tmin, longitude, latitude, elevation and record duration for the two stations is given in table 3.1. WeaGETS has been used and tested extensively at several other locations under various climates (Caron, 2006; Chen et al., 2010). These two stations were selected simply to outline the typical outputs and results.

Table 3.1 Location, record period, average annual precipitation, maximum and minimum temperatures (Tmax and Tmin) for Ottawa and Churchill stations

Station name	Latitude (°N)	Longitude (°W)	Elevation (m)	Records of data	Annual precip	Annual Tmax	Annual Tmin
Ottawa	45.26	75.74	93	1891-2008 (118)	882	10.98	0.79
Churchill	58.73	94.05	29	1947-2006 (60)	439.1	-2.71	-10.91

The observed daily precipitation, Tmax and Tmin, were used to run WeaGETS to generate synthetic time series without parameter smoothing. The length of the generated series is 10 times that of the observed series. Statistics including mean, standard deviation, percentiles and extreme values are calculated for both observed and synthesize time series for each meteorological variable.

3.5.1 Precipitation occurrence

The precipitation occurrences are produced using first, second and third-order Markov chains. The statistics of dry and wet spells calculated from those time series are presented in table 3.2. Each Markov model produces a good replication of the mean of both dry and wet spells for both stations. However, the standard deviation of dry spells is slightly underestimated by each model, while the two higher-order models perform somewhat better than the first-order model. Each Markov model reproduced the 25^{th}, 50^{th} and 75^{th} percentiles of both dry and wet spells for both stations. The longest dry spells are overestimated for the Ottawa station and underestimated for the Churchill station. Overall, the performance at the Ottawa station is slightly better that at the Churchill station. The differences between stations are due to the different climate zones they belong to. Churchill is a relative dry station and Ottawa is much wetter. The third-order Markov model is, not surprisingly the best. Wilks (1999b) observed that the first-order Markov model may be inadequate at generating long dry spells in very wet and or dry regions. Here, the replication of long wet spells is better than for long dry spells, especially for the Ottawa station.

3.5.2 Precipitation quantity

To compare the exponential and gamma distributions in terms of accurately producing precipitation quantity, two time series of precipitation occurrence are generated using the first-order Markov model, and then the wet day precipitations are simulated with exponential and gamma distributions, respectively. The results show that both the exponential and gamma distributions reproduce the daily precipitation mean very well (table 3.3). However, they both underestimate the standard deviations of daily precipitation with mean relative

errors (MREs) of -25.8% for exponential distribution and -14.6% for gamma distribution over two stations. This indicates that both distributions underestimate the high-frequency variability of precipitation. Both distributions overestimate the 25^{th}, 50^{th} and 75^{th} percentiles of daily precipitation for both stations, while underestimating the all time maximum daily precipitations. This is understandable because neither the exponential nor the gamma distribution is tailed to generated extreme precipitation events. It is well-documented that extreme precipitation values follow different distribution functions. Both distributions, however, perform well in producing monthly and annual mean precipitation, while they underestimate the standard deviation of monthly precipitation with MREs of -16.0% for exponential distribution and -11.7% for gamma distribution. The standard deviation of annual precipitation is also considerably underestimated with MREs of -31.4% for the exponential distribution and -29.1% for the gamma distribution. As discussed earlier, this indicates that the exponential and gamma distributions underestimate the inter-annual and intra-annual variability of precipitation. Both distributions generate the percentiles of monthly and yearly precipitations very well for the Ottawa station. In contrast, for the Churchill station, both distributions overestimate the lower percentiles of monthly and yearly precipitations, and underestimate the higher percentiles. This indicates (again) that weather generators generally perform better when simulating precipitation for wetter regions than for dry regions. Moreover, the gamma distribution is consistently better than the exponential distribution at simulating precipitation.

3.5.3 Maximum and minimum temperatures

Tmax and Tmin are generated using both unconditional and conditional schemes, conditioned on wet and dry states simulated with first-order Markov model. Table 3.4 presents the statistics of observed and synthetic Tmax and Tmin. The results show that both unconditional and conditional schemes produce the mean of daily temperatures well, although there is a small underestimation of Tmin with the unconditional scheme. This is because Tmax and Tmin are generated independently, resulting in several cases where Tmin is greater than Tmax in a single day. Thus, a range check is imposed to force the generated

Tmin to be less than Tmax. This procedure affects the statistics of Tmin. Overall, both unconditional and conditional schemes provide good simulations of standard deviations of Tmax and Tmin, even though there are some biases. Both schemes poorly reproduce the all time maximum and minimum temperatures, especially for the Churchill station. The conditional scheme is consistently better than the unconditional one for all statistics overall.

Table 3.2 Statistics of dry and wet spells for the Ottawa and Churchill stations (Obs=observed data, Order 1= first-order Markov chain, Order 2= second-order Markov chain, Order 3= third-order Markov chain, and Std = standard deviation)

Station	**Source**	**Dry spell**				**Wet spell**			
		Obs	**Order 1**	**Order 2**	**Order 3**	**Obs**	**Order 1**	**Order 2**	**Order 3**
Ottawa	Mean	3.0	3.0	3.0	3.0	2.0	2.0	2.0	2.0
	Std	2.6	2.4	2.5	2.5	1.3	1.4	1.3	1.3
	25th percentile	1	1	1	1	1	1	1	1
	50th percentile	2	2	2	2	2	1	2	2
	75th percentile	4	4	4	4	2	2	2	2
	Longest	25	29	30	28	16	17	14	14
Churchill	Mean	3.2	3.2	3.2	3.2	2.2	2.2	2.2	2.2
	Std	3.0	2.8	2.8	2.9	1.7	1.7	1.6	1.7
	25th percentile	1	1	1	1	1	1	1	1
	50th percentile	2	2	2	2	2	2	2	2
	75th percentile	4	4	4	4	3	3	3	3
	Longest	43	32	31	39	17	26	19	23

Table 3.3 Statistics of daily, monthly and yearly precipitation quantities for Ottawa and Churchill stations (Obs=observed data, Exp=exponential distribution, Gam=gamma distribution and Std =standard deviation)

Station	**Source**	**Daily**			**Monthly**			**Yearly**		
		Obs	**Exp**	**Gam**	**Obs**	**Exp**	**Gam**	**Obs**	**Exp**	**Gam**
Ottawa	Mean	6.1	6.1	6.1	73.5	73.3	73.6	882.0	879.1	882.8
	Std	7.6	6.2	6.9	33.9	30.2	31.9	112.9	97.7	99.2
	25th percentile	1.3	1.8	1.4	48.7	51.8	50.7	814.1	813.8	816.5
	50th percentile	3.3	4.2	3.8	69.5	69.2	69.4	872.5	880.1	881.9
	75th percentile	8.1	8.4	8.2	94.5	91.5	91.5	961.6	939.4	943.8
	Maximum	108.6	84.1	95.0	250.2	261.7	242.2	1159.2	1273.0	1183.4
Churchill	Mean	2.9	2.9	2.9	36.6	36.4	36.7	439.1	436.9	440.6
	Std	4.8	3.3	3.9	29.1	23.0	24.1	102.5	52.0	55.3
	25th percentile	0.5	0.8	0.6	15.0	18.0	18.0	361.9	400.2	403.3
	50th percentile	1.2	1.8	1.6	28.5	31.0	30.9	426.2	434.7	437.6
	75th percentile	3.2	3.8	3.7	50.3	50.9	50.8	503.3	469.1	476.6
	Maximum	62.3	44.3	84.2	247.0	166.1	183.5	748.5	587.1	644.7

Table 3.4 Statistics of maximum and minimum temperatures for Ottawa and Churchill stations (Std = standard deviation and Max or Min = all time maximum of maximum temperature and all time minimum of minimum temperature, Obs=observed, Uncon=unconditional, con=conditional)

Station	**Source**	**Tmax**			**Tmin**		
		Obs	**Uncon**	**Con**	**Obs**	**Uncon**	**Con**
Ottawa	Mean	11.0	11.0	11.0	0.8	0.4	0.8
	Std	13.0	12.3	12.7	12.0	12.5	11.9
	25th percentile	1.0	-0.2	-0.7	-7.2	-8.8	-8.8
	50th percentile	11.7	12.1	12.0	1.8	2.2	2.3
	75th percentile	22.2	22.5	22.4	10.6	10.6	11.0
	Max or Min	37.8	35.5	38.7	-38.9	-51.6	-47.4
Churchill	Mean	-2.7	-2.7	-2.7	-10.9	-11.7	-10.9
	Std	15.5	14.5	15.3	15.0	15.5	15.2
	25th percentile	-15.2	-15.4	-14.9	-24.6	-24.5	-23.6
	50th percentile	-1.4	-2.4	-2.2	-8.0	-10.3	-9.5
	75th percentile	9.3	10.8	11.0	1.9	2.5	2.8
	Max or Min	36.9	30.0	36.3	-45.4	-70.3	-65.4

Auto and cross-correlations of and between daily Tmax and Tmin are computed for observed and synthetic (unconditional and conditional) time series (figure 3.3). The autocorrelation is a measure of the persistence of temperature trends, and is an important characteristic to reproduce. The unconditional scheme reproduces the observed lag 1 autocorrelation well, but for larger lags its values are consistently greater than those of observed data for both stations. The conditional scheme reproduces the day-to-day persistence much better. Similar conclusion can also been found when looking at cross-correlation.

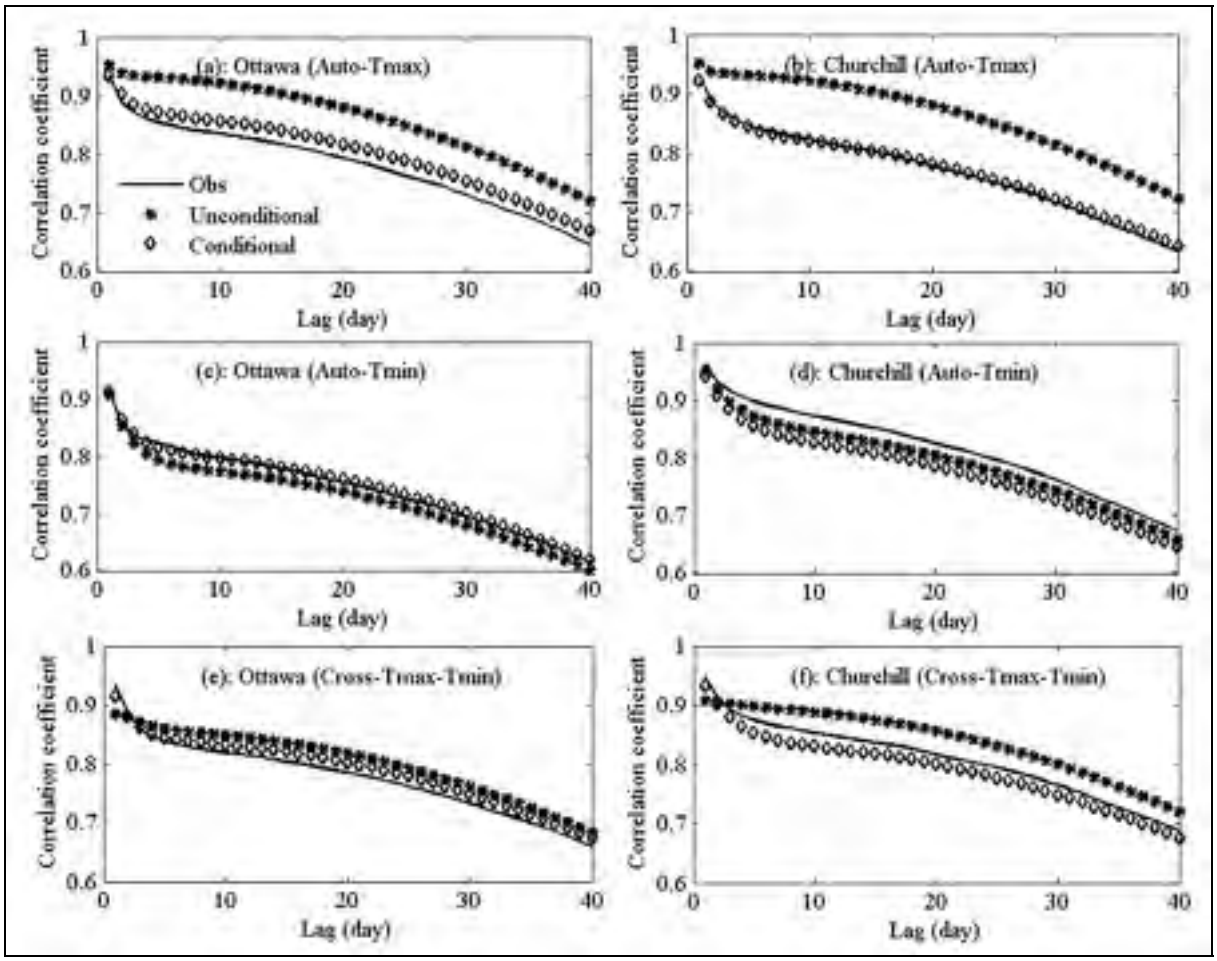

Figure 3.3 40 days of lagged auto and cross-correlation of and between observed (OBS), unconditional and conditional generated data for maximum and minimum temperatures for the Ottawa and Churchill stations.

3.5.4 Low-frequency variability correction

A main advantage of WeaGETS over most other stochastic weather generators is that an approach to correct for the underestimation of the low-frequency variability for both precipitation and temperature is built in. This section illustrates the performance of the spectral correction approach in dealing with this problem. Two data sets (both including precipitation, Tmax and Tmin) were generated using a first-order Markov model for precipitation occurrence, gamma distribution for wet day precipitation quantity and the

conditional scheme for Tmax and Tmin. One data set is corrected using the spectral correction method and the other is not. The mean and standard deviations of monthly precipitation are compared for both data sets, as well as the means, standard deviations and auto correlations of annual precipitation, Tmax and Tmin.

Figure 3.4 presents the ratios of the mean and standard deviations of monthly and annual precipitations derived from the synthesized weather series to those derived from the observed series. Without spectral correction, WeaGETS reproduces monthly and annual averaged precipitations well (figure 3.4a and 3.4b), but it underpredicts the variance of monthly and yearly precipitation, as shown in figures 3.4c and 3.4d. Spectral correction significantly improves this performance.

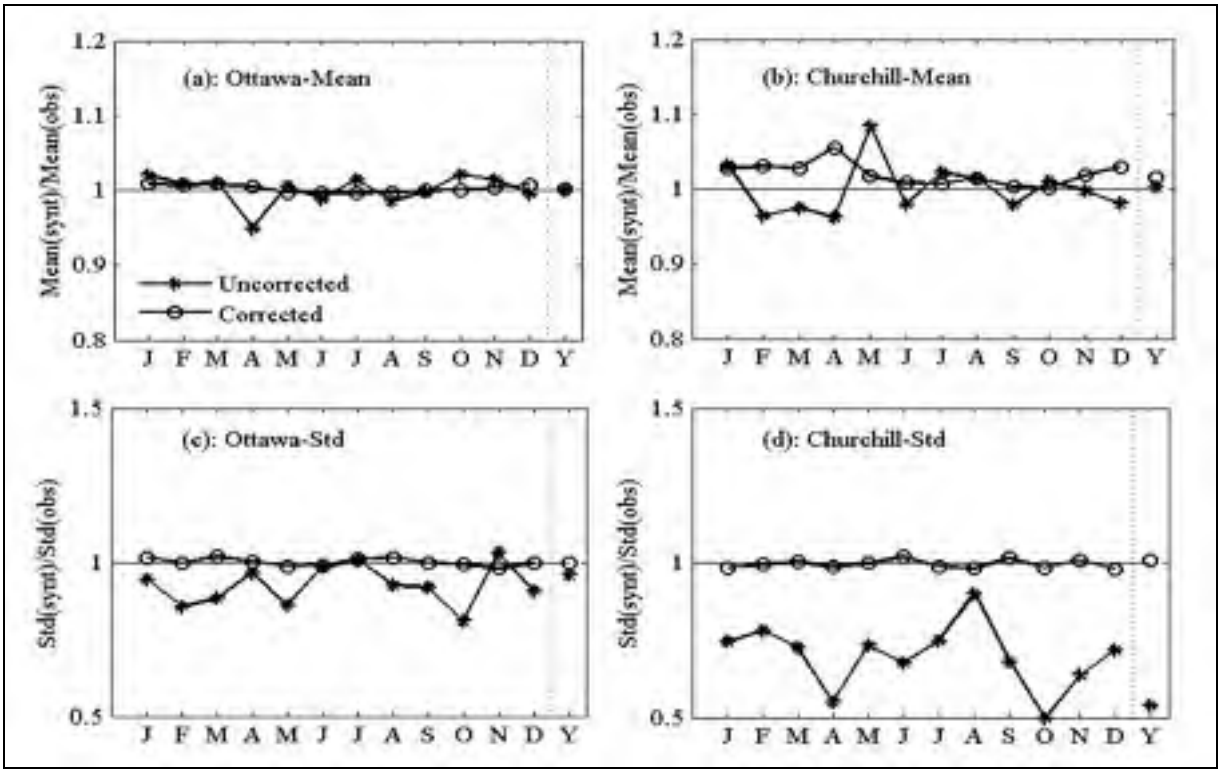

Figure 3.4 The ratios of the mean and standard deviations (std) of monthly and annual precipitations derived from the synthetic weather series (synt) to the mean and standard deviations derived from the observed series (obs) for the Ottawa and Churchill stations. The synthetic precipitation series includes both uncorrected and corrected time series.

The means of yearly Tmax and Tmin are reproduced very well by the conditional scheme at both stations, with or without correction (table 3.5). Without correction, as was the case for precipitation, WeaGETS underestimates the inter-annual variability of temperature data, as represented by its standard deviation. In contrast, the spectral correction method preserves the standard deviations of yearly Tmax and Tmin very well.

Table 3.5 Mean and standard deviations of yearly Tmax and Tmin derived from the synthesized and observed series for Ottawa and Churchill stations. The synthesized precipitation series includes both uncorrected and corrected time series

Source	Ottawa					Churchill				
	Tmax			Tmin		Tmax			Tmin	
	Mean	Std		Mean	Std	Mean	Std		Mean	Std
Obs	10.98	0.84		0.79	1.09	-2.71	1.25		-10.91	1.18
Uncorrected	11.00	0.43		0.44	0.51	-2.70	0.66		-10.90	0.71
Corrected	10.98	0.83		0.79	1.08	-2.71	1.21		-10.91	1.12

The annual autocorrelation functions of observed annual precipitation, Tmax and Tmin presented in figure 3.5, display clear trends, indicating that dryer and wetter years, and warmer and cooler years, do not occur in random order. Without correction, weather generators simply aim to reproduce the same mean climatology year after year, as shown in figure 3.5. The spectral correction method successfully reproduces the observed autocorrelation of precipitation, Tmax and Tmin for both stations.

3.6 Discussion and conclusions

WeaGETS is a Matlab-based daily stochastic weather generator that can generate precipitation, Tmax and Tmin time series of unlimited length, thus permitting impact studies of rare occurrences of meteorological variables. Furthermore, by perturbing its parameters according to changes projected by climate models, it can be used as a downscaling tool for climate change studies. WeaGETS has the advantage of incorporating the computational

schemes of other well-known weather generators, as well as offering unique options, such as correction of the underestimation of inter-annual variability, and the ability to use Markov chains of varying orders. More importantly, the use of Matlab allows for easy modification of the source code to suit the specific needs of users. It would be very easy, for example, to add additional precipitation distribution functions. Finally, Matlab offers an integrated environment to further analyze the data generated by WeaGETS.

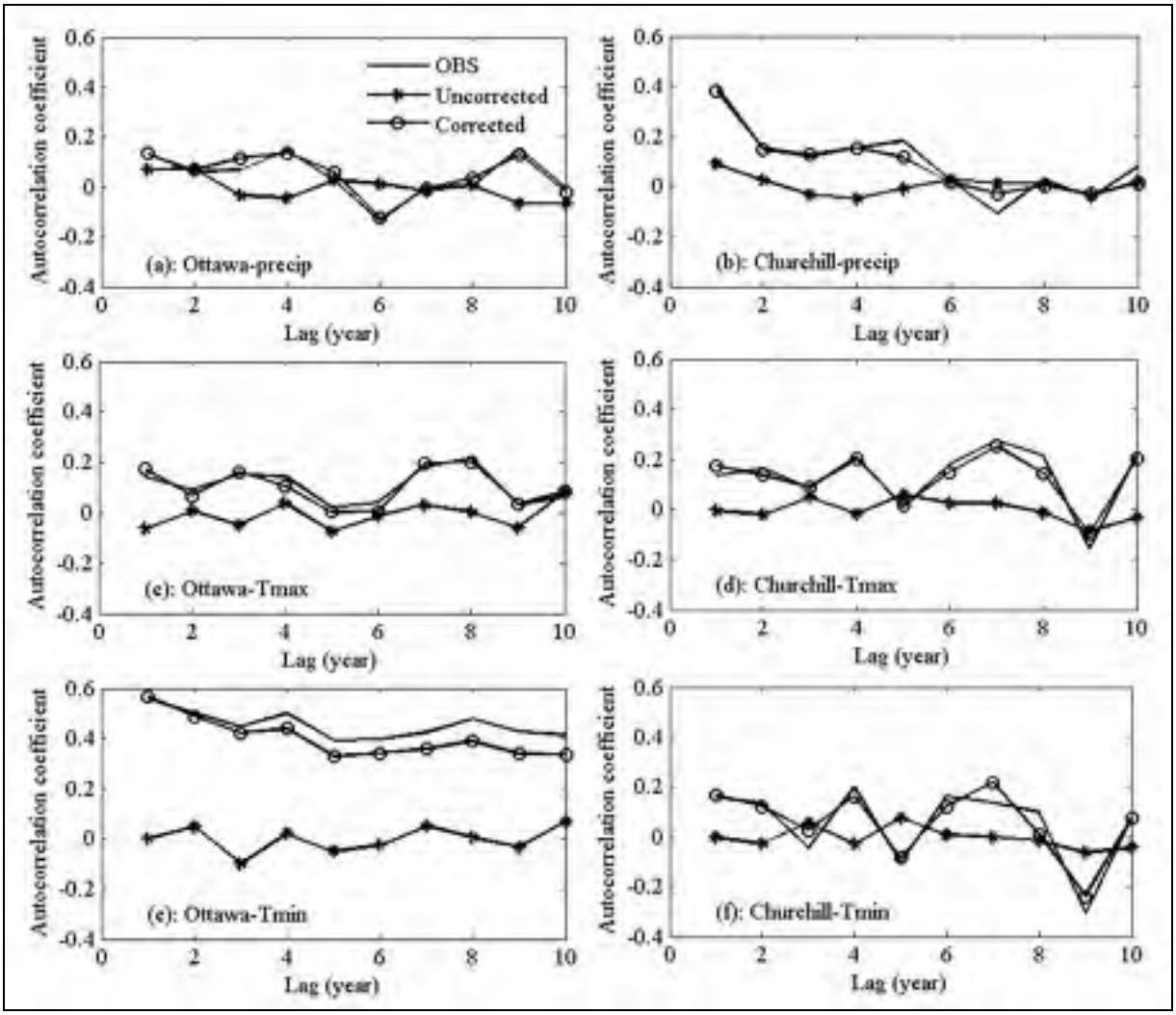

Figure 3.5 10-year lagged autocorrelation of observed (OBS), weather generator produced (uncorrected and corrected) average yearly precipitation, Tmax and Tmin for the Ottawa and Churchill stations.

Two Canadian stations are selected to illustrate WeaGETS' performance. The results demonstrate that the most widely used model, a first-order Markov model, is adequate at producing precipitation occurrence, but it underestimates the longest wet and especially dry spells. The higher-order models have positive effects. The gamma distribution is consistently better than the exponential distribution in generating precipitation quantity, and the conditional scheme is better than the unconditional scheme at simulating temperatures. As is the case for all available weather generators, WeaGETS underestimates the monthly and inter-annual variances of precipitation and temperatures. The included spectral correction approach option is very successful in resolving this underestimation problem.

Although WeaGETS is more flexible than other available weather generators in generating precipitation, Tmax and Tmin, it does have a few limitations. Firstly, the exponential and gamma distributions are inadequate at reproducing the extremes of precipitation, because they are not heavy-tailed. The three-parameter Pearson III distribution or Fréchet distribution may be better. However, the extremes of precipitation have been drawn from rather different populations than most daily precipitation observations that the distribution has been fit to (Wilks, 1999b), because they are associated with unusual meteorological events. Moreover, the distribution of extreme precipitation can vary quite drastically on a regional basis, and it is no simple task to find a distribution that is suitable for all climate zones. As mentioned earlier, users working with a specific distribution function can easily add it to WeaGETS. Another limitation is linked to the spectral correction approach that keeps the precipitation occurrence process constant. Ongoing work shows that the transition probabilities also display inter-annual variability. However, a relatively simply approach to adjust the low-frequency variability of precipitation occurrence remains elusive. Finally, the low-frequency variability of temperatures is only corrected at the yearly scale. Consequently, the monthly variability is improved, but it is not as good as that at the yearly scale (results not shown). This is because the correction of inter-annual variability has a limited effect at the monthly scale (Chen et al., 2010). Thus, it may be necessary to correct the monthly variability at the same time, but this may bring along overfitting problems resulting in cases where Tmin is greater than Tmax in a given day. Therefore, this type of correction is not incorporated into

this version of WeaGETS. When working with weather generators, there is always the danger that more complex schemes dealing with secondary statistics may have a negative impact on the more fundamental distribution properties of the generated variables. The authors plan to address these problems in future versions of WeaGETS.

CHAPTER 4

COUPLING STATISTICAL AND DYNAMICAL METHODS FOR SPATIAL DOWNSCALING OF PRECIPITATION

Jie Chen[1], François P. Brissette[1], Robert Leconte[2]

1. Department of Construction Engineering, École de technologie supérieure, Université du Québec, 1100, rue Notre-Dame Ouest, Montréal, Québec, Canada, H3C 1K3.
2. Department of Civil Engineering, Université de Sherbrooke, 2500, boul. de l'Université, Sherbrooke, Québec, Canada, J1K 2R1

This article was submitted to the Climatic Change in February, 2010.

4.1 Abstract

The resolution of General Circulation Models (GCMs) is too coarse for climate change impact studies at the catchment or site-specific scales. To overcome this problem, both dynamical and statistical downscaling methods have been developed. Each downscaling method has its advantages and drawbacks, which have been described in great detail in the literature. This paper evaluates the improvement in statistical downscaling (SD) predictive power when using predictors from a Regional Climate Model (RCM) over a GCM. Our approach uses mixed downscaling, combining both dynamic and statistical methods. Precipitation, a critical element of hydrology studies that is also much more difficult to downscale than temperature, is the only variable evaluated in this study. The SD method selected here uses a stepwise linear regression approach for precipitation quantity and occurrence (similar to the well-known Statistical Downscaling Model (SDSM) and called SDSM-like herein). In addition, a discriminant analysis (DA) was tested to generate precipitation occurrence, and a weather typing approach was used to derive statistical relationships based on weather types, and not only on a seasonal basis as is usually done. To compare the relative efficiency of the SD approaches, relationships were derived at the same

sites using the same predictors at a 300km scale (the National Center for Environmental Prediction (NCEP) reanalysis) and at a 45km scale with data from the limited-area Canadian Regional Climate Model (CRCM) driven by NCEP data at its boundaries. Predictably, using CRCM variables as predictors rather than NCEP data resulted in a much-improved explained variance for precipitation, although it was always less than 50% overall. For precipitation occurrence, the SDSM-like model slightly overestimated the frequencies of wet and dry periods, while these were well-replicated by the DA-based model. Both the SDSM-like and DA-based models reproduced the percentage of wet days, but the wet and dry statuses for each day were poorly downscaled by both approaches. Overall, precipitation occurrence downscaled by the DA-based model was much better than that predicted by the SDSM-like model. Despite the added complexity, the weather typing approach was not much better at downscaling precipitation than approaches without classification. Overall, despite significant improvements in precipitation occurrence prediction by the DA scheme, and even going to finer scales predictors, the SD approach tested here still explained less than 50% of the total precipitation variance. While going to even smaller scale predictors (10-15 km) might improve results even more, such smaller scales would basically transform the direct outputs of climate models into impact models, thus negating the need for statistical downscaling approaches.

Keywords: Downscaling; Statistical downscaling, Weather typing; Precipitation; Regional climate model

4.2 Introduction

Mismatches of spatial and temporal resolutions between General Circulation Model (GCM) outputs and the data requirements of hydrological models pose major obstacles to the quantification of the hydrologic impacts of climate change. This is because GCMs generally run at a resolution of 150-300 km (IPCC 2007) while impact study models usually require data at a much finer resolution, from station data to resolutions of a just few kilometers. Therefore, “downscaling” techniques have been developed to deal with scale and resolution.

There are two widely used downscaling techniques: dynamic downscaling (regional climate models (RCMs)) and statistical downscaling (SD). RCMs are limited-area dynamic models that use GCMs data at their boundary, both spatially and temporally. The main drawback of RCMs is that they are computationally costly complex models (Solman and Nunez 1999). As such, RCM data is relatively scarce, fewer greenhouse gas emission scenarios are run and, except for a few inter-comparison studies, data from more than one model is rarely available for climate change uncertainty studies. Moreover, despite improvements, the output of RCMs is still too coarse for several practical applications, such as smaller watersheds and site-specific agricultural impact studies, which may need local and site-specific climate scenarios. SD involves linking the states of certain variables that represent a large-scale (GCMs or RCMs grid-scale - predictors) model, and the states of certain variables representing a much smaller-scale (catchment or site0scale - predictands) model. SD approaches are computationally cheap and relatively simple and easy to apply. Thus, a wide range of SD techniques have been developed. Those techniques fall into three main categories: transfer function, weather typing, and weather generator (Wilby and Wigley 1997; von Storch et al. 2000; Zhang 2005). In reality, many downscaling studies use more than one of these categories (Wilby and Wigley 1997).

4.2.1 Transfer function approaches

Transfer function approaches involve establishing statistical linear or nonlinear relationships between observed local climatic variables (predictands) and large-scale GCM or RCM outputs (predictors). The most commonly used methods for deriving those relationships include multivariate linear or nonlinear regressions, principle component analysis (PCA), canonical correlation analysis (CCA), singular value decomposition (SVD), and artificial neural networks (ANN). The most commonly used predictors from GCM outputs include vorticity, airflow indices, wind velocity and direction, mean sea level pressure, geopotential heights, and relative humidity (Wilby et al. 1998a; Solman and Nunez 1999; Sailor and Li 1999; Trigo and Palutikof 2001). Widmanm et al. (2003) and Zhang (2005) downscaled precipitation using GCM precipitation as a predictor. The results showed that the

performance was better using GCM precipitation as a predictor than with conventional methods using other predictors. However, most authors agree that predictors selected should be variables that are reasonably well-reproduced by GCM (or RCM), and precipitation may not fit this criterion, especially at the GCM scale.

The most typical transfer function approach makes use of the statistical downscaling model (SDSM) developed by Wilby et al. (2002a) for the rapid development of single-site, ensemble scenarios of daily weather variables. This model is good at downscaling temperature with a percentage of explained variance normally in excess of 70%, but its performance is not as good for precipitation, with an explained variance usually less than 30%. The linear regression scheme of the SDSM also results in downscaled precipitation that has a much smaller standard deviation than observed precipitation. To overcome this problem, a stochastic component is added to the downscaled data.

The main strength of the transfer function approach to future climate scenario generation is the relative ease of application. A potential obstacle is the probable lack of a temporally stable relationship between predictors and predictands. For example, Wilby (1997) has shown that, even within a single circulation regime, precipitation diagnostics may vary considerably from year to year.

4.2.2 Weather typing schemes

Weather typing downscaling methods involve grouping local meteorological variables in relation to different classes of atmospheric circulation based on a given weather classification scheme (Bardossy and Plate 1992; von Storch et al. 1993). In general, weather classification procedures include PCA (White et al. 1991; Shoof and Pryor 2001), cluster analysis (Wilks 1995), CCA (Gyalistras et al. 1994), fuzzy rules (Bardossy et al. 1995), ANN (Bardossy et al. 1994), analogue procedures (Martin et al. 1997; Timbal et al. 2009) and Lamb Weather Types (Lamb 1972; Jones et al. 1993; Conway and Jones 1998). Within a classification scheme, weather types are grouped and the relationships between large-scale variables and

local meteorological variables may be established separately for each weather type. The analogue approach is a weather typing scheme that involves finding the event in the past when the situation most closely resembles the day in the future. The benefits of the analogue approach are that it is able to preserve the spatial correlation of predictands and it is easy to apply, even if the predictands do not follow a normal distribution. However, only events that have occurred in the past can be modeled; thus, it cannot study rare events under future climate changes.

Shoof and Pryor (2001) downscaled precipitation and temperatures based on the PCA classification scheme. PCA was first employed to reduce the number of inter-correlated variables to a smaller set of uncorrelated components. Principle component elements were then calculated for each day and used as predictors to fit linear (for temperatures) and Poisson (for precipitation) transfer functions with the local meteorological variables. The results showed that the precipitation models exhibited poorer predictive capabilities. This may be due to the use of principal component elements as predictors rather than circulation climate variables, such as vorticity, airflow indices and wind speed.

The main advantage of weather typing schemes is that local variables are sensitively linked to large-scale atmospheric circulations. Compared to other downscaling techniques, it provides a greater understanding of the problems involved. The drawbacks of this method are that the reliability depends on the stationary relationship between large-scale circulation and local climate, and that it requires the additional task of weather classification.

4.2.3 Weather generator approaches

Over the past decade, stochastic weather generators have been used in climate change studies as downscaling tools (Wilks 1992, 1999a; Semenov and Barrow 1997; Pruski and Nearing 2002; Zhang et al. 2004, Zhang 2005; Zhang and Liu 2005; Minville et al. 2008). This is achieved by perturbing their parameters according to the changes of future climates, derived from GCMs or RCMs.

Wilby et al. (2002b) explored the use of synoptic-scale predictor variables to downscale both the high- and low-frequency variability of daily precipitation at sites across Great Britain. The results showed that conditionally stochastic rainfall models displayed positive effects on monthly rainfall statistics, but they did not completely remove overdispersion. As mentioned earlier, Zhang (2005) used a transfer function approach to spatially downscale monthly GCM output from grid-scale to site-scale using only GCM monthly precipitation as a predictor. Subsequently, the monthly precipitation was temporally downscaled to a daily time scale using the weather generator CLIGEN. The method is relatively simple and can produce infinite-length time series with the same statistical properties of climate scenarios. However, this method adjusts the precipitation occurrence according to the relationship between monthly precipitation and transition probability used to describe the precipitation occurrence process. There is frequently no strong relationship. Similarly to Zhang's method, Wilks (1999a) and Chen et al. (2006) also downscaled precipitation with weather generators by adjusting their statistical parameters based on the changes in monthly precipitation. The downscaled daily precipitation series are then generated by weather generators using adjusted parameters. The results illustrated that the proposed method was capable of reproducing the mean precipitation quantity.

Overall, the most appealing feature of using a weather generator approach is its ability to rapidly produce sets of climate scenarios for studying the impacts of rare climate events. The disadvantages are that the precipitation occurrence parameters cannot be easily adjusted for future climate conditions, and unanticipated effects on secondary variables may be induced which then changes the quantity of one variable; for example, adjusting the precipitation occurrence may affect the precipitation amount, because both determine the precipitation amount.

4.2.4 Comparison of statistical downscaling methods

Given the range of possible downscaling techniques, a comparison in their predictive ability is needed for a given application. Wilby et al. (1998b) investigated the abilities of six downscaling methods: two weather generator techniques (WGEN and a method based on spell-length duration (SPEL)), two methods using vorticity as a predictor (B-Circ and C-Circ), and two variations of ANN using circulation data and circulation with temperature data as predictors. The validation tests showed that the WGEN and SPEL methods performed better than all the other methods for the majority of diagnostics. However, they both underestimated the standard deviation of monthly precipitation. The B-Circ and C-Circ methods performed well, and were better than the ANN methods, which consistently overestimated the frequency of wet days.

Widmann et al. (2003) compared three SD methods: local rescaling, SVD, and local rescaling with a dynamical correction, using precipitation as a predictor. The results demonstrated that the SVD method explained over 60% of the observed monthly precipitation variability at almost all locations in the studied region. The local scaling method also performed very well over most parts of the region, but it was not as good as the SVD method. Moreover, the local rescaling with a dynamical correction method performed almost as well as the SVD approach. This research indicated that using GCM-simulated precipitation as a predictor may have positive effects. Diaz-Nieto and Wilby (2005) compared the abilities of "change factor" (CF) and SD methods to assess the impact of climate change on low flow in a river basin. The results illustrated that the changes of low flow related to the SD scenarios are generally more complex than those arising from CF methods. Wetterhall et al. (2007) evaluated four downscaling methods: two analog (one using PCA and one using gradients in the pressure field (Teweles-Wobus scores, TWS)) and two conditional-probability methods (one using classification of weather patterns (MOFRBC) and one using SDSM. The results showed that MOFRBC and SDSM, the conditional-probability methods, were superior to the analog methods for the ranked probability scores; analog methods were better than other methods in

winter and autumn; and SDSM and TWS were most accurate in the spring and MOFRBC in the summer.

Overall, each SD method has its advantages and drawbacks. The choice of one method over another should be made according to the application purposes, time of year and data availability. Moreover, more robust SD methods need to be developed for impact assessment studies of climate change.

The objectives of this research are to (1) evaluate the improvement in SD using RCM variables as predictors over GCM, based on an SDSM-like model, and (2) assess the efficiency of a weather typing approach in downscaling precipitation using Canadian RCM (CRCM) variables as predictors.

4.3 Methodology

The SD method selected here uses a stepwise linear regression approach for precipitation quantity and occurrence (similar to the well-known SDSM model and called SDSM-like herein). In addition, a discriminant analysis (DA) was used to generate precipitation occurrence, and a weather typing approach was used to derive statistical relationships based on weather types and not only on a seasonal basis as is usually done. Predictor variables were derived from the Canadian RCM (CRCM4.2.0), and, at the GCM-scale, from the National Center for Environmental Prediction (NCEP) re-analysis data interpolated to the CGCM3.1 grid. The data used in this research covers the period 1970 to 1999. The NCEP and the CRCM predictors considered are listed in tables 4.1 and 4.2, respectively.

4.3.1 Downscaling precipitation occurrence

Two methods are used to downscale precipitation occurrence, one based on linear regression (the SDSM-like model) and one based on DA.

Table 4.1 NCEP predictor variables used to select precipitation predictors for downscaling

Predictor variable	**Abbreviation**	**Predictor variable**	**Abbreviation**
Mean sea level pressure	ncepmslp	500hPa Divergence	ncepp5zh
1000hPa Wind Speed	ncepp_f	850hPa Wind Speed	ncepp8_f
1000hPa U-component	ncepp__u	850hPa U-component	ncepp8_u
1000hPa V-component	ncepp__v	850hPa V-component	ncepp8_v
1000hPa Vorticity	ncepp__z	850hPa Vorticity	ncepp8_z
1000hPa Wind Direction	ncepp_th	850hPa Geopotential	ncepp850
1000hPa Divergence	ncepp_zh	850hPa Wind Direction	ncepp8th
500hPa Wind Speed	ncepp5_f	850hPa Divergence	ncepp8zh
500hPa U-component	ncepp5_u	500hPa Specific Humidity	ncep s500
500hPa V-component	ncepp5_v	850hPa Specific Humidity	nceps850
500hPa Vorticity	ncepp5_z	1000hPa Specific Humidity	ncepshum
500hPa Geopotential	ncepp500	Temperature at 2m	nceptemp
500hPa Wind Direction	ncepp5th		

4.3.1.1 SDSM-like model

The SDSM uses a conditional process to downscale precipitation. Local precipitation amounts depend on wet-/dry-day occurrence, which in turn depend on regional-scale predictors such as mean sea level pressure, specific humidity and geopotential height (Wilby et al. 1999; Wilby and Dawson 2007). Specifically, downscaling of precipitation occurrence is achieved by linking daily probabilities of non-zero precipitation (P_{wet}) with large-scale predictor variables (Wilby et al. 1999).

Table 4.2 Surface and upper-air variables of CRCM used for synoptic classification of circulation indices and to select precipitation predictors for downscaling

Surface variables	**Abbreviation**	**Surface variables**	**Abbreviation**
East component of wind at 10-meter height	ESU	Total precipitation rate	PCP
East component of wind at 10-meter height	NSV	Specific humidity at 2-meter height	SQ
Screen temperature at 2-meter height	ST	Surface pressure	PS
Upper-air variables	Abbreviation	Upper air variables	Abbreviation
Air temperature		North component of wind	
850 hPa	TEMP850	850 hPa	NV850
700 hPa	TEMP700	700 hPa	NV 700
500 hPa	TEMP500	500 hPa	NV 500
Relative humidity		Cloud by layer	
850 hPa	RHUM850	850 hPa	CLD850
700 hPa	RHUM700	700 hPa	CLD700
500 hPa	RHUM500	500 hPa	CLD500
East component of wind		Absolute vorticity	
850 hPa	EU850	850 hPa	AVRT850
700 hPa	EU700	700 hPa	AVRT700
500 hPa	EU500	500 hPa	AVRT500

Similarly to the SDSM, P_{wet} for a given day was downscaled using NCEP and CRCM variables, respectively, and a lag-1 autocorrelation parameter as predictors in this study (referred to as the SDSM-like model). The steps are: (1) A partial correlation analysis was applied to identify the relationship between NCEP (or CRCM) variables and P_{wet}. Variables with significant correlation to the P_{wet} plus lag-1 autocorrelation parameter of P_{wet} were selected as predictors; (2) A multiple linear regressive equation was fitted between P_{wet} and

step (1)-identified predictors plus lag-1 P_{wet}; and (3) A uniformly distributed random number r ($0 \leq r \leq 1$) was used to determine whether precipitation occurs. For any given day, a wet-day occurred if $r \leq P_{wet}$.

4.3.1.2 Discriminant analysis

The other downscaling method is based on the DA using NCEP (or CRCM) variables, respectively, and their lag-1 variables as predictors. With DA, it is necessary to have an available "training sample" in which it is known that each of the vectors is classified correctly (Wilks 1995). In this research, NCEP (or CRCM) variables and their lag-1 variables were used as the training sample. The precipitation series were first divided into two groups, a wet-day group (daily precipitation amount ≥1mm) and a dry-day group (daily precipitation amount < 1mm). The future observation of unknown groups (wet - and dry - days) was similarly classified according to rules constructed based on training sample and corresponding groups.

A weather typing approach described in section of 4.3.2.2 was also used to downscale precipitation occurrence based on the DA and using CRCM variables as predictors to assess the efficiency of the weather typing approach in downscaling precipitation occurrence.

4.3.2 Downscaling of the daily precipitation amount

Precipitation amounts were downscaled using an SDSM-like model and a weather typing approach. For the SDSM-like model, precipitation amounts were downscaled from both GCM scale (NCEP data) and CRCM scale to site-specific scale in order to assess the improvement in SD using RCM variables over GCM.

4.3.2.1 SDSM-like model

The SDSM-like model was used in this research as a benchmark method to compare with the weather typing approach and to assess the improvement in SD using predictors at the RCM scale over the GCM scale. The main difference from the SDSM package is that we only look at the predictive power of the statistical functions without the stochastic component of SDSM (variance inflation and bias correction) that acts as a weather generator superimposed over the SD scheme. The main procedures of the SDSM-like model are the following:. 1-Identification of the screen variable: a partial correlation analysis was used to identify the relationship between NCEP (or CRCM) variables and precipitation amounts. Their lag-1 variables were also used as candidate predictors. Variables which significantly correlated to precipitation amounts were then selected as predictors; 2-Model calibration: multiple linear regressive equations were established between precipitation amounts and step one-identified predictors for each season. Since the distribution of the daily precipitation is highly skewed, a fourth root transformation was applied to the original data before fitting the transfer function; and 3-Application of transfer functions: established transfer functions were further used to downscale precipitation amounts for data series at the validation period.

4.3.2.2 Weather typing scheme

The local meteorological conditions are controlled by the synoptic-scale meteorological system (Orlanski, 1975). For certain meteorological applications it is useful to group weather into distinct types. By doing this, the weather within the same type is more or less homogeneous, while it is markedly different in other types. Generally speaking, the weather forces may be similar in a weather type but inhomogeneous in different types. When this concept is used for downscaling, the weather types are first classified using either GCM or RCM-scale variables, and different predictor sets are then selected to downscale the local variables according to each weather type. This provides for a greater physical understanding of the climate sensitivity and variability. In contrast, a traditional downscaling model like SDSM does not specifically consider the climate sensitivity and variability because it uses

the same predictors for a given time period (monthly, seasonal or annual). Thus, one of the goals of this research is to assess the efficiency of a weather typing approach in downscaling precipitation amount and occurrence. The weather typing approach was only tested with the CRCM4.2.0 data.

The specific procedures are: 1-Synoptic classification: CRCM variables were first subjected to PCA. The first few components that explain most of the variance of the original dataset were selected. By doing this, a number of inter-correlated variables were reduced to a smaller set of uncorrelated principle components. Principal component elements were then calculated for each principal component and cluster analysis was applied to them to obtain a number of different weather types; 2-Determining the screen variables for each weather type: similarly to the SDSM-like model, partial correlation analysis was used to identify the relationship between CRCM variables and precipitation amounts for each weather type. The variables that significantly correlated to daily precipitation were used as predictors for a specific weather type; 3- Model calibration: multiple linear regressive equations were established between precipitation amounts and step 2-identified predictors for each weather type. Similarly to the SDSM-like model, a fourth root transformation was applied to the original data before fitting the transfer function; and 4- Model validation: the same as for the SDSM-like model described above in 4.3.2.1.

4.3.3 Model validation

The observed precipitation series were divided into two periods: 1970-1984 and 1985-1999. The first half period of data was used to calibrate the model. For the SDSM-like model and weather typing approach, this dataset was used to fit the transfer function; for the DA based model, this dataset was used as a known group to build the discriminant function to derive unknown precipitation occurrence. The second data period was used for validation. The following diagnostics were used to validate the capabilities of each downscaling model (table 4.3).

Table 4.3 Diagnostics used to validate the downscaling method

Diagnostics	
Precipitation occurrence	Precipitation amount
Frequency distribution of dry and wet periods	Mean of daily precipitation
The longest wet and dry spells	Standard deviation of daily precipitation
Total wet days	Distribution of daily precipitation (Q-Q plot)
Successful rates of identified wet and dry days	Explained variance

4.3.4 Studied river basin and data

Results from four stations over the Gatineau River Watershed (Southwestern portion of the Quebec province in Canada) are presented in this paper (table 4.4).

Table 4.4 Location, record period, and average annual precipitation for 4 stations

Station	**Latitude (°N)**	**Longitude (°W)**	**Elevation (m)**	**Records of daily precipitation**	**Precipitation (mm)**
svir219	47.53	74.41	461	1970-1999 (30)	981.1
svir293	47.19	76.30	387	1970-1999 (30)	980.4
svir559	46.04	76.03	142	1970-1999 (30)	973.9
svir689	45.51	76.26	81	1970-1999 (30)	861.6

4.4 Results

4.4.1 Downscaling of daily precipitation occurrence

The frequencies of the observed, SDSM-like and DA-based model's downscaled wet and dry spells at station svir293 using CRCM variables as predictors are plotted in figure 4.1. Since similar results were obtained from all four stations, for illustration purposes only results from

the svir293 station are shown. The SDSM-like model slightly overestimated the frequencies of the wet and dry periods, especially at low frequencies. However, the longest wet and dry periods were slightly underestimated, with 13 and 11 days the observed and DA-downscaled longest wet periods, and 21 and 18 days the longest observed and DA-downscaled dry periods. Wilby et al. (2002a) reported a similar result when precipitation occurrence was downscaled using SDSM. In contrast, the frequencies of both wet and dry periods were well replicated by the DA-based model. The longest wet and dry periods were also reasonably well-produced, with 13 and 13 days for the longest wet periods, and 21 and 18 days for the observed and downscaled longest dry periods.

NCEP variables were used as predictors to downscale precipitation occurrence to assess the improvement in SD using RCM-scale over GCM-scale variables (table 4.5). The results showed that both downscaling methods, the SDSM-like and the DA-based models, well-reproduced the total wet days. Consequently, the total dry days were also well-produced. Moreover, there were no distinct differences noted from using these models.

However, the reproduction of total wet or dry days is not adequate to judge the ability of downscaling models, because if both the wet and dry days are poorly produced and have a similar number of error cases, the errors may be offset. A more useful metric is the percentage of correct wet and dry day classifications (Wilks 1995). The results presented in table 4.5 indicate that neither of the precipitation occurrence downscaling models was successful in producing wet and dry days, although the DA-based model was better than the SDSM-like model. For the SDSM-like model, there was essentially no difference from the observed results whether using NCEP or CRCM variables as predictors. It reproduced dry days better than wet days; the averaged success rate for the dry days was 61.5% with NCEP variables as predictors and 61.3% when using CRCM variables. For wet days, these numbers were 38.9% and 39.0%, respectively.

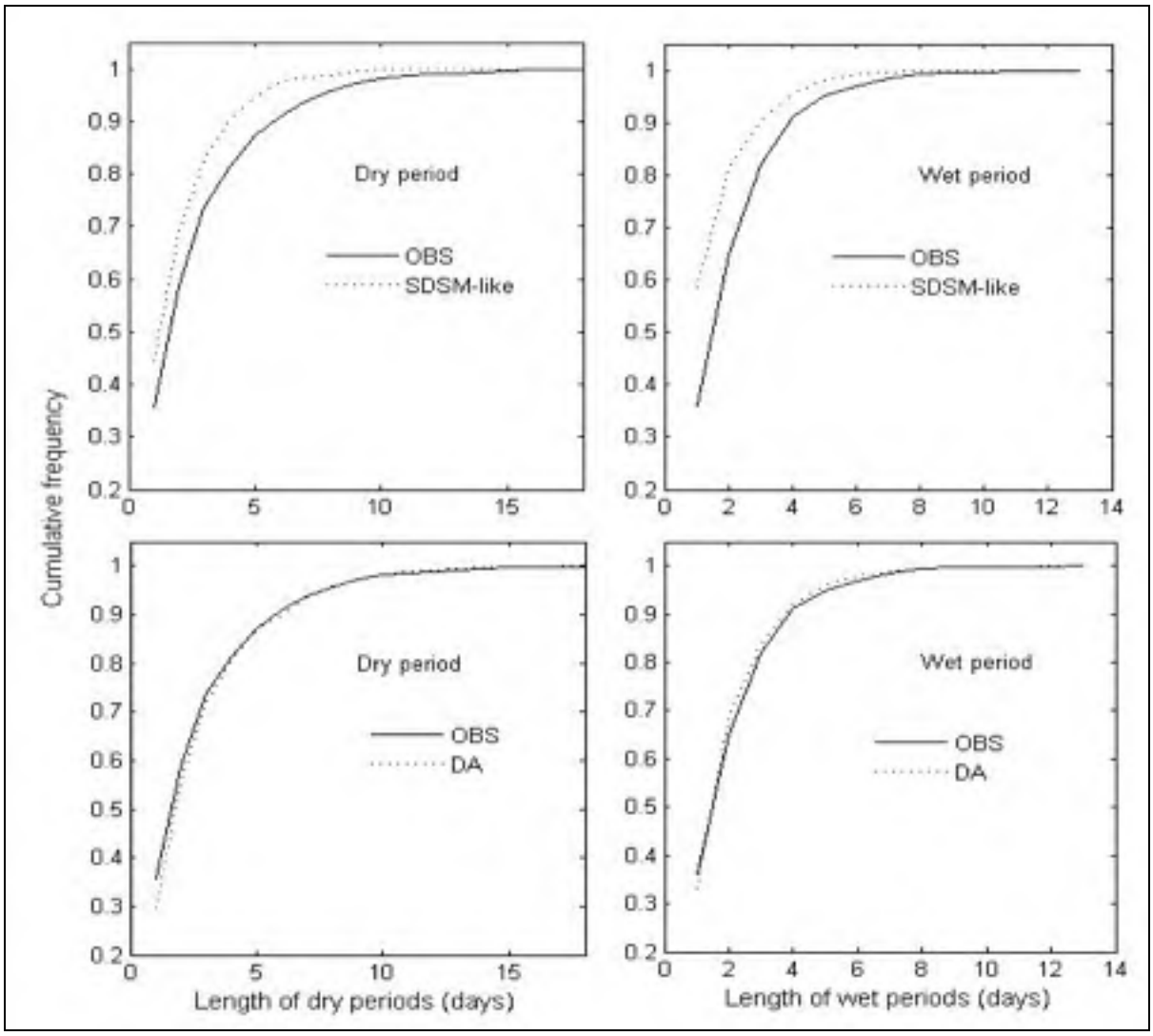

Figure 4.1 Frequency distribution of wet and dry periods extracted from observed (OBS) and downscaled daily precipitation occurrences at the svir293 station. The downscaling methods include the SDSM-like model and discriminant analysis (DA).

A similar success rate of wet and dry days were found by Wilby et al. (1999) in their studies using HadCM2 variables, including mean sea level pressure, specific humidity and 500hpa geopotential height as predictors in Colorado, US. However, in their research, the reproduction of wet days was better than for dry days. This may be because the research was conducted in different regions and used different GCMs and variables. The results obtained from the DA- based model for downscaling precipitation occurrence were better than those

of the SDSM-like approach. In addition, the use of CRCM variables as predictors yielded a slightly improved results over using NCEP variables. The averaged success rates for wet days were 73.0% when using CRCM variables as predictors and 68.8% when using NCEP variables. The numbers for dry days were 81.9%, and 74.1%, respectively. Dry days were better reproduced than wet days for both approaches.

Table 4.5 Downscaling of precipitation occurrence using SDSM-like and discriminant analysis-based models

station		**SDSM-like model**			**Discriminant Analysis**	
		NCEP scale	**CRCM scale**		**NCEP scale**	**CRCM scale**
	tot_day	5475				
svir219	cor_wet_day	42.8%	43.8%		66.3%	72.0%
	cor_dry_day	58.0%	56.1%		75.4%	80.1%
	obs_wet_day	2400				
	dow_wet_day	2320 (-3.3%)	2356 (-1.8%)		2347 (-2.2%)	2340 (-2.5%)
svir293	cor_wet_day	43.6%	45.1%		68.5%	74.8%
	cor_dry_day	56.6%	56.0%		75.1%	82.5%
	obs_wet_day	2452				
	dow_wet_day	2379 (-3.0%)	2435 (-0.7%)		2432 (-0.8%)	2362 (-3.7%)
svir559	cor_wet_day	35.7%	34.6%		70.1%	73.2%
	cor_dry_day	64.6%	64.9%		72.5%	81.9%
	obs_wet_day	1929				
	dow_wet_day	1944(0.9%)	1913 (-0.7%)		2326 (20.8%)	2052 (6.5%)
svir689	cor_wet_day	33.3%	32.4%		70.1%	71.9%
	cor_dry_day	66.7%	68.1%		73.4%	83.1%
	obs_wet_day	1818				
	dow_wet_day	1824 (0.3%)	1757 (-3.4%)		2248 (23.7%)	1926 (5.9%)

Note: tot_day = the total days used to verify the downscaling approach; cor_wet_day = the percentage of correctly identified wet days; cor_dry_day = the percentage of correctly identified dry days; obs_wet_day = the observed wet days within the total days; and dow_wet_day = the downscaled wet days within the total days. The value in parentheses is the relative error of downscaled wet days.

Since the results presented in table 4.5 indicate that the DA-based model is the best, it was the scheme chosen to assess the weather typing approach.

The results pertaining to the coupled weather typing and DA methods are presented in table 4.6. Similar results were obtained from all four stations, but only those results from the svir293 station are shown. Based on the classification scheme of the PCA and cluster analysis, the whole time series of precipitation was classified into 4 weather types and first compared with a 4-season classification scheme. For precipitation occurrence, results indicate that the weather classification scheme resulted in worse results than with a simple seasonal classification. The averaged success rates for the weather typing approach were 70.1% for wet days and 75.4% for dry, compared to 74.4% and 80.8%, respectively, with seasonal classification. Since weather conditions are more homogeneous within a weather type, it increases the difficulty of identifying wet and dry states, which likely explains the decreased performance for precipitation occurrence.

Table 4.6 Downscaling of seasonal precipitation occurrence
using the weather typing scheme at station svir293

	SDSM-like				**Weather types**			
	Spring (MAM)	**Summer (JJA)**	**Autumn (SDN)**	**Winter (DJF)**	**Type1**	**Type2**	**Type3**	**Type4**
tot_day	1380	1380	1365	1350	1365	2005	1131	976
cor_wet_day	75.2%	70.1%	76.8%	75.5%	68.4%	69.6%	66.0%	76.3%
cor_dry_day	85.0%	76.5%	81.0%	80.8%	75.2%	79.8%	74.7%	71.9%
obs_wet_day	529	652	664	607	228	728	764	738
dow_wet_day	526 (-0.6%)	628 (-3.7%)	643 (-3.2%)	601 (-1.0%)	438 (92.1%)	765 (5.1%)	597 (-21.9%)	630 (-14.6%)

Note: tot_day = the total days used to verify the downscaling approach; cor_wet_day = the percentage of correctly identified wet days; cor_dry_day = the percentage of correctly identified dry days; obs_wet_day = the observed wet days within the total days; and dow_wet_day = the downscaled wet days within the total days. The value in parentheses is the relative error of downscaled wet days.

4.4.2 Downscaling of daily precipitation amount

The results for precipitation amounts are presented in table 4.7. Overall, the results show improvements in all cases when using RCM-scale variables as predictors over GCM-scale, and additional (although more modest) improvements when using a weather typing scheme at the seasonal time scale. The means of daily precipitation amounts downscaled by an SDSM-like model using NCEP variables as predictors was markedly underestimated for each season, with mean relative errors (MRE) of -31.2% for spring, -42.6% for summer, -37.5% for autumn and -32.6% for winter across four stations. Precipitation amounts downscaled by an SDSM-like model using CRCM variables as predictors were improved, but still underestimated precipitation amounts with an MRE of -27.0% . Adding a weather typing scheme resulted in a modest improvement in the underestimation of precipitation amounts, with an MRE of -25.2%.

Similarly to results for the mean, the standard deviation of daily precipitation amounts was markedly underpredicted by the SDSM-like model using NCEP variables as predictors, with the MRE at -70.5% across the four stations (table 4.8). Downscaling using CRCM variables as predictors significantly improved the standard deviation of the precipitation amount, although it was still underestimated for most seasons with an MRE of -37.5%. Adding weather typing resulted in no additional improvements (MRE of -37.4%).

Percentile plots of downscaled precipitation amounts using the following models: SDSM-like with NCEP predictors, SDSM-like with CRCM predictors, and SDSM-like with CRCM predictors conditioned on weather types are presented in figure 4.2. Similar results were obtained at all stations, but only the results of station svir293 are shown. The results indicate that the downscaled precipitation amounts were too high for light precipitation (below the 50th percentile) and too small for heavier precipitation (above the 50th percentile). This pattern was consistent for all seasons and all downscaling approaches. However, the distribution of downscaling using CRCM variables as predictors was much better than those

using NCEP variables as predictors. The weather typing approach did not show any advantage, even though it is more physically based.

Table 4.7 Comparison of the mean daily precipitation downscaled by an SDSM-like model and a weather typing scheme using NCEP and CRCM-scale variables as predictors (The value in parentheses is the percentage of relative error for each season. WT=weather typing)

Station	Season	Observed	SDSM_NCEP	SDSM_CRCM	WT_CRCM
sivr219	spring (MAM)	4.16	2.87 (-31.1)	3.12 (-25.0)	3.40 (-18.4)
	summer (JJA)	5.68	3.36 (-40.8)	3.69 (-35.1)	3.57 (-37.1)
	autumn (SON)	4.61	2.67 (-42.2)	3.60 (-21.9)	3.63 (-21.3)
	winter (DJF)	3.26	2.16 (-33.8)	2.37 (-27.4)	2.52 (-22.7)
svir293	spring (MAM)	3.53	2.67 (-24.5)	2.79 (-20.9)	2.94 (-16.6)
	summer (JJA)	5.02	3.08 (-38.6)	3.31 (-34.1)	3.43 (-31.7)
	autumn (SON)	4.35	2.72 (-37.3)	3.38 (-22.2)	3.46 (-20.4)
	winter (DJF)	2.75	2.06 (-25.2)	2.32 (-15.7)	2.45 (-10.8)
svir559	spring (MAM)	5.54	3.95 (-28.8)	4.16 (-25.0)	4.29 (-22.5)
	summer (JJA)	6.37	3.99 (-37.4)	3.85 (-39.6)	3.90 (-38.9)
	autumn (SON)	6.08	3.76 (-38.2)	4.03 (-33.7)	4.06 (-33.2)
	winter (DJF)	4.33	3.51 (-18.9)	4.13 (-4.6)	4.08 (-5.8)
svir689	spring (MAM)	4.85	2.98 (-38.5)	3.30 (-32.0)	3.38 (-30.4)
	summer (JJA)	6.14	3.14 (-48.8)	3.29 (-46.4)	3.08 (-49.8)
	autumn (SON)	5.19	3.33 (-35.9)	3.85 (-25.8)	3.91 (-24.7)
	winter (DJF)	3.60	2.27 (-36.9)	2.79 (-22.3)	2.94 (-18.3)
Mean relative error (%)		--	-34.8	-27.0	-25.2

Table 4.8 Comparison of the standard deviation of daily precipitation downscaled by an SDSM-like model and by a weather typing scheme using NCEP and CRCM variables as predictors (The value in parentheses is the percentage of relative error for each season. WT=weather typing)

Station	Season	Observed	SDSM_NCEP	SDSM_CRCM	WT_CRCM
sivr219	spring (MAM)	4.71	1.90 (-59.6)	3.71 (-21.2)	3.64 (-22.6)
	summer (JJA)	6.56	1.52 (-76.8)	3.12 (-52.4)	2.60 (-60.3)
	autumn (SON)	5.96	1.52 (-74.5)	5.25 (-11.9)	5.15 (-13.7)
	winter (DJF)	4.00	1.50 (-62.5)	2.86 (-28.5)	2.60 (-34.9)
svir293	spring (MAM)	4.67	1.77 (-62.0)	3.74 (-19.9)	3.73 (-20.1)
	summer (JJA)	6.28	1.67 (-73.4)	2.49 (-60.4)	2.75 (-56.2)
	autumn (SON)	6.10	1.75 (-71.3)	4.49 (-26.4)	4.27 (-30.0)
	winter (DJF)	3.47	1.39 (-59.9)	4.47 (28.9)	3.79 (9.2)
svir559	spring (MAM)	6.06	1.94 (-67.9)	3.35 (-44.7)	3.57 (-41.1)
	summer (JJA)	8.27	1.53 (-81.5)	1.55 (-81.2)	2.17 (-73.8)
	autumn (SON)	7.77	2.06 (-73.5)	3.49 (-55.1)	3.46 (-55.4)
	winter (DJF)	4.97	1.74 (-64.9)	4.46 (-10.3)	4.07 (-18.0)
svir689	spring (MAM)	5.68	1.47 (-74.2)	3.58 (-36.9)	3.37 (-40.6)
	summer (JJA)	8.10	1.00 (-87.7)	1.57 (-80.6)	1.35 (-83.3)
	autumn (SON)	7.04	2.07 (-70.6)	4.69 (-33.4)	4.54 (-35.5)
	winter (DJF)	4.59	1.50 (67.3)	4.20 (-8.5)	4.39 (-4.3)
Mean relative error (%)		--	-70.5	-37.5	-37.4

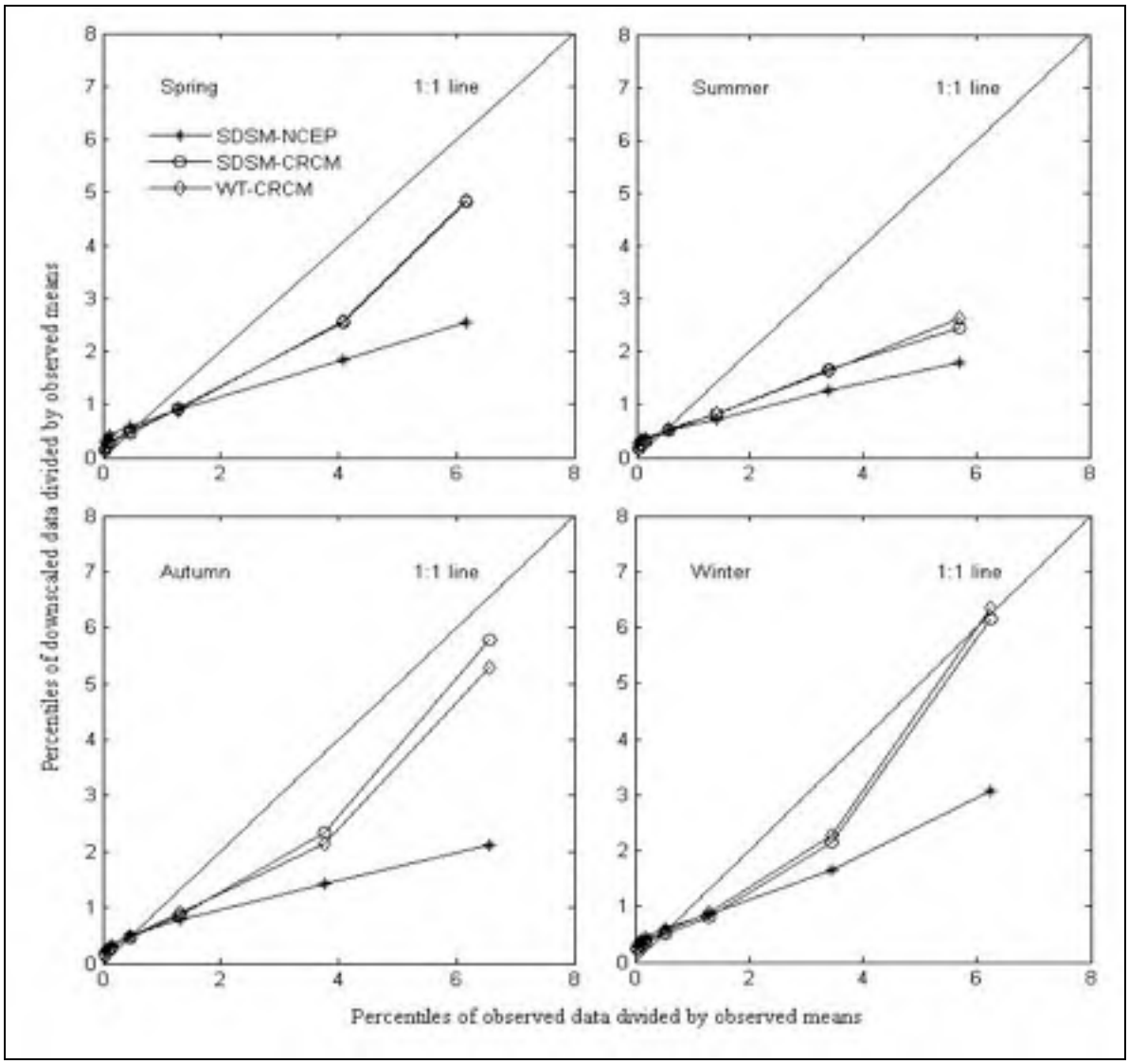

Figure 4.2 Plots of 5, 15, 25, 50, 75, 95 and 99 percentiles of observed vs. downscaled daily precipitation for each season at station svir293. The percentiles of each season were divided by the corresponding observed mean of each season (SDSM-NCEP = SDSM-like with NCEP predictors; SDSM-CRCM = SDSM-like with CRCM predictors; and WT-CRCM = SDSM-like with CRCM predictors conditioned on weather types.

The percentage of explained variance indicates the extent to which daily variations in the local predictands are determined by regional forcing (Wilby et al., 2002a). For temperature, an explained variance over 70% is quite normal, but for precipitation, it is generally less than 30%. Using SDSM, Wilby et al. (2002a) found explained variances of 28%, 73% and 72%

for precipitation amounts, maximum and minimum temperatures, respectively. The results for the percentage of explained variance are presented for precipitation amounts in table 4.9. In this research, the averaged explained variance for precipitation amounts was only 13.8% using NCEP variables and the SDSM-like model for calibration, and 13.3% for validation across 4 seasons and four stations. In particular, these were extremely low in the summer; only 8.0% and 8.4% for calibration and validation, respectively. The explained variance was higher in winter, with a percentage of explained variance of 18.3 for calibration and 15.4 for validation. Across all seasons and stations, the explained variances were distinctly improved when using CRCM variables as predictors. These were 30.2% and 32.2% for calibration and validation, respectively. Adding weather typing modestly improved the explained variance to 33.6% and 33.5% for calibration and validation, respectively. The explained variance was still lower in the summer (<20%) and the best in winter at more than 40%. The improvement with weather typing was at their maximum over winter, indicating the winter precipitation was controlled by large-scale atmospheric circulation to a greater degree.

4.5 Discussion and conclusion

4.5.1 Downscaling of daily precipitation occurrence

This paper compared the ability of two approaches to downscale precipitation occurrence (the linear regression approach of an SDSM-like model, and a DA-based model) at the GCM and RCM scales. The results showed that the SDSM-like model slightly overestimated the frequencies of wet and dry periods. In contrast, the frequencies of both wet and dry periods were well replicated by the downscaling model based on DA. Both approaches reproduce total wet days and dry days accurately. However, this apparently good performance is an illusion, since the wet or dry status for each day was poorly downscaled. Wet days were frequently predicted to be dry and vice-versa. In fact, with a 61% success rate, the SDSM-like model was only slightly better than a random draw. The observed accuracy in total wet days (and dry days) simply reflects the fact that each model had the same percentage of errors in wet and dry days. Despite the above limitation, precipitation occurrence downscaled by the DA-based model was better than that obtained using the SDSM-like model. This

should not be a surprise, since discriminant analysis finds the optimal linear combination of predictors that separate two different groups. Discriminant analysis has much in common with linear regression, and it can be shown that linear regression may, at best, match DA performance, but cannot possibly exceed it. Hence, the performance of DA-based model indicates the best possible outcome for a linear method. As such its performance is relatively disappointing in that it fails to adequately reproduce wet and dry states at all stations and seasons. While the success rates may seem adequate (between 66% and 83%), it should be observed that a perfectly random scheme would result in a 50% success rate. Perhaps even more disappointing is the fact that DA did not do significantly better in separating wet days from dry days identified using a much higher precipitation threshold (results not shown). In other words, extremely wet days were not categorized as 'wet' any more frequently than moderately wet days. This indicates that there is simply not enough information present in the predictors to accurately downscale precipitation occurrence, particularly at the GCM scale. The improvements resulting from using RCM predictors clearly show that some additional information is added at the finer scale, but it is still not sufficient for the approaches to be used in a climate change context. This is also reflected in the fact that weather typing was not useful in downscaling precipitation occurrence, although this is likely at least partly due to the more homogeneous conditions within each weather type, rendering identification of wet/dry states more challenging.

Overall, downscaling of daily precipitation occurrence was largely unsuccessful with the linear techniques used. Daily precipitation occurrence is controlled by many factors, some of which are linked to large scale atmospheric circulation. Clearly, for the selected stations, sub-grid processes play a significant role in determining whether or not precipitation occurs. The selected variables were unable to capture a major portion of the variability. The addition of lag-1 variables did not improve results significantly.

Table 4.9 Comparison of explained variance of daily precipitation downscaled by SDSM-like models and a weather typing scheme using NCEP and CRCM variables as predictors (WT=weather typing)

Station	**Season**	**Explained variance (%) of calibration**			**Explained variance (%) of validation**		
		SDSM_ NCEP	**SDSM_ CRCM**	**WT_ CRCM**	**SDSM_ NCEP**	**SDSM_ CRCM**	**WT_ CRCM**
sivr219	spring (MAM)	15.7	36.7	42.6	12.4	31.7	32.4
	summer (JJA)	9.6	23.9	21.7	6.5	19.2	21.2
	autumn (SON)	12.0	36.1	38.4	13.6	42.0	40.2
	winter (DJF)	20.0	35.4	41.1	13.8	34.9	36.2
svir293	spring (MAM)	18.5	43.9	45.3	21.5	48.2	48.1
	summer (JJA)	11.4	24.1	27.5	13.9	28.1	28.0
	autumn (SON)	15.4	39.2	44.1	15.2	51.4	50.2
	winter (DJF)	21.5	41.4	47.6	16.9	45.3	47.7
svir559	spring (MAM)	14.6	28.7	32.2	11.8	26.1	28.2
	summer (JJA)	6.9	7.3	11.9	7.1	12.3	11.4
	autumn (SON)	12.2	23.7	26.4	14.9	33.4	35.7
	winter (DJF)	14.3	33.4	38.3	12.4	28.0	30.1
svir689	spring (MAM)	13.0	33.6	36.3	11.3	26.8	27.0
	summer (JJA)	3.9	8.6	8.9	5.9	11.1	18.4
	autumn (SON)	13.8	28.8	31.6	17.0	38.7	37.6
	winter (DJF)	17.5	38.4	43.9	18.6	38.1	44.1
Mean		13.8	30.2	33.6	13.3	32.2	33.5

A better approach may be to try to downscale monthly or seasonal transition probabilities such as P01 (a wet day following a dry day) and P11 (a wet day following a wet day). Since these variables are only needed at the monthly or seasonal scales, more robust relationships may be derived with monthly or seasonal averaged values from GCM and RCM data. The downscaled monthly or seasonal transition probabilities can then be disaggregated at the

daily scale using a stochastic weather generator. There are three advantages to linking weather generator parameters with RCM or GCM variables. Firstly, the spatial scales of RCMs and GCMs indicate that their variables are more likely to be linked to the monthly or seasonal climate variability rather than to daily scales. Secondly, RCM and GCM outputs are considered more robust at the monthly or seasonal scales than at daily scales (Maurer and Hidalgo 2007). Finally, downscaling weather generator parameters allows the generation of time-series of infinite length, thus allowing the study of rare events. However, as mentioned earlier, Wilby et al. (2002b) explored the use of synoptic-scale predictor variables to downscale both high- and low-frequency variability of precipitation based on conditional stochastic rainfall models at sites across Great Britain. Their results showed that their conditional rainfall models displayed positive effects on monthly rainfall statistics relative to the control, but they did not completely remove overdispersion. This may be because the applied predictors did not accurately explain the local climate variability. Moreover, Zhang (2005) used the mean of monthly precipitation to downscale weather generator parameters (P01 and P11), but there is frequently no strong relationship between monthly precipitation and transition probability. Therefore, to better simulate the low-frequency variability, predictors that strongly correlate with transition probabilities are needed. Clearly, there are research opportunities in this area.

4.5.2 Downscaling of daily precipitation amount

This paper compared the ability of two approaches to downscale precipitation amounts (the linear regression approach of an SDSM-like model, with and without weather typing) at the GCM and RCM scales. Both the mean and standard deviations were markedly underestimated for the two approaches tested. These results are consistent with other SD studies and were observed using GCM and RCM scale predictors, for all seasons and all stations. The weather typing approach was somewhat better than the SDSM-like model (without weather typing) in downscaling the precipitation mean, but there was the same mediocre ability at downscaling the standard deviation of precipitation. The downscaled precipitation amounts were too high for the observed light precipitation (below the 50th

percentile) and too small for the observed heavier precipitation (above the 50th percentile). This pattern was consistent for all seasons, stations and approaches.

Downscaling using RCM variables as predictors distinctly improved the mean and standard deviation for both approaches. In particular, the explained variance, which was very low with GCM scale predictors, was improved with RCM scale predictors. Clearly, the finer resolution of RCMs increased a models' ability to capture regional details affecting the local climate. However, going from a 300km scale to a 45km scale did not yield spectacular improvements. Considering that wet days were diagnosed incorrectly up to 28% of the time, and that dry days were identified as wet up to 20% of the time, it would seem that the information contained in GCM and RCM variables is more about the likelihood of precipitation and less about precipitation itself. The marked lack of success of weather typing in this paper testifies to that. Grouping days into weather types makes physical sense, but did not improve the success rate, indicating that a large part of the information on the processes leading to precipitation is generally not present at the GCM and RCM scales. Nevertheless, the improvements observed when going to the RCM scale raise the obvious question of how much better would SD get with an RCM run at an even finer resolution. At a 15km grid, much of the precipitation process would still have to be parameterized within RCMs, thus limiting potential improvements in SD. It should be emphasized that at the 45km scale, direct inclusion of RCM outputs into hydrological models is possible on larger watersheds (with or without bias correction). With a 15 km grid, biases would be reduced even more, enabling direct use of RCM data in even more applications. With a 1km grid, the physical equations could resolve convective processes on their own and precipitation accuracy should (in theory at least) improve dramatically. However, at this scale, for most applications, SD would not be needed anymore. In this sense, for the approaches and stations presented in this paper, SD seems to have hit a dead-end for precipitation, while it still has an advantage in uncertainty studies. With the exception of intercomparison studies, RCM data is scarce and difficult to obtain. Data is rarely available from more than one RCM (driven by one GCM) over a given area while GCM data is now abundant with global coverage. With regards to the uncertain future, it is essentially impossible to adequately cover the major source of uncertainty

(climate models) at the regional scale. Consequently, downscaling techniques from GCM data will continue to be an avenue of research.

CHAPTER 5

ASSESSMENT OF REGRESSION-BASED STATISTICAL APPROACHES FOR DOWNSCALING PRECIPITATION FOR NORTH AMERICA

Jie Chen[1], François P. Brissette[1], Robert Leconte[2]

1. Department of Construction Engineering, École de technologie supérieure, Université du Québec, 1100, rue Notre-Dame Ouest, Montréal, Québec, Canada, H3C 1K3.
2. Department of Civil Engineering, Université de Sherbrooke, 2500, boul. de l'Université, Sherbrooke, Québec, Canada, J1K 2R1

This article was submitted to the Journal of Climate in January, 2011.

5.1 Abstract

The mismatch of spatial resolution between General Circulation model (GCM) outputs and the data requirements of hydrological models are major obstacles for quantifying the hydrologic impacts of climate change. Downscaling methods have been developed to overcome this problem. Among the different methods available, regression-based statistical approaches have been the most widely used, due to their low computational cost and relative ease of application. However, while these approaches work relatively well for downscaling temperatures, they often account for only a small percentage of the observed precipitation variance. The objective of this paper is to assess the reliability of regression-based approaches in downscaling precipitation for North America across different scales from GCMs to mid and high resolution Regional Climate Models (RCM) all the way to station scale. Overall, nine downscaling experiments were performed, combining four spatial scales starting from GCM (300km), going to RCMs at 45km and 15km, and finally to the station scale. The statistical downscaling method selected here uses discriminant analysis for precipitation occurrence and a stepwise linear regression approach for precipitation amounts. The percentages of correct wet and dry day classifications and percentages of explained variance for both calibration and

validation were used as criteria to assess these methods. The results showed that the downscaling of daily precipitation occurrence was mostly unsuccessful at all scales, although results did constantly improve with the increased resolution of climate models. Results for downscaling of dry day occurrence at the station scale went from 75.4% (GCM predictors) to 77.7% (45-km RCM predictors) and finally to 82.0% (15-km RCM predictors). For precipitation amounts, the average explained variances when downscaling to the station scale were less than 25% when using GCM predictors. Using RCM predictors at 45-km yielded a clear improvement in downscaling ability although explained variance rarely got above 40%. Using predictors at the 15-km scale yielded little improvement over the 45-km predictors. To gain a better understanding of those results, precipitation was also downscaled across all scales (GCM to GCM, GCM to 45-km RCM, GCM to 15-km RCM, 45-km RCM to 45-km RCM, 45-km RCM to 15-km RCM, and finally, 15-km RCM to 15-km RCM). The percentages of explained variance for downscaled GCM precipitation from GCM predictors were consistently lower than 40%. Downscaling of 45-km RCM precipitation amounts using 45-km RCM predictors distinctly improved the explained variances for both calibration and validation, but going to the 15-km RCM scale resulted in little improvement. The average explained variance was always less than 85% for both calibration and validation. While downscaling GCM precipitation from GCM predictors (or RCM precipitation from RCM predictors) cannot really be considered downscaling, as there is no change in scale, the exercise yields interesting information as to the theoretical limit in predictive ability at the station scale. This was especially clear at the GCM scale, where the inability of downscaling GCM precipitation from GCM predictors demonstrates that GCM precipitation-generating processes are largely at the sub-grid scale, thus indicating that downscaling daily precipitation at the station scale from GCM scale is virtually a dead-end. While results got better at the RCM scale, the results indicate that overall, regression-based approaches did not perform well in downscaling precipitation.

Keywords: Statistical downscaling; discriminant analysis; stepwise linear regression; precipitation

5.2 Introduction

The Intergovernmental Panel on Climate Change (IPCC) stated that continued greenhouse gas emissions at or above current rates would cause further warming and consequently induce many changes in the global climate system during the 21st century (IPCC, 2007). This kind of climate change will severely affect terrestrial water resources in the future (Srikanthan and McMahon, 2001; Xu and Singh, 2004). In order to quantify the impacts of climate change, the development of tools or approaches to generate future climate projections is necessary. General Circulation Models (GCMs) have been developed to simulate the present climate and predict future climate change. However, the spatial and temporal resolutions of GCMs are too coarse to assess the regional and site-specific impacts of climate change (Leavesley, 1994; Hostetler, 1994). It is necessary to perform some post-processing to improve upon these global-scale models for impact studies. Consequently, two widely used classes of downscaling techniques have been developed: dynamic downscaling and statistical downscaling.

Dynamical downscaling was developed based on dynamic formulations using initial and time-dependent lateral boundary conditions of GCMs to achieve a higher spatial resolution by nesting limited-area Regional Climate Models (RCMs). The main drawback of RCMs is their high computational cost (Solman and Nunez, 1999). Therefore, they are only available for limited regions, and, except for a few intercomparison studies, there is rarely more than one RCM operating over a given area, thus limiting the ability to sample the uncertainty linked to climate modeling. Moreover, despite improvements, the outputs of most RCMs are still too coarse to enable their direct use for impact studies over small to medium size watersheds which may require local and site-specific climate projections. Statistical downscaling involves linking the states of some variables representing a large scale (GCM or RCM grid scale, predictors) to the states of some variables representing a much smaller scale (catchment or site scale, predictands). The main strengths of statistical downscaling approaches are that they are computationally inexpensive and relatively easy to apply. Thus, they are often used to downscale GCM outputs. However, there is often a marked lack of

strong relationships between predictors and predictands, especially for precipitation. Over the past two decades, a diverse range of statistical downscaling methods have been developed. They fall into three categories: transfer function (regression based, Wilby et al., 1998a; Wilby et al., 2002a), weather generator (Wilks, 1999a; Zhang, 2005), and weather typing (von Storch et al., 1993; Schoof and Pryor, 2001).

Transfer functions are the most widely used statistical downscaling approaches. They involve establishing statistical linear or nonlinear relationships between observed local climatic variables (predictands) and large-scale GCM output (predictors). The most commonly used predictors from GCM outputs include vorticity, airflow indices, wind velocity and direction, mean sea-level pressure, geopotential heights and relative humidity (Wilby et al., 1998a; Solman and Nunez, 1999; Sailor and Li, 1999; Trigo and Palutikof, 2001). A typical transfer function approach is with the one used by the statistical downscaling model (SDSM) developed by Wilby et al. (2002a). This model works relatively well in downscaling temperature at the station scale, with a percentage of explained variance usually over 70%. However, it underestimates the daily precipitation (both mean and variance), because the percentage of explained variance is generally less than 30% (Wilby et al, 1999). To address this problem, bias correction and variance inflation schemes were incorporated within the SDSM to ensure that observed and downscaled precipitation totals were equal for the simulation period. When using bias correction and variance inflation, the SDSM essentially becomes a weather generator, where a stochastic component is superimposed on top of the downscaled variable. Another statistical downscaling approach is based on the use of stochastic weather generators. Weather generator parameters are perturbed according to the changes of future climate projected by climate models (Wilks, 1992, 2010; Semenov and Barrow 1997, Wilby et al, 2002b; Zhang, 2005, Qian et al., 2010). The appealing property of the weather generator approach is its ability to rapidly produce ensembles of climate scenarios for studying the impacts of rare climate events. The main disadvantages are that changes in one variable may affect secondary variables (adjusting the precipitation occurrence may affect the precipitation amount), and that the link between parameters and future climate may not be easy to establish. Weather typing schemes have also been used as a

downscaling method, which involves grouping local meteorological variables in relation to different classes of atmospheric circulation based on a given weather classification scheme (Bardossy and Plate, 1992; von Storch et al., 1993). The main advantage is that local variables are sensitively linked to the large scale atmospheric circulation. The drawbacks are that the reliability depends on the stationary relationship between large scale circulation and the local climate of each weather type, and that it requires the additional task of weather classification.

Overall, even though there are a number of statistical downscaling methods, regression-based approaches are the type most widely used. The ease of application, especially with the SDSM freeware package, explains in large part the popularity of these methods. Accordingly, this paper aims at assessing the reliability of regression-based approaches in downscaling daily precipitation for North America through statistical downscaling across several scales, from GCM to mid and high resolution RCMs, all the way to station scale. To better reflect the real ability of the statistical downscaling method, this paper only considers the results of the regression scheme, with no stochastic component added on top of the downscaled component.

5.3 Study area and data

5.3.1 Study area

The study was conducted over North America (except Greenland) in a zone extending from within 10° of latitude of both the equator and the North Pole. It embraces every climatic zone, from tropical rain forest and savanna in the lowlands of Central America to ice fields in Northern Canada, which adequately represents the spatial climate variability (figure 5.1). Two hundred and fifty-eight Canadian GCM3 (CGCM3) 300km grid points dispersed across North America were selected to test the ability of regression-based statistical downscaling methods. Since the Canadian RCM (CRCM) has many more grid points than the number of CGCM3 grid points due to its higher resolution, the 258 grid points closest to CGCM3 grid points were chosen for downscaling. The use of 15-km CRCM data was restricted to the

Manicouagan river basin in Quebec, Canada with 1369 grid points (37×37 grid). One hundred and fifty-six (12×13) grid points were selected for the downscaling from the 45-km CRCM to the 15-km CRCM and from the 15-km CRCM to the 15-km CRCM. In addition, six grid points within or close to the Manicouagan river basin were used for the downscaling from GCM to the 15-km CRCM. Moreover, sixteen stations dispersed across Canada and the United States were used for downscaling from GCM and 45-km CRCM to the station scale, and six stations within or close to the Manicouagan river basin were used to downscale precipitation at the station scale from the 15-km CRCM predictors (figure 5.1). Basic information, including latitude, longitude, elevation, average annual precipitation and record duration for these stations is given in table 5.1. The downscaling experiments and the number of selected grid points or stations are presented in table 5.2.

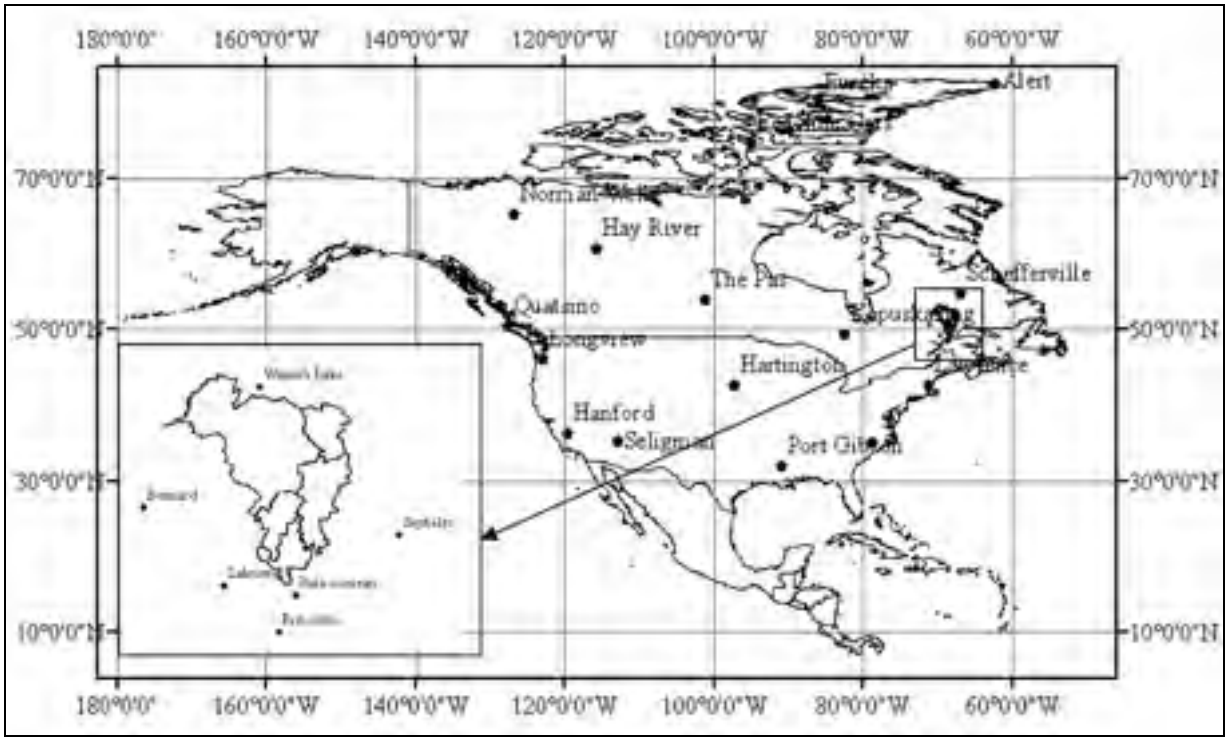

Figure 5.1 Selected study stations over North America and Manicouagan river basin in Quebec, Canada.

5.3.2 Data

This project made use of several different climatic databases. The CGCM3 data and the National Center for Environmental Prediction (NCEP) reanalysis data interpolated to the CGCM3 grid (Kalnay et al., 1996; DAI CGCM3 Predictors, 2008) were used at the GCM scale. The regional scale is covered at the 15-km and 45-km scales by the CRCM (version 4.2.3) as discussed in Music and Caya (2007, 2009) over the North-American domain for the 45-km resolution, and over the Quebec domain for the 15-km resolution. CRCM is driven by NCEP data at its boundaries in the former, and by the 45-km CRCM over the Quebec domain in the latter. Although the results are from the same version of the CRCM, the 15-km CRCM data was driven at its boundary conditions by a different run (over the Quebec domain) than the one used in this paper at the 45-km scale (over the North American domain). This is important to mention as this may have implications on the results. Since the NCEP is the parent of the CRCM, it is further used to represent GCM data for downscaling from 300-km scale to finer scale (experiments 2, 4 and 7). CGCM data was used for the first downscaling experiment (GCM to GCM).

The data in this research covers the period 1961 to 2000, with the exception of some stations within or close to the Manicouagan river basin that have a record shorter than 40 years, as shown in table 5.1. The first half-period of data was used to calibrate the model (establishing the transfer function), and then the second period of data was used to verify the ability of the fitted transfer function. The GCM, NCEP, 45-km CRCM and 15-km CRCM predictors considered are listed in table 5.3.

Table 5.1 Location, record period, and average annual precipitation for 16 stations (ID 1-16) dispersed throughout North America and 6 stations (ID 17-22) within or close to the Manicouagan river basin (Lat=latitude; Lon=longitude and Ele=elevation)

ID	State or Province	Station name	Lat (°N)	Lon (°E)	Ele (m)	Records of daily precip	Annual precip
1	British Columbia	Quatsino	50.53	-127.65	3	1961-2000 (40)	2491.9
2	Northwest Territories	Norman Wells	65.28	-126.80	73	1961-2000 (40)	298.4
3	Northwest Territories	Hay River	60.84	-115.78	165	1961-2000 (40)	328.2
4	Nunavut	Alert	82.52	-62.28	31	1961-2000 (40)	158.7
5	Nunavut	Eureka	79.98	-85.93	10	1961-2000 (40)	70.6
6	Nunavut	Resolute Cars	74.72	-94.99	66	1961-2000 (40)	144.9
7	Manitoba	The Pas	53.97	-101.10	270	1961-2000 (40)	444.5
8	Ontario	Kapuskasing	49.40	-82.47	227	1961-2000 (40)	849.0
9	Quebec	Schefferville	54.80	-66.82	522	1961-2000 (40)	768.1
10	Massachusetts	Lawrence	42.70	-71.17	18	1961-2000 (40)	1106.2
11	North Carolina	Fayetteville	35.06	-78.86	29	1961-2000 (40)	1175.9
12	Mississippi	Port Gibson	31.99	-90.97	37	1961-2000 (40)	1449.4

ID	State or Province	Station name	Lat (°N)	Lon (°E)	Ele (m)	Records of daily precip	Annual precip
13	Nebraska	Hartington	42.62	-97.26	418	1961-2000 (40)	660.3
14	Arizona	Seligman	35.33	-112.88	1601	1961-2000 (40)	315.8
15	Washington	Longview	46.15	-122.92	4	1961-2000 (40)	1190.1
16	California	Hanford	36.32	-119.64	75	1961-2000 (40)	209.6
17	Quebec	Bain-Someau	49.13	-68.2	21.6	1967-2000 (34)	997.5
18	Quebec	Labrieville	49.30	-69.55	152	1961-1992 (32)	847.5
19	Quebec	Sept-Iles	50.22	-66.27	55	1961-2000 (40)	1126.1
20	Quebec	Rimouski	48.45	-68.52	36	1966-1999 (34)	877.1
21	Quebec	Bonnard	50.73	-71.05	506	1965-1998 (34)	934.6
22	Newfoundland	Wabush Lake	52.93	-68.87	551	1961-2000 (40)	854.8

5.4 Methodology

The precipitation occurrence was downscaled using discriminant analysis and the wet day precipitation amounts were downscaled using a stepwise linear regression. Discriminant analysis is a technique for classifying a set of observations into predefined classes (Wilks, 1995). The purpose is to determine the class of an observation based on a set of variables known as predictors or input variables. It has much in common with linear regression, as it

finds the optimal linear combination of predictors that separate predefined groups (two groups: wet and dry in this case). In other words, its performance indicates the best possible outcome for a linear method.

Table 5.2 Downscaling experiments and number of selected grid points or stations

No.	Experiment	Number of grid points or stations
1	CGCM to CGCM	258 grid points over North America
2	NCEP to 45-km CRCM	258 grid points over North America
3	45-km CRCM to 45-km CRCM	258 grid points over North America
4	NCEP to 15-km CRCM	6 grid points within or close to the Manicouagan river basin
5	45-km CRCM to 15-km CRCM	156 grid points within or close to the Manicouagan river basin
6	15-km CRCM to 15-km CRCM	156 grid points within or close to the Manicouagan river basin
7	NCEP to station	16 stations dispersed across the North America
8	45-km CRCM to station	16 stations dispersed across the North America
9	15-km CRCM to station	6 stations within and or close to the Manicouagan river basin

With discriminant analysis for downscaling of precipitation occurrence, it is necessary to have an available "training sample" in which each of the vectors are known to be classified correctly. In this paper, the first half period of climate model (CGCM, NCEP, 45-km CRCM or 15-km CRCM) predictors and their lag-1 predictors were used as the training sample. The precipitation series were first divided into two groups, a wet-day group (daily precipitation amount ≥1mm) and a dry-day group (daily precipitation amount < 1mm). Other threshold values for the determination of wet days were tested and yielded similar results. The precipitation occurrence at the validation period was similarly classified according to rules constructed based on training samples and corresponding groups.

A stepwise linear regression approach was selected to downscale wet day precipitation amounts. All of the CGCM (NCEP) or CRCM variables and the lag-1 variables of the first half period were used to select predictors using the stepwise regressive method. Multiple linear regressive equations were then fitted between the precipitation and the predictors for each season. Since the distribution of the daily precipitation is highly skewed, a fourth root transformation was applied to the original data before fitting the transfer function. The established transfer functions were then used to downscale daily precipitation for the second half period using CGCM, NCEP or CRCM variables and their lag-1.

This research downscales daily precipitation occurrence and amounts from CGCM scale to CRCM scale (45-km and 15-km) and then to station scale. As mentioned earlier, this results in nine downscaling experiments combining four spatial scales (table 5.2). In the cases where precipitation was downscaled from predictors at the same scale (experiments 1, 3 and 6 from table 5.2), the predictors were those listed in table 5.3 as well as their lag-1 counterparts, and daily precipitation was used as the predictand. Technically speaking, these experiments cannot be classified as downscaling since the scale remains constant, but the results can give interesting information about the ability to downscale at a finer scale. For the other downscaling experiments (going to a finer scale), the larger scale variables were used as predictors and the finer scale or station precipitation was used as the predictand.

Table 5.3 CGCM, NCEP, 45-km CRCM and 15-km CRCM variables used to select precipitation predictors for downscaling

	GCM and NCEP variables	**45-km CRCM variables**	**15-km CRCM variables**
Surface variables	Mean sea level pressure	East component of wind	East component of wind
	Temperature at 2m	North component of wind	North component of wind
		Total precipitation rate	Total precipitation rate
		Screen specific humidity	Screen specific humidity
		Tmin	Tmin
		Tmax	Tmax
		Surface geopotential	Screen temperature
		Snow on ground	Mean sea level pressure
Upper-air variables	East component of wind (500, 850 and 1000 hPa)	East component of wind (500, 700 and 850 hPa)	East component of wind (500, 700 and 850 hPa)
	North component of wind (500, 850 and 1000 hPa)	North component of wind (500, 700 and 850 hPa)	North component of wind (500, 700 and 850 hPa)
	Geopotential (500 and 850 hPa)	Geopotential (500, 700 and 850 hPa)	Geopotential (500, 700 and 850 hPa)
	Specific humidity (500, 850 and 1000 hPa)	Relative humidity (500, 700 and 850 hPa)	Relative humidity (500, 700 and 850 hPa)
	Vertical vorticity (500, 850 and 1000 hPa)	Vertical vorticity (500, 700 and 850 hPa)	Vertical vorticity (500, 700 and 850 hPa)
	Divergence (500, 850 and 1000 hPa)	Clouds by layer (500, 700 and 850 hPa)	Clouds by layer (500, 700 and 850 hPa)
	Wind direction (500, 850 and 1000 hPa)		Air temperature (500, 700 and 850 hPa)
	Wind speed (500, 850 and 1000 hPa)		

5.5 Results

5.5.1 Downscaling of precipitation occurrence

The percentage of correct wet and dry day classifications is a useful metric to judge the accuracy of a downscaling model (Wilks, 1995). Figure 5.2 presents the percentages of dry and wet days downscaled from CGCM to CGCM (experiment 1), from NCEP to 45-km CRCM (experiment 2), and from 45-km CRCM to 45-km CRCM (experiment 3) for 258 grid points over North America. Generally, discriminant analysis was not successful in producing dry and wet days for all grid points. However, the reproduction of dry days was consistently better than those of wet days for all downscaling experiments. Moreover, the success rates of dry and wet days were higher for the west coast of North America and the northern part of Canada. In these regions, precipitation is strongly affected by the Pacific and Arctic oceans and accordingly, precipitation occurrence is more correlated to large scale atmospheric circulation.

On the other hand, the interior and eastern coasts of North America are under a continental climate where regional details such as topography play a much more important role in precipitation occurrence. Specifically, for experiment 1 (CGCM to CGCM), the success rates of dry and wet days ranged between 53.1% and 90.0% and between 65.4% and 84.9% with means of 77.8% and 73.2%, respectively, across the 258 grid points of North America. These numbers should be interpreted by keeping in mind that a success rate of 50% is no better than having a random assignation of dry and wet days. Experiment 1 clearly shows that precipitation generation in a climate model is largely controlled by sub-grid processes, and that important information is missing from grid-scale predictors. It should then not be a surprise to observe worse results when downscaling from NCEP to 45-km CRCM scale (experiment 2). The success rates changed from 57.5% to 88.5% for dry days and from 57.8% to 82.5% for wet days with means of 70.1% and 67.9% across the 258 grid points of North America, respectively. Better results were obtained when downscaling from 45-km CRCM to 45-km CRCM scale (experiment 3).The mean success rates were 89.7% for dry state and 83.9% for wet state with maximum success rates of 96.9% and 90.1%, respectively,

across the 258 grid points of North America. These numbers outline the increased potential of the higher resolution RCMs for downscaling to the station scale.

Downscaling from 45-km CRCM to 15-km CRCM scale (experiment 5), the percentages of correct dry and wet days ranged between 67.0% and 73.0% and between 59.4% and 73.5% with means of 69.5% and 69.3%, respectively, across the 156 grid points within or close to the Manicouagan river basin (figure 5.3). In percentage values, the results seem worse than downscaling from NCEP to 45-km CRCM scale, but since the experiments were not carried out over the same domains, a direct comparison is not possible. However, since the percentages of correct dry and wet days of Quebec were lower than other parts of North America (figures 5.2c and 5.2d), it appears that the results from experiment 5 are slightly better.

Due to availability restrictions on the 15-km CRCM data, only six NCEP and 15-km CRCM grid points were selected for downscaling from NCEP to 15-km scale (experiment 4). The average percentages of correct dry and wet days were 73.2% and 68.8%, respectively (table 5.4). Overall, results were similar to those obtained when going from 45-km CRCM to 15-km CRCM with average percentages of correct dry and wet days of 69.5% and 69.3%, and when downscaling from NCEP to 45-km CRCM (70.1% and 67.9%). Again, it should be noted a direct comparison is not possible since the former case only averaged 6 grid points over the Manicouagan river basin, while the latter two averaged 156 grid points over the Manicouagan river basin and 258 grid points over North America, respectively.

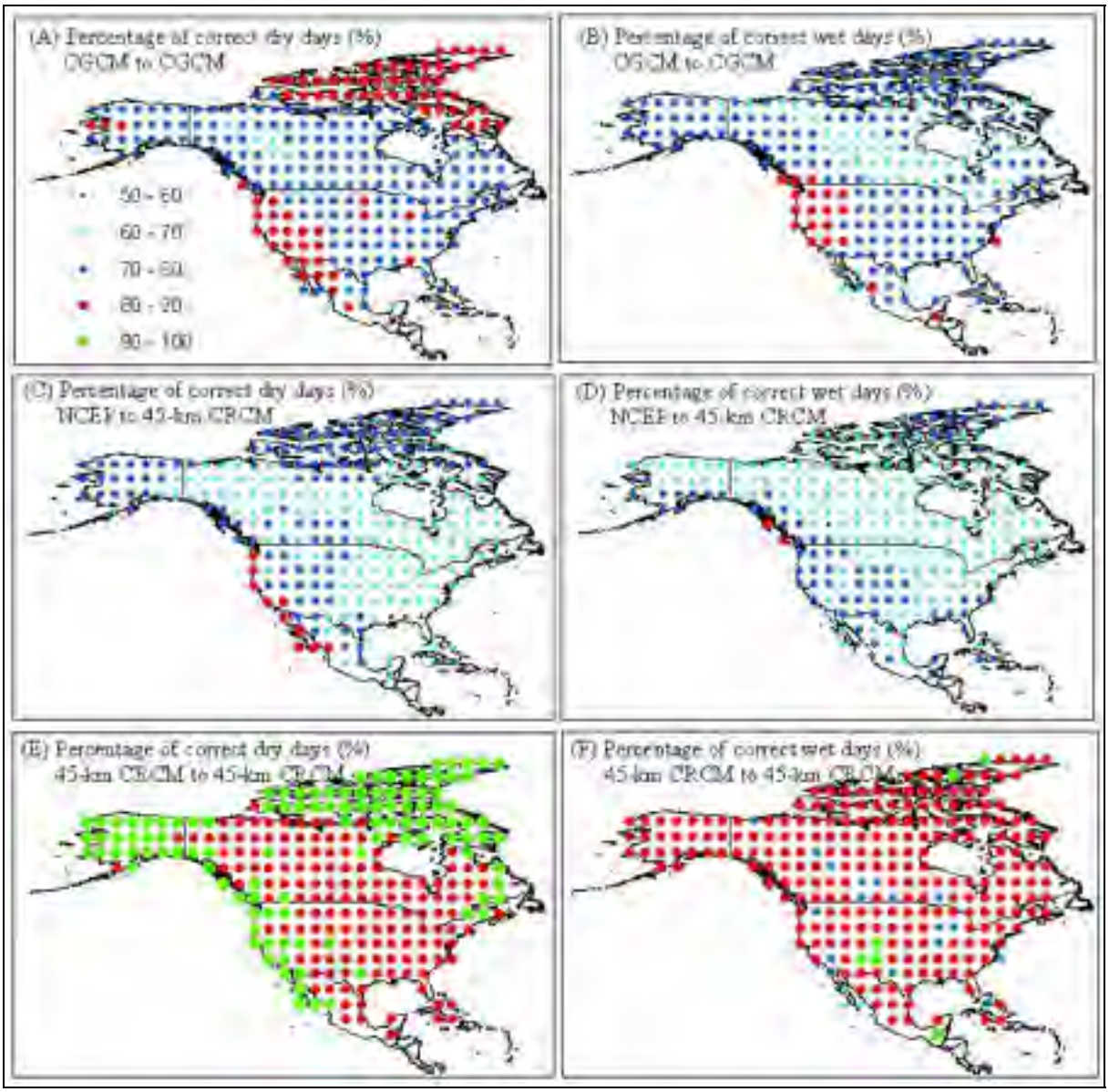

Figure 5.2 Percentages of correct wet and dry day classifications downscaled from CGCM to CGCM scale (A and B), from NCEP to 45-km CRCM scale (C and D) and from 45-km CRCM to 45-km CRCM scale (E and F).

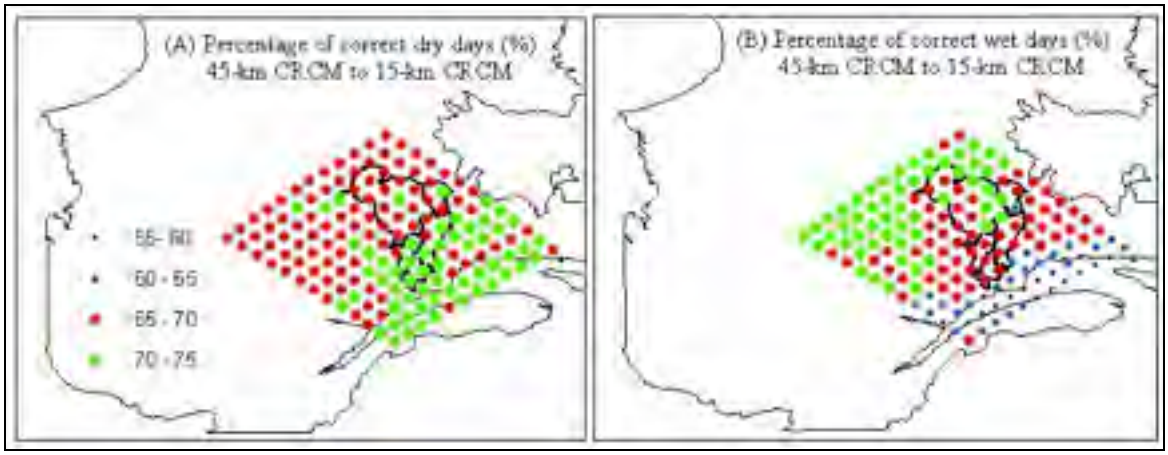

Figure 5.3 Percentages of correct wet and dry day classifications downscaled from 45-km CRCM to 15-km CRCM scale.

Table 5.4 Percentages of correct wet and dry day classifications downscaled from NCEP to 15-km CRCM scale.

Grid	**Downscaling from NCEP to 15-km CRCM**	
	Percentage of correct dry days (%)	**Percentage of correct wet days (%)**
Grid 1	73.2	67.6
Grid 2	72.2	72.1
Grid 3	73.7	67.8
Grid 4	73.8	71.7
Grid 5	72.8	66.5
Grid 6	73.5	67.0
Mean	73.2	68.8

The best results were obtained then downscaling 15-km precipitation occurrence from 15-km predictors (experiment 6) over the Manicouagan river basin (figure 5.4). The percentages of correct dry and wet states ranged between 88.2% and 94.6% and between 77.0% and 87.9% with means of 91.3% and 83.6%, respectively, across the 156 grid points. In addition, for both downscaling from 45-km CRCM and 15-km CRCM to 15-km CRCM scale (experiments 5 and 6), the success rates for dry states at the southeastern Manicouagan river

basin were greater than those at the northwestern river basin, but the success rates of wet states show an opposite pattern. This is likely linked to the observed precipitation pattern showing a north to south gradient of increasing precipitation. This pattern is an example of the ability of the 15-km CRCM to detect patterns of precipitation at this fine scale, and indicates the positive potential of downscaling to the station scale, as will be evaluated next.

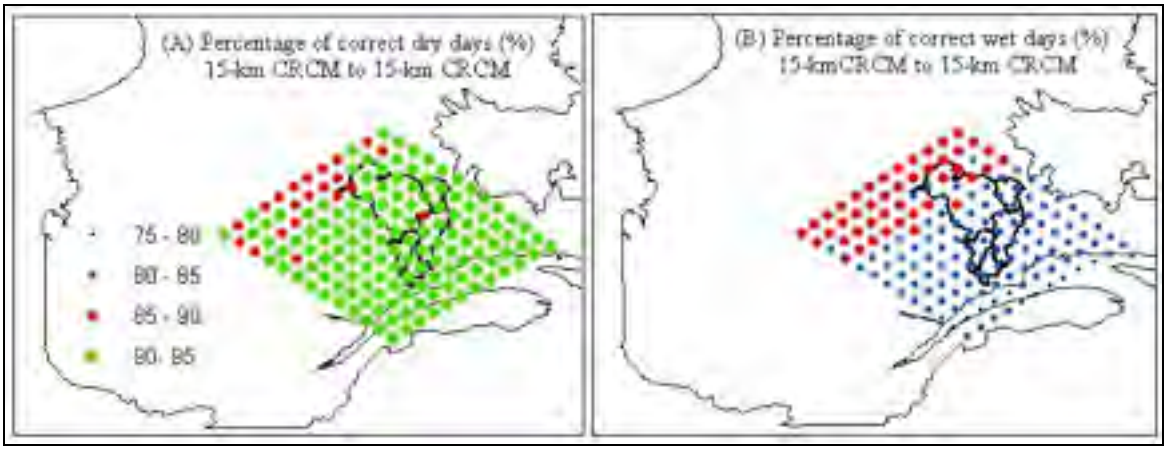

Figure 5.4 Percentages of correct wet and dry day classifications downscaled from 15-km CRCM to 15-km CRCM scale.

For climate change impact studies, the GCM or RCM outputs are normally downscaled to the station scale. Accordingly, daily precipitation occurrence was downscaled from NCEP, 45-km CRCM and15-km CRCM to the station scale. As discussed above, success rates were expected to be smaller than when predicting precipitation occurrence from same-scale predictors, and this is exactly what was observed. The prediction of dry states was also consistently better than that of wet states for all downscaling experiments, as shown in table 5.5. For downscaling from NCEP to station scale (experiment 7), the percentages of correct dry and wet states ranged between 69.7% and 89.1% and between 56.7%and 82.4%, respectively, with means of 75.4% and 69.6% across all 16 North American stations (ID 1-16). The success rates indicate a large spatial variability. The use of 45-km CRCM variables as predictors (experiment 8) yielded only small improvements over using NCEP predictors. The averaged success rates for dry and wet days were 77.7% and 70.2% across the same 16

stations. Even though a direct comparison is not possible, it is interesting to note that the average percentages of correct dry and wet days for the six stations over the Manicouagan river basin were slightly better when downscaling from 15-km CRCM to station (experiment 9). The percentages of correct dry and wet days were 82.0% and 71.6%, respectively, when going to 15-km CRCM scale.

Table 5.5 Percentages of correct wet and dry day classifications (%) downscaled from NCEP, 45-km CRCM and 15-km CRCM to station scale

ID	Downscaling from NCEP to station		Downscaling from 45-km CRCM to station		ID	Downscaling from 15-km CRCM to station	
	Correct dry days (%)	Correct wet days (%)	Correct dry days (%)	Correct wet days (%)		Correct dry days (%)	Correct wet days (%)
1	82.9	82.3	85.4	80.6	17	84.3	73.1
2	71.9	74.7	78.3	75.1	18	79.9	68.0
3	79.6	69.2	79.9	72.3	19	83.9	73.9
4	76.9	73.7	77.8	71.7	20	81.6	69.0
5	70.7	63.0	73.7	65.6	21	81.2	72.3
6	75.4	63.1	76.8	66.8	22	81.0	73.4
7	72.4	64.2	74.7	65.2			
8	73.7	63.6	76.0	63.4			
9	74.0	65.0	70.1	66.0			
10	69.7	56.7	68.8	60.0			
11	69.7	68.7	74.8	69.2			
12	70.3	72.1	75.2	70.7			
13	71.7	66.4	70.1	67.8			
14	76.9	82.4	83.1	72.7			
15	81.0	78.1	86.5	79.3			
16	89.1	70.9	91.8	76.1			
Mean	75.4	69.6	77.7	70.2	--	82.0	71.6

5.5.2 Downscaling of precipitation amounts

The percentage of explained variance indicates the extent to which daily variations in the local predictands are determined by regional forcing (Wilby et al., 2002b). For temperature, an explained variance over 70% is quite normal, but for precipitation, it is generally less than 30% for downscaling from GCM to station scale (Wilby et al., 1999).

Figures 5.5-5.7 present the percentages of explained variances for the calibration and validation of each season for downscaling from CGCM to CGCM (experiment 1) and from NCEP and 45-km CRCM to 45-km CRCM scale (experiments 2 and 3). Similarly to precipitation occurrence, the explained variances over the western coast of North America and the northern part of Canada were higher than those in the interior and eastern coast regions for all downscaling experiments, especially for the downscaling from 45-km CRCM to 45-km CRCM scale. Percentages of explained variance were lower in the summer and higher in the winter for all downscaling experiments. This is consistent with previous work and simply indicates that convective precipitation, typically occurring during summers, is less controlled by regional atmospheric circulation than is cyclonic precipitation. More specifically, for downscaling from CGCM to CGCM, the averaged explained variance for daily precipitation amounts was 32.7% for calibration and 28.3% for validation across four seasons and 258 grid points. The maximum explained variance was 58.1% for calibration and 56.1% for validation. On average, this indicates that only about 30% of the information is presented within the chosen predictors. These results again outline the fact that the precipitation generating processes within climate models are parameterized at a sub-grid scale. These relatively poor results also indicate that downscaling from GCM to a finer scale can only yield even poorer results for precipitation amounts. This is indeed the case when downscaling from NCEP to 45-km CRCM scale (experiment 2). The explained variance was only 15.8% for calibration and 11.3% for validation across four seasons and all 258 grid points, even though the 45-km CRCM model was driven by NCEP data at its boundaries. Downscaling precipitation amounts from 45-km CRCM using 45-km CRCM predictors yielded much improved results with average explained variances of 73.8% and 71.6% for

calibration and validation, respectively. Results were predictably poorer when downscaling precipitation amounts at the 15-km scale using 45-km CRCM predictors (figure 5.8, experiment 5), even though the selected grid points were different between the two downscaling experiments. The percentages of explained variances were 16.8% for calibration and 18.4% for validation across four seasons and 156 grid points within or close to the Manicouagan river basin. In particular, they were extremely low in the summer with only 9.9% and 14.0% for calibration and validation, respectively. The explained variance was higher in winter, with a percentage of explained variance of 22.5% for calibration and 23.0% for validation. As discussed earlier, the low explained variance is possibly due in part to the fact that the 45-km CRCM data used in this research was not run on the same domain as the 15-km CRCM. Nevertheless, these results have significant implications on the potential validity of finer-scale RCMs and their ability to statistically downscale precipitation at a finer scale, as will be discussed in more detail later. Downscaling precipitation amounts at the 15-km CRCM scale from 15-km CRCM predictors (experiment 6) showed slightly more consistency than the same experiments at the NCEP and 45-km CRCM scales (experiments 1 and 3). The average explained variance was 77.2% for calibration and 75.2% for validation across four seasons and 156 grid points within or close to the Manicouagan river basin. Moreover, the explained variances of the northern part of Manicouagan river basin were higher than those of the other parts of the river basin for both calibration and validation.

Experiment 4 looked at downscaling 15-km CRCM precipitation amounts from NCEP predictors. The average explained variances were 28.6% for calibration and 21.8% for validation across four seasons and all six grid points (table 5.6).

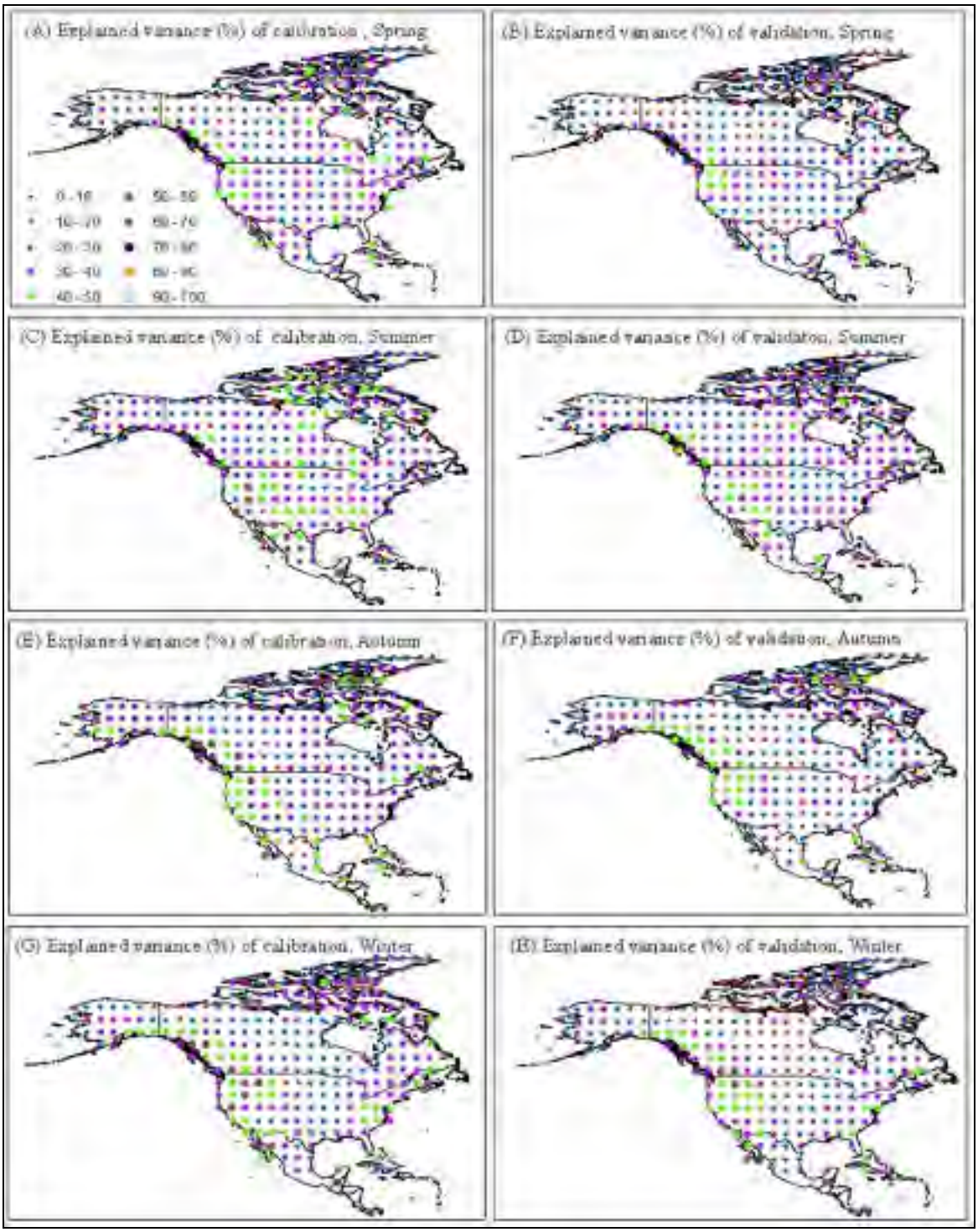

Figure 5.5 Explained variance of daily precipitation downscaled from CGCM to CGCM scale for calibration and validation of each season (Spring = Mar. + Apr. + May; Summer = Jun. + Jul. + Aug.; Autumn= Sep. + Oct. + Nov; Winter = Dec. + Jan. + Feb.).

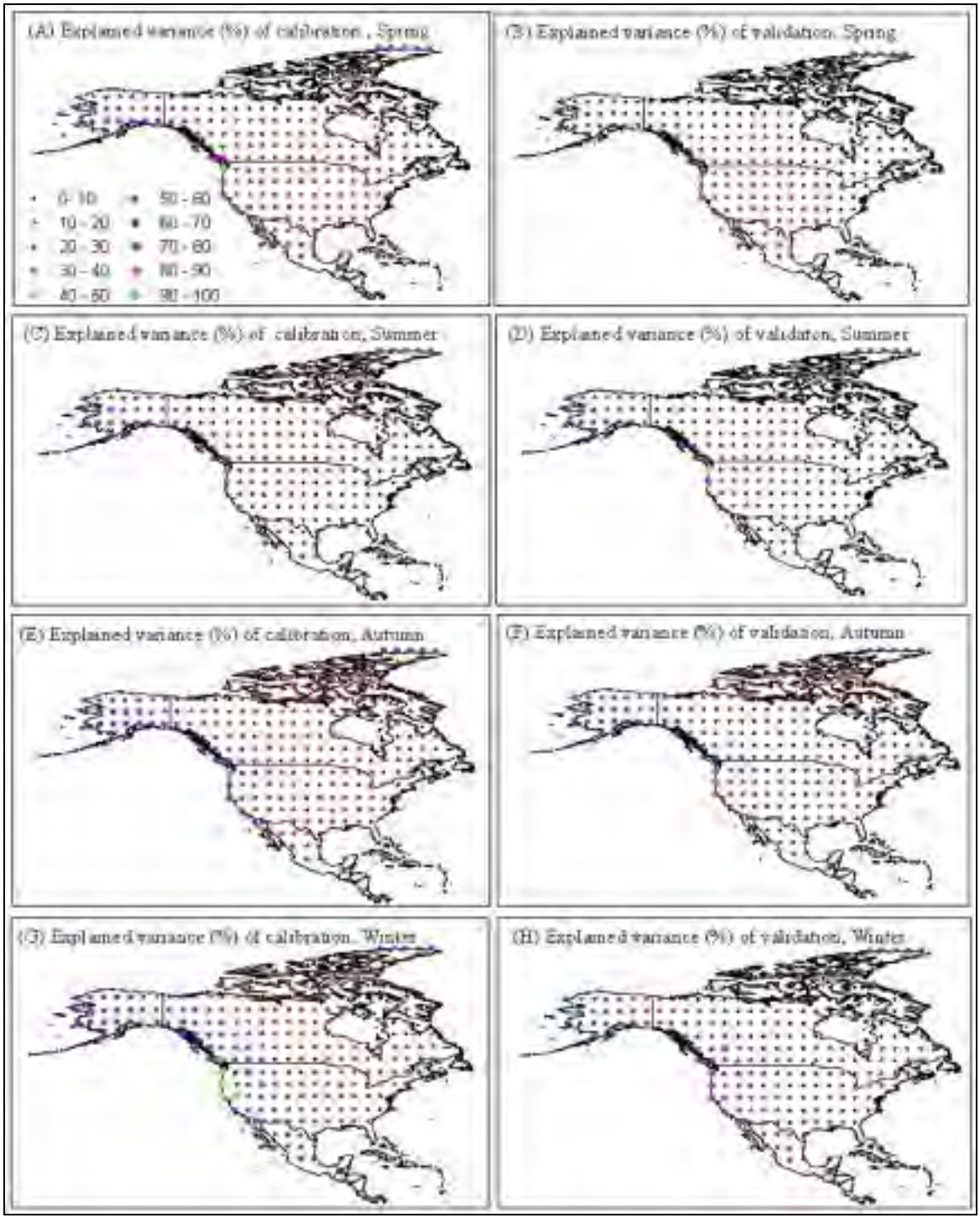

Figure 5.6 Explained variance of daily precipitation downscaled from NCEP to 45-km CRCM scale for calibration and validation of each season (Spring = Mar. + Apr. + May; Summer = Jun. + Jul. + Aug.; Autumn = Sep. + Oct. + Nov; Winter = Dec. + Jan. + Feb.).

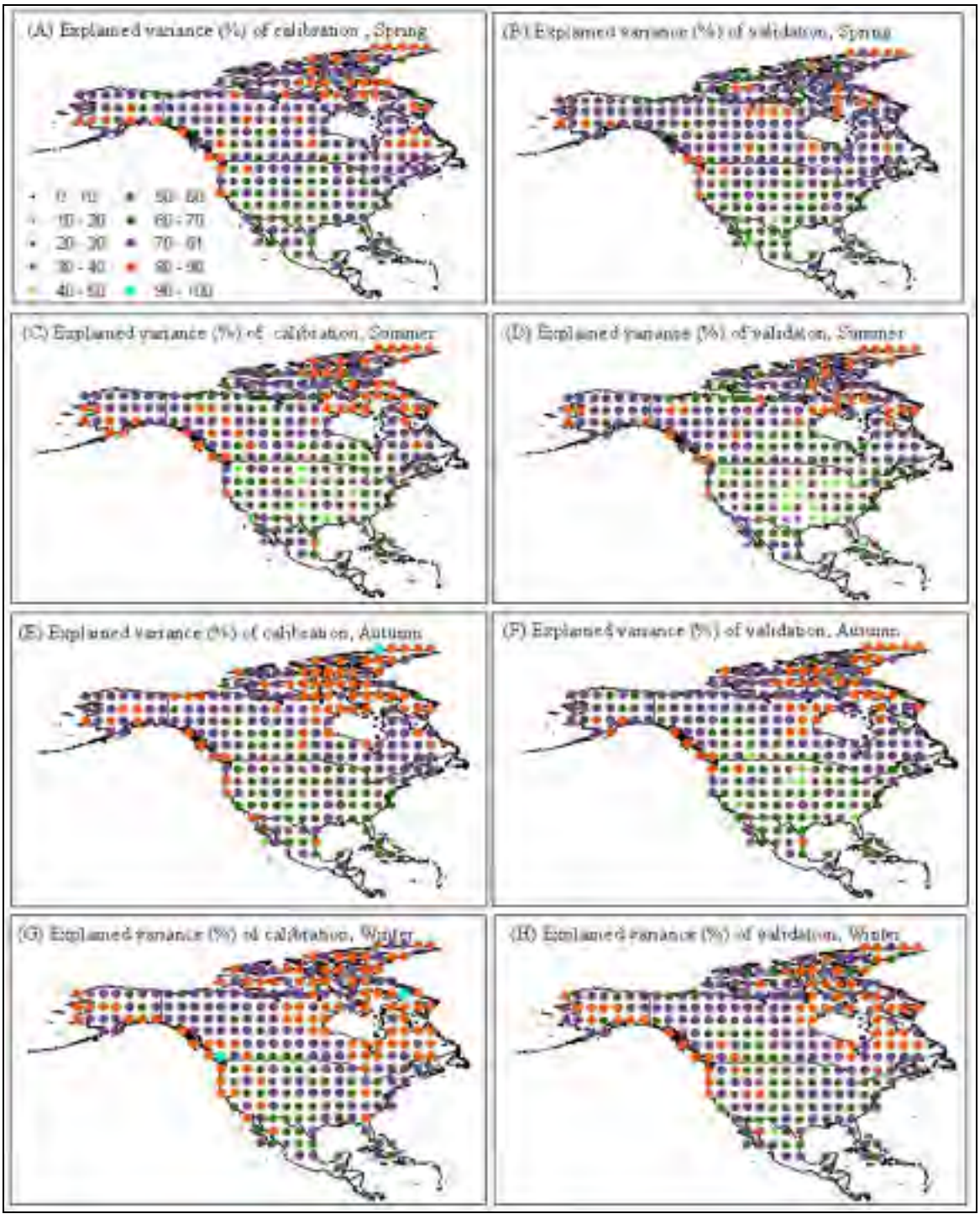

Figure 5.7 Explained variance of daily precipitation downscaled from 45-km CRCM to 45-km CRCM scale for calibration and validation of each season (Spring = Mar. + Apr. + May; Summer = Jun. + Jul. + Aug.; Autumn = Sep. + Oct. + Nov.; Winter = Dec. + Jan. + Feb.).

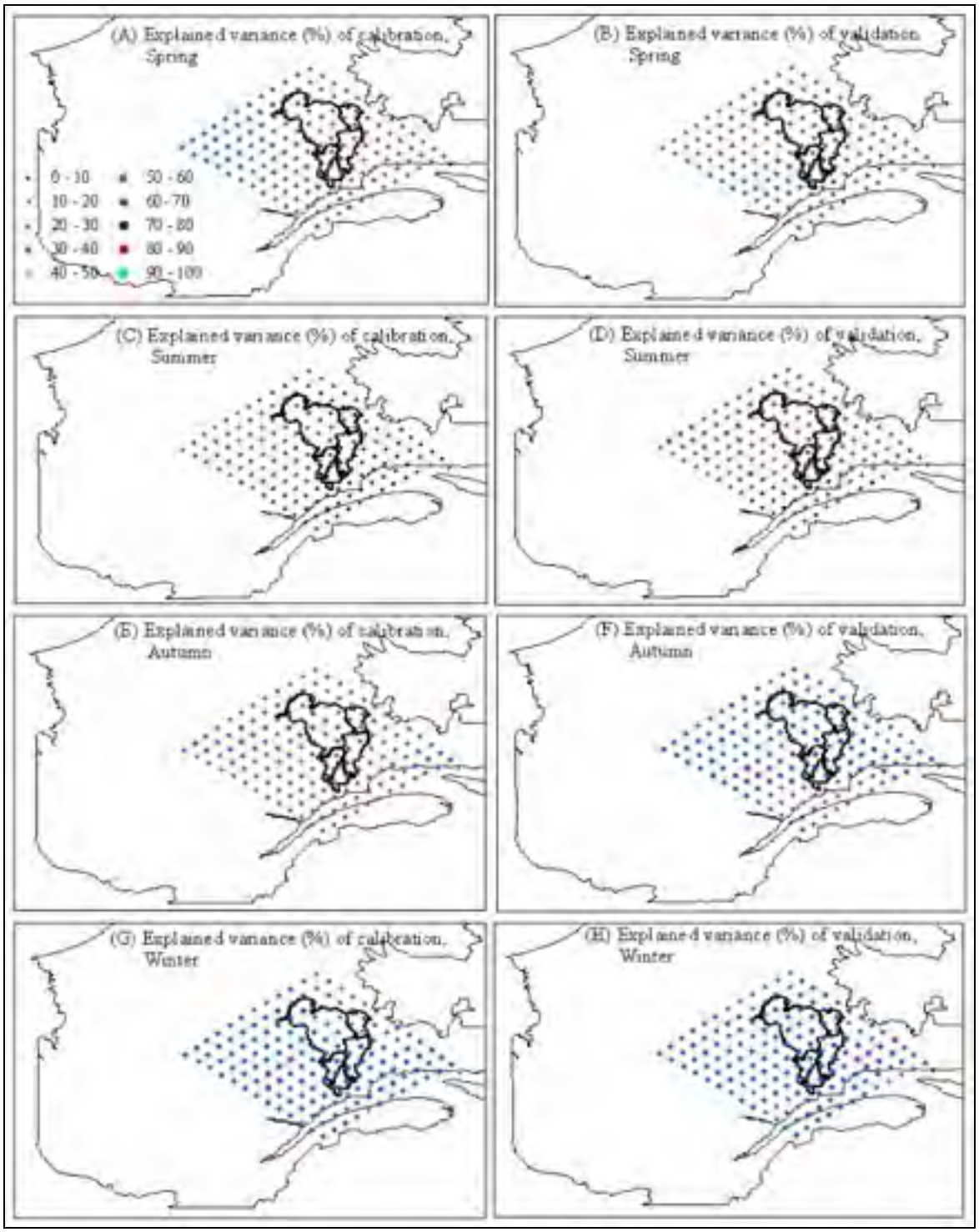

Figure 5.8 Explained variance of daily precipitation downscaled from 45-km CRCM to 15-km CRCM scale for calibration and validation of each season (Spring = Mar. + Apr. + May; Summer = Jun. + Jul. + Aug.; Autumn = Sep. + Oct. + Nov; Winter = Dec. + Jan. + Feb.).

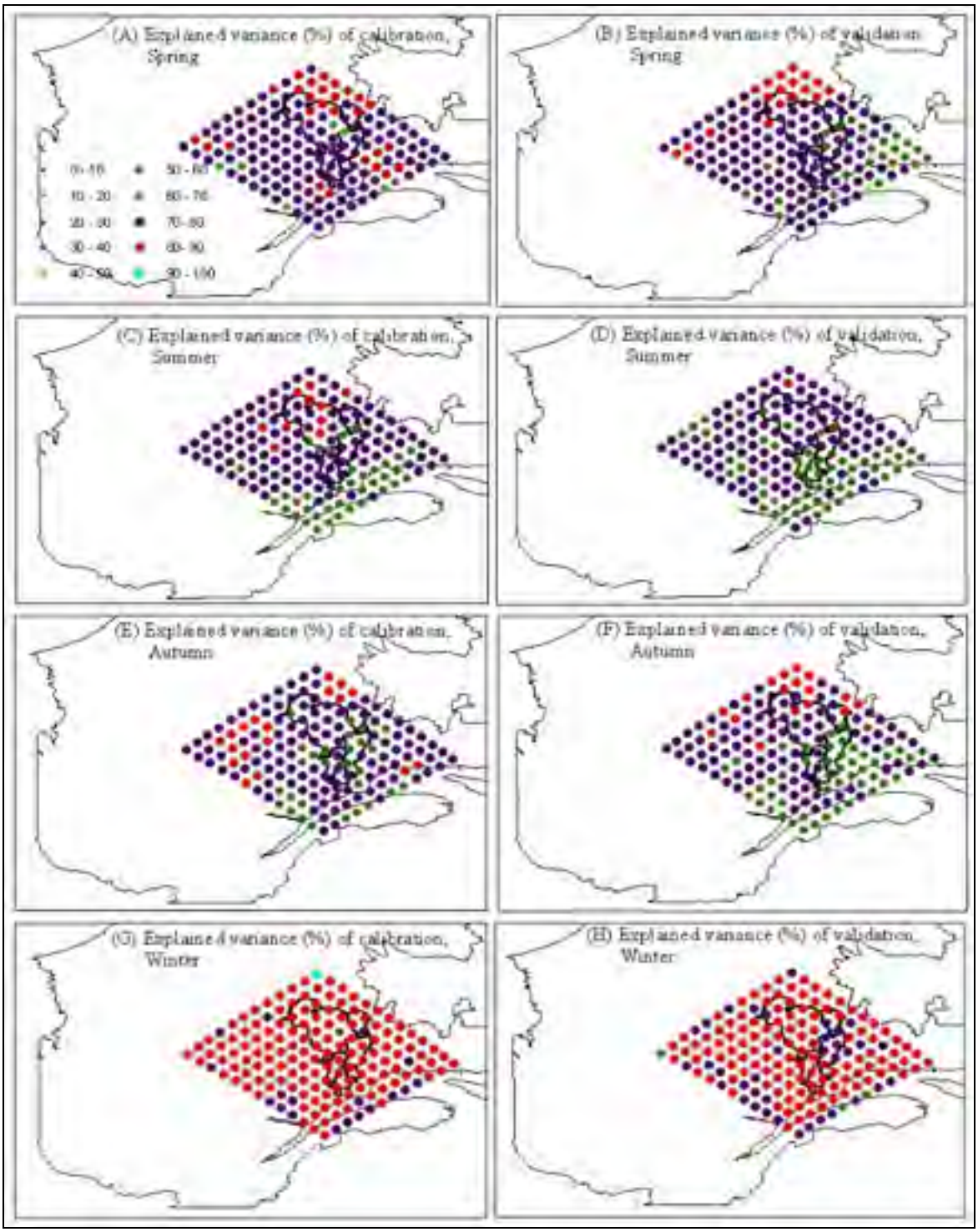

Figure 5.9 Explained variance of daily precipitation downscaled from 15-km CRCM to 15-km CRCM scale for calibration and validation of each season (Spring = Mar. + Apr. + May; Summer = Jun. + Jul. + Aug.; Autumn = Sep. + Oct. + Nov; Winter = Dec. + Jan. + Feb.).

Table 5.6 Explained variance of daily precipitation downscaled from NCEP to 15-km CRCM scale for calibration and validation of each season

Grid	Explained variance of calibration (%)				Explained variance of validation (%)			
	MAM	JJA	SON	DJF	MAM	JJA	SON	DJF
Grid 1	30.8	25.8	27.1	31.8	21.6	14.8	23.5	27.2
Grid 2	31.3	19.0	29.8	31.5	23.4	19.5	23.6	25.4
Grid 3	20.7	18.8	24.8	38.8	20.6	17.7	24.0	22.9
Grid 4	27.2	19.4	29.9	37.3	23.6	16.7	26.0	28.6
Grid 5	27.6	16.2	27.9	42.7	20.1	11.7	19.7	31.5
Grid 6	35.6	14.0	32.3	45.3	20.6	11.3	17.9	31.9
Mean	28.9	18.9	28.6	37.9	21.7	15.3	22.4	27.9

Finally, daily precipitation amounts were downscaled to the station scale from NCEP, 45-km CRCM and 15-km CRCM scales (experiments 7, 8 and 9). Results are presented in tables 5.7, 5.8 and 5.9, respectively. Going from large scale predictors to the station scale is the goal for most climate change impact studies, and these are ultimately the most relevant results for most users. The explained variances of daily precipitation amount were only 17.8% for calibration and 10.6% for validation across four seasons and all 16 stations when using NCEP predictors. Values were especially low in the summer (11.6% for calibration and 7.0% for validation) and slightly higher in the winter (22.0% for calibration and 11.0% for validation). As discussed above, the explained variances also reflect a large spatial variability depending on station location. For example, in the spring, the maximum explained variance was 35.7% (station 9), while the minimum was 5.0% (station 12). Across all seasons and stations, the explained variances were somewhat improved when using 45-km CRCM variables as predictors. These were 21.6% and 13.2% for calibration and validation, respectively. When downscaling from 15-km CRCM to station scale, the average explained variance was 33.4% for calibration and 30.3% for validation. However, the explained variance was still lower in the summer (<20%) and was the highest in the winter at more than 40%. As discussed earlier, although the selected stations were different in experiment 9, results nonetheless indicate the added value of the finer 15-km CRCM scale. The

improvements observed with finer scale predictors were the greatest in winter, again indicating the better ability of the finer scale climate model at describing regional atmospheric circulation. Convective precipitation events again proved to be a more complex problem, and will be discussed below.

Table 5.7 Explained variance of daily precipitation downscaled from NCEP to station scale for calibration and validation of each season

Station	Explained variance of calibration (%)				Explained variance of validation (%)			
	MAM	JJA	SON	DJF	MAM	JJA	SON	DJF
1	30.3	19.7	33.9	32.9	33.3	25.1	32.3	30.8
2	11.6	19.9	23.4	23.9	11.1	5.1	18.4	3.2
3	13.9	5.0	15.7	18.7	7.9	0.6	14.6	5.2
4	20.5	17.9	28.1	7.5	12.1	7.6	18.4	2.7
5	16.6	14.4	16.0	17.9	16.9	6.9	6.7	8.8
6	22.3	14.7	15.5	20.5	13.4	4.9	13.9	7.6
7	21.9	14.5	22.9	22.1	13.3	12.8	14.3	19.0
8	35.7	18.6	26.8	35.4	16.1	13.8	23.3	23.5
9	30.5	16.1	11.6	25.7	15.6	8.6	19.5	22.9
10	18.8	3.8	24.3	22.8	3.9	4.0	5.4	1.9
11	10.0	11.4	20.9	9.9	3.3	3.2	2.9	4.4
12	5.0	2.0	5.9	16.4	2.9	0.8	6.5	3.7
13	13.7	7.4	13.5	22.1	2.6	0.7	6.4	4.6
14	8.8	6.0	15.3	23.6	5.0	0.7	1.8	9.5
15	16.0	7.1	21.6	29.9	12.1	12.4	16.0	18.3
16	14.4	7.1	17.9	22.1	10.0	5.7	10.5	10.0
Mean	18.1	11.6	19.6	22.0	11.2	7.0	13.2	11.0

Table 5.8 Explained variance of daily precipitation downscaled from 45-km CRCM to station scale for calibration and validation of each season

Station	Explained variance of calibration (%)				Explained variance of validation (%)			
	MAM	JJA	SON	DJF	MAM	JJA	SON	DJF
1	33.8	22.3	38.8	33.7	40.7	27.8	45.0	40.1
2	15.4	22.1	26.4	26.2	18.0	8.2	19.3	5.0
3	22.7	11.6	25.6	34.2	12.9	0.9	17.2	8.3
4	24.1	18.9	25.8	17.4	16.3	8.0	17.4	5.9
5	19.4	22.9	12.9	19.1	18.8	7.7	6.4	8.0
6	26.0	16.9	22.3	15.9	11.2	5.2	16.9	8.4
7	24.5	18.0	25.0	26.4	18.9	15.3	16.2	14.1
8	34.3	17.9	25.8	18.7	19.0	15.7	26.1	26.8
9	30.8	18.3	21.0	29.5	18.6	9.4	16.4	23.4
10	18.8	7.0	28.0	24.4	3.6	6.2	6.2	2.5
11	12.2	5.3	14.9	13.1	9.2	4.4	6.0	10.7
12	13.2	7.3	5.8	19.1	4.3	4.4	7.4	9.7
13	19.9	6.1	33.8	40.5	2.0	2.0	6.2	5.9
14	18.7	8.4	12.9	30.0	7.5	1.3	2.3	4.3
15	24.6	11.0	35.3	39.5	23.6	9.3	34.1	33.4
16	24.2	20.0	14.9	29.1	6.7	7.0	13.8	14.4
Mean	22.7	14.6	23.1	26.0	14.5	8.3	16.0	13.8

5.6 Discussion and conclusion

Regression-based statistical downscaling methods were evaluated with respect to precipitation. The methodology involved nine downscaling experiments at four different spatial scales, from GCM scale all the way to station scale. The precipitation occurrence was downscaled using discriminant analysis and a stepwise linear regression method was used for downscaling daily

precipitation amounts. The approaches tested are representative of the most commonly used statistical downscaling method in the literature.

Table 5.9 Explained variance of daily precipitation downscaled from 15-km CRCM to station scale for calibration and validation of each season

Station	Explained variance of calibration (%)				Explained variance of validation (%)			
	MAM	**JJA**	**SON**	**DJF**	**MAM**	**JJA**	**SON**	**DJF**
17	39.5	25.7	36.0	47.8	35.2	14.6	36.5	46.9
18	25.1	11.4	30.6	48.1	22.8	13.4	31.9	33.5
19	40.8	21.6	35.8	44.6	33.3	14.5	51.5	52.8
20	29.5	11.7	28.2	38.3	13.8	7.7	33.1	19.0
21	29.8	19.8	40.3	52.0	30.5	15.9	31.5	57.1
22	39.0	22.3	31.9	50.5	27.3	21.4	35.7	48.2
Mean	33.9	18.8	33.8	46.9	27.1	14.6	36.7	42.9

Prior to going to the station scale, downscaling experiments were first performed within the realm of climate models to gain insights on the maximum potential ability of the approach (experiments 1 to 6). Clearly, if the tested downscaling method is not successful when applied between a RCM and its parent GCM (or NCEP data), there is little hope of having any success at the station scale.

With respect to downscaling precipitation occurrence, table 5.10 summarizes the average percentages of correct dry and wet days of all of the downscaling experiments. Within the first six experiments, not surprisingly, the best predictions of precipitation occurrence were all obtained from downscaling precipitation from predictors at the same scale. Results improved when going from CGCM to CRCM scale, but overall, the differences were very small between the 15-km and 45-km CRCM. Even in these best-case experiments, the performance was less than stellar, especially for wet days, clearly indicating that within climate models, precipitation

generation is a lot more complex than a linear combination of atmospheric variables. It is important to keep in mind that these are same-scale experiments that represent an upper bound in terms of potential performance when downscaling to a finer scale using linear transfer functions. Results rapidly deteriorated for the 'true' downscaling experiments (experiments 2, 4 and 5), for which both average success rates of correct dry and wet days were below 75%. The results show quite clearly that there is an important loss of information when trying to downscale at a finer scale, even within the same parent GCM and associated CRCM. Once the GCM (or NCEP) information is transmitted at the boundaries of the RCM, the regional model is now free within its own domain and there are no guarantees that storm patterns will not move a little bit further south or north. While regional patterns should on average stay the same, daily precipitation may differ markedly within a few grid points, which explains the relatively poor performance. The same limitation also applies to downscaling at the station scale. For downscaling from NCEP and CRCM to station scale, the average percentage of correct dry days increased slightly as the climate model resolution gets finer. However, there was little change for wet days across all three scales. The maximum average percentage of correct days was 82.0% for dry days and 71.6% for wet days. While better than a random guess, this performance is certainly not adequate for modeling series of consecutive wet or dry days. Since these series are critical to many agricultural or hydrological climate change impact studies, the obvious conclusion is that linear regression-based statistical downscaling methods are inappropriate for modeling precipitation occurrence, at least over North America. Since results are dependent upon geographical location, it is not possible to state that these methods could not yield acceptable results somewhere else, but the fact remains that any climate change impact study based on linear regression downscaling, should be suspect unless the ability of properly modeling precipitation occurrence is clearly demonstrated, or unless precipitation occurrence is not an important factor. One example of such an application is snowmelt-related flooding. In Nordic climates, precipitation accumulated over several months usually melts within a few weeks at most. In this context, it does not matter that much if snowfall occurrence was not well reproduced, as long as there is the right amount of snow accumulation at the onset of the spring thaw. In contexts such as these the results for downscaling precipitation amounts would be worthwhile.

The average seasonal percentages of the explained variances of precipitation amounts for the calibration and validation periods for all downscaling experiments were also summarized in table 5.10.

Table 5.10 Average percentages of correct dry and wet day classifications and average explained variance of daily precipitation for each downscaling combination

ID	Experiment	Correct dry days (%)	Correct wet days (%)	Average explained variance of calibration (%)				Average explained variance of validation (%)			
				MAM	JJA	SON	DJF	MAM	JJA	SON	DJF
1	CGCM to CGCM	77.8	73.2	30.7	33.8	33.3	32.8	26.4	30.2	28.5	28.0
2	NCEP to 45-km CRCM	70.1	67.9	15.2	12.7	16.0	19.1	10.3	9.5	13.0	12.5
3	45-km CRCM to 45-km CRCM	89.7	83.9	74.3	70.7	73.5	76.6	72.4	68.0	71.1	74.7
4	NCEP to 15-km CRCM	73.2	68.8	28.9	18.9	28.6	37.9	21.7	15.3	22.4	27.9
5	45-km CRCM to15-km CRCM	69.5	69.3	17.6	9.9	17.2	22.5	16.1	14.0	20.4	23.0
6	15-km CRCM to 15-km CRCM	91.3	83.6	77.2	73.7	74.5	83.5	74.5	71.4	73.2	81.7
7	NCEP to station	75.4	69.6	18.1	11.6	19.6	22.0	11.2	7.0	13.2	11.0
8	45-km CRCM to station	77.7	70.2	22.7	14.6	23.1	26.0	14.5	8.3	16.0	13.8
9	15-km CRCM to station	82.0	71.6	33.9	18.8	33.8	46.9	27.1	14.6	36.7	42.9

As was done earlier for precipitation occurrence, downscaling experiments within the realm of climate models (experiments 1- 6) will first be discussed prior to examining station scale downscaling. When performing same-scale downscaling (experiments 1, 3 and 6), results increased from about 30% at the CGCM scale to around 73% for 45-km CRCM, to an average

of 76% for the 15-km CRCM. These numbers are not interesting by themselves since they do not represent true downscaling experiments, but they are very relevant in helping to understand the limits of the tested approach at the station scale, the ultimate goal for most impact studies. These numbers indicate that downscaling from GCM scale to the station scale is likely a futile exercise, but that the use of predictors at the finer regional scales may yield better results. The results from experiments 2, 4 and 5 (downscaling from NCEP to CRCM (45-km and 15-km) or from 45-km CRCM to 15-km CRCM) demonstrated that even within climate models, linear regression at best explains 37.9% of the observed variance for daily precipitation amounts.

Results of experiments 7, 8 and 9, where downscaling was performed at the station scale, demonstrated quite convincingly the poor performance of linear regression schemes for downscaling precipitation amounts at the station level. The average percentage of explained variance was always less than 14.2% (as low as 7% for summer) when downscaling from GCM scale. A disappointing increase of around 3% in explained variance was observed when using 45-km CRCM predictors. Many studies have shown a large reduction in precipitation biases when using RCM over GCM. Our results indicate that these improvements mostly do not transfer to the tested statistical downscaling approach. Even at the finer 45-km scale, the world seen by the climate model is vastly different than the real world. As discussed earlier, even when driven by NCEP data, the model is free to create its own dynamics and the chaotic nature of the climate system virtually insures that storm patterns will not be recreated in the same positions and at the same time as they are in the real world. Since it is difficult for linear methods to reproduce precipitation occurrence, it should not be surprising to find an even poorer performance for precipitation amounts.

However, the percentages of explained variance almost doubled when downscaling from 15-km CRCM predictors. This improvement is clear, even though we are not comparing results over the same domains. This seems to indicate that the much better representation of the real physical world (especially in terms of digital elevation models, vegetation and humidity zones) allows for a much better resemblance between the virtual world of the climate model and the real world. While they are improved, the percentages of explained variance remain relatively

low, with a maximum of 46.9% for winter and a minimum of 14.6% for summer. However, these downscaling results are not of much practical use, because at that scale, CRCM precipitation exhibits small precipitation biases (at least over southern Quebec where it was tested here) and can be directly input into impact models without the need for further downscaling .

The main conclusion of this study is that linear regression statistical approaches are mostly an ineffective downscaling tool for both precipitation occurrence and precipitation amounts, at least for most parts of North America. In light of these results, it is difficult to understand why the use of this method has been so prevalent in the last decade. One of the reasons is probably because it works relatively well for downscaling temperatures, and that it is only natural to extend it to other predictands such as precipitation. Another reason is very likely due to how easy the SDSM freeware is to use. The built-in bias correction and variance inflation tools may yield apparently adequate results for the wrong reasons in the hands of untrained users. For example, the proper amount of bias correction and variance inflation may give nearly perfect QQ plots between downscaled and observed precipitation amounts, even with predictors explaining less than 10% of the total variance.

There remains the last caveat of all statistical downscaling methods -- which the established links between predictors and predictands must hold in a changed climate. This is a leap of faith for all statistical methods but particularly for the commonly used regression-based approaches that use NCEP predictors and then apply the extracted relationships to GCM predictors. While they do share many similarities, NCEP data and GCM data are completely independent. NCEP data aims at representing the real world, whereas GCMs operate in their own virtual world. NCEP reanalysis data is based on the assimilation of real world observed data into a climate model, whereas GCMs operate on their own, in their own world at a scale that limits the resemblance between both worlds. This explains in large part why GCMs exhibit relatively large biases for both temperature and precipitation. Under these conditions, it is in fact unlikely that rules established from NCEP predictors will hold with GCM data, under both current and future climate conditions.

CHAPTER 6

DOWNSCALING OF WEATHER GENERATOR PARAMETERS FOR QUANTIFYING THE HYDROLOGICAL IMPACTS OF CLIMATE CHANGE

Jie Chen[1], François P. Brissette[1], Robert Leconte[2]

1. Department of Construction Engineering, École de technologie supérieure, Université du Québec, 1100, rue Notre-Dame Ouest, Montréal, Québec, Canada, H3C 1K3.
2. Department of Civil Engineering, Université de Sherbrooke, 2500, boul. de l'Université, Sherbrooke, Québec, Canada, J1K 2R1

This article was submitted to the Climate Research in March, 2011.

6.1 Abstract

A major obstacle in quantifying the hydrological impacts of climate change is the mismatch between the coarse resolution of General Circulation Models' (GCMs) and Regional Climate Models' (RCMs) outputs and the fine resolution requirements of hydrological models. Both dynamical and statistical downscaling approaches have been developed to overcome this problem. This research presents a statistical downscaling approach combining the attributes of both the stochastic weather generator (WG) and the change factor (CF) method using an RCM projected precipitation and temperatures as predictors. It is further compared against the commonly used CF method in terms of quantifying the hydrological impacts of climate change over the next century for a Canadian watershed (Quebec province). Both downscaling methods suggested increases in winter (November - April) discharge and decreases in summer (June - October), especially for those downscaled by the WG-based method. The WG-based method predicted higher peak discharges than the CF method. The two downscaling methods suggested significantly different increases in annual and seasonal discharges and particularly for low flows. Hydrology results show that precipitation and temperature variability play a very important role in the runoff generating process and that

neglecting to address these changes can lead to biased results. The results also outline the uncertainty linked to the choice of a downscaling method. The proposed WG approach has the significant advantage over the CF method of allowing for different probabilities of precipitation and variability in a changed climate, and is arguably a better approach than the more widely used CF method.

Keywords: Statistical downscaling; stochastic weather generator; change factor method; hydrology; climate change

6.2 Introduction

The Intergovernmental Panel on Climate Change (IPCC, 2007) states that the average surface air temperature of Earth will likely increase between 1.8-4.0 ºC by the end of this century. Climate models predict that extreme events such as severe storms will increase in frequency, and that the variability of precipitation will also be on the rise (IPCC, 2007). Climate change will affect the global hydrological cycle and consequently, assessing the changes in future precipitation (quantity and variability) is a priority. Quantifying the impacts of climate change requires a tool or an approach that is able to produce climate projections. General Circulation Models (GCMs) were developed over several years to meet this requirement. However, the resolution of current GCMs is too coarse to assess the watershed and site-specific impacts of climate change (IPCC, 2007). Dynamical and statistical downscaling methods have been developed to resolve this issue. Dynamical downscaling is developed based on dynamic formulations using the initial and time-dependent lateral boundary conditions of GCMs to achieve a higher spatial resolution by nesting Regional Climate Models (RCM) (Caya and Laprise, 1999). The spatial resolution of RCMs is much better than that of GCMs. However, this method remains too coarse for small and medium-size watersheds as well as for site-specific impact studies. Moreover, RCM data is only available for limited regions, due to the large computational cost of running the models (Solman and Nunez, 1999). To overcome this problem, statistical downscaling methods have been developed. These involve linking the states of some variables representing a large scale

(GCM or RCM grid scale, predictors) to the states of some variables representing a much smaller scale (catchment or site scale, predictands). A range of statistical downscaling methods have been developed, and can be classified into three categories: transfer function (Wilby et al., 1998a; Wilby et al., 2002a), weather typing (von Storch et al. 1993; Schoof and Pryor, 2001) and weather generator (WG)-based approaches (Wilks, 1999a; Zhang, 2005; Kilsby et al., 2007; Qian et al., 2005, 2010). Each category has its advantages and drawbacks. For transfer functions and weather typing schemes, the chief drawback is that they do not consistently provide a stable relationship between predictors and predictands (Chen et al., 2011a). In the case of WG approaches, the adjustment of transition probabilities, such as a wet day following a wet day (P11) and a wet day following a dry day (P01) is still a challenge. Transfer functions are the most widely used methods, with vorticity, airflow indices, wind velocity and direction, mean sea-level pressure, geopotential heights and relative humidity as the most commonly used predictors (Wilby et al., 1998a; Solman and Nunez, 1999; Sailor and Li, 1999; Trigo and Palutikof, 2001).

Over the past decade, stochastic weather generators (WGs) have been commonly used as downscaling tools for climate change studies (Wilby et al. 2002b, Zhang, 2005, Kilsby et al., 2007; Qian et al., 2005, 2010; Wilks, 2010). Daily stochastic WGs like WGEN (Richardson, 1981; Richardson and Wright, 1984), CLIGEN (Nicks et al., 1995), and WeaGETS (Chen et al., 2011b) can rapidly produce climate projections at a daily time scale that can be used to quantify the impacts of climate change (Wilks, 1992; Pruski and Nearing, 2002; Zhang et al., 2004, Zhang, 2005; Zhang and Liu, 2005). There are two main approaches for parametric adjustments of WGs (Wilks, 2010). The first involves a day-by-day change to the WG parameters based on daily variations in atmospheric circulation (Wilby et al., 2002b). The other one is the most commonly used method, and involves changes in WG parameters based on assumed changes in the corresponding monthly statistics of atmospheric circulation (Zhang, 2005, Kilsby et al., 2007; Qian et al., 2005, 2010; Wilks, 2010). Wilby et al. (2002b) explored the use of synoptic-scale predictor variables (North Atlantic Oscillation and Sea Surface Temperature) to downscale both high- and low-frequency variability of daily precipitation at sites across Great Britain. The results showed that conditionally stochastic

rainfall models displayed positive effects on monthly rainfall statistics. However, the relationship between precipitation parameters and indices was very weak for most of the tested stations. Other work indicates that statistical downscaling using GCM precipitation directly as a predictor performed much better than using other predictors (Widmann et al., 2003; Zhang, 2005). Zhang (2005) presented a method for statistically downscaling GCM monthly outputs from GCM grid scale to site-specific scale using GCM-projected precipitation and temperature as predictors. GCM-projected monthly precipitation was first spatially downscaled from a grid box to a target station using transfer functions. The spatially downscaled monthly precipitation was then downscaled to daily precipitation series at the target station using CLIGEN. For the downscaling of precipitation occurrence, transition probabilities were adjusted based on spatially downscaled monthly precipitation. This method has not been tested in different climates, and the relationships between transition probabilities and monthly precipitation may strongly depend on geographical location.

The change factor (CF) method is a straightforward and widely used downscaling method (Diaz-Nieto and Wilby, 2005). It establishes a baseline climatology using long-term climate data for the target site. The changes between present and future climates derived from a GCM grid point close to the target site, usually at a monthly scale, are added to (for temperature) or multiplied by (for precipitation) each day in the baseline time series. This method is computationally straightforward and easy to apply. The most significant drawback is that the temporal sequencing of wet and dry days and the variance of each variable are unchanged.

The objective of this work is to present a statistical downscaling method combining the attributes of both stochastic WG and the CF methods, using RCM-projected precipitation and temperatures as predictors. This new method is further compared to the CF method by quantifying the hydrological impacts of climate change for a Canadian watershed (Quebec province). The huge advantage of the developed method over the CF method is that differences in precipitation occurrence and variance of all variables can be specifically taken

into account. In addition, time series of any length can be generated -- an advantage for the study of extremes.

6.3 Study area and data

6.3.1 Study area

This study was conducted for the Manicouagan 5 river basin (figure 6.1) located in central Quebec, Canada. It covers 24,610 km^2 of mostly forested area. It has a rolling to moderately hilly topography with a maximum elevation of 952 m above sea level. The reservoir at the basin outlet has a mean level of 350 m above sea level. Population density is extremely low and logging is the only industrial activity over the basin. The basin drains into the Manicouagan 5 reservoir, a 2000 km^2 annular reservoir within an ancient eroded impact crater. The basin ends at the Daniel Johnson dam which is the largest buttressed multiple arch dam in the world. The installed hydropower capacity is 2.6GW. The annual mean discharge of the Manicouagan 5 River is 529m^3/s. Snowmelt peak discharge usually occurs in May and averages 2200 m^3/s.

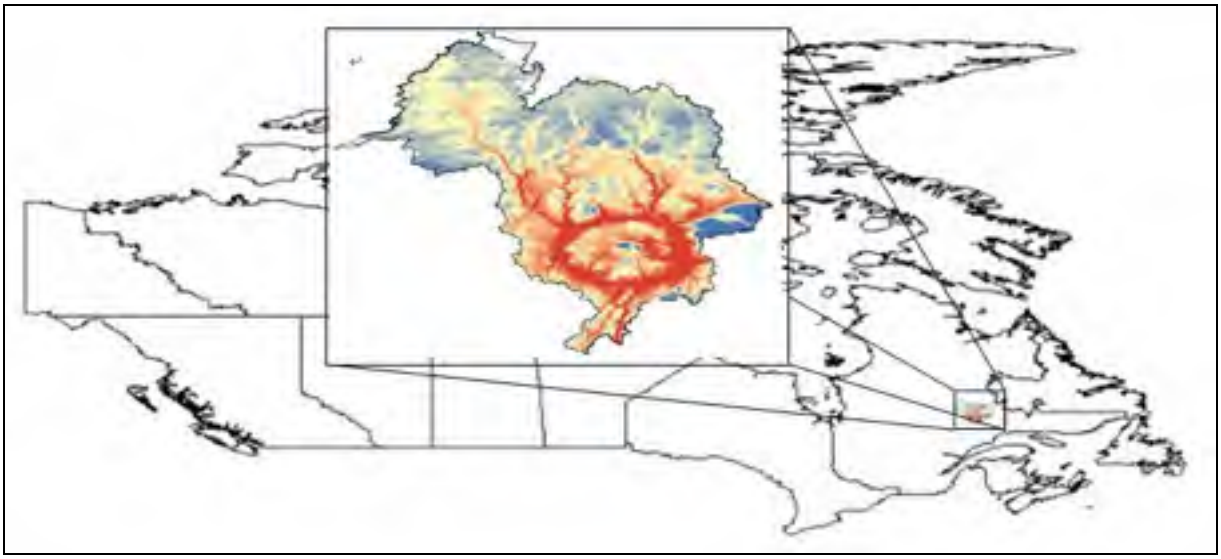

Figure 6.1 Location map of Manicouagan 5 river basin.

6.3.2 Data

The observed data consisted of precipitation, maximum and minimum temperatures (Tmax and Tmin) interpolated on a 10 km grid by the National Land and Water Information Service (www.agr.gc.ca/nlwis-snite). The interpolation is performed using a thin plate smoothing spline surface fitting method (Hutchinson et al., 2009). Discharge data at the basin outlet was obtained from mass balance calculations at the dam and provided by Hydro-Québec. Climate data consisted of RCM-projected precipitation, Tmax and Tmin. Data from the Canadian Regional Climate Model (CRCM) (v.4.2.0) with a grid resolution of 45km driven by the Canadian General Circulation Model (v3.1) (CGCM3) was used. This work covers the 1970-1999 period (reference period) for calibration and the 2011-2099 period in climate change mode. Thirty-year moving averages were calculated for climate data for the 2011- 2099 period, which resulted in 60 30-year horizons centered over 2025-2084.

6.4 Methodology

A new downscaling method based on WG is presented below. Precipitation, Tmax and Tmin were downscaled from the CRCM scale to the site-specific scale over the 2025-2084 period (centered by 30-year moving averages from 2011-2099) using CRCM precipitation and temperatures as predictors. The results were compared against the widely-used CF method in downscaling precipitation, Tmax and Tmin and in simulating hydrological impacts using a lumped conceptual hydrological model.

6.4.1 Downscaling of weather generator parameters

This section presents a method based on stochastic WGs for statistically downscaling CRCM-projected precipitation, Tmax and Tmin. The method can also be applied to GCM outputs. A WG is first calibrated using observed data. The parameters of the WG are then modified to take into account variations projected by a climate model (GCM or RCM). This variation is based on a delta change approach. For example, take the probability of occurrence of P01, a common parameter of weather generators using a two-state Markov

chain for precipitation occurrence. For various reasons, P01 from GCM or RCM data will not match P01 measured at a station. Thus, similarly to the CF method, the difference between P01 projected by GCM (or RCM) in present and future climate will be applied to the observed data. The same method is also applied to the probability of occurrence of P11 and the monthly mean precipitation (MMP). The prerequisite for using this method is that the GCM (or RCM) simulated P01, P11 and MMP should display gradual changes as the climate varies. Figure 6.2 displays the 30-year moving averages of CGCM3- and CRCM-simulated seasonal MMP, P01 and P11 for the 1961-2099 period. The results show that MMP, P01 and P11 change gradually from 1960 to 2099 for all four seasons. The correlations between each change trend and its linear regression are very significant for both CGCM3 and CRCM data at the P=0.01 level (table 6.1). Thus, this method is feasible for downscaling the MMP, P01 and P11 of GCM and RCM outputs.

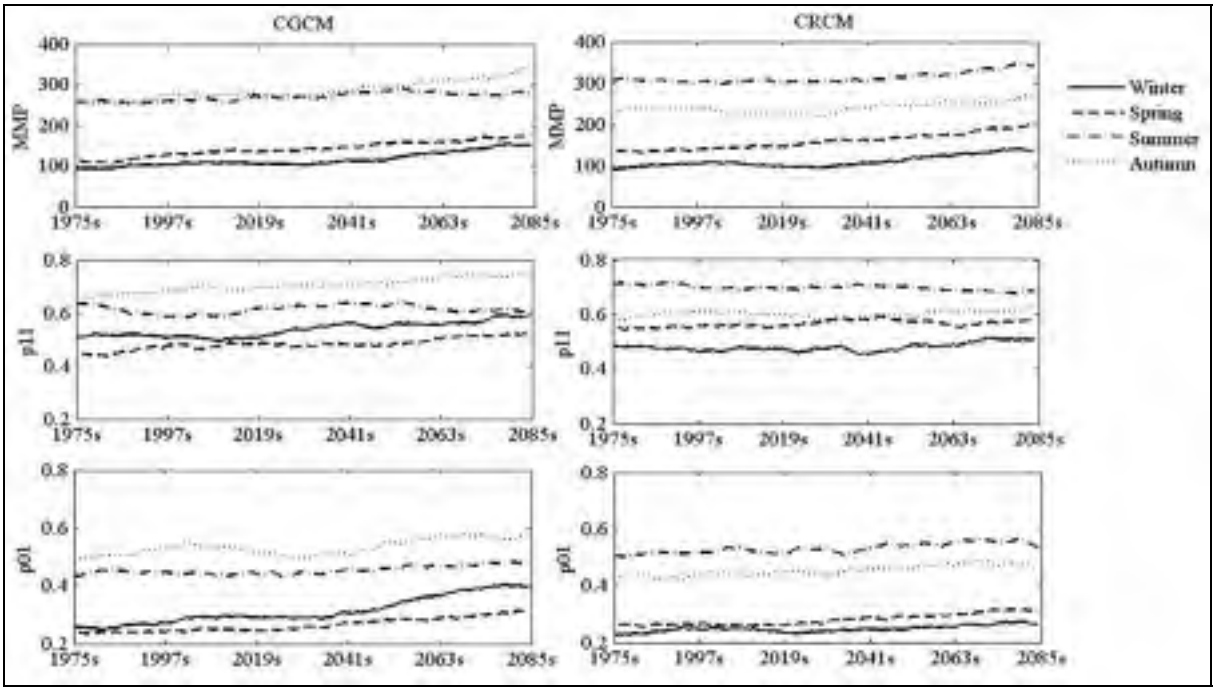

Figure 6.2 The 30-year moving averages of monthly mean precipitation (MMP), P01 and P11 for CRCM and CGCM data over the 1961-2099 period.

Table 6.1 The correlation coefficient of the linear regression for CRCM and CGCM statistics, including monthly mean precipitation (MMP), P01 and P11 for the 2025-2084 period

	CGCM						CRCM					
	MMP		P01		P11		MMP		P01		P11	
	R2	P	R2	P	R2	P	R2	P	R2	P	R2	P
Winter	0.83	<0.01	0.89	<0.01	0.80	<0.01	0.70	<0.01	0.62	<0.01	0.43	<0.01
Spring	0.97	<0.01	0.92	<0.01	0.81	<0.01	0.96	<0.01	0.87	<0.01	0.50	<0.01
Summer	0.73	<0.01	0.61	<0.01	0.46	<0.01	0.62	<0.01	0.76	<0.01	0.59	<0.01
Autumn	0.89	<0.01	0.53	<0.01	0.95	<0.01	0.50	<0.01	0.83	<0.01	0.38	<0.01

The WG used in this research is CLIGEN (Nicks and Lane, 1989). In this study, only the functions to generate precipitation (occurrence and quantity), Tmax and Tmin were used. Other WGs could also have been used. A first-order two-state Markov chain is used to generate the occurrence of wet or dry days. The probability of precipitation on a given day is based on the wet or dry status of the previous day, which can be defined in terms of the two transition probabilities: P01 and P11. For a predicted wet day, a three-parameter skewed normal Pearson III distribution was used to generate daily precipitation quantity for each month (Nicks and Lane, 1989). A normal distribution was used to simulate Tmax and Tmin. The temperature with the smaller standard deviation between Tmax and Tmin is computed first, followed by the other temperature (Chen, et al, 2008). The mean and standard deviation of Tmax and Tmin were calculated monthly and smoothed with Fourier interpolation to a daily scale.

A total of nine monthly parameters are needed by CLIGEN to generate precipitation, Tmax and Tmin. These include P01 and P11 for generating precipitation occurrence, the mean, standard deviation and skewness for generating daily precipitation quantity and the means and standard deviations of Tmax and Tmin. The skewness of precipitation is supposed to be unchanged in the future for this study. The other eight parameters are modified based on the projected climate change as predicted by a GCM or an RCM by following these steps:

1) Similarly to the CF method, the adjusted monthly mean Tmax and Tmin for the future horizon ($\overline{T}_{adj,fut}$) are estimated as:

$$\overline{T}_{adj,fut} = \overline{T}_{obs} + (\overline{T}_{CM,fut} - \overline{T}_{CM,ref}) \tag{6.1}$$

The adjusted values are obtained by adding the differences predicted by a GCM or an RCM between the future horizon and the reference period ($\overline{T}_{CM,fut} - \overline{T}_{CM,ref}$) to the observed mean monthly observed temperatures ($\overline{T}_{obs}$).

2) Monthly means and variances of precipitation, monthly variances of Tmax and Tmin and the transition probabilities of precipitation occurrence P01 and P11 for the future horizon are adjusted by:

$$X_{adj,fut} = X_{obs} \times (X_{CM,fut} / X_{CM,ref}) \tag{6.2}$$

where X represents the variable to be adjusted. The subscripts are the same as above.

3) The P01 and P11 values are expressed in terms of an unconditional probability of daily precipitation occurrence (π) and the lag-1 autocorrelation of daily precipitation (r) for further adjustments.

$$\pi = \frac{P_{01}}{1 + P_{01} + P_{11}} \tag{6.3}$$

$$r = P_{11} - P_{01} \tag{6.4}$$

4) The adjusted mean daily precipitation per wet day (u_d) is estimated as (Wilks, 1999a; Zhang, 2005):

$$\mu_d = \frac{\mu_m}{N_d \pi} \tag{6.5}$$

where N_d is the number of days in a month, $N_d \pi$ is the average number of wet days in a month, and u_m is the step (2)-adjusted monthly precipitation.

5) The adjusted daily variance (σ_d^2) is approximated using equation (6.6), based on the step (2)-adjusted variance of the monthly precipitation (σ_m^2) (Wilks, 1999a).

$$\sigma_d^2 = \frac{\sigma_m^2}{N_d \pi} - \frac{(1-\pi)(1+r)}{1-r}\mu_d^2 \tag{6.6}$$

All adjusted precipitation, Tmax and Tmin parameter values are input into CLIGEN to generate 900-year long time series of daily meteorological data. Long time series are used to obtain the true expectancy of a WG. Short time series could results in biases due to the random nature of the stochastic process. Each 900-year time series is representative of a 30-year horizon as defined earlier. All in all, sixty 900-year time series (centered over 2025-2084) were generated. The flow chart of WG-based downscaling is presented in figure 6.3.

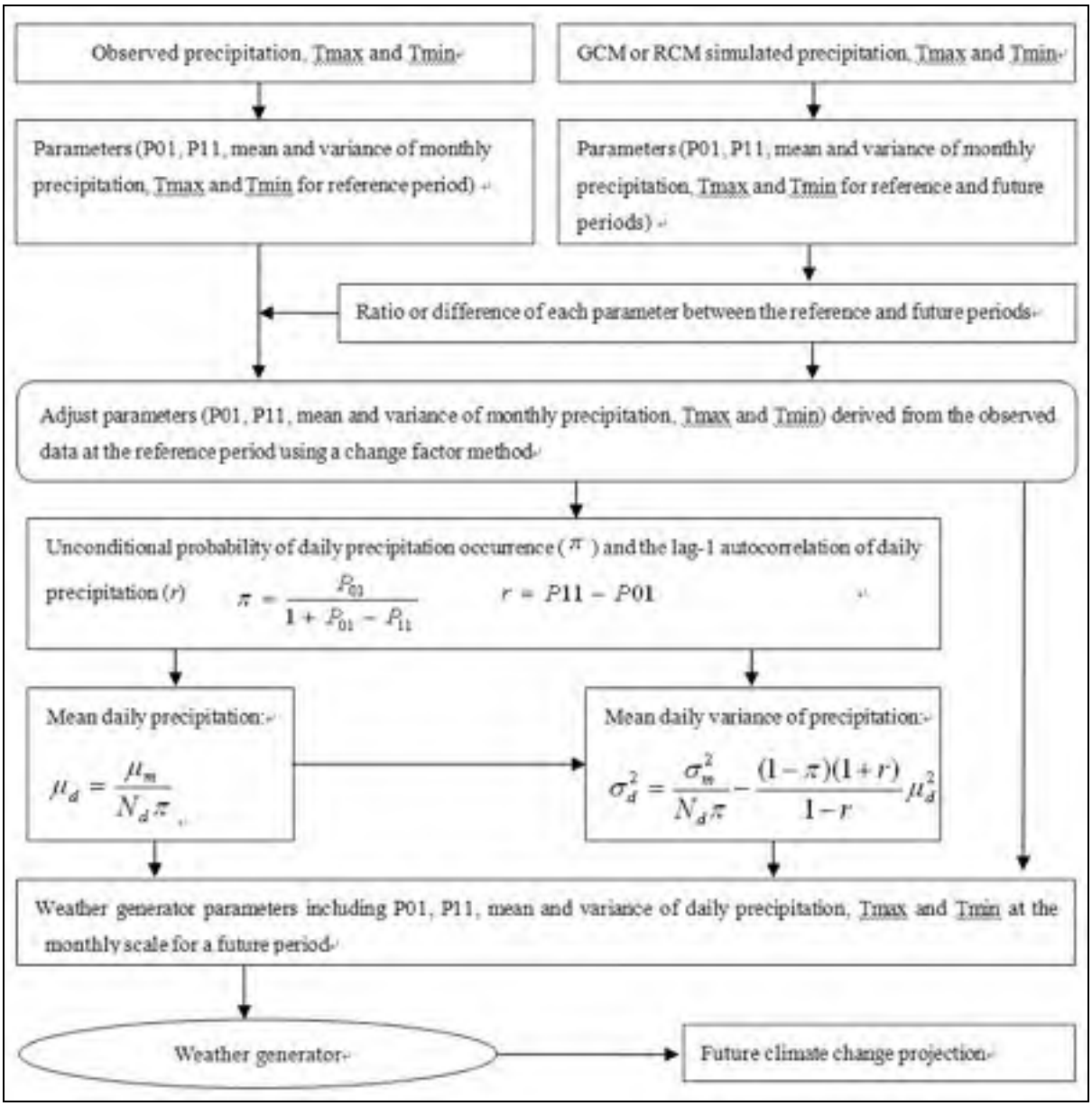

Figure 6.3 Flow chart of downscaling of weather generator parameters.

6.4.2 Change factor method

The CF method involves adjusting the observed daily temperature ($T_{obs,d}$) by adding the difference in monthly temperature between the future horizon and the reference period predicted by the climate model (GCM or RCM) ($\overline{T}_{CM,fut,m} - \overline{T}_{CM,ref,m}$) to obtain the daily temperature at the future horizon ($T_{adj,fut,d}$) (equation (6.7)) (Chen et al., 2011c). The adjusted

daily precipitation for the future horizon ($P_{adj,fut,d}$) is obtained by multiplying the precipitation ratio ($\overline{P}_{CM,fut,m} / \overline{P}_{CM,ref,m}$) by the observed daily precipitation ($P_{obs,d}$) (equation (6.8)).

$$T_{adj,fut,d} = T_{obs,d} + (\overline{T}_{CM,fut,m} - \overline{T}_{CM,ref,m}) \tag{6.7}$$

$$P_{adj,fut,d} = P_{obs,d} \times (\overline{P}_{CM,fut,m} / \overline{P}_{CM,ref,m}) \tag{6.8}$$

6.4.3 Hydrological simulation

The hydrological simulation used the HSAMI hydrological model developed by Hydro-Québec, and which has been used to forecast natural inflows for over 20 years (Fortin, 2000). HSAMI is used by Hydro-Québec for hourly and daily forecasting of natural inflows over 84 watersheds with surface areas ranging from 160 km^2 to 69,195 km^2. Hydro-Québec's total installed hydropower capacity on these basins exceeds 40GW. HSAMI is a 23-parameter, lumped, conceptual, rainfall-runoff model. Two parameters account for evapotranspiration, six for snowmelt, ten for vertical water movement, and five for horizontal water movement. Vertical flows are simulated with four interconnected linear reservoirs (snow on the ground, surface water, unsaturated and saturated zones). Horizontal flows are filtered through two hydrograms and one linear reservoir. Model calibration is done automatically using the shuffled complex evolution optimization algorithm (Duan, 2003). The model takes snow accumulation, snowmelt, soil freezing/thawing and evapotranspiration into account.

The basin-averaged minimum required daily input data for HSAMI are: Tmax, Tmin, liquid and solid precipitation. Cloud cover fraction and snow water equivalent can also be used as inputs, if available. A natural inflow or discharge time series is also needed for proper calibration/validation. For this study, thirty years (1970-1999) of daily discharge data were used for model calibration/validation. The optimal combination of parameters was selected based on Nash-Sutcliffe criteria. The set of parameters thus chosen yielded Nash-Sutcliffe criteria values of 0.89 for both the validation (20 years) and calibration periods (10 years).

This high Nash-Sutcliffe criteria value is representative of the good quality of the weather inputs and observed discharge values.

6.5 Results

6.5.1 Validation of the weather generator and the hydrological model

The validation of the hydrological model HSAMI was based on the performance of the simulated hydrographs (labeled OBS-SIM) at the basin outlet compared to the observed hydrograph. Mean hydrograph results are presented in figure 6.4. The mean hydrograph simulated by HSAMI using CLIGEN-generated data (labeled OBS-WG) for the reference period is also displayed to validate the ability of CLIGEN at generating weather data representative of its training period. The mean hydrograph from the observed discharge (labeled OBS) is also presented for comparison. The observed precipitation and temperatures resulted in a mean hydrograph that is very close to the observed one. A slight bias was introduced by CLIGEN in late fall and winter. However, the overall fits are quite good.

6.5.2 Climate change projections

6.5.2.1 Dry and wet day spells

The CF method does not take into account the temporal sequencing of dry and wet days, which is its main drawback. The WG-based method modifies the transition probabilities of precipitation occurrence based on RCM-projected variations. Thus, the dry and wet day spells change according to the differences in RCM-projected dry and wet day spells between the future and reference periods. Figures 6.5 and 6.6 show the average dry and wet day spells downscaled by the CF and WG-based methods, respectively, for 12 months over the 2025-2084 period (30-year moving average from 2011-2099) for the Manicouagan 5 river basin. Changes in precipitation occurrence are not taken into account by the CF method. Thus, the average dry and wet day spells are stationary over the 2025-2084 period for all months (horizontal dashed lines in figures 6.5 and 6.6). The WG-based method displays clear trends

throughout the century, which is markedly different from the situation at the reference period. The WG-based method suggested shorter dry day spells for all months of the 2025-2084 period, comparing to those of the reference period, indicating that wet days will become more common. However, there is no uniform pattern for monthly average wet day spells, which are predicted to be longer for April and November and shorter for July and August for the 2025-2084 period. In addition, this pattern would be first shorter and then longer than that of the reference period for January, March, September, October and December throughout the 2025-2084 period. In contrast, February wet day spells would have an opposite trend than that of the reference period.

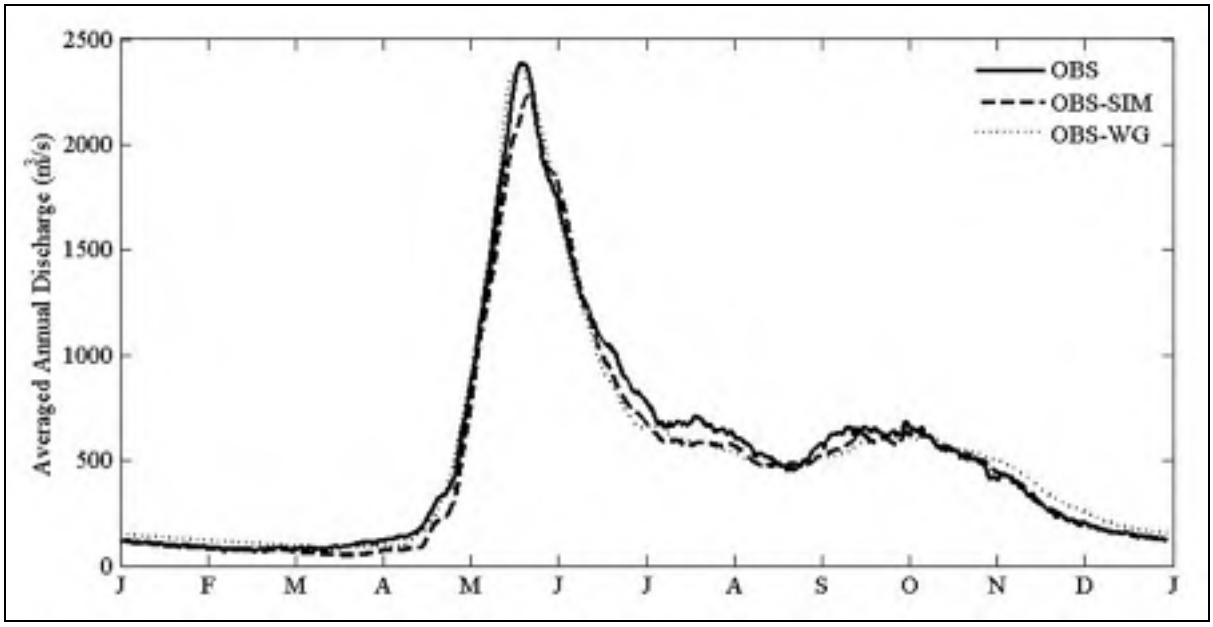

Figure 6.4 Observed (OBS) and HSAMI modeled averaged hydrograph (OBS-SIM) for the reference period (1970-1999) at the Manicouagan 5 watershed. An HSAMI-simulated hydrograph using CLIGEN-produced meteorological data at the reference period (OBS-WG) is also plotted.

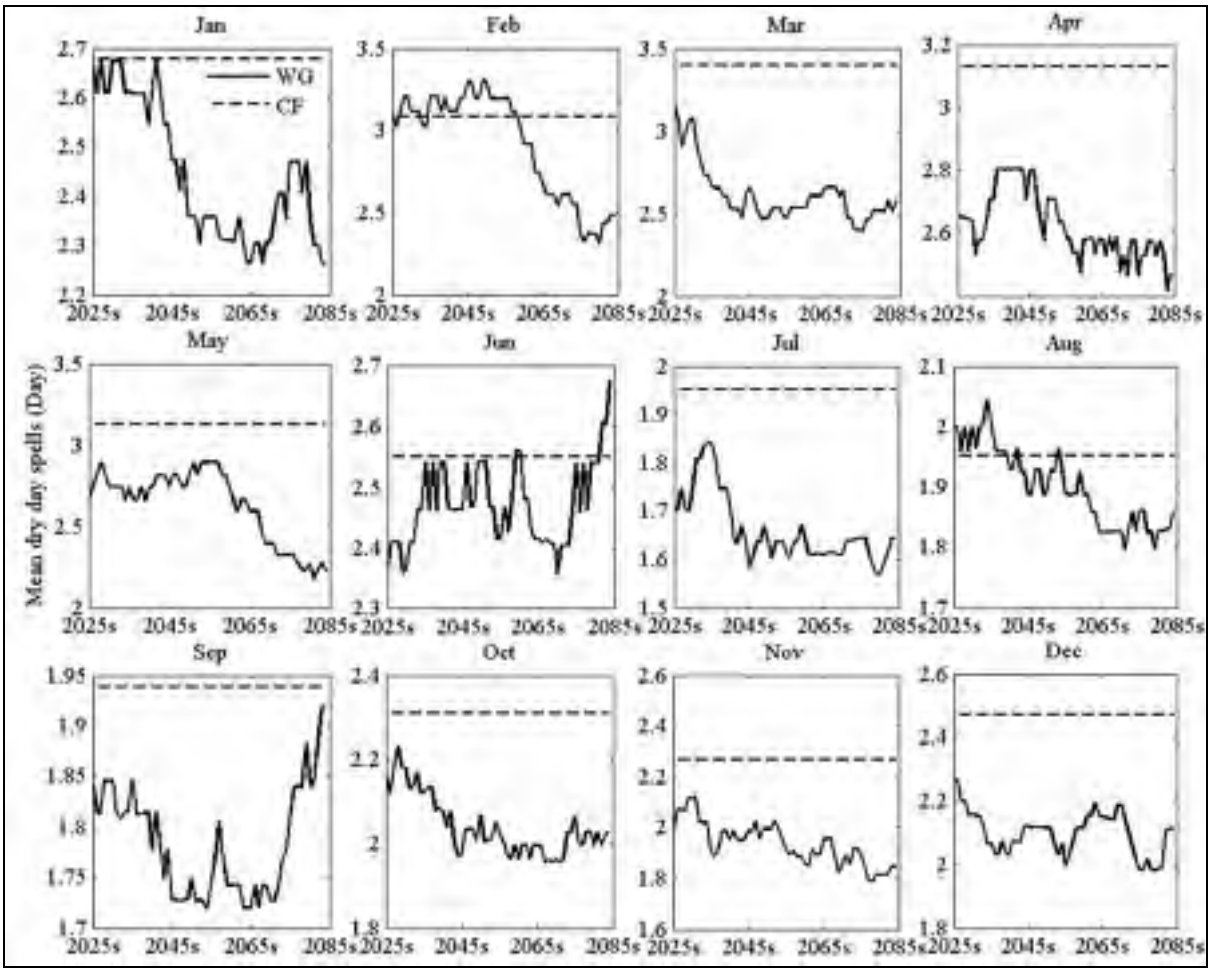

Figure 6.5 Mean dry day spells downscaled by change factor (CF) and weather generator-based (WG) methods for each month over the 2025-2084 period for the Manicouagan 5 river basin.

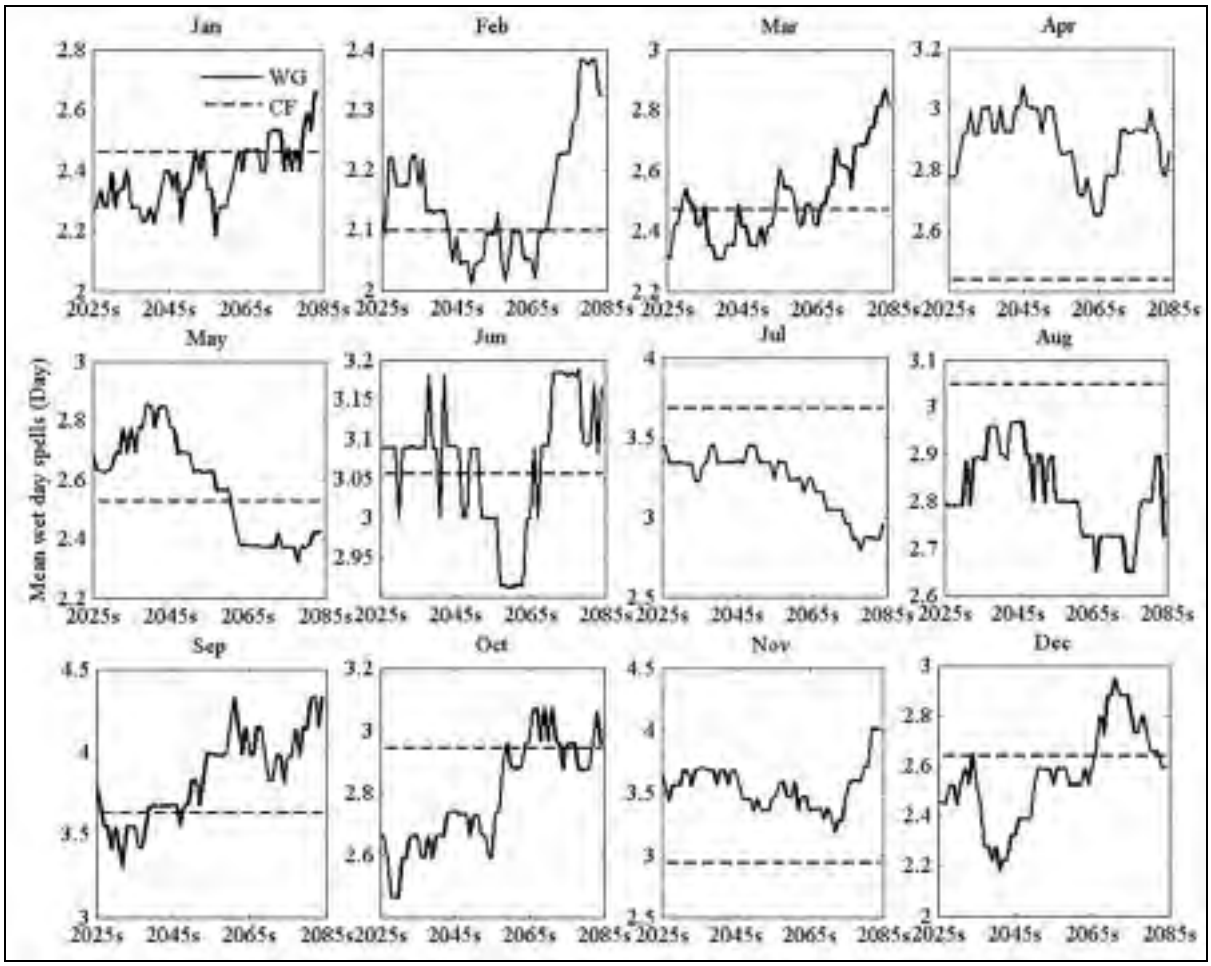

Figure 6.6 Mean wet day spells downscaled by change factor (CF) and weather generator-based (WG) methods for each month over the 2025-2084 period for the Manicouagan 5 river basin.

6.5.3 Annual and seasonal precipitation

Figure 6.7 shows the annual and seasonal evolutions of mean precipitations downscaled by the CF and WG-based methods for the 2025-2084 period. Both downscaling methods suggest very similar general increases in annual mean precipitations, reaching 200 mm by the end of the century. Similarities are not surprising since the CF and WG-based methods are essentially the same with respect to mean precipitation. The slight differences can be attributed to the stochastic nature of precipitation generation by WG. The seasonal

precipitations would also increase, with the largest increase in winter (DJFM). Similar results were obtained by Minville et al. (2009) for a study over the Peribonka River watershed.

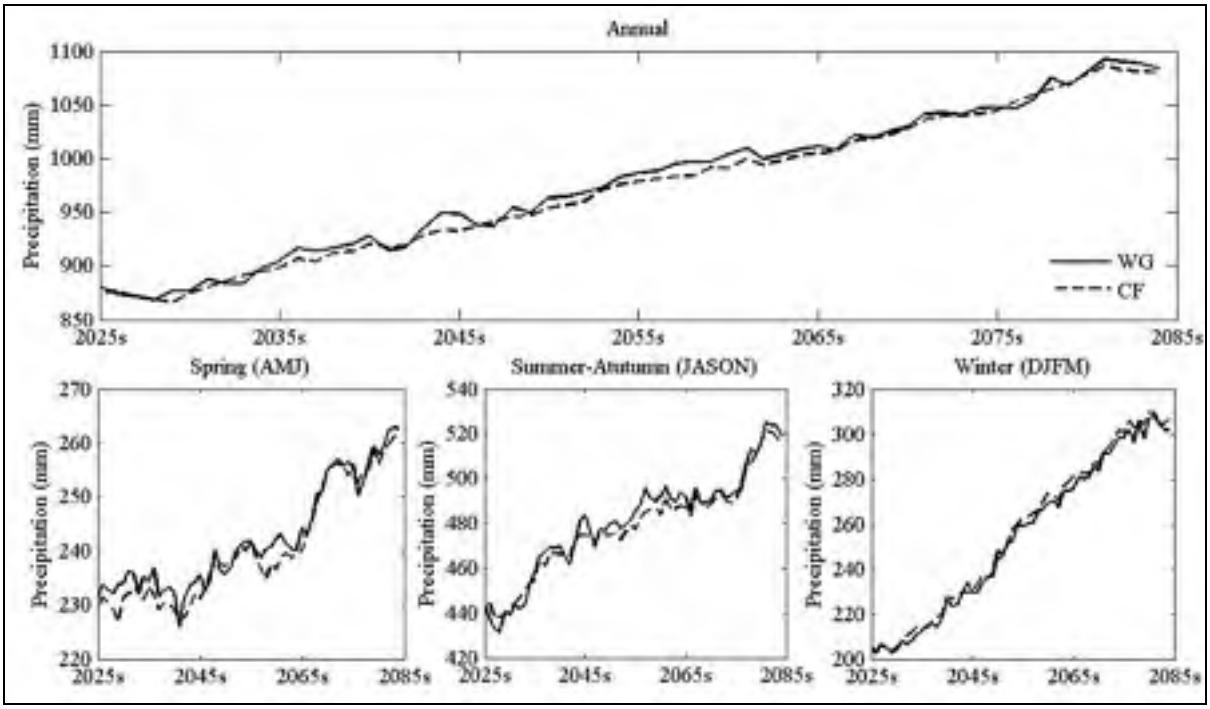

Figure 6.7 Annual and seasonal precipitation downscaled by change factor (CF) and weather generator-based (WG) methods over the 2025-2084 period for the Manicouagan 5 river basin.

6.5.3.1 Annual and seasonal temperatures

Figure 6.8 presents the annual and seasonal evolutions of Tmax (higher lines) and Tmin (lower lines) downscaled by the CF and WG methods over the Manicouagan 5 river basin. Similarly to precipitation, the annual and seasonal mean Tmaxs and Tmins are non-stationary, and increase gradually over the 2025-2084 period. The CF and WG-based methods predict increases in annual Tmax and Tmin by nearly 3.0°C and 3.4°C, respectively, and by the end of the century. As was the case for mean precipitation, both methods are essentially equivalent with respect to mean temperature, with the slight differences due to the stochastic nature of the WG-based approach.

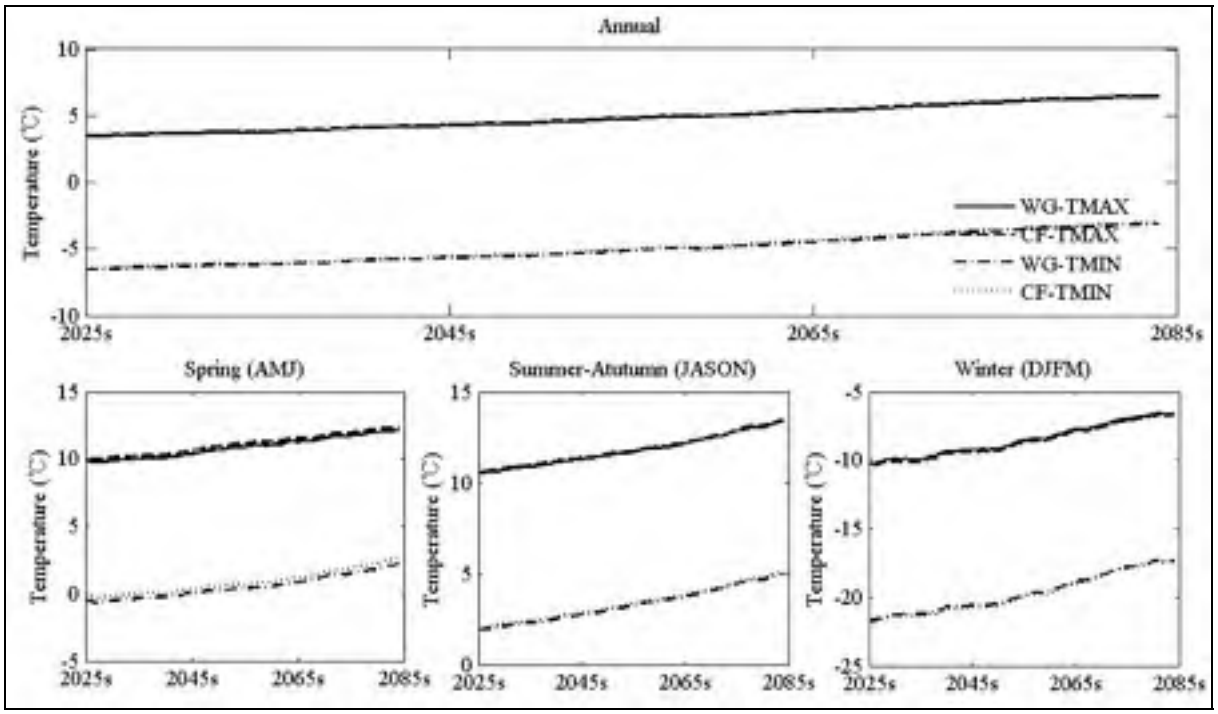

Figure 6.8 Annual and seasonal Tmaxs and Tmins downscaled by change factor (CF) and weather generator-based (WG) methods over the 2025-2084 period for the Manicouagan 5 river basin.

6.5.3.2 Mean daily precipitation

The CF and WG-based methods suggest similar increases in annual and seasonal precipitations for the 2025-2084 period, but the dry and wet day spells are significantly different. Specifically, mean daily precipitation changes in the opposite direction than that of the wet day frequency. Figure 6.9 demonstrates the mean daily precipitation downscaled by the two methods for 12 months over the 2025-2084 period. Both downscaling methods show gradual increases in mean daily precipitation for all months of the 2025-2085 period. However, the CF method suggests more increases in mean daily precipitation than the WG-based method. This is because the CF method predicts more wet days with similar annual and seasonal precipitations than the WG-based method.

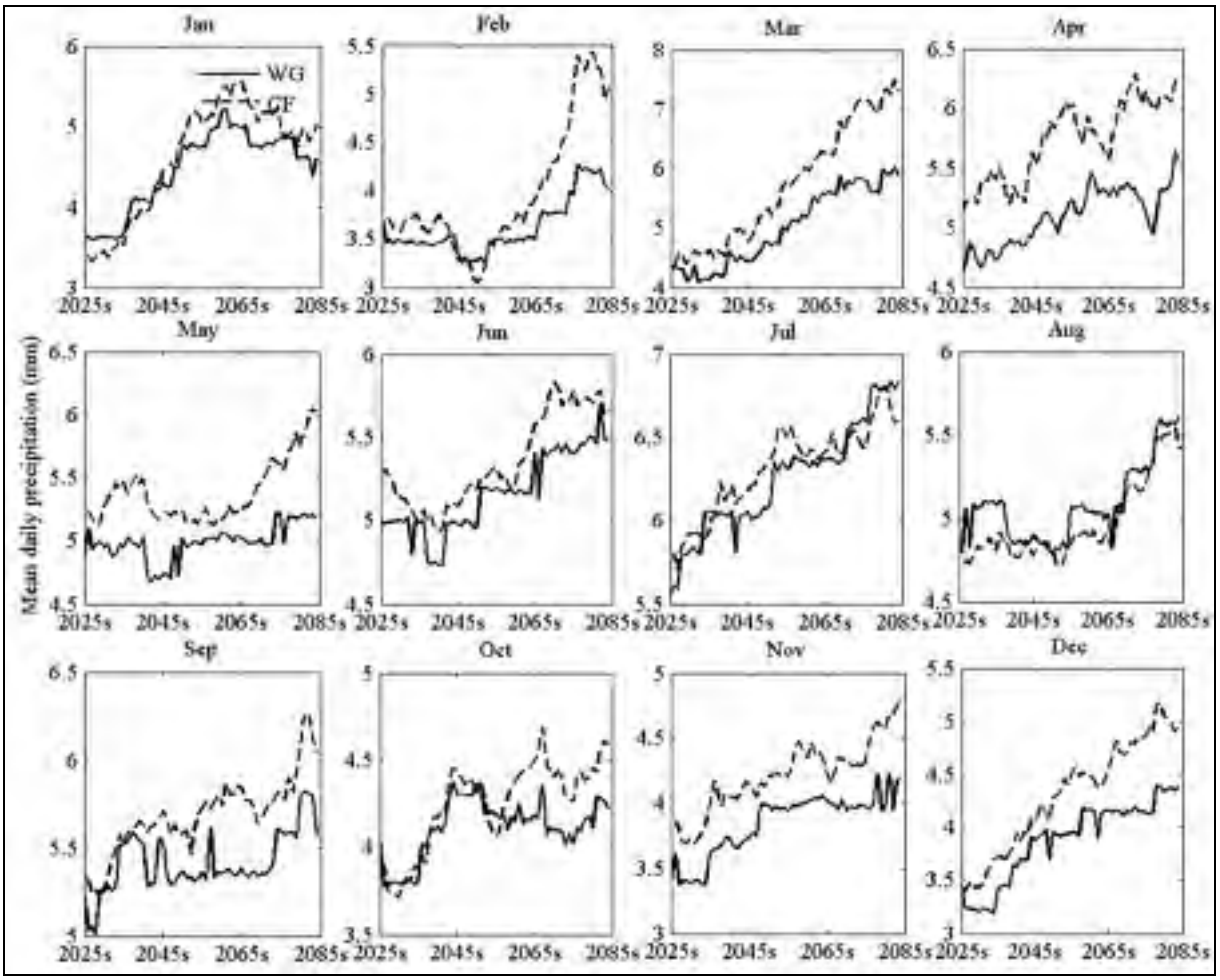

Figure 6.9 Mean daily precipitation downscaled by change factor (CF) and weather generator-based (WG) methods for each month over the 2025-2084 for the Manicouagan 5 river basin.

6.5.3.3 Standard deviation of daily precipitation

Both CF and WG-based methods suggest changes in daily precipitation variance. The change of variance predicted by the CF method is based on the change of mean daily precipitation, because the CF method does not specifically modify the precipitation variance. However, the WG-based method specifically takes into account the variance of precipitation based on RCM-projected variations. Figure 6.10 presents the standard deviation of daily precipitation downscaled by CF and WG-based methods for 12 months over the 2025-2084 period. Both

downscaling methods suggest general increases in the standard deviations of daily precipitation for all months. For the CF method, the change in standard deviation of daily precipitation is consistent with the change in the mean precipitation. The WG-based method suggests more future variability for the most of months, consistent with that predicted by the RCM.

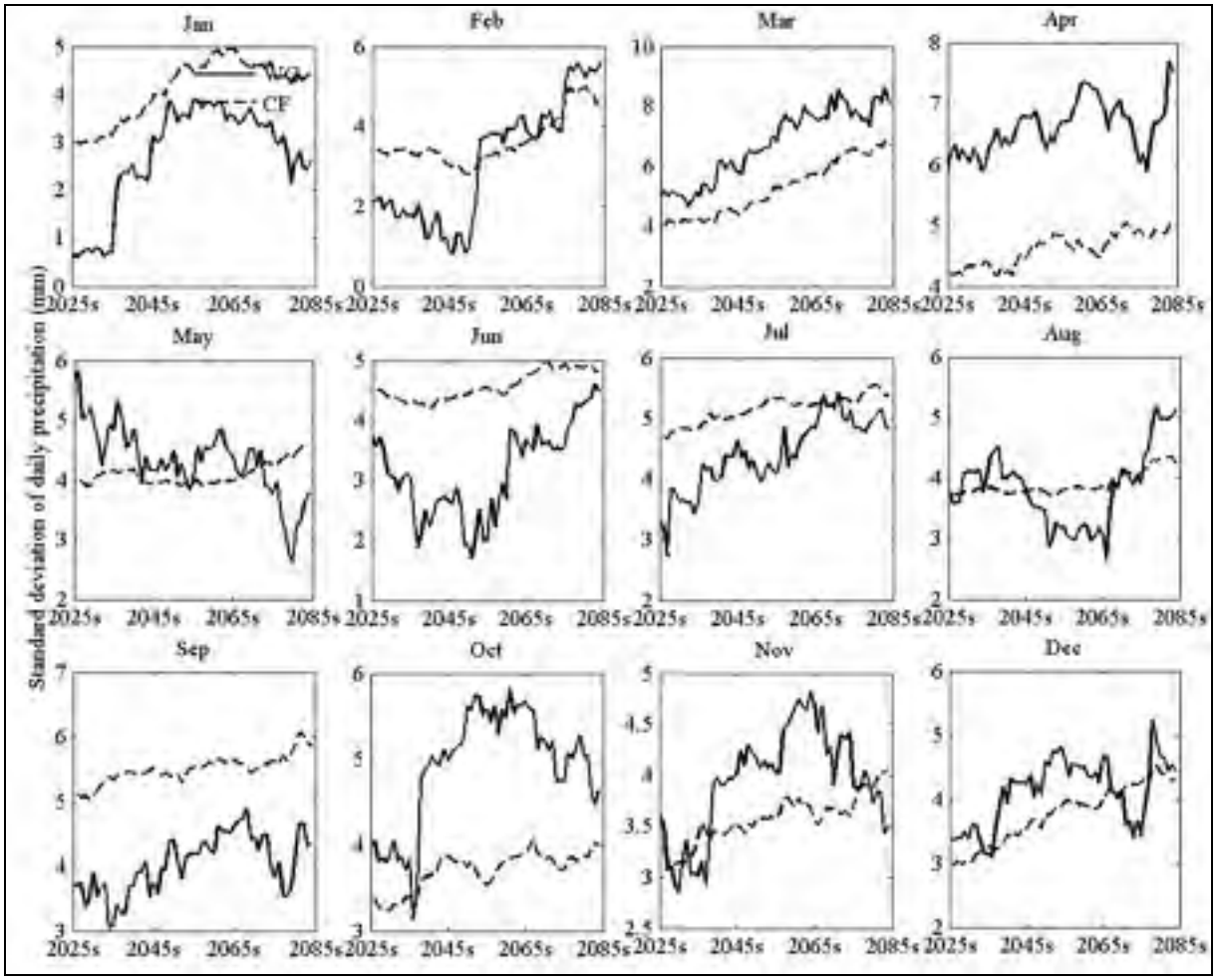

Figure 6.10 Standard deviation of daily precipitation downscaled by change factor (CF) and weather generator-based (WG) methods for each month over the 2025-2084 period for the Manicouagan 5 river basin.

6.5.3.4 Standard deviation of daily Tmax and Tmin

The CF method does not take into account the change of variance for Tmax and Tmin. Standard deviations of Tmax and Tmin downscaled by the CF method are constant for the 2025-2084 period, which is exactly equal to that of the reference period as presented in figures 6.11 and 6.12. However, similarly to the transition probabilities of precipitation occurrence, the WG-based method adjusts the variances of Tmax and Tmin based on the RCM-projected changes. Compared to the reference period (1970-1999), the WG-based method suggests decreases in the variability of winter (December, January and February) Tmax, while it suggests increases for all other months.

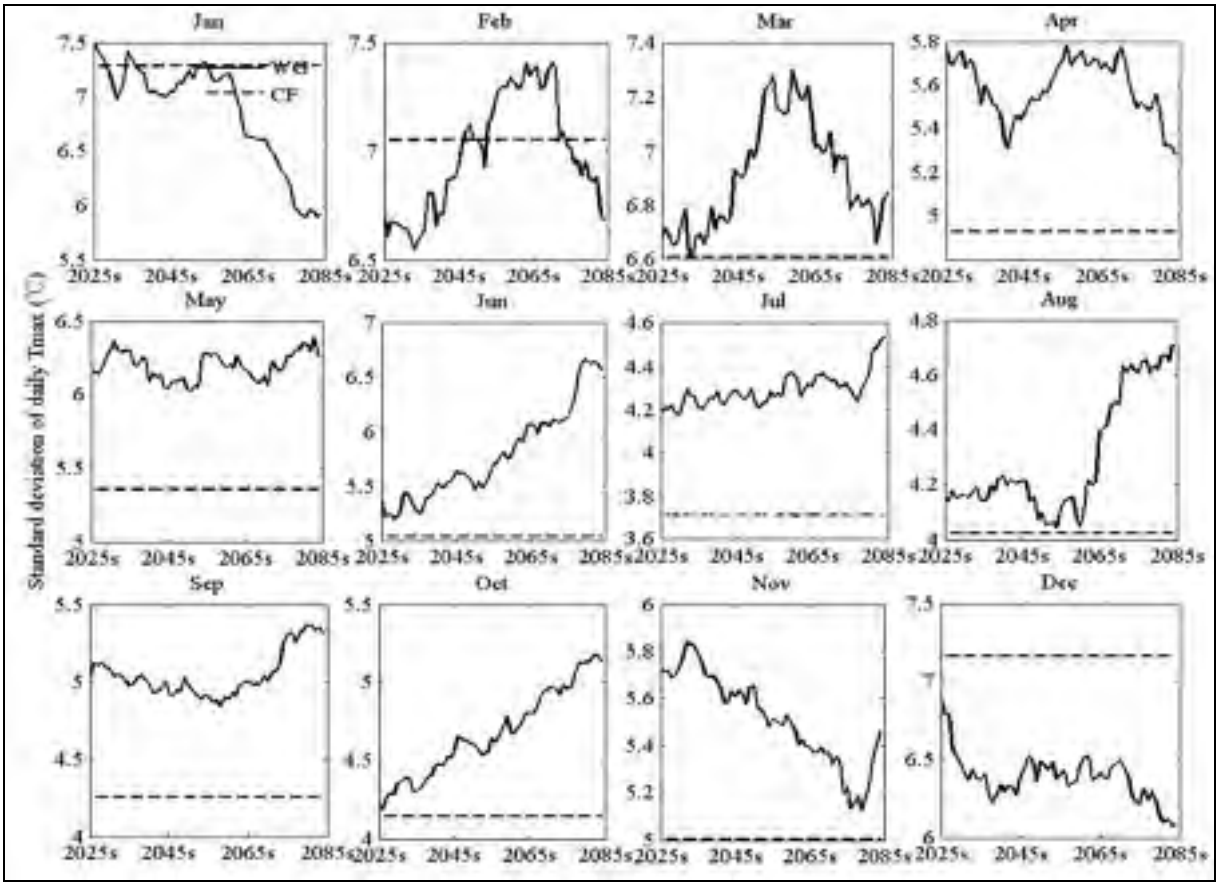

Figure 6.11 Standard deviation of daily Tmax downscaled by change factor (CF) and weather generator-based (WG) methods for each month over the 2025-2084 period for the Manicouagan 5 river basin.

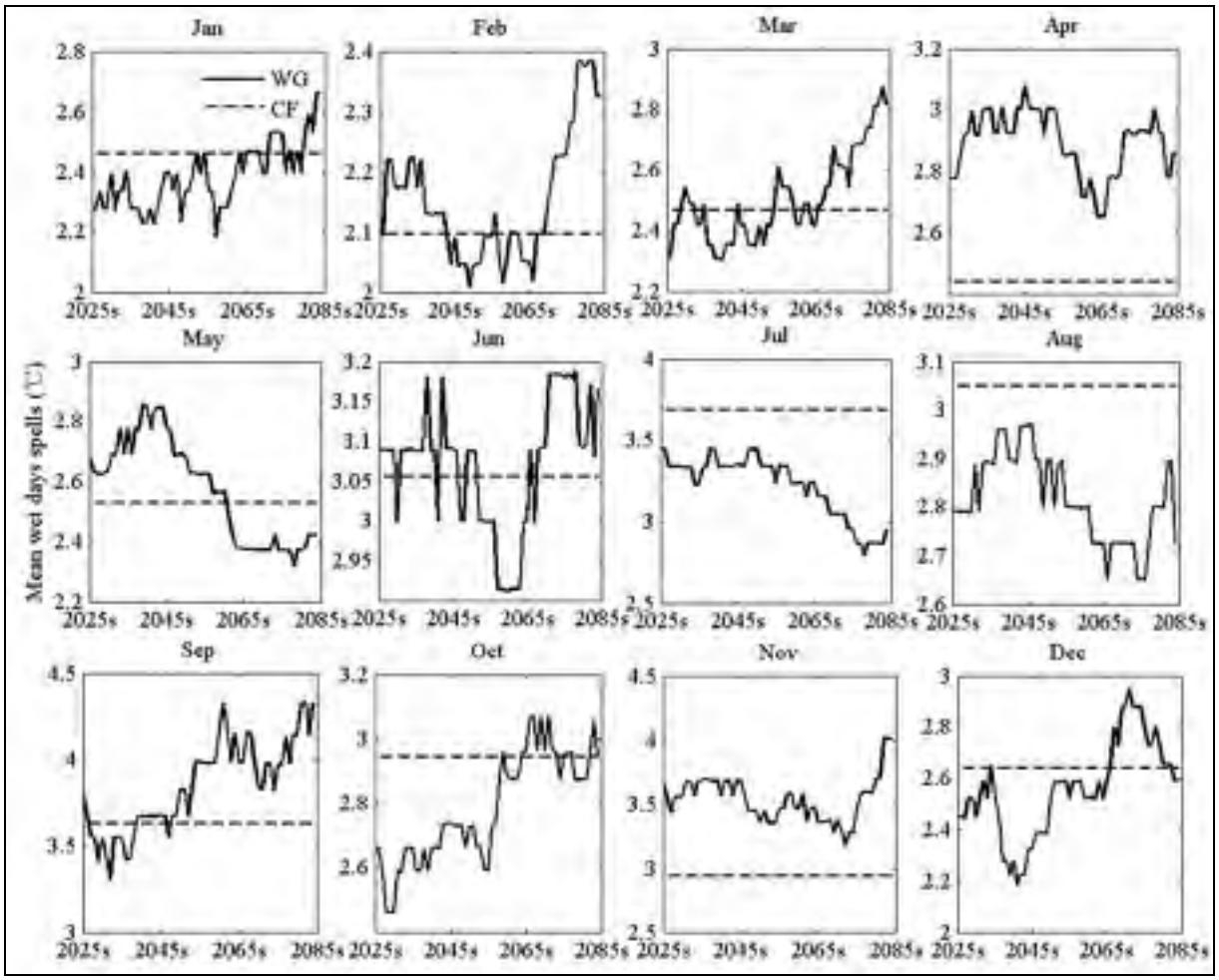

Figure 6.12 Standard deviation of daily Tmin downscaled by change factor (CF) and weather generator-based (WG) methods for each month over the 2025-2084 period for the Manicouagan 5 river basin.

6.5.4 Hydrological impacts

6.5.4.1 Average annual hydrograph

Figure 6.13 presents the envelope of the averaged annual hydrographs simulated with the weather variables downscaled by the CF and WG-based methods. Each envelope is represented by 60 averaged annual hydrographs (2025-2084 period). When the time period is near the reference period, the averaged annual hydrograph of the future period is close to that of the reference period. To avoid the minor bias resulting from the hydrological model when

comparing the future to the reference period, the discharge at the reference period is represented by model data and not by the observed discharge. The results showed that both downscaling methods suggest increases in winter (November - April) discharge. Decreases in summer (June - October) are predicted for most future horizons, especially for those downscaled by the WG-based method. The WG-based method suggests peak discharges higher than both those of the CF method and the simulated peak discharges at the reference period. Significantly, the peak discharges increase even more as the future advances, especially for WG-based method. Peak discharges over the 2025-2085 period are predicted to be earlier than those at the reference period by both downscaling methods. Lags vary from 12 days (May 12th) to 19 days (May 5th) for the WG-based method and from 6 days (May 18th) to 22 days (May 2nd) for the CF method.

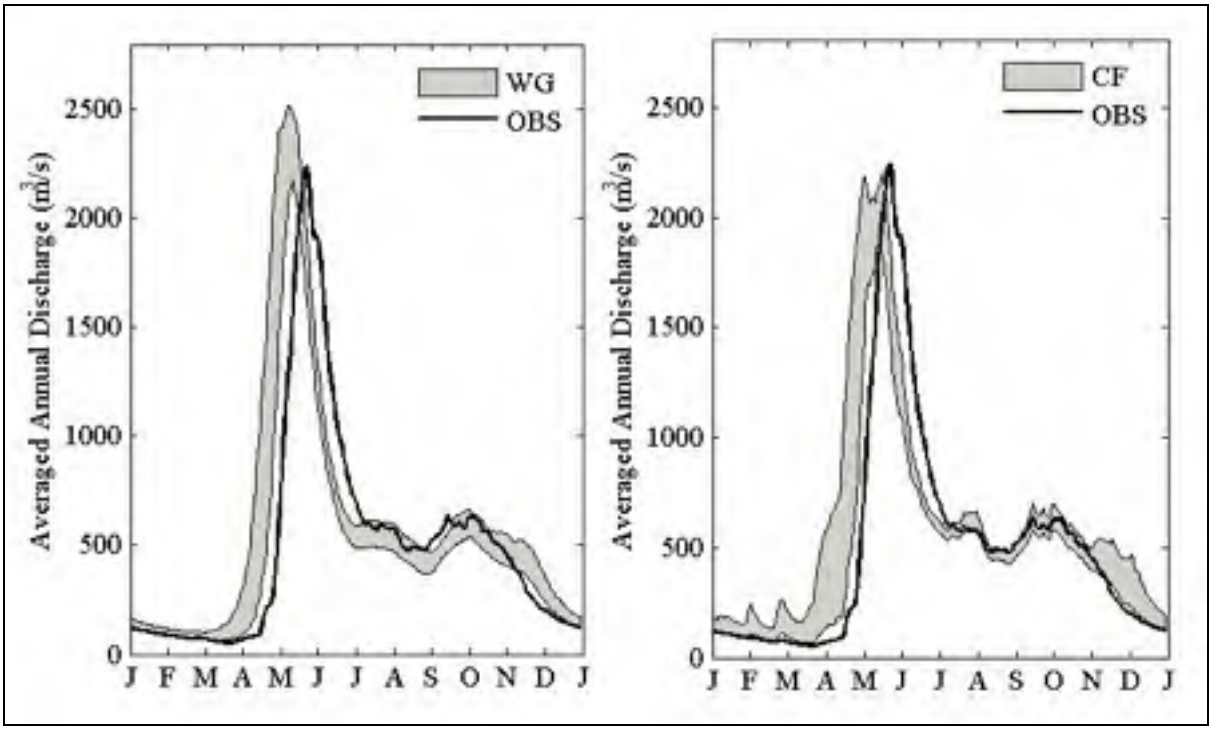

Figure 6.13 Envelopes of 60 averaged annual hydrographs simulated with change factor (CF) and weather generator-based (WG) methods' downscaled precipitation, Tmaxs and Tmins over the 2025 -2084 period at the Manicouagan 5 river basin. The observed hydrograph for the 1970-1999 period is displayed for comparison.

6.5.4.2 Annual and seasonal discharges

Figure 6.14 presents the 30-year moving averages of annual and seasonal discharges simulated by HSAMI using weather data downscaled by the CF and WG-based methods. Compared to the reference period discharge (straight dashed line in figure 6.14), both methods suggest increases in annual, spring and winter discharges over the 2025-2084 period. The summer-autumn discharge predicted by CF method is less than that at the reference period for most horizons, but WG-based method suggests increase in summer-autumn discharge for most horizons. Even though both downscaling methods predict similar annual and seasonal mean precipitations and temperatures, the annual and seasonal discharges are different, especially for seasonal discharge. This indicates that the annual and seasonal discharges are not only affected by the means of the precipitation and temperatures, but also by their variance and by precipitation occurrence. In addition, these results reflect that the process by which climate projections become hydrologic variables is not a linear one. Annual discharge suggested by the CF method is slightly more than that predicted by the WG-based method over the 2025-2085 period. The discharges differ more at the seasonal scale than at the annual scale. Compared to the CF method, the WG-based method suggests larger increases in spring (AMJ) discharge, and smaller increases in summer-autumn (JASON) and winter (DJFM) discharges.

6.5.4.3 Annual and seasonal low flows

Changes in monthly precipitation averages can conceal subtle variations in dry spells that are potentially significant for low flows (Diaz-Nieto and Wilby, 2005). The two downscaling methods suggest similar changes in monthly precipitation, but different changes in precipitation occurrence, resulting in noticeable differences in mean low flows (Q95, derived from mean hydrographs) at the river basin. Figure 6.15 presents the 30-year moving averages of mean annual and seasonal low flows for the 2025-2084 period. Both downscaling methods suggest general increases in average annual and seasonal low flows, but there are considerable differences in their predictions. The CF method predicts larger increases in

mean annual low flow than the WG-based method. These greater increases, compared to the WG-based method, occur in spring and winter low flows, resulting in the larger increases in annual low flow.

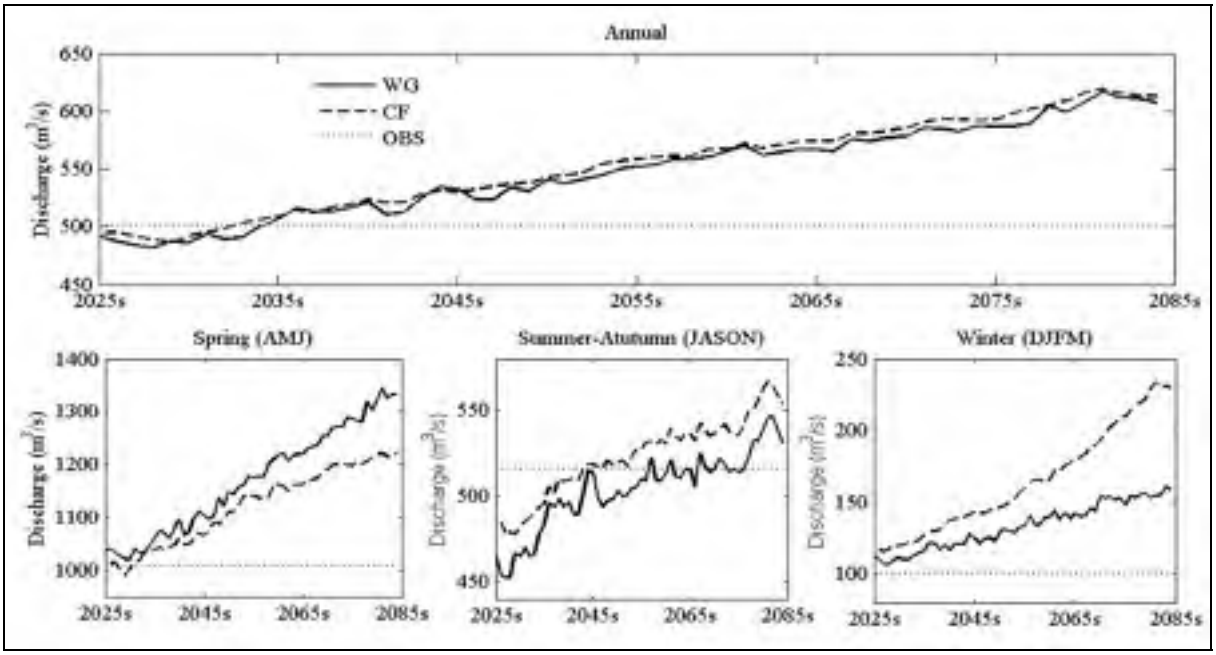

Figure 6.14 Annual and seasonal mean discharge simulated with change factor (CF) and weather generator-based (WG) methods' downscaled precipitation, Tmaxs and Tmins over the 2025 -2084 period at the Manicouagan 5 river basin. The annual and seasonal mean discharge over the reference period (1970-1999) is shown, for comparison.

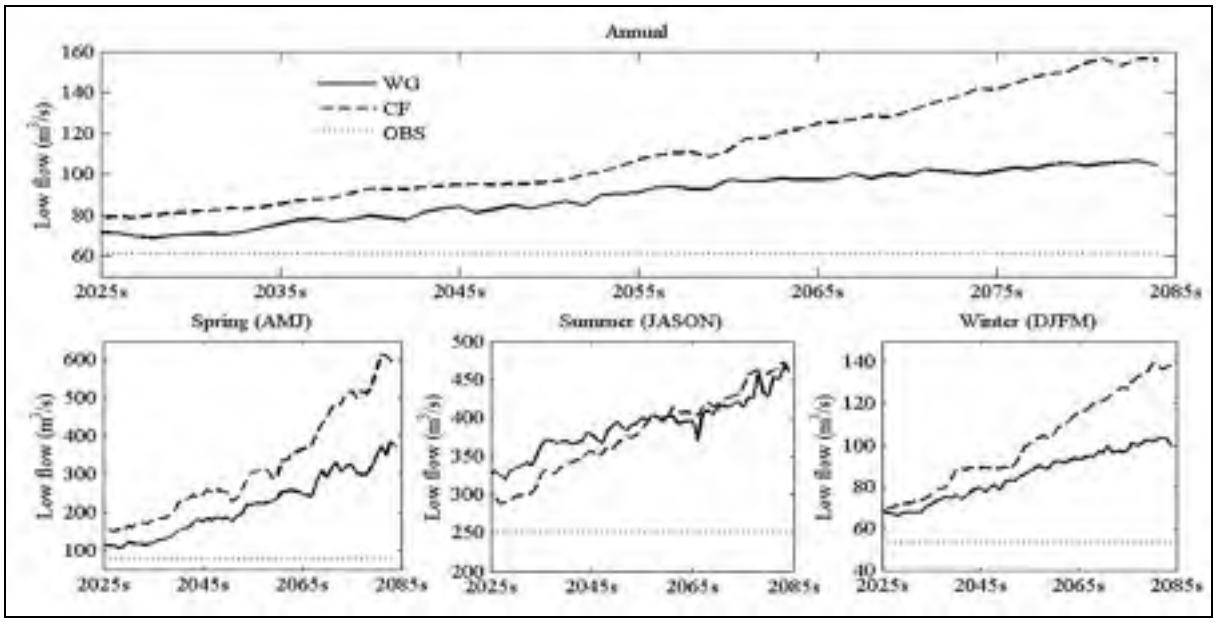

Figure 6.15 Annual and seasonal mean low flow simulated with change factor (CF) and weather generator-based (WG) methods' downscaled precipitation, Tmax and Tmin over the 2025 -2084 period at the Manicouagan 5 river basin. The annual and seasonal low flow for the reference period (1970-1999) is plotted for comparison.

Figure 6.16 presents the 30-year moving averages of the annual and seasonal minimal low flows (minimums of 30-year for CF method and 900-year for WG-based method) for the 2025-2084 period and those for the reference period. Similarly to the mean low flows shown in figure 6.15, both downscaling methods suggest increases in annual and seasonal minimal low flows, but those predicted by WG-based figures display more variability. The WG method has a much longer time series (900 years compared to 30 years) that is better at sampling climate variability. The CF method predicts larger increases in minimal low flow, especially for the more distant future period, and larger increases in spring and winter minimal low flows than the WG-based method. The WG-based method is better able to capture long series of dry days that lead to low flows. The WG-predicted summer-autumn minimal low flows for the 2025-2084 period are considerably larger than those for the reference period. Both methods give similar results, although the WG-based method predicts low flows that are 10% smaller than those of the CF method, on average.

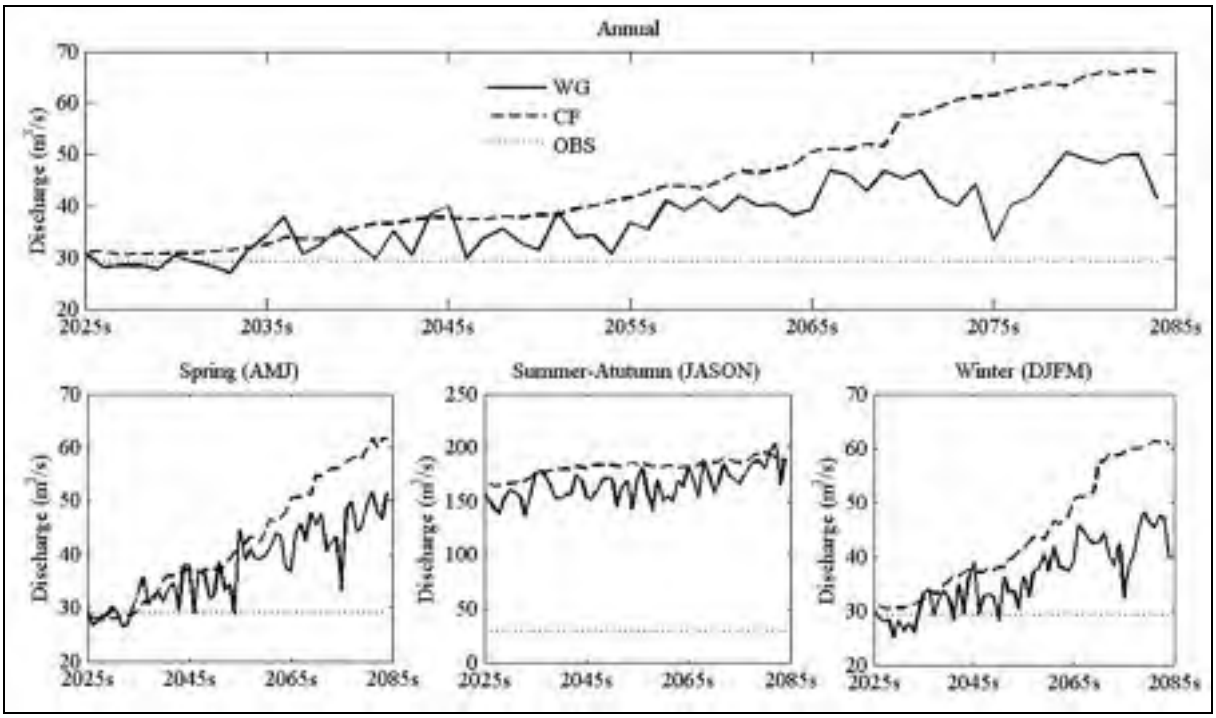

Figure 6.16 The minimal annual and seasonal low flow (Q5) simulated with the change factor (CF) and weather generator-based (WG) downscaling methods over the 2025 -2084 period at the Manicouagan 5 river basin. The minimal annual and seasonal low flow for the reference period (1970-1999) is also plotted, for comparison.

6.6 Discussion and Conclusions

A new statistical downscaling method combining a stochastic WG and some aspects of the CF method was presented in this paper. The parameters of the WG are perturbed to take into account the relative variations in the means and variances of weather variables projected by a climate model. The precipitation and temperature parameters projected by climate models display gradual (significantly non-stationary) changing patterns, which form the basis for the parameter perturbation of the WG. This downscaling method is relatively simple to use and negates the prerequisite of a strong relationship between local-scale variables (predictants) and large scale climate model variables (predictors) common to most statistical downscaling methods.

The proposed downscaling method is compared to the CF method in downscaling precipitation, Tmax and Tmin and further quantifying the hydrological impacts of climate change over the 2025-2084 period for the Manicouagan 5 river basin. Both downscaling methods suggest similar increases in annual and seasonal precipitations and temperatures for the 2025-2084 period. This was as expected, since both approaches are similar with respect to their treatment of precipitation and temperature means. Analysis of climate change scenarios shows that monthly dry and wet spells for the 2025-2084 period predicted by the WG-based method would be considerably different from those of the reference period. The CF method does not consider any change in precipitation occurrence over the reference period, a clear weakness of the approach. Compared to the reference period, the WG-based method predicts shorter dry day spells for the 2025-2084 period, thus indicating an increasing wet day frequency. Different dry and wet day spells and similar seasonal precipitation results in different mean daily precipitations between the two downscaling approaches. The standard deviation of daily precipitation, Tmax and Tmin differ markedly depending on the downscaling method. This should not be a surprise, since the WG-based method specifically takes the variance change of precipitation and temperatures into account, while the CF method does not. To evaluate how those changes translate into hydrological variables, weather variables derived from both downscaling methods were fed into the lumped semi-conceptual hydrology model HSAMI.

Both downscaling methods suggest general increases in winter (November - April) discharge and decreases in summer (June - October), the increases being larger when downscaled by the WG-based method. The WG-based method suggests higher peak discharges than those predicted by the CF method and those of the reference period. Peak discharges over the 2025-2084 period would be observed earlier than those at the reference period according to both downscaling methods. The differences between the weather variables downscaled from the two methods are amplified when transferred to hydrologic variables. Even though both downscaling methods suggest similar increases in annual and seasonal precipitations and temperatures, the annual and seasonal discharges are markedly different, especially for

seasonal discharge. This indicates that precipitation and temperature variability play an important role in the processes leading to runoff.

The comparison of the two downscaling methods reveals the main weakness of the CF method; that it keeps the precipitation occurrence and variability of all weather variables constant. This fallibility is probably not a major obstacle with respect to spring snowmelt, as shown in figure 6.14, because spring floods are the result of several months of snow accumulation followed by rapid melting. As such, the most important feature to have in a climate change study is the correct total quantity of solid precipitation. The variability of solid precipitation during the winter months is likely a less important feature, unless variability adds the frequent mid-winter thaws that cannot be captured by the CF method. For summer and fall events, damages often result from one major rainfall event, or from droughts that occur after long periods with little to no precipitation. In such cases, the CF method would be totally inappropriate for climate change studies. This situation is clearly delineated by the low flow results, where the two downscaling approaches display very different trends. The proposed WG-based method takes into account the change of precipitation occurrence and the variance of all variables, so it should arguably result in better climate projections for impact studies. Time series of any length can be generated with this method, another advantage for the study of rare events.

CHAPTER 7

UNCERTAINTY OF DOWNSCALING METHOD IN QUANTIFYING THE IMPACT OF CLIMATE CHANGE ON HYDROLOGY

Jie Chen[1], François P. Brissette[1], Robert Leconte[2]

1. Department of Construction Engineering, École de technologie supérieure, Université du Québec, 1100, rue Notre-Dame Ouest, Montréal, Québec, Canada, H3C 1K3.
2. Department of Civil Engineering, Université de Sherbrooke, 2500, boul. de l'Université, Sherbrooke, Québec, Canada, J1K 2R1

This article was published in the Journal of Hydrology in March, 2011.

7.1 Abstract

Uncertainty estimation of climate change impacts has been given a lot of attention in the recent literature. It is generally assumed that the major sources of uncertainty are linked to General Circulation Models (GCMs) and Greenhouse Gases Emissions Scenarios (GGES). However, other sources of uncertainty such as the choice of a downscaling method have been given less attention. This paper focuses on this issue by comparing six downscaling methods to investigate the uncertainties in quantifying the impacts of climate change on the hydrology of a Canadian (Quebec province) river basin. The downscaling methods regroup dynamical and statistical approaches, including the change factor method and a weather generator-based approach. Future (2070-2099, 2085 horizon) hydrological regimes simulated with a hydrological model are compared to the reference period (1970-1999) using the average hydrograph, annual mean discharge, peak discharge and time to peak discharge as criteria. The results show that all downscaling methods suggest temperature increases over the basin for the 2085 horizon. The regression-based statistical methods predict a larger increase in autumn and winter temperatures. Predicted changes in precipitation are not as unequivocal as

those of temperatures, they vary depending on the downscaling methods and seasons. There is a general increase in winter discharge (November - April) while decreases in summer discharge are predicted by most methods. Consistently with the large predicted increases in autumn and winter temperature, regression-based statistical methods show severe increases in winter flows and considerable reductions in peak discharge. Across all variables, a large uncertainty envelope was found to be associated with the choice of a downscaling method. This envelope was compared to the envelope originating from the choice of 28 climate change projections from a combination of 7 GCMs and 3 GGES. Both uncertainty envelopes were similar, although the latter was slightly larger. The regression-based statistical downscaling methods contributed significantly to the uncertainty envelope. Overall, results indicate that climate change impact studies based on only one downscaling method should be interpreted with caution.

Keywords: Climate change; uncertainty; downscaling; hydrology; precipitation; temperature

7.2 Introdution

The Intergovernmental Panel on Climate Change (IPCC, 2007) stated that there is high confidence that recent climate changes have had discernible impacts on physical and biological systems. Many General Circulation Models (GCMs) consistently predict increases in frequency and magnitudes of extreme climate event and variability of precipitation (IPCC, 2007). This will affect terrestrial water resource in the future, perhaps severely (Srikanthan and McMahon, 2001; Xu and Singh, 2004). For continental water resources, hydrological models are frequently used to quantify the hydrological impacts of climate change using GCM data as inputs (Salathe, 2003; Diaz-Nieto and Wilby, 2005; Minville et al., 2008, 2009). However, the spatial resolution mismatch between GCMs outputs and the data requirements of hydrological models is a major obstacle (Leavesley, 1994; Hostetler, 1994; Xu, 1999). It is therefore necessary to perform some post-processing to improve upon these global-scale models for impact studies. Consequently, dynamical downscaling (regional climate models, RCMs) and statistical downscaling (SD) methods have been developed to

meet this requirement. RCMs are developed based on dynamic formulations using initial and time-dependent lateral boundary conditions of GCMs to achieve a higher spatial resolution at the expense of limited area modeling (Caya and Laprise, 1999). The main problem of RCMs is the computational cost (Solman and Nunez, 1999). Thus, it is only available for limited regions. Moreover, despite improvements, outputs of RCMs are still too coarse for some practical applications, like small watershed hydrological and field agricultural impact studies, which may need local and site-specific climate scenarios. SD techniques have been developed to overcome these challenges. They involve linking the state of some variables representing a large scale (GCM or RCM grid scale, the predictors) and the state of other variables representing a much smaller scale (catchment or site scale, the predictands). These techniques are computationally cheap and relatively easy to implement.

These SD techniques fall into three categories: transfer function (Wilby et al., 1998a; Wilby et al., 2002a), weather typing (von Storch et al. 1993; Schoof and Pryor, 2001) and weather generator (WG) (Wilks, 1999a; Zhang, 2005). Transfer function approaches involve establishing statistical linear or nonlinear relationships between observed local climatic variables (predictands) and large-scale GCM outputs (predictors) (Wilby et al. 2002a). They are relatively easy to apply, but their main drawback is the probable lack of a stable relationship between predictors and predictands (Wilby and Wigley, 1997). Weather typing scheme involves grouping local meteorological variables in relation to different classes of atmospheric circulation (Bardossy and Plate 1992; von Storch et al. 1993). The main advantage is that local variables are closely linked to global circulation. However, its reliability depends on a stationary relationship between large-scale circulation and local climate. Especially for precipitation, there is frequently no strong correlation between daily precipitation and large-scale circulation. The WG method is based on the perturbation of its parameters according to the changes projected by climate models (Zhang, 2005; Kilsby et al., 2007; Qian et al., 2005, 2010; Wilks, 2010). The appealing property is its ability to rapidly produce sets of climate scenarios for studying the impacts of rare climate events and investigating natural variability.

Another relatively straightforward and popular downscaling method for rapid impact assessment of climate change is the change factor (CF) method (Minville et al., 2008; Diaz-Nieto and Wilby, 2005; Hay et al, 2000). It involves adjusting the observed time series by adding the difference (for temperatures) or multiplying the ratio (for precipitation) between future and present climates as simulated by the RCMs or GCMs. The most significant drawbacks are that the temporal sequencing of wet and dry days, and that the variances of temperatures are unchanged.

The unique advantages and drawbacks of each downscaling method result in different future climate projections. In particular, some downscaling methods are unable to capture the extremes of climate events that are often of particular concern in hydrology. Differences in future climate projections imply that downscaling methods add uncertainties in quantifying the impacts of climate change on hydrology. Many studies have focused on uncertainties linked to GCMs (Graham et al., 2007a, b; Maurer and Hidalgo, 2008; Minville et al., 2008; Christensen and Lettenmaier, 2007; Hamlet and Lettenmaier, 1999). Rowell (2006) compared the effect of different sources of uncertainty including emissions scenario, GCM, RCM and initial condition ensembles on changes in seasonal precipitation and temperature for the UK. The uncertainty from a GCM was found to be the largest. Prudhomme and Davies (2009) used three GCMs, two greenhouse gas emission scenarios (GGES) and two downscaling techniques (statistical downscaling model (SDSM) and HadRM3) to investigate their uncertainty in propagating river flow, and demonstrated that uncertainties from GCMs are larger than those from downscaling methods and GGES. Kay et al. (2009) also investigated different sources of uncertainties including GGES, GCM's structure (five GCMs), downscaling method (CF and RCM), hydrological model structure (two models), hydrological model parameters (jack-knifed calibrated parameter sets) and the internal variability of the climate system on the impact of climate change on flood frequency in England. With this research, each different source of uncertainty was done individually rather than in combination with each other. The results showed that the uncertainty related to GCM structure is the largest, but that other sources of uncertainty are significant if the GCM structure's influence was not taken into account. Wilby and Harris (2006) presented a

probabilistic framework for quantifying different sources of uncertainties on future low flow. They used four GCMs, two GGES, two downscaling techniques (SDSM and CF), two hydrological model structures and two sets of hydrological model parameters. The results indicated that GCMs revealed the greatest uncertainty, followed by downscaling methods. Uncertainties due to hydrological model parameters and GGES were less important.

Generally, GCMs are considered to be the largest source of uncertainty for quantifying the impacts of climate change. However, the uncertainty related to the downscaling and bias-correction methods must be taken into account for better estimation of the impact of climate change (Quintana Segui et al, 2010). Moreover, although some studies attempted to investigate the uncertainty related to downscaling techniques, only two methods were involved. A better method may use multi-downscaling techniques (more than two) for quantifying their uncertainty propagation in hydrology.

The objective of this study is to quantify the impacts of climate change on a Canadian river basin (Quebec province), while investigating the uncertainties related to downscaling techniques, using six downscaling methods. The downscaling methods include both dynamical and statistical approaches, including the CF method and a WG-based approach.

7.3 Study area and data

7.3.1 Study area

This study was conducted for the Manicouagan 5 river basin located in central Quebec, Canada. It covers 24,610 km^2 of mostly forested areas (figure 7.1). It has a rolling to moderately hilly topography with a maximum elevation of 952 m above sea level. The reservoir at the basin outlet has a mean level of 350 m above sea level. Population density is extremely low and logging is the only industrial activity over the basin. The basin drains into the Manicouagan 5 reservoir, a 2000 km^2 annular reservoir within an ancient eroded impact crater. The basin ends at the Daniel Johnson dam which is the largest buttressed multiple arch dam in the world. The installed capacity of the dam is 2.6GW. The annual mean discharge of

the Manicouagan 5 River is 529 m^3/s. Snowmelt peak discharge usually occurs in May and averages 2200 m^3/s.

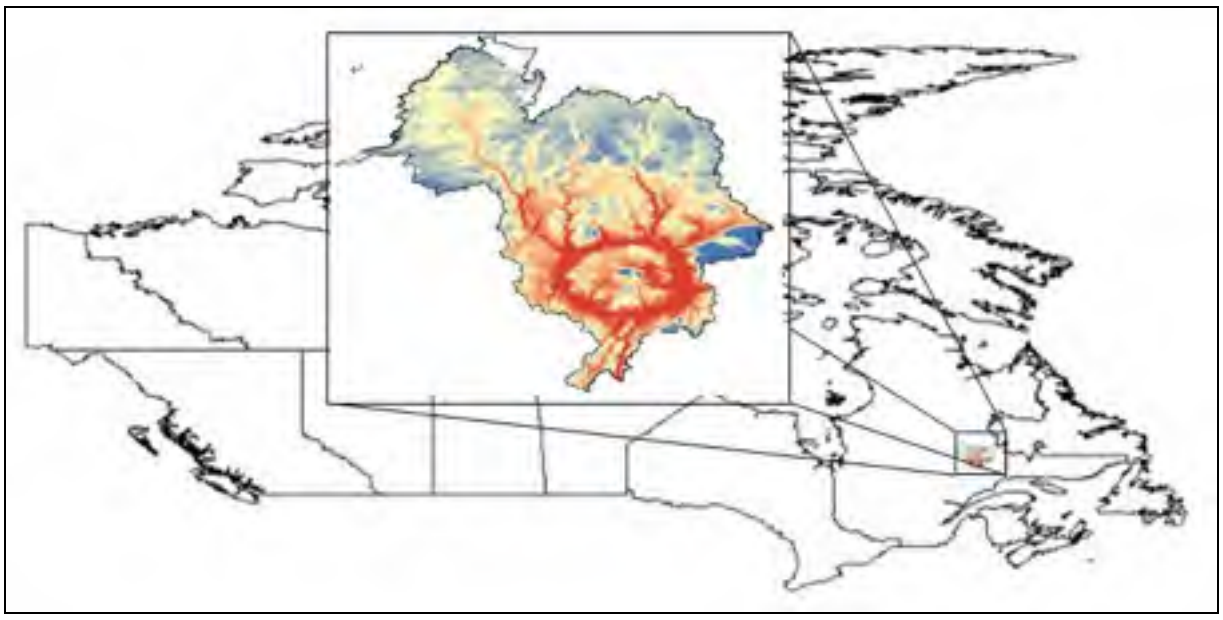

Figure 7.1 Location map of Manicouagan 5 river basin.

7.3.2 Data

The different datasets used in this work are summarized in table 7.1. Observed data consisted of precipitation, maximum temperature (Tmax) and minimum temperature (Tmin) interpolated on a 10 km grid by the National Land and Water Information Service (www.agr.gc.ca/nlwis-snite). The interpolation is performed using a thin plate smoothing spline surface fitting method (Hutchinson et al., 2009). Discharge data at the basin outlet was obtained from mass balance calculations at the dam and were provided by Hydro-Québec. Climate data consisted of reanalysis, GCM and RCM data. Data from the Canadian GCM (v3.1) (CGCM) and the Canadian RCM (v.4.2.0) (CRCM) was used. Average grid resolution was about 300 km for the CGCM and 45 km for the CRCM. The National Center for Environmental Prediction (NCEP) reanalysis data was used as a proxy to GCM data, to calibrate some of the downscaling used in this paper. This data uses a T62 (~ 209 km) global

spectral model to consistently collect observational data from a wide variety of observed sources (Kalnay et al., 1996; DAI CGCM3 Predictors, 2008). It includes information from both models and observations. SD techniques were calibrated using NCEP predictors interpolated at the CGCM scale. In climate change mode, predictors from the CGCM were used directly. The CRCM data driven by NCEP was also used for calibration purposes, while in climate change mode it was driven by the CGCM at its boundary and initial conditions. This work covers the 1970 - 1999 period (reference period) for calibration and the 2070 - 2099 period (2085 horizon) in climate change mode. The atmospheric predictors considered (NCEP and CGCM) are listed in table 7.2.

Table 7.1 The datasets used in this research

NO	Dataset	Purpose	Time period
1	Observed P, Tmax and Tmin (interpolated at a 10km scale - NLWIS dataset), measured discharge	Baseline, calibration of Hydrological model and WG	1970-1999
2	CGCM P, Tmax and Tmin	Downscaling of CF and WG methods	1970-1999, 2070-2099
3	CRCM P, Tmax and Tmin	Downscaling of CF and WG, and CRCM with and without BC methods	1970-1999, 2070-2099
4	NCEP predictors interpolated to CGCM grid	Calibration of SDSM and DASR	1970-1999
5	CGCM predictors	Downscaling of SDSM and DASR	2070-2099
6	CRCM P, Tmax and Tmin driven by NCEP	Calibration of HM for the method of CRCM without BC	1970-1999

Note: P=precipitation; Tmax=maximum temperature; Tmin=minimum temperature; BC=bias correction; WG=weather generator; SDSM=statistical downscaling model, and DASR=discriminant analysis coupled with stepwise linear regression downscaling method

Table 7.2 NCEP and CGCM predictor variables used to select precipitation predictors for downscaling

Predictor variable	**Abbreviation**	**Predictor variable**	**Abbreviation**
Mean sea level pressure	ncepmslp	500hPa Divergence	ncepp5zh
1000hPa Wind Speed	ncepp_f	850hPa Wind Speed	ncepp8_f
1000hPa U-component	ncepp__u	850hPa U-component	ncepp8_u
1000hPa V-component	ncepp__v	850hPa V-component	ncepp8_v
1000hPa Vorticity	ncepp__z	850hPa Vorticity	ncepp8_z
1000hPa Wind Direction	ncepp_th	850hPa Geopotential	ncepp850
1000hPa Divergence	ncepp_zh	850hPa Wind Direction	ncepp8th
500hPa Wind Speed	ncepp5_f	850hPa Divergence	ncepp8zh
500hPa U-component	ncepp5_u	500hPa Specific Humidity	ncep s500
500hPa V-component	ncepp5_v	850hPa Specific Humidity	nceps850
500hPa Vorticity	ncepp5_z	1000hPa Specific Humidity	ncepshum
500hPa Geopotential	ncepp500	Temperature at 2m	nceptemp
500hPa Wind Direction	ncepp5th		

7.4 Methodology

7.4.1 Downscaling methods

Six downscaling methods will be compared in this work. They consist of using CRCM data with (1) and without (2) bias correction, CF (3) and WG (4) methods at both CGCM and CRCM scales and two statistical downscaling methods: SDSM (5) and discriminant analysis coupled with step-wise regression method (6) at CGCM scale. Table 7.3 briefly describes all of the methods. Details follow below.

Table 7.3 Downscaling methods used in this work

Method	Brief description	Acronym used in the paper
1	Direct use of CRCM precipitation and temperature data without any bias correction, but with a specific hydrology model calibration.	CRCM-NONBC
2	Direct use of CRCM precipitation and temperature data with bias correction.	CRCM-BC
3	Change factor method, based on CRCM and CGCM data.	CRCM-CF CGCM-CF
4	Weather generator method based on CRCM and CGCM data.	CRCM-WG CGCM-WG
5	Statistical approach using the SDSM package with variance inflation and bias correction. GCM scale predictors are used (NCEP/CGCM).	CGCM-SDSM
6	Statistical approach using discriminant analysis for precipitation occurrence and stepwise linear regression for precipitation and temperature data. GCM scale predictors are used (NCEP/CGCM).	CGCM-DASR

7.4.1.1 Canadian RCM without bias correction

With the improved resolution of RCMs and the relatively small biases of RCM output data (compared to GCM data), it is now possible to envision direct use of RCM data as proxies to observed data. This is especially appealing in the cases where basins are much larger than the grid resolution. In this method, no bias correction is made, but the hydrology model is specifically calibrated to this data against observed discharge. The assumption behind this method is that biases are sufficiently small to be overcome by the hydrology model through the calibration process. While many take the accuracy of observed precipitation and

temperature data for granted, it is known that such data can also be biased. For example, rain gauges are known to underestimate real precipitation and weather station density is often low, especially in remote areas or at higher altitude, thus introducing spatial biases. If the specifically calibrated hydrology model is able to adequately reproduce observed discharge with realistic internal parameters, it can be argued that RCM data is no more biased than observed data. It is just biased differently, and thus the need for a specific calibration.

7.4.1.2 Canadian RCM with bias correction

While RCM data has been shown to be much more precise than their GCM counterparts, simulated monthly mean precipitation and temperatures are nevertheless biased when compared to observed data (Minville et al., 2009). These biases are large enough to induce significant errors if introduced directly into models such as hydrology models. In this method, bias correction is applied to both temperature and precipitation data. For precipitation, a correction is made to both monthly mean frequency and quantity, using the Local Intensity Scaling Method developed by Schmidli et al. (2006). This method involves three steps: (1) A wet-day threshold is determined from the daily RCM precipitation series of each month such that the threshold exceedence matches the wet-day frequency of the observed time series; (2) A scaling factor is calculated to insure that the mean of the observed precipitation is equal to that of RCM precipitation at the reference period for each month; and (3) The monthly thresholds and factors determined in the reference climate are used to adjust monthly precipitation for the 2085 horizon.

A three-step bias correction is also carried out for both the mean and variance of monthly temperatures (including Tmax and Tmin) of RCM data.

1) Daily RCM temperatures are corrected on a monthly basis using the following equation:

$$T_{cor,2085} = T_{RCM,2085} + (\overline{T}_{obs} - \overline{T}_{RCM,ref}) \quad (7.1)$$

Where $T_{cor,2085}$ is the daily corrected temperature at the horizon 2085 obtained by adding the difference in mean monthly temperatures between observed data and RCM reference period ($\overline{T}_{obs} - \overline{T}_{RCM,ref}$) to the RCM temperature data for the 2085 horizon ($T_{RCM,2085}$).

2) In a subsequent step, the standard deviation of monthly temperatures '*S'* at the 2085 horizon is corrected using the following equation:

$$S_{cor,2085} = S_{RCM,2085} \times (S_{obs} / S_{RCM,ref}) \quad (7.2)$$

Equation (7.2) effectively corrects the standard deviation of RCM temperatures based on the standard deviation ratio between observed and RCM temperatures over the reference period (subscripts are the same as defined for equation (7.1).

3) In a last step, downscaled temperatures at the daily scale for the 2085 horizon are obtained by adjusting temperatures obtained in step 1 to the standard deviation calculated in step 2. This is done by normalizing the step 1 temperatures to a zero mean and standard deviation of one, and transforming back to the step 2 standard deviation. This technique assumes that biases are time-invariant and ensures that the temperatures of the RCM over the reference period have the same monthly mean and standard deviation as those of the observed data.

7.4.1.3 Change factor (CF) method

The CF method involves adjusting the observed daily temperature ($T_{obs,d}$) by adding the difference in monthly temperature predicted by the climate model (GCM or RCM) between the 2085 horizon and the reference period ($\overline{T}_{CM,2085,m} - \overline{T}_{CM,ref,m}$) to obtain daily temperature at the 2085 horizon ($T_{adj,2085,d}$) (equation (7.3)). The adjusted daily precipitation for the 2085

horizon ($P_{adj,2085,d}$) is obtained by multiplying the precipitation ratio ($\overline{P}_{CM,2085,m} / \overline{P}_{CM,ref,m}$) with the observed daily precipitation ($P_{obs,d}$) (equation (7.4)).

$$T_{adj,2085,d} = T_{obs,d} + (\overline{T}_{CM,2085,m} - \overline{T}_{CM,ref,m}) \quad (7.3)$$

$$P_{adj,2085,d} = P_{obs,d} \times (\overline{P}_{CM,2085,m} / \overline{P}_{CM,ref,m}) \quad (7.4)$$

7.4.1.4 Weather generator (WG)-based method

The WG used in this research is CLImate GENerator (CLIGEN, Nicks and Lane, 1989). In this study, only the functions to generate precipitation occurrence and quantity, Tmax and Tmin were used. Other weather generators could also have been used.

In CLIGEN, a first-order two-state Markov chain is used to generate the occurrence of wet or dry days. The probability of precipitation on a given day is based on the wet or dry status of the previous day, which can be defined in terms of the two transition probabilities: wet day following a dry day (P01) and a wet day following a wet day (P11). For a predicted wet day, a three-parameter skewed normal Pearson III distribution was used to generate daily precipitation intensity for each month (Nicks and Lane, 1989).

A normal distribution was used to simulate Tmax and Tmin. The temperature with the smaller standard deviation between Tmax and Tmin is computed first, followed by the other temperature (Chen, et al, 2008). The mean and standard deviation of Tmax and Tmin were calculated monthly and smoothed with Fourier interpolation at a daily scale.

Overall, CLIGEN requires a total of 9 monthly parameters to generate precipitation, Tmax and Tmin. They include p01, and p11 for generating precipitation occurrence, mean, standard deviation and skewness for generating daily precipitation intensity and means and standard deviations of Tmax and Tmin. The skewness of precipitation is supposed to be unchanged in

the future for this study. Thus, there are 8 parameters that require modification for every future climate change scenario.

The parameters of CLIGEN are modified to take into account the variations predicted by a climate model (GCM or RCM). This variation is based on a delta change approach. For example, take the probability of precipitation occurrence P01. For various reasons, the P01 from GCM or RCM data will not match the P01 measured at a particular station. Thus, similarly to the CF method, the difference obtained from the GCM (or RCM) between the future and the reference periods will be applied to the observed data. This is a hybrid method combining attributes of both statistical and CF methods. The huge advantage over the CF method is that differences in precipitation occurrence and variance of all variables can be taken into account. Time series of any length can be generated, which is another advantage for the studies of extremes.

Details of this approach are as follows:

1) Similarly to the CF method, the adjusted monthly mean Tmax and Tmin for the 2085 horizon ($\overline{T}_{adj,2085}$) are estimated as:

$$\overline{T}_{adj,2085} = \overline{T}_{obs} + (\overline{T}_{CM,2085} - \overline{T}_{CM,ref}) \tag{7.5}$$

The adjusted values are obtained by adding the differences predicted by a climate model (GCM or RCM) between the 2085 horizon and the reference period ($\overline{T}_{CM,2085} - \overline{T}_{CM,ref}$) to the observed mean monthly observed temperatures ($\overline{T}_{obs}$).

2) Monthly means and variances of precipitation, monthly variances of Tmax and Tmin and transition probabilities of precipitation occurrence p01 and p11 for the 2085 horizon are adjusted by:

$$X_{adj,2085} = X_{obs} \times (X_{CM,2085} / X_{CM,ref}) \tag{7.6}$$

where *X* represents the variable to be adjusted. The subscripts are the same as above.

3) The p01 and p11 values are expressed in terms of an unconditional probability of daily precipitation occurrence (π) and the lag-1 autocorrelation of daily precipitation (*r*) for further adjustments.

$$\pi = \frac{P_{01}}{1 + P_{01} - P_{11}} \tag{7.7}$$

$$r = P_{11} - P_{01} \tag{7.8}$$

4) The adjusted mean daily precipitation per wet day (u_d) was estimated as (Wilks, 1999a; Zhang, 2005):

$$\mu_d = \frac{\mu_m}{N_d \pi} \tag{7.9}$$

where N_d is the number of days in a month, $N_d \pi$ is the average number of wet days in a month, and u_m is the step (2)-adjusted monthly precipitation.

5) The adjusted daily variance (σ_d^2) was approximated using equation (7.10), based on the step (2)-adjusted variance of the monthly precipitation (σ_d^2) (Wilks, 1999a).

$$\sigma_d^2 = \frac{\sigma_m^2}{N_d \pi} - \frac{(1-\pi)(1+r)}{1-r} \mu_d^2 \tag{7.10}$$

All of the adjusted precipitation, Tmax and Tmin parameter values were input to CLIGEN to generate 900 years of daily time series (Thirty 30-year realizations). An ensemble of realizations was used to insure that the method converges toward its true mean response. Due to the stochastic nature of the WG, a single realization of 30 years could have resulted in a biased estimate.

7.4.1.5 Statistical downscaling model (SDSM)

The SDSM is a downscaling tool developed by Wilby et al. (2002a) that can be used to develop climate change scenarios. The SDSM uses a conditional process to downscale precipitation. Local precipitation amounts depend on wet-/dry-day occurrences, which in turn depend on regional-scale predictors such as mean sea level pressure, specific humidity and geopotential height (Wilby et al., 1999; Wilby and Dawson, 2007). Specifically, downscaling of precipitation occurrence is achieved by linking daily probabilities of non-zero precipitation with large-scale predictors selected from the variables listed in table 7.2.

The main procedures of the SDSM for downscaling wet day precipitation intensity, Tmax and Tmin (predictands) are the following: (1) Identification of the screen variable: a partial correlation analysis was used to identify the relationship between NCEP variables and predictands. Variables that significantly correlated to predictands were then selected as predictors; (2) Model calibration: multiple linear regressive equations were established between predictands and step (1)-identified predictors for each season. Since the distribution of the daily precipitation is highly skewed, a fourth root transformation was applied to the original precipitation before fitting the transfer function (Wilby and Dawson, 2007); and (3) Application of transfer functions: established transfer functions were further used to downscale precipitation amounts, Tmax and Tmin for the 2085 horizon.

The SDSM bias correction was applied to insure that observed and downscaled precipitation totals were equal for the simulation period. The variance inflation scheme was also used, to increase the variance of precipitation and temperatures to agree better with observations. When using bias correction and variance inflation, SDSM essentially becomes a weather generator, where a stochastic component is superimposed on top of the downscaled variable. This is especially true for precipitation, where the explained variance is generally less than 30% (Wilby et al., 1999).

7.4.1.6 Discriminant analysis coupled with step-wise regression method (DASR)

This approach is similar to that of the SDSM, but with no stochastic component added on top via bias correction and variance inflation. The main difference is that precipitation occurrence is downscaled using a discriminant analysis and the daily precipitation intensity of wet days is downscaled using a stepwise linear regression approach.

With discriminant analysis for the downscaling of precipitation occurrence, it is necessary to have an available "training sample" in which it is known that each of the vectors is classified correctly (Wilks, 1995). In this research, the NCEP variables interpolated to the CGCM grid and their lag-1 variables were used as the training sample. The precipitation series were first divided into two groups, a wet-day group (daily precipitation amount ≥1mm) and a dry-day group (daily precipitation amount < 1mm). The future precipitation occurrence was similarly classified according to rules constructed based on a training sample and corresponding groups.

The SD method selected here uses a stepwise linear regression for the precipitation quantity of wet days, Tmax and Tmin (predictands). Twenty-five NCEP variables and the lag-1 variables for the reference period were used to select predictors using the stepwise regressive method. Multiple linear regressive equations were then fitted between predictands and selected predictors for each season. A fourth root transformation was also applied to the original precipitation before fitting the transfer function. The established transfer functions were then used to downscale daily precipitation for the 2085 horizon using CGCM predictors.

7.4.2 Hydrological simulation

The impacts of climate change on hydrology at the catchment were quantified based on discharges simulated with the hydrological model HSAMI, developed by Hydro-Québec, and which has been used to forecast natural inflows for over 20 years (Fortin, 2000). HSAMI is

used by Hydro-Québec for hourly and daily forecasting of natural inflows on 84 watersheds with surface areas ranging from 160 km^2 to 69,195 km^2. Hydro-Québec's total installed hydropower capacity on these basins exceeds 40GW. HSAMI is a 23-parameter, lumped, conceptual, rainfall-runoff model. Two parameters account for evapotranspiration, 6 for snowmelt, 10 for vertical water movement, and 5 for horizontal water movement. Vertical flows are simulated with 4 interconnected linear reservoirs (snow on the ground, surface water, unsaturated and saturated zones). Horizontal flows are filtered through 2 hydrograms and one linear reservoir. Model calibration is done automatically using the shuffled complex evolution optimization algorithm (Duan, 2003). The model takes snow accumulation, snowmelt, soil freezing/thawing and evapotranspiration into account.

The basin-averaged minimum required daily input data for HSAMI are: Tmax, Tmin, liquid and solid precipitations. Cloud cover fraction and snow water equivalent can also be used as inputs, if available. A natural inflow or discharge time series is also needed for proper calibration/validation. For this study, thirty years (1970-1999) of daily discharge data were used for model calibration/validation. The optimal combination of parameters was chosen based on Nash-Sutcliffe criteria. The chosen set of parameters yielded Nash-Sutcliffe criteria values of 0.89 for both validation and calibration periods. This high value of the Nash-Sutcliffe criteria is representative of the good quality of weather inputs and observed discharge.

7.5 Results

7.5.1 Validation of downscaling methods

The validation of each downscaling method was based on the quality of the simulated hydrographs at the basin outlet, when compared to the hydrograph developed from observed weather data. Mean hydrograph results are presented in figure 7.2. The mean hydrograph from observed discharge (labeled OBS) and a hydrograph simulated from observed weather data (labeled OBS-SIM) show the small biases introduced by the hydrological model. The overall fit is quite good, with a Nash-Sutcliffe coefficient of 0.89 over the length of the time

series, as mentioned above. The mean hydrograph simulated from WG generated weather data (labeled OBS-WG) is also displayed to verify the possibility of using the WG method. The other curves represent the downscaling approaches presented in table 7.3, with the exception of the CF method which requires no validation. Overall, all of the methods, with the exception of CGCM-DASR, result in hydrographs that are very close the one simulated using observed precipitation and temperatures time series. The best methods were found to be CRCM data with bias correction and the SDSM. In addition, the performance of CLGEN was also qualified to use in this research. The performance of the hydrological model when calibrated with raw RCM data indicates that the biases of the climate model are small enough to be accounted for by the hydrology model. However, the Nash-Sutcliffe coefficient was better when using the standard calibration and correcting the biases (0.89 for CRCM-BC versus 0.81 for CRCM-NONBC), indicating that RCM data is either more biased than the observed values or less coherent with the observed discharge.

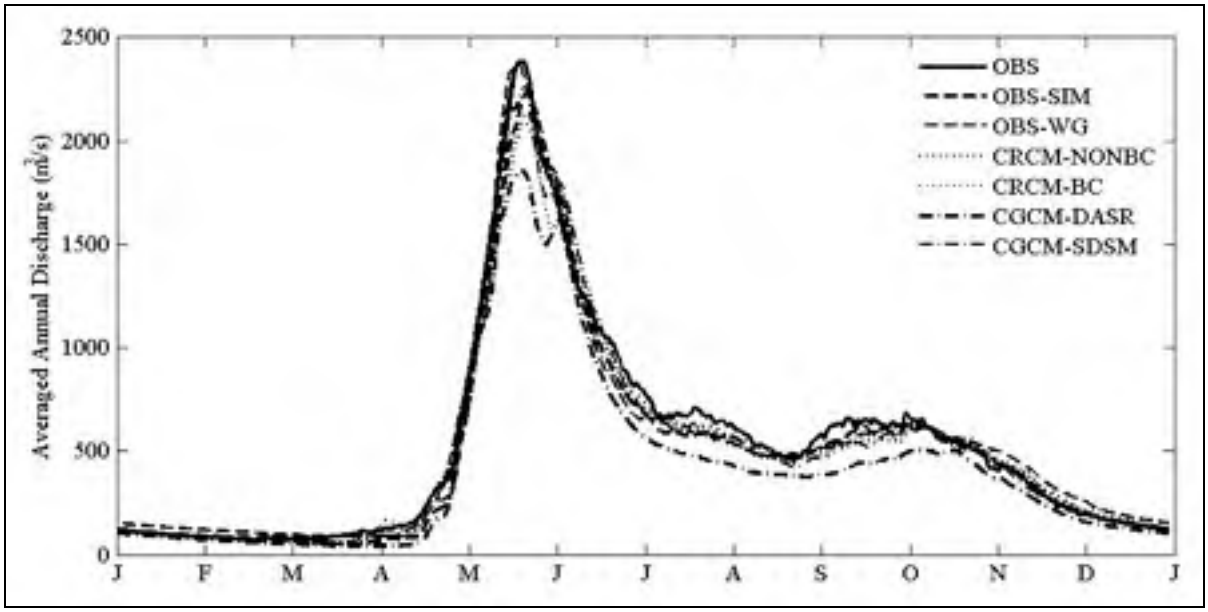

Figure 7.2 Averaged annual hydrographs for the reference period (1970-1999) at the Manicouagan 5 river basin. Observed (OBS), observed weather data simulated (OBS-SIM), and weather generator data simulated (OBS-WG) discharges are also plotted for comparison. See Table 1 for the downscaling method acronyms.

As mentioned above, discharges simulated with the precipitation, Tmax and Tmin downscaled by DASR were underestimated. This is because DASR underestimated the precipitation (mean and standard deviation), while the SDSM reproduced it very well (figure 7.3). This indicates that the explained variance of the linear regression approach is not sufficient to properly resolve discharge. The stochastic component added by the SDSM via bias correction and variance inflation makes up for the basic flaw of the approach (a small percentage of explained variance) with respect to precipitation. Results are much better for temperatures because of the much larger percentage of explained variance. The DASR and SDSM methods are very similar and the observed differences between these approaches outline the differences in the raw predictive power of the statistical scheme and with the added stochastic component. This will be further discussed after the results in a changed climate are presented.

7.5.2 Climate change scenarios

7.5.2.1 Monthly and daily mean precipitations

All downscaling methods show increases in total seasonal precipitation for the 2085 horizon (figure 7.4a). The ratios of increase range from 6% to 67% for spring, 1% to 20% for summer, 3% to 21% for autumn and between 5 and 45% for winter. Although both CGCM-SDSM and CGCM-DASR are regression-based methods, the former suggests more increases in monthly precipitation than the latter. This is partly due to the underestimation of mean precipitation by the CGCM-DASR model (figure 7.3b). A bias correction is used with the SDSM to insure the downscaled mean precipitation agrees better with the observation.

The CGCM-DASR suggests 12% winter daily precipitation increase and 5% decrease for spring, 8% decrease for summer and 2% decrease for autumn (figure 7.4b). However, the other downscaling methods, with the exception of CGCM-WG, predict increases in daily precipitation for all seasons. The increased/decreased ratios range from 11% to 68% for spring, -4% (predicted by CGCM-WG) to 19% for summer, -1% (predicted by CGCM-WG)

to 29% for autumn and between 12% and 40 % for winter. The variation of daily precipitation in each season is not consistent with that of totally seasonal precipitation. This is because the daily precipitation quantity is affected not only by the seasonal precipitation quantity, but also by precipitation occurrence. The precipitation occurrence is different for each downscaling method (results not shown).

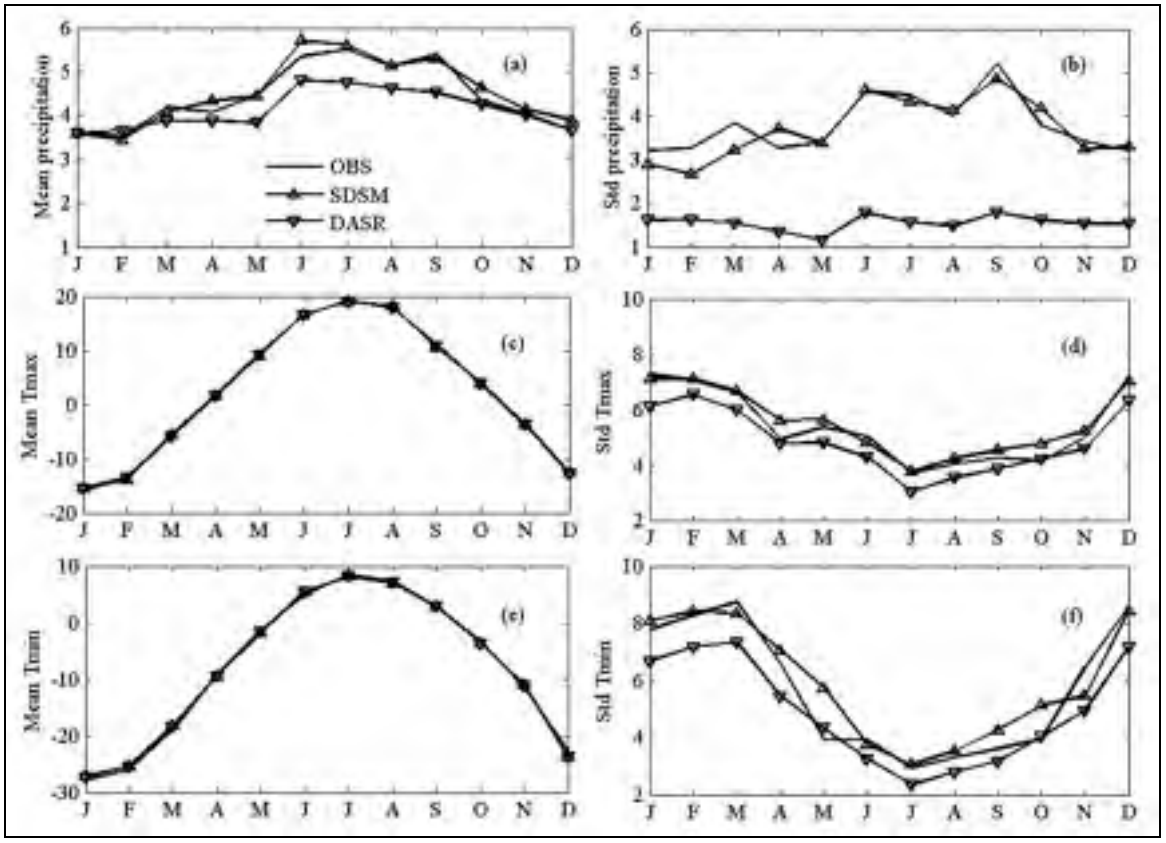

Figure 7.3 Means and standard deviations of observed (OBS) and DASR and SDSM downscaled monthly precipitations, Tmax and Tmin at the Manicouagan 5 river basin for the reference period (1970-1999).

The CGCM-DASR predicts a 26% standard deviation increase for total winter precipitation and a decrease for all other seasons (8% for spring, 26% for summer and 19% for autumn) for the 2085 horizon (figure 7.4c). This decrease is partly due to the underestimation of the variance of precipitation as shown in figure 7.3b. As mentioned earlier, the SDSM uses a stochastic component to increase downscaled variances to better agree with observations.

Other downscaling methods suggest increases in the standard deviation of seasonal precipitation for each season (20-59% for spring, 4-19% for summer and autumn and between 18% and 50% for winter). Although the CF and WG methods share similarities, the observed increases are different, because the CF method adjusts precipitation variance through a modification of the mean, while WG-based methods adjust it from changes of not only precipitation quantity but also occurrence. In addition, variances downscaled from CGCM and CRCM data are also different, although the CRCM is driven by the CGCM. Predicted changes in the standard deviation of daily precipitation are not unequivocal (figure 7.4d). The CGCM-DASR suggests reductions in the standard deviation of daily precipitation (between 50% and 63% depending on the season) while the other methods suggest increases for most of the seasons.

7.5.2.2 Average temperatures

Figure 7.5 presents annual temperature (average of Tmax and Tmin) cycles for all downscaling methods for the 2085 horizon and for the observed data (reference period). All of the downscaling methods suggest increases in temperatures for the 2085 horizon. Increases range between 3.6 °C and 6.3 °C for spring, 0.4 °C and 4.1°C for summer, 1.8 °C and 4.8°C for autumn and between 5.7 °C and 9.1°C for winter. Winter temperature increases are greater than for other seasons. The CRCM-NONBC method suggests lower increases in temperature than other methods. The regression-based statistical methods predict a much larger increase in autumn and winter average temperatures. Average temperature cycle graphs display the freezing dates when the average temperature climbs above and descends below zero degrees. These dates are April 27th and October 15th for the reference period. Depending on the specific downscaling method, this period could start as early as April 11th and as late as November 13th for the 2085 horizon, which implies that the freezing season could be shortened by up to 42 days. These changes would affect the snow accumulation in the winter and the spring snowmelt.

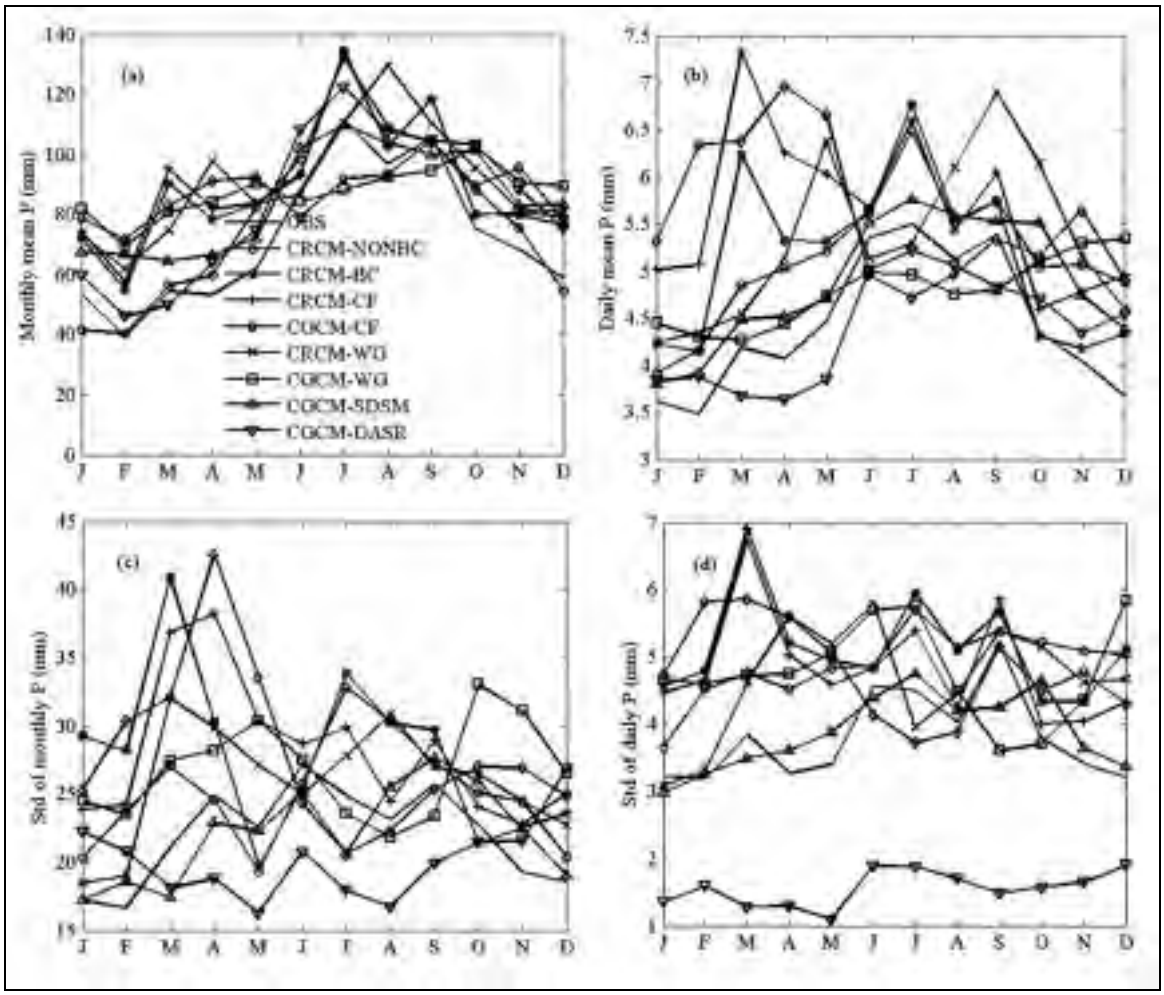

Figure 7.4 Mean and standard deviation of the observed (1970-1999) and downscaled (2070-2099) monthly and daily precipitations at the Manicouagan 5 river basin. (a): mean monthly precipitation; (b): mean daily precipitation; (c): standard deviation of monthly precipitation; and (d): standard deviation of daily precipitation.

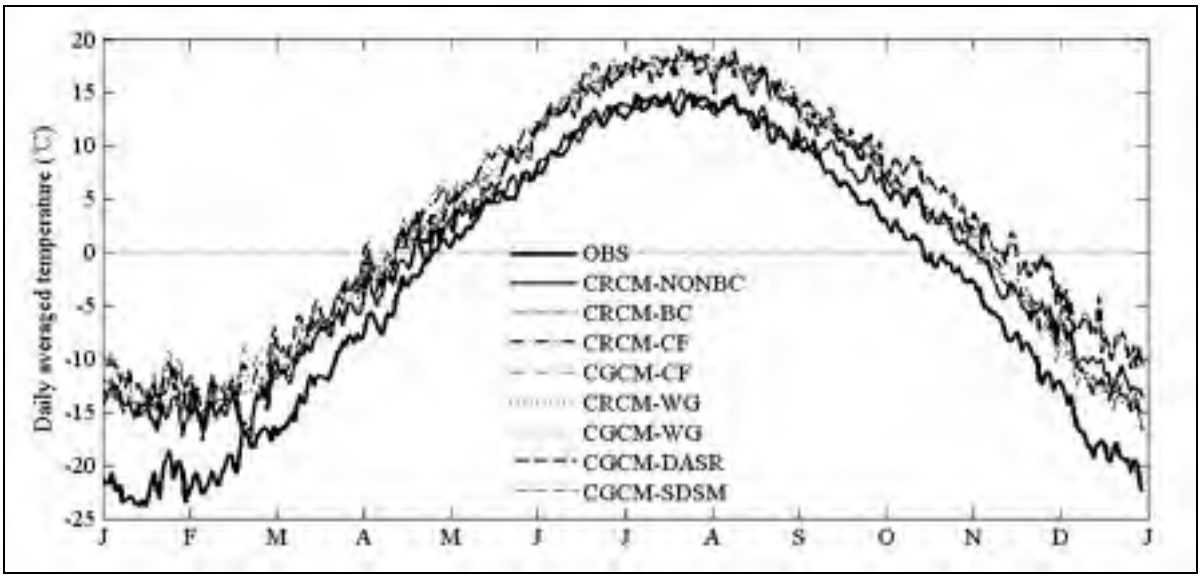

Figure 7.5 Observed (1970-1999) and downscaled (2070-2099) average annual temperature cycle at the Manicouagan 5 river basin.

7.5.3 Uncertainty of annual precipitation and maximum and minimum temperatures

Probability density functions (PDFs) of the annual precipitation, Tmax and Tmin, were built to show the uncertainties related to downscaling methods (figure 7.6). The probability of a variable (precipitation, Tmax or Tmin) falling within a given set is given by the integral of its density over the set. The total area under each PDF is equal to one. The annual precipitations for the reference period are between 557.8 mm and 1230.8 mm with a median value of 863.7 mm (there is a 50% probability of annual precipitation being greater or less than 863.7 mm) and a mode (most frequent value) of 850.1 mm. The PDFs show that all downscaling methods predict an increase in annual precipitation for the 2085 horizon; the magnitude of increase varies from one method to the other ranging between 75.0 (CRCM-NONBC) and 219.1 mm (CRCM-WG). The CRCM-WG predicts the largest increase in annual precipitation. Medians of annual precipitation would also increase by between 9% and 26% in the 2085 horizon. The CRCM-NONBC predicts the lowest increase in the median and the CRCM-WG predicts the highest. Figure 7.6a shows that an average year of precipitation in the current climate would become a very dry year in the 2085 future climate.

Each downscaling method suggests increases in annual mean Tmax and Tmin for the 2085 horizon. The magnitude of the increases varies from one method to the other, ranging between 3.6 °C and 5.4 °C for Tmax and between 2.4 °C and 5.8 °C for Tmin. In addition, all downscaling methods predict increases in the medians of annual mean Tmax (3.7-5.6°C) and Tmin (2.7-6.1°C). The CRCM-NONBC predicts the smallest increases in temperatures, while the two regression-based methods (CGCM-SDSM and CGCM-DASR) suggest the largest increases.

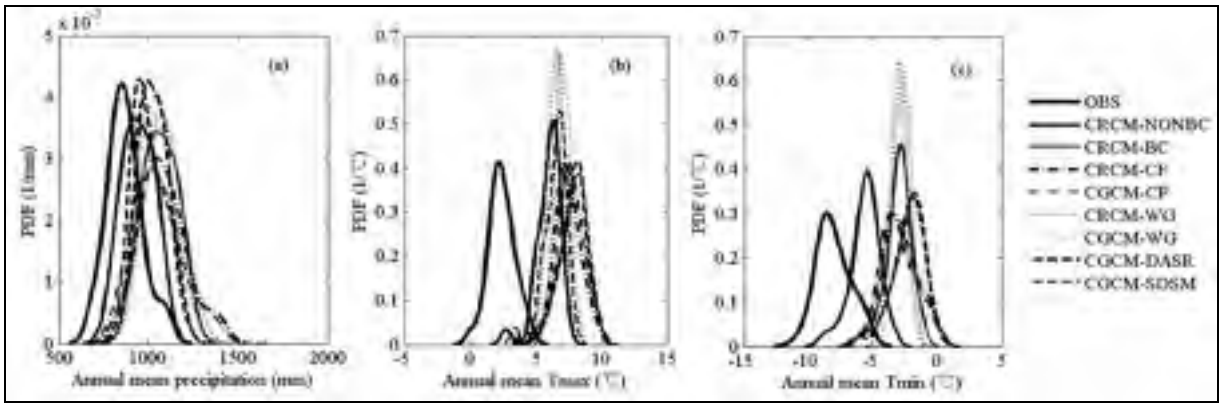

Figure 7.6 Probability density functions (PDF) of the observed (1970-1999) and downscaled (2070-2099) annual mean precipitation and maximum and minimum temperatures at the Manicouagan 5 river basin.

7.5.4 Hydrologic impacts of climate change

7.5.4.1 Hydrologic variables

Figure 7.7 presents average hydrographs simulated with precipitation and temperature downscaled from the different methods. To avoid any bias resulting from the hydrological modeling process, discharge for the reference period is represented by modeled discharge and not by observations. The results showed that all downscaling methods suggest increases in winter discharge (November-April) and decreases in summer (June-October). The two

regression-based methods predict much larger increases in winter flows than other methods, and, consequently, their snowmelt peak discharges are much lower. These two methods predict a larger increase in autumn and winter temperatures; the liquid winter precipitation rapidly contributes to runoff instead of being accumulated in the snow cover. Thus, there is not very much snowmelt in spring to contribute to peak discharge. For annual discharges, the only simulation that predicts a decrease comes from the CGCM-DASR method, largely because this method underestimates precipitation. All other downscaling methods show increases in annual discharges ranging between 3.5% (CRCM-NONBC) and 20.9% (CRCM-WG). By the 2085 horizon, the two regression-based methods and the CRCM-NONBC suggest decreases in peak discharges between 4.1% (CRCM-NONBC) and 25.1% (CGCM-DASR). The slight decrease predicted by CRCM-NONBC is due to a smaller increase in annual precipitation, relative to a larger increase in temperature. However, the CGCM-WG predicts an increase in peak discharge, as do the CRCM-WG and the CRCM-BC. For these three methods, increases in winter temperature are not sufficient to offset the precipitation increase. In addition, for all downscaling methods the peak discharges of the 2085 horizon are observed earlier than for the reference period. Lags vary from 12 days (May 12th) for the CRCM-NONBC to 27 days (April 27) for the CGCM-CF.

7.5.4.2 Uncertainty of hydrologic variables

In order to better quantify the uncertainties of hydrologic variables, PDFs were constructed for peak discharge, time to peak discharge and annual mean discharge (figure 7.8). These graphs display the global uncertainty linked to downscaling techniques. Figure 7.8a shows that the two regression-based methods predict the largest decreases in peak discharges. All of the downscaling methods predict an earlier peak discharge (figure 7.8b), although there is significant inter-annual variability. Inter-annual variability is very large for the two regression-based methods as shown by their very flat PDFs. Large inter-annual variability is also shown with future annual mean discharge (figure 7.8c). As mentioned earlier, the CGCM-DASR method is the only that shows decreases in future annual mean discharge. The

CF methods (CGCM-CF and CRCM-CF) display the largest future inter-annual variability of mean discharge (flattest PDFs in figure 7.8c).

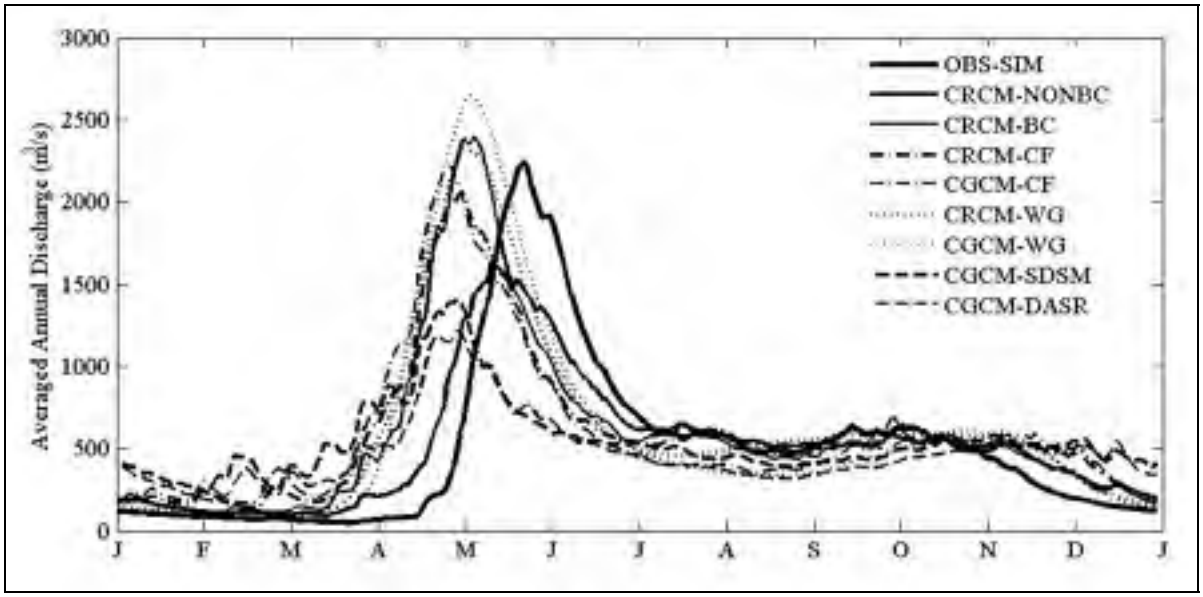

Figure 7.7 Average annual hydrographs for the future (2070-2099) and reference (1970-1999) periods at the Manicouagan 5 river basin.

7.6 Discussion and conclusions

The uncertainty of climate change impacts on hydrology has been given more and more attention in the scientific literature. By far the largest focus has been on investigating the roles of GCMs and GGES in the uncertainty cascade. Other sources of uncertainty, such as the choice of downscaling method, have been given much less attention. Six downscaling methods were compared to investigate the uncertainty of downscaling methods in quantifying the impact of climate change on the hydrology of a Canadian (Quebec province) River basin. The downscaling methods regroup dynamical and statistical approaches including the CF method and a WG-based approach. Two regression-based methods (SDSM and DASR) are also used for comparison. The downscaling methods were first validated based on the modeling of discharge. Overall, all of the methods, with the exception of CGCM-DASR, result in hydrographs that are very close to the hydrograph simulated by

using observed precipitation and temperature time series. The best methods were CRCM data with bias correction and the SDSM. The DASR method underestimates the hydrograph, clearly indicating that the explained variance of the linear regression approach is not sufficient to properly resolve discharge issues. The stochastic component added by the SDSM via bias correction and variance inflation makes up for the basic flaw of the approach (only a small percentage of variance is explained) with respect to precipitation.

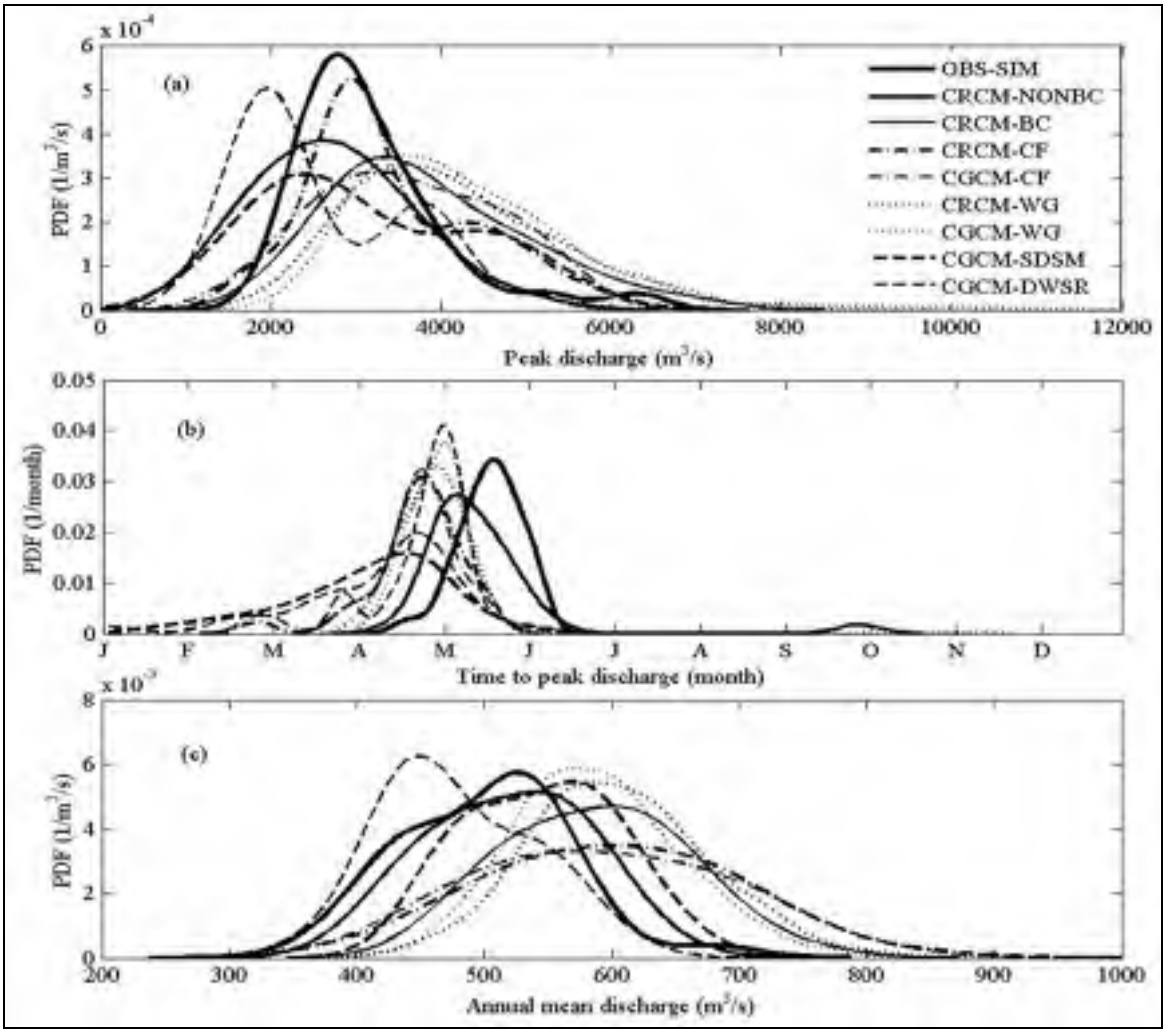

Figure 7.8 Probability density functions (PDF) of (a) peak discharge, (b) time to peak discharge and (c) annual mean discharge for the future (2070-2099) and reference (1970-1999) periods at the Manicouagan 5 river basin.

The analysis of climate change scenarios shows that all downscaling methods suggest increases in temperature over the basin for the 2085 horizon. The two regression-based methods show larger increases in autumn and winter temperatures than the others. Depending on the specific downscaling method, the freezing season would be shortened by 26-42 days. Predicted changes in precipitation are not as unequivocal as those for temperature. Results vary seasonally and depend on the downscaling method. The combined effects of precipitation and temperature changes influence discharge differently depending on the downscaling method. All of the methods show a general increase in winter discharge (November-April) and most show a decrease in summer discharge. Winter flows are especially large for the two regression-based methods, which also predict the largest temperature increases in autumn and winter. Liquid winter precipitation rapidly contributes to runoff instead of being temporarily stored in the snow cover. This leads to strongly attenuated snowmelt peak flows. Peak discharges appear earlier for all downscaling methods, but their timing varies according to the downscaling method.

The results indicate that climate change impact studies based only on one downscaling method should be interpreted with caution. General speaking, it is assumed that the major sources of uncertainty are linked to GCMs and GGES (Kay et al., 2009; Wilby and Harris, 2006). To make a comparison with GCM-linked uncertainty, the uncertainty envelope derived from the choice of downscaling method in this paper is compared to that originating from a combination of 28 climate projections from a combination of 7 GCMs and 3 GGES (figure 7.9). Both uncertainty envelopes display the same characteristics. Downscaling contributes to a larger uncertainty in winter flows, but GCM-GGES projections give a much larger uncertainty over the snowmelt season. Both envelopes are very similar in the summer and fall seasons. Comparing six downscaling methods to 28 projections (from 7 GCMs and 3 GGES) should contribute to a larger uncertainty envelope in the latter case, and overall this is what was observed. On the other hand, the two regression-based SD methods contributed proportionally more to the uncertainty envelope, because their behavior was markedly different in several instances.

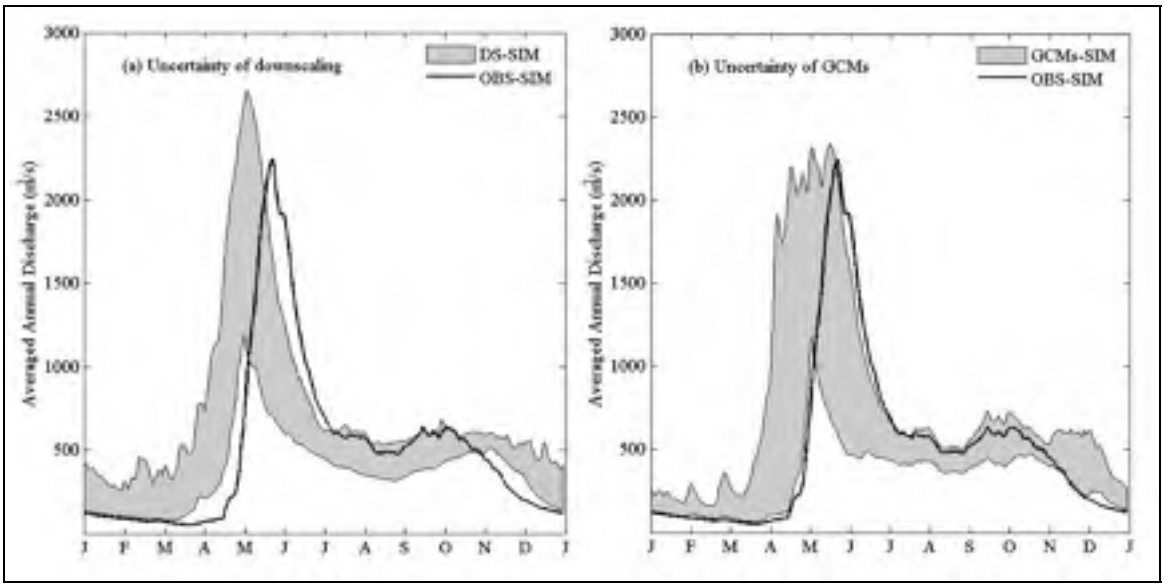

Figure 7.9 Envelopes of simulated discharge with (a) six downscaling methods and (b) 28 GCMs and GGES using the change factor downscaling method at the Manicouagan 5 river basin for the future period (2070-2099). The discharge simulated with observed climate data for the reference period (1970-1999) is also plotted for comparison.

The results indicated quite clearly that the choice of a downscaling method is critical for any climate change impact study on hydrology. Can the results outlined in this paper help in selecting an appropriate method? For the most part, the answer would be 'no' and that additional research is needed. However, these results do raise some important points. It can be argued that regression-based methods should be used with caution due to their distinctive behavior compared to other downscaling methods; their downscaled future temperatures are very high, especially when compared to the direct outputs from the regional climate models (which exhibit relatively small biases in the current climate). So despite the fact that a high percentage of temperature variance is explained by regression-based methods in the current climate, the anomalous downscaled future temperatures raise serious questions about the stationary nature of the regression. This was always a weak point of regression-based methods that could never be clearly disproved or confirmed. If there is doubt that regression equations are stationary for temperature, the case of the validity of the approach for precipitation is even harder to make, mostly because the percentage of explained variance is very low to begin with. The CGCM-DASR model (a regression-based model with no bias or

variance correction) was included for comparison purposes only. It is clearly inadequate at reproducing adequate precipitation in the current climate. However, both this flawed method (CGCM-DASR) and the one correcting for precipitation bias and variance (CGCM-SDSM) give nearly identical future mean hydrographs (figure 7.7), further raising doubts as to the validity of transposing regression equations in changed climate predictions.

The strength and weaknesses of the CF method have been discussed in several papers. This method gives similar results whether factors are derived from the GCM or the RCM (driven by the same GCM at its boundaries). Its main weakness (that it does not modify future variance and precipitation occurrence) is probably not a major obstacle with respect to spring snowmelt. Since spring floods are the result of several months of snow accumulation followed by rapid melting, the most important feature to have in a climate change study is the correct total quantity of solid precipitation. The variability of solid precipitation during the winter months is a less important feature to have. On the other hand, for summer and fall events, damages often result from one major rainfall event, and droughts from long periods with little to no precipitation. In such cases, the CF method would be totally inappropriate for climate change studies and another downscaling method would be necessary. In such cases, WG based approaches may be more successful in resolving extremes series of dry days and high temperature. This would especially be the case for arid and semi-arid areas.

An interesting result from this paper is that the biases in the RCM that was used are small enough that they can be dealt with by the hydrological model, thus negating any bias correction on the outputs from the CRCM. As discussed earlier, this approach stems from the assumption that biases present in observed weather data (especially for precipitation) are of the same order as those from the RCM precipitation. As such, a specific calibration of the hydrology model to each dataset is sufficient. While this has proved to be the case in the present climate, there are large differences in future predicted outflows between the direct inputs of RCM data (CRCM-NONBC) and the use of RCM data with bias corrections (CRCM-BC). This is partly because CRCM precipitation used to calibrate the hydrological model (1970-1999) was driven by initial and boundary conditions of NCEP, while it was

driven by initial and boundary conditions of CGCM for the future period (2070-2099). However, both datasets were considerably different for the reference period (results not shown). It should be not a surprise, since NCEP data and GCM data are not entirely comparable. NCEP data aims at representing the real world, whereas GCMs operate in their own virtual world. It is difficult to say which method is the most correct from both practical and theoretical viewpoints. The fact that they give a markedly different future hydrology indicates that either the assumption of constant bias does not hold, or that the choice of different calibration parameters (in the case of CRCM-NONBC) results in significant future uncertainty. However, recent work (Poulin et al., 2011) demonstrates that the uncertainty derived from hydrology model parameters is relatively small, raising doubts toward the common assumption of constant biases over time. Even if the direct use of RCM data had proved to be the most interesting method, the problem remains that it would not be possible to sample GCM uncertainty with this approach, as it would require outputs from several RCMs, all driven by different GCMs, over the same basin.

Clearly, more research is needed before this problem is settled. In particular, it would be interesting to get results from basins in different climate zones (especially arid and semi-arid climates) as the hydrological response to a choice of a given downscaling method may be related to a given climate. It is not possible at this stage to recommend a specific downscaling method for a given application, or even to use several downscaling methods to produce an ensemble of forcings for hydrology models, such as commonly done with GCM and GGES. Cases where the downscaling uncertainty envelope is contained within other uncertainties sources should not be treated with the same attention than cases where downscaling is the main source of uncertainty. The first conclusion of this paper is that the choice of a downscaling method does matter, and that the uncertainty linked to the choice of a downscaling method should not be ignored in any climate change impact study. The second conclusion is that downscaling methods are not created equal and that the choice of one or more approach should be evaluated on a case by case basis with respect to the objectives of the climate change impact study.

CHAPTER 8

GLOBAL UNCERTAINTY STUDY OF THE HYDROLOGICAL IMPACTS OF CLIMATE CHANGE FOR A CANADIAN WATERSHED

Jie Chen[1], François P. Brissette[1], Annie Poulin[1], Robert Leconte[2]

1. Department of Construction Engineering, École de technologie supérieure, Université du Québec, 1100, rue Notre-Dame Ouest, Montréal, Québec, Canada, H3C 1K3.
2. Department of Civil Engineering, Université de Sherbrooke, 2500, boul. de l'Université, Sherbrooke, Québec, Canada, J1K 2R1

This article was submitted to the Water Resources Research in February, 2011.

8.1 Abstract

General Circulation Models (GCMs) and Greenhouse Gas Emissions Scenarios (GGES) are generally considered to be the two major sources of uncertainty in quantifying the climate change impacts on hydrology. Other sources of uncertainty have been given less attention. This study considers global uncertainty by combining results from an ensemble of six GCMs, two GGES, five GCM initial conditions, four downscaling techniques, three hydrological model structures and 10 sets of hydrological model parameters. Each climate projection is equally weighted to predict the hydrology on a Canadian watershed for the 2081-2100 horizon. The results show that the choice of GCM is consistently a major contributor to uncertainty. However, other sources of uncertainty, such as the choice of a downscaling method and the GCM initial conditions also have a comparable or even larger uncertainty for some hydrological variables. Uncertainties linked to GGES and the hydrological model structure are somewhat less than those related to GCMs and downscaling techniques. Uncertainty due to the hydrological model choice of parameters has the least important contribution among all the variables considered. Overall, this research underlines the importance of adequately covering all sources of uncertainty. A failure to do so may result in

moderately to severely biased climate change impact studies. Results further indicate that the major contributors to uncertainty vary depending on the hydrological variables selected, and that the methodology presented in this paper is successful at identifying the key sources of uncertainty to consider for a climate change impact study.

Keywords: Climate change, hydrology, uncertainty, hydrological model, general circulation model, downscaling

8.2 Introduction

The Intergovernmental Panel on Climate Change (IPCC, 2007) stated that climate change will have discernible impacts on continental water resources, due to changes in precipitation and temperatures that will have an effect on the global water circulation. Thus, water resources management, already stressed with the hazards of natural variability, will face additional challenges. General Circulation Models (GCMs) are the major tools that provide information about future climate. General speaking, there are two steps to follow to quantify the hydrological impacts of climate change based on GCMs outputs: (1) GCM outputs (usually precipitation and temperatures) are first downscaled to a watershed or site-specific scale to obtain climate change projections at an appropriate scale; and (2) climate change projections are then input into hydrological models to simulate future hydrological conditions. A decision-maker can then make long-term decisions according to the predicted hydrological conditions and variability. However, given the large number of GCMs, Greenhouse Gas Emissions Scenarios (GGES) and downscaling methods available, it is becoming increasingly difficult to assess the uncertainties that result from their combination. This difficulty is further amplified when taking into account the choice of an impact model (such as a hydrological model) and its parameters, which also contribute to global uncertainty. Various sources of uncertainty have been clearly identified and it has been recognized that they should be taken into account in climate change impact studies. A failure to cover the full range of uncertainty may result in severely biased impact studies. The uncertainty cascade can be classified as follows: (1) GCM structures; (2) GGES; (3)

downscaling methods; (4) hydrological model structures; (5) hydrological model parameters; and (6) GCM initial conditions. Running GCMs with different initial conditions is a way to assess natural variability as perceived by the climate model. Some of these uncertainty sources may be reduced in the future (through higher resolution GCMs for example), but some causes of uncertainty will always remain. The acknowledgement and proper quantification of uncertainty are vital to facilitate a risk-based approach to decision making. As such, a non-biased framework to properly sample all sources of uncertainty is very much needed. To date, there have been several hydrological impact studies that have taken some causes of uncertainties into account, but only a rare few have investigated most of the entire cascade of uncertainties listed above.

Jenkins and Lowe (2003) studied changes in global mean rainfall from different GCMs and GGES and showed that GCM uncertainty dominates GGES uncertainty. This finding has been confirmed by several other studies. Rowell (2006) investigated the uncertainty arising from RCM formulation, and compared it with three other sources of uncertainty (GCMs, GGES and GCM initial conditions (ensemble runs)) with respect to changes in seasonal precipitation and temperature for the United Kingdom. The results showed that the uncertainty due to RCM formulation was relatively small, while GCMs consistently demonstrated a dominant role for each season. These two studies investigated the uncertainty on the primary outputs of climate models (temperature and/or precipitation) rather than on river flow. Different results may be obtained when transferring climate projections to watershed streamflows, since it is a non-linear process.

Prudhomme and Davies (2009) used three GCMs, two GGES and two downscaling techniques (a statistical downscaling model (SDSM) and the RCM HadRM3) to investigate the uncertainty in river flows, and demonstrated that GCMs were the main contributors to monthly mean flow uncertainty. The downscaling of originating uncertainty was also important, but the contribution of GGES to uncertainty was negligible. Kay et al. (2009) also investigated different sources of uncertainties including five GCMs, four GGES (A1F1, A2, B1 and B2), two downscaling methods (change factor (CF) and RCM)), two hydrological

models, hydrological model parameters and GCM initial conditions on the impact of climate change on flood frequency in England. With this research, each source of uncertainty was assessed individually rather than in combination with each other. The results showed that the uncertainty related to GCM structure was the largest, but other sources of uncertainty were also important, although less so than GCM uncertainty. However, Booij (2005) found that the uncertainty related to GCM initial conditions was larger than that of GCMs and RCMs.

Wilby and Harris (2006) presented a probabilistic framework for quantifying different sources of uncertainties on future low flows. They used four GCMs, two GGES, two downscaling methods (SDSM and CF), two hydrological model structures and two sets of hydrological model parameters. The results again showed that GCMs are the main contributor to global uncertainty, followed by downscaling methods. Uncertainties due to hydrological model parameters and GGES were less important. This is probably the most thorough study so far, in terms of inclusion of the most sources of uncertainty. However, it also has several limitations. Firstly, two downscaling methods, two hydrological model structures and two sets of hydrological model parameters are likely to be insufficient to represent their uncertainty envelope. In particular, using only two downscaling methods results in an underestimation of the true contribution of downscaling to uncertainty (Chen et al., 2011c). They also did not consider hydrological models with different levels of complexity and structure. The study did not consider the uncertainty due to the GCM initial conditions. As mentioned earlier, the uncertainty linked to GCM initial conditions is even larger than that of GCMs in some cases (Booij, 2005). Finally, since the purpose of this research was to provide a framework for assessing uncertainties in climate change impact studies, the only quantified variable was river low flows. Other hydrological variables such annual, seasonal and peak discharges may respond quite differently with respect to global uncertainty.

The objective of this research is to outline the contribution of six sources of uncertainty, with respect to the impacts of climate change on the hydrology of a Canadian river basin (Quebec province). The uncertainties considered include (1) six GCMs; (2) two GGES; (3) four

downscaling methods; (4) three hydrological model structures; (5) ten sets of hydrological model parameters; and (6) five GCM initial conditions. Future (2081-2100) hydrological regimes are compared to the reference period (1971-1990) using mean annual and seasonal discharges, annual low flow (95%), peak discharge, time to the beginning of flood, time to peak discharge and time to the end of flood as criteria.

8.3 Study area and data

8.3.1 Study area

This study was conducted over the Manicouagan 5 river basin, which is located in the center of Quebec province, Canada (figure 8.1). It is the biggest sub-basin of the Manicouagan watershed, which covers 24,610 km^2 of mostly forested areas. It has a rolling to moderately hilly topography with a maximum elevation of 952 m above sea level. The reservoir at the basin outlet has a mean level of 350 m above sea level. Population density is extremely low and logging is the only industrial activity over the basin. The basin drains into the Manicouagan 5 reservoir, a 2000 km^2 annular reservoir within an ancient eroded impact crater. The basin ends at the Daniel Johnson dam, which is the largest buttressed multiple arch dam in the world. The installed capacity of the dam is 2.6GW. The annual mean discharge of the Manicouagan 5 River is 529m^3/s. Snowmelt peak discharge usually occurs in May and averages 2200 m^3/s.

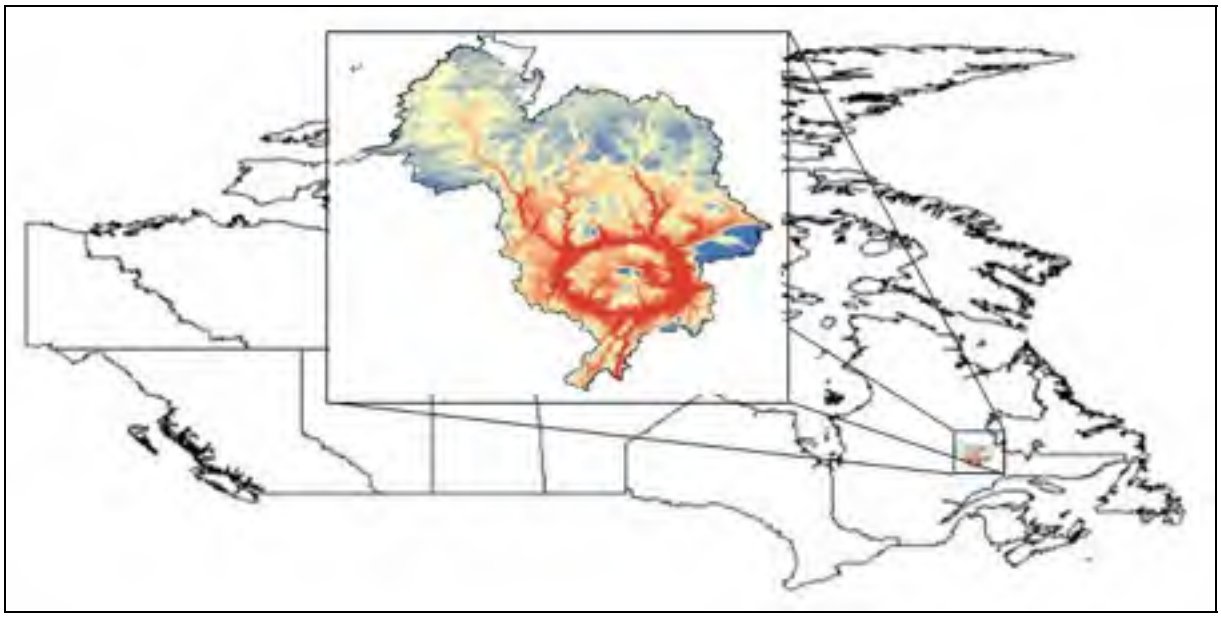

Figure 8.1 Location map of Manicouagan 5 river basin.

8.3.2 Data

Observed data consisted of precipitation, maximum temperature (Tmax) and minimum temperature (Tmin) interpolated on a 10km grid by the National Land and Water Information Service (www.agr.gc.ca/nlwis-snite). The interpolation is performed using a thin plate smoothing spline surface fitting method (Hutchinson et al., 2009). Discharge data at the basin outlet was obtained from mass balance calculations at the dam and was provided by Hydro-Quebec. Daily precipitation, Tmax and Tmin projected by six GCMs (CGCM3, CSIRO-Mk3.5, GFDL-CM2.0, MPI-ECHAM5, MIROC3.2-Medres and MRI-CGCM2.3) under two emission scenarios (A2, B1) from the Fourth Assessment Report (IPCC, 2007) were used. To investigate the uncertainty of GCM initial conditions, the daily precipitation, Tmax and Tmin, from five runs of MRI-CGCM2.3 under either A2 or B1 scenarios were also used. Table 8.1 presents the general information of the chosen GCMs. Since statistical downscaling requires GCM variables as predictors to calibrate the model and create future climate change projections, the National Center for Environmental Prediction (NCEP) reanalysis data interpolated to the Canadian GCM (CGCM3) grid was used to calibrate the

statistical method. In climate change mode, predictors from the CGCM3 under the A2 emission scenario were used directly. The atmospheric predictors considered (NCEP and CGCM3) are listed in table 8.2. This work covers the 1971 - 1990 period (reference period) for calibration and the 2081 - 2100 period (future horizon) in climate change mode.

Table 8.1 General information of selected GCMs

Acronym	**Country**	**Resolution**	**Scenario**	**Run**	**Number of grid points**
CGCM3	Canada	3.75° x 3.75°	A2, B1	Run1	4
CSIRO-Mk3.5	Australia	1.87° x 1.87°	A2, B1	Run1	10
GFDL-CM2.0	United States	2.0° x 2.5°	A2, B1	Run1	6
MPI-ECHAM5	Germany	1.87° x 1.87°	A2, B1	Run1	10
MIROC3.2-Medres	Japan	2.8° x 2.8°	A2, B1	Run1	6
MRI-CGCM2.3	Japan	2.8° x 2.8°	A2, B1	Run1-Run5	6

Table 8.2 NCEP and CGCM3 variables used to select precipitation predictors for the statistical downscaling model

Source	**Predictor**	**Predictor**
Surface variables	Mean sea level pressure	Temperature at 2m
Upper-air variables	East component of wind (500, 850 and 1000 hPa)	Vertical vorticity (500, 850 and 1000 hPa)
	North component of wind (500, 850 and 1000 hPa)	Divergence (500, 850 and 1000 hPa)
	Geopotential (500 and 850 hPa)	Wind direction (500, 850 and 1000 hPa)
	Specific humidity (500, 850 and 1000 hPa)	Wind speed (500, 850 and 1000 hPa)

Since Manicouagan 5 is a large watershed, several GCM grid points were selected to represent the climate of the river basin, using the following procedure. A 600km diameter circle was drawn around the center point of the watershed and all GCM grid points within the circle were chosen. By doing this, at least four grid points were selected for each GCM. Then, the average climate (precipitation and temperatures) over the river basin was calculated using the Inverse Distance Weighting method. The number of selected grid points for each GCM is presented in the last column of table 8.1.

8.4 Methodology

This research investigates the contributions of GCMs, GGES, GCM initial conditions, downscaling techniques, hydrological model structures and parameters to the global uncertainty of future hydrologic regimes. Each climate projection is equally weighted to predict the hydrology on the Manicouagan 5 watershed for the 2081-2100 horizon. Figure 8.2 presents the framework of the considered uncertainty cascade.

8.4.1 GCM, GGES and GCM initial conditions

Six GCMs under two emission scenarios were selected to investigate the uncertainty of hydrological impacts under climate change (table 8.1). They are a subset of the climate models and emission scenarios that contributed to the IPCC Fourth Assessment Report (IPCC, 2007). The six GCMs were selected to cover most of the uncertainty displayed on a mean yearly precipitation-temperature dispersion diagram. According to IPCC (2007), A2 describes a very heterogeneous world with high population, slow economic development and slow technological change; B1 describes a convergent world with global population peaking during the mid-century and with very rapid changes in economic structures towards a service and information economy. These two scenarios are two extremes of greenhouse gas emissions. Thus, they represent a large range of uncertainty.

There are two methods with which to consider the uncertainty related to the internal variability of a climate system. The first is a climate model-based approach that consists of

running an ensemble of simulations using different initial conditions, with subsequent identical forcing (Kay et al, 2009). The other method is to use a stochastic weather generator to produce an ensemble of climate projections. The former approach was used in this study with five runs of MRI-CGCM2.3 under either A2 or B1 scenarios. Due to the limitation of the available climate data, only one simulation run (run 1) was used for the other five GCMs.

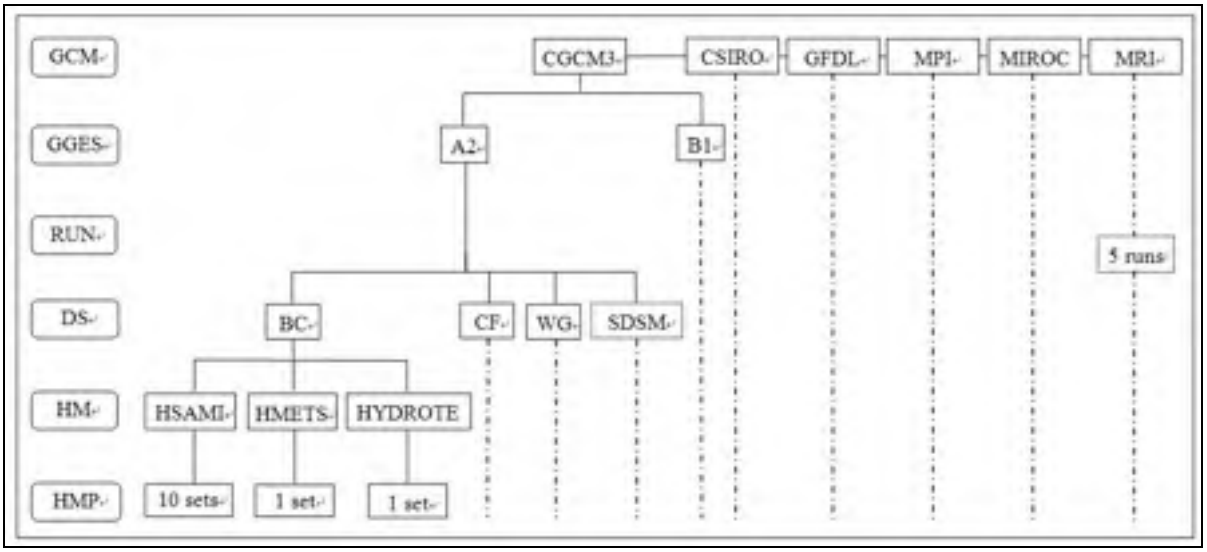

Figure 8.2 A framework of the uncertainty cascade considered; a vertical dashed line indicates that the flow chart under its linked text box is identical to the previous one. Ensemble runs were only available for MRI, and SDSM was used with CGCM3 predictors only. GCM = Global Circulation Models; GGES = Greenhouse gas emission scenarios; DS=downscaling methods; HM = hydrological model; HMP = hydrological model parameters; BC = bias correction, CF = change factor; and WG = weather generated based method.

8.4.2 Downscaling techniques

Four downscaling methods were used to downscale GCM outputs to watershed scale in this study. These include bias correction, the change factor method (CF), a weather generator (WG) based method and the SDSM. Each approach is detailed below.

8.4.2.1 Bias correction method

In this method, a monthly bias correction is applied to both temperature and precipitation data. For precipitation, a correction is made to both monthly mean frequency and quantity, using the Local Intensity Scaling Method developed by Schmidli et al. (2006). This method contains three steps: (1) A wet-day threshold is determined from the daily GCM precipitation series of each month such that the threshold exceedence matches the wet-day frequency of the observed time series; (2) A scaling factor is calculated to insure that the mean of the observed monthly precipitation is equal to that of the GCM precipitation multiplied by the scaling factor for the reference period; and (3) The monthly thresholds and factors determined in the reference climate are used to adjust monthly precipitation for the future horizon.

Daily GCM temperatures are corrected on a monthly basis using the following equation (Chen et al. 2011c):

$$T_{cor,fut} = T_{GCM,fut} + (\overline{T}_{obs} - \overline{T}_{GCM,ref}) \tag{8.1}$$

where $T_{cor,fut}$ is the daily corrected temperature at future horizon (2081-2100) obtained by adding the difference in mean monthly temperatures between observed data and the GCM reference period ($\overline{T}_{obs} - \overline{T}_{GCM,ref}$) to the GCM temperature data for the future horizon ($T_{GCM,fut}$). After the monthly mean correction is done, the standard deviation of monthly temperatures '*S'* at the future horizon is corrected using the following equation:

$$S_{cor,fut} = S_{GCM,fut} \times (S_{obs} / S_{GCM,ref}) \tag{8.2}$$

Equation (8.2) effectively corrects the standard deviation of GCM temperatures based on the standard deviation ratio between observed and GCM temperatures over the reference period

(subscripts are the same as those defined for equation (8.1)). In a last step, downscaled temperatures at the daily scale for the future horizon are obtained by adjusting temperatures obtained in step 1 to the standard deviation calculated in step 2. This is done by normalizing the step 1 temperatures to a zero mean and standard deviation of one, and transforming back to the step 2 standard deviation. This technique assumes that biases are time-invariant, and ensures that the temperatures of the GCM over the reference period have the same monthly mean and standard deviation as those of the observed data. .

8.4.2.2 Change factor (CF) method

The CF method involves adjusting the observed daily temperature ($T_{obs,d}$) by adding the difference in monthly temperature between the future horizon and the reference period predicted by the GCM ($\overline{T}_{GCM,fut,m} - \overline{T}_{GCM,ref,m}$) to obtain the daily temperature at the future horizon ($T_{adj,fut,d}$) (equation (8.3)) (Chen et al., 2011c). The adjusted daily precipitation for the future horizon ($P_{adj,fut,d}$) is obtained by multiplying the precipitation ratio ($\overline{P}_{GCM,fut,m} / \overline{P}_{GCM,ref,m}$) by the observed daily precipitation ($P_{obs,d}$) (equation (8.4)).

$$T_{adj,fut,d} = T_{obs,d} + (\overline{T}_{GCM,fut,m} - \overline{T}_{GCM,ref,m}) \tag{8.3}$$

$$P_{adj,fut,d} = P_{obs,d} \times (\overline{P}_{GCM,fut,m} / \overline{P}_{GCM,ref,m}) \tag{8.4}$$

8.4.2.3 Weather generator (WG) based method

The WG used in this research is CLIGEN (Nicks and Lane, 1989), which was used to generate daily precipitation occurrence and amounts, as well as Tmax and Tmin. CLIGEN was chosen because it generates precipitation and temperature independently, and the mean and standard deviation of each variable are explicitly used in its probability distribution function, so that the incorporation of GCM projected monthly changes in statistical moments

is straightforward (Zhang, 2005; Chen et al. 2009). However, other weather generators could also have been used.

In CLIGEN, a first-order two-state Markov chain is used to generate the occurrence of wet or dry days. The probability of precipitation on a given day is based on the wet or dry status of the previous day, which can be defined in terms of the two transition probabilities: a wet day following a dry day (P01) and a wet day following a wet day (P11). For a predicted wet day, a three-parameter skewed normal Pearson III distribution was used to generate daily precipitation intensity for each month (Nicks and Lane, 1989).

A normal distribution was used to simulate Tmax and Tmin. The temperature with the smaller standard deviation between Tmax and Tmin is computed first, followed by the other temperature (Chen, et al, 2008). The mean and standard deviation of Tmax and Tmin were calculated monthly and smoothed with Fourier interpolation to a daily scale.

CLIGEN requires a total of nine monthly parameters to the generate precipitation, Tmax and Tmin. These include p01 and p11 for generating precipitation occurrence, mean, standard deviation and skewness for generating daily precipitation intensity and mean and standard deviations of Tmax and Tmin. The skewness of precipitation is assumed to be unchanged in the future for this research. Thus, there are eight parameters that require modification at every future climate change scenario.

The parameters are modified to take into account the variations predicted by a GCM (Chen et al. 2011c). This variation is based on a CF approach that has the following steps:

1) Similarly to the CF method, the adjusted monthly mean Tmax and Tmin for the future horizon ($\overline{T}_{adj,fut}$) are estimated as:

$$\overline{T}_{adj,fut} = \overline{T}_{obs} + (\overline{T}_{GCM,fut} - \overline{T}_{GCM,ref}) \quad (8.5)$$

The adjusted values are obtained by adding the differences predicted by a GCM between the future horizon and the reference period $(\overline{T}_{GCM,fut} - \overline{T}_{GCM,ref})$ to the observed mean monthly observed temperatures $(\overline{T}_{obs})$.

2) Monthly means and variances of precipitation, monthly variances of Tmax and Tmin and transition probabilities of precipitation occurrence p01 and p11 for the future horizon are adjusted by:

$$X_{adj,fut} = X_{obs} \times (X_{GCM,fut} / X_{GCM,ref}) \tag{8.6}$$

where X represents the variable to be adjusted. The subscripts are the same as above.

3) The p01 and p11 values are expressed in terms of an unconditional probability of daily precipitation occurrence (π) and the lag-1 autocorrelation of daily precipitation (r) for further adjustments.

$$\pi = \frac{P_{01}}{1 + P_{01} + P_{11}} \tag{8.7}$$

$$r = P_{11} - P_{01} \tag{8.8}$$

4) The adjusted mean daily precipitation per wet day (u_d) is estimated as (Wilks, 1999a; Zhang, 2005):

$$\mu_d = \frac{\mu_m}{N_d \pi} \tag{8.9}$$

where N_d is the number of days in a month, $N_d \pi$ is the average number of wet days in a month, and u_m is the step (2)-adjusted monthly precipitation.

5) The adjusted daily variance (σ_d^2) is approximated using equation (8.10), based on the step (2)-adjusted variance of the monthly precipitation (σ_m^2) (Wilks, 1999a).

$$\sigma_d^2 = \frac{\sigma_m^2}{N_d \pi} - \frac{(1-\pi)(1+r)}{1-r}\mu_d^2 \tag{8.10}$$

All of the adjusted precipitation, Tmax and Tmin parameter values were input to CLIGEN to generate 600 years of daily time series (Thirty 20-year realizations).

8.4.2.4 Statistical downscaling model (SDSM)

The SDSM is a downscaling tool that can be used to develop climate change scenarios (Wilby et al., 2002a). It uses a conditional process to downscale precipitation. Local precipitation amounts depend on wet-/dry-day occurrences, which in turn depend on regional-scale predictors such as mean sea level pressure, specific humidity and geopotential height (Wilby et al. 1999; Wilby and Dawson 2007). Specifically, downscaling of precipitation occurrence is achieved by linking daily probabilities of non-zero precipitation with large-scale predictor variables.

The main procedures of the SDSM for downscaling wet day precipitation intensity, Tmax and Tmin (predictands) are the following: (1) Identification of the screen variable: a partial correlation analysis was used to identify the relationship between NCEP variables (table 8.2) and predictands (precipitation, Tmax and Tmin). Variables that were significantly correlated to predictands were then selected as predictors; (2) Model calibration: multiple linear regressive equations were established between predictands and step (1)-identified predictors for each season. Since the distribution of the daily precipitation is highly skewed, a fourth root transformation was applied to the original precipitation before fitting the transfer function (Wilby and Dawson, 2007); and (3) Application of transfer functions: established transfer functions were further used to downscale precipitation amounts, Tmax and Tmin for the future horizon.

The SDSM bias correction was applied to insure that observed and downscaled precipitation totals were equal for the simulation period. A variance inflation scheme was also used, to increase the variance of precipitation and temperatures to better agree with observations. When using bias correction and variance inflation, a SDSM essentially becomes a WG, in which a stochastic component is superimposed on top of the downscaled variable. This is especially true for precipitation, where the explained variance is generally less than 30% (Wilby et al, 1999). Since a large number of variables are required to use an SDSM, only CGCM3 under A2 emission scenario was used with this downscaling method.

8.4.3 Hydrological model structures and parameters

Two lumped conceptual models and one physically-based distributed model were used to investigate the contributions of model structure and choice of model parameters to the global uncertainty.

8.4.3.1 Hydrological model structures

1) HSAMI model :

HSAMI is a lumped conceptual rainfall-runoff model developed by Hydro-Québec and which has been used to forecast natural inflows for over 20 years (Fortin, 2000). It is used by Hydro-Québec for hourly and daily forecasting of natural inflows on 84 watersheds with surface areas ranging from 160 km^2 to 69,195 km^2. Hydro-Québec's total installed hydropower capacity on these basins exceeds 40GW. HSAMI has up to 23 model parameters. Two parameters account for evapotranspiration, six for snowmelt, ten for vertical water movement, and five for horizontal water movement. Vertical flows are simulated with four interconnected linear reservoirs (snow on the ground, surface water, unsaturated and saturated zones). Horizontal flows are filtered through two hydrograms and one linear reservoir. Model calibration is done automatically using the shuffled complex evolution

optimization algorithm (SCE-UA) (Duan, 2003). The model accounts for snow accumulation, snowmelt, soil freezing/thawing and evapotranspiration.
The basin-averaged minimum required daily input data for HSAMI are: Tmax, Tmin, liquid and solid precipitations. Cloud cover fraction and snow water equivalent can also be used as inputs, if available. A natural inflow or discharge time series is also needed for proper calibration/validation. The optimal combination of parameters was chosen based on Nash-Sutcliffe criteria.

2) HMETS model:

HMETS is a lumped conceptual rainfall-runoff model developed at the Ecole de Technologie Supérieure (Brissette, 2010). It is a MATLAB-based freeware, and has up to 20 free parameters: ten parameters for snowmelt, one for evapotranspiration, four for infiltration and five for upper and lower soil reservoirs. Similarly to HSAMI, model calibration is done automatically using the SCE-UA (Duan, 2003), and as with the HSAMI, it accounts for snow accumulation, snowmelt, soil freezing/thawing and evapotranspiration.

The basin-averaged minimum required daily input data for HMETS are: Tmax, Tmin, liquid and solid precipitations or total precipitation. A natural inflow or discharge time series is needed for proper calibration/validation. The optimal combination of parameters was chosen based on Nash-Sutcliffe criteria.

3) HYDROTEL model:

The HYDROTEL model is a spatially-distributed and physically-based simulation tool developed by a research team from the Institut National de la Recherche Scientifique in Quebec City, Canada (Fortin et al. 2001). It has been applied to several watersheds located in the province of Quebec and in other countries such as southern France (Fortin et al. 1995; Fortin et al. 2007). Currently, it is used operationally by the Centre d'expertise hydrique du Québec for flow forecasting in the context of river and reservoir management.

To run this model, a given watershed must first be divided into several simulation units (or elementary subwatersheds) called relatively homogeneous hydrological units (RHHUs). The number of RHHU subdivisions on a given river basin depends on the hydrological network's discretization specified by the user. Each RHHU comprises a river reach, may include various land occupations and is assumed to be characterized by a single soil type. The simulation process is based on five sub-models: (1) snowpack accumulation and melting, (2) potential evapotranspitation (PET), (3) vertical water budget in the subsurface, unsaturated and saturated zones, (4) flow on sub-watersheds, and (5) channel flow in river reaches. Simulations can be executed at a daily or sub-daily time step. In this study, simulations were run on a daily basis. To reduce the calibration time, only the twelve most sensitive parameters out of 26 were calibrated automatically using the SCE-UA (Duan, 2003). The remaining parameters were set to fixed values according to the results of previous studies (Turcotte et al., 2007).

The required meteorological inputs are daily precipitation, Tmax and Tmin (see section 2.2). To simplify the comparison with the other two lumped conceptual models, the time series of precipitation and temperatures for the future period were aggregated and used as a lumped input, instead of using spatially distributed data to run the model.

8.4.3.2 Hydrological model parameters

To analyze the parameter space uncertainty, HSAMI was automatically calibrated ten times using the SCE-UA. In each calibration, the SCE-UA method looks for an optimal parameter set within a bounded parameter space, based on maximization of the Nash-Sutcliffe efficiency criterion. All 23 parameters were invariably considered in each calibration. Twenty years (1971-1990) of daily discharge was used for model calibration and 10 year of data (1991-2000) was used for validation. The optimal combination of parameters was selected, based on Nash-Sutcliffe criteria. This set of parameters yielded Nash-Sutcliffe criteria values of 0.90 for calibration and 0.85 for validation. These high values for Nash-

Sutcliffe criteria are representative of the good quality of weather inputs and observed discharge for the Manicouagan 5 river basin.

Since a previous study showed that the calibration of a hydrological model contributes small uncertainty on hydrological impacts of climate change (Poulin et al., 2011), only HSAMI was used to investigate parameter space uncertainty. Both HMETS and HYDROTEL were only calibrated once. The daily discharge from 1971-1990 was used to calibrate HMETS and the data from 1991-2000 was used for validation with Nash-Sutcliffe values of 0.85 for calibration and 0.73 for validation. Since HYDROTEL calibration is time-consuming, even when using a multi-processor computer (64-bit system with four 2.94-GHz processors), only ten years of daily discharge data (1979-1988) with a mean annual discharge similar to that of the 20-year time series (1971-1990) was used for calibration with a Nash-Sutcliffe value of 0.85. The other ten years of data (1989-1998) with a mean annual discharge similar to that of the calibration time series (1979-1988) was used for validation with a Nash-Sutcliffe value of 0.75.

8.4.4 Statistical analysis

The annual hydrographs were calculated from all daily discharge time series simulated by the three hydrological models. They were further grouped into six uncertainty sources. For example, to investigate the uncertainty linked to GCMs, hydrographs were grouped by GCMs (six GCMs), each group including hydrographs from two emission scenarios, three downscaling methods and three hydrological models. To ensure that each projection was weighted equally, projections involving hydrological model parameters and downscaling SDSM were not included. The combination and sample size of each group for each source of uncertainty are presented in table 8.3.

The mean annual hydrograph was calculated for each group. For example, eighteen hydrographs were averaged for each GCM. Nine hydrological parameters (table 8.4) were then calculated as criteria to investigate each source of uncertainty. Time to the beginning

and to the end of flood (Criteria 7 and 9) is determined by the following procedures: (1) A cumulative hydrograph is calculated based on the mean annual hydrograph. (2) Four breakpoints of the cumulative mean hydrograph are then determined insuring that the Root-Mean-Square error between the cumulative mean hydrograph and a straight line approximation (5 lines) is minimized. The time to the first breakpoint is the beginning of spring flood, and the time to the second is the end of flood.

Table 8.3 The combination and sample size of each group for each source of uncertainty

ID	Source	Group size	Combination of each group	Sample size of each group
1	GCM	6	2 (GGES) × 3 (DS)×3 (HM)	18
2	GGES	2	6 (GCM) × 3 (DS)×3 (HM)	54
3	GCM initial conditions	5	2 (GGES) × 3 (DS)×3 (HM)	18
4	Downscaling method (DS)	4*	6 (GCM) × 2 (GGES)×3 (HM)	36
5	Hydrological model (HM)	3	6 (GCM) × 2 (GGES)×3 (DS)	36
6	Hydrological model parameters	10	6 (GCM) × 2 (GGES)×3 (DS)	36

*SDSM is only used to investigate downscaling uncertainty, since only CGCM3 under A2 emission scenario was used with this method.

Table 8.4 Nine criteria used to investigate each source of uncertainty

ID	Criterion	ID	Criterion	ID	Criterion
1	Annual mean discharge	4	Winter (DJFM) mean discharge	7	Time to the beginning of flood
2	Spring (AMJ) mean discharge	5	95% low flow dishcang	8	Time to peak discharge
3	Summer-autumn (JASON) mean discharge	6	Magnitude of peak discharge	9	Time to the end of flood

A paired t-test was performed for each combination of uncertainty sources to assess its contribution in predicting mean annual and seasonal (spring, summer-autumn and winter) discharges. For example, for the assessment of GCM uncertainty, the paired t-test was conducted by emission scenarios, downscaling methods and hydrological models (n=18). Furthermore, annual and seasonal discharges of the future horizon (2081-2100) were tested against the discharges at the reference period (1971-1990) for significant changes, using a t-test. The significance level used in this research is P=0.05 -- referring to a Type 1 error. The larger the P value, the more likely two populations are similar, and vice versa.

The statistical tests could not be conducted for the other five chosen criteria (ID 5-9, table 8.4), because the mean value of each criteria is different when computing from the mean hydrograph versus averaging the criteria obtained from each individual hydrograph within a group. For example, if the peak discharges from two hydrographs are 2000 m^3/s and 3000 m^3/s, when the two hydrographs are averaged, the peak discharge will necessarily be smaller than 2500 m^3/s, unless the peak discharge of each hydrograph occurs on the exact same day.

8.5 Results

8.5.1 Validation of downscaling methods and hydrological models

The validation of each hydrological model was based on the quality of the simulated mean hydrographs at the basin outlet, when compared to the observed mean hydrograph. Mean hydrograph results are presented in figure 8.3. Mean hydrographs simulated by HSAMI using input data from the CLIGEN (labeled CLIGEN-SIM) and from the SDSM (labeled SDSM-SIM) at the reference period are also displayed. These two curves are an indirect validation of the ability of CLIGEN and SDSM to produce unbiased estimates of precipitation and temperatures. The mean hydrograph from observed discharge (labeled OBS) is also presented for comparison. Overall results are very good, although small biases were introduced by the hydrological models, especially HYDROTEL, which somewhat overestimated late summer and autumn streamflows. The results indicate that all three hydrological models perform

well, and that CLIGEN and SDSM generate precipitation and temperature data of excellent quality.

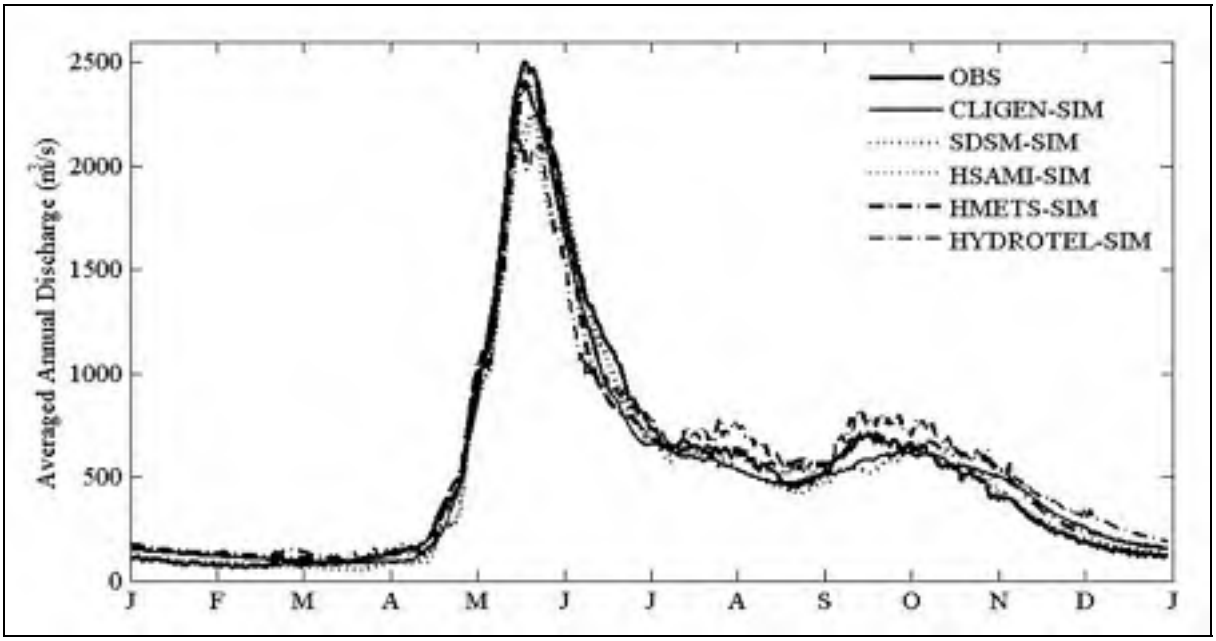

Figure 8.3 Observed (OBS) and modeled averaged hydrographs for the reference period (1971-1990) for the 'Manicouagan 5' watershed. The simulated hydrographs include HSAMI modeled using CLIGEN (CLIGEN-SIM) and SDSM (SDSM-SIM) generated input data, as well as simulations with HSAMI, HMETS and HYDROTEL models using observed meteorological data for the reference period (HSAMI-SIM, HMETS-SIM and HYDROTEL-SIM).

8.5.2 Climate change projections

The seasonal (spring, summer-autumn and winter) and annual changes of precipitation (ratio) and mean temperature (difference) are plotted by GCMs, GGES, GCM initial conditions and downscaling techniques in figure 8.4 to illustrate each source of uncertainty. Climate projections from the same source are first grouped and then averaged to a mean climate projection. For example, eighteen hydrographs were averaged for each GCM for assessing the GCM uncertainty.

All of the GCMs, GGES, GCM initial conditions and downscaling techniques suggest increases in seasonal and annual precipitations and mean temperatures for the 2081-2100 horizon. GCMs and GGES are the major contributors to uncertainty, although GCM initial conditions and downscaling techniques can be important depending on the season. Figure 8.4 shows that the MIROC3 model contributes significantly to the uncertainty envelope, particularly with respect to temperature. The uncertainty related to GCMs is larger than that linked to GGES, even though two emission scenarios are compared to six GCMs, because these two scenarios represent two extremes of greenhouse gas emissions. The uncertainty linked to the GCM initial conditions is much smaller than for GCMs and GGES, with the exception of spring precipitation.

Downscaling method uncertainty proved to be the least important in predicting precipitation and mean temperature. The CF, WG and bias correction methods are similar in downscaling quantities of precipitation and temperature. Thus, they suggest very similar changes in both mean precipitation and temperature, as shown in figure 8.4. However, since the WG and bias correction methods modify precipitation occurrence, and the CF method does not, these three methods may result in different hydrologic responses. The SDSM predicts larger increases in annual average temperatures, with the exception of the spring season.

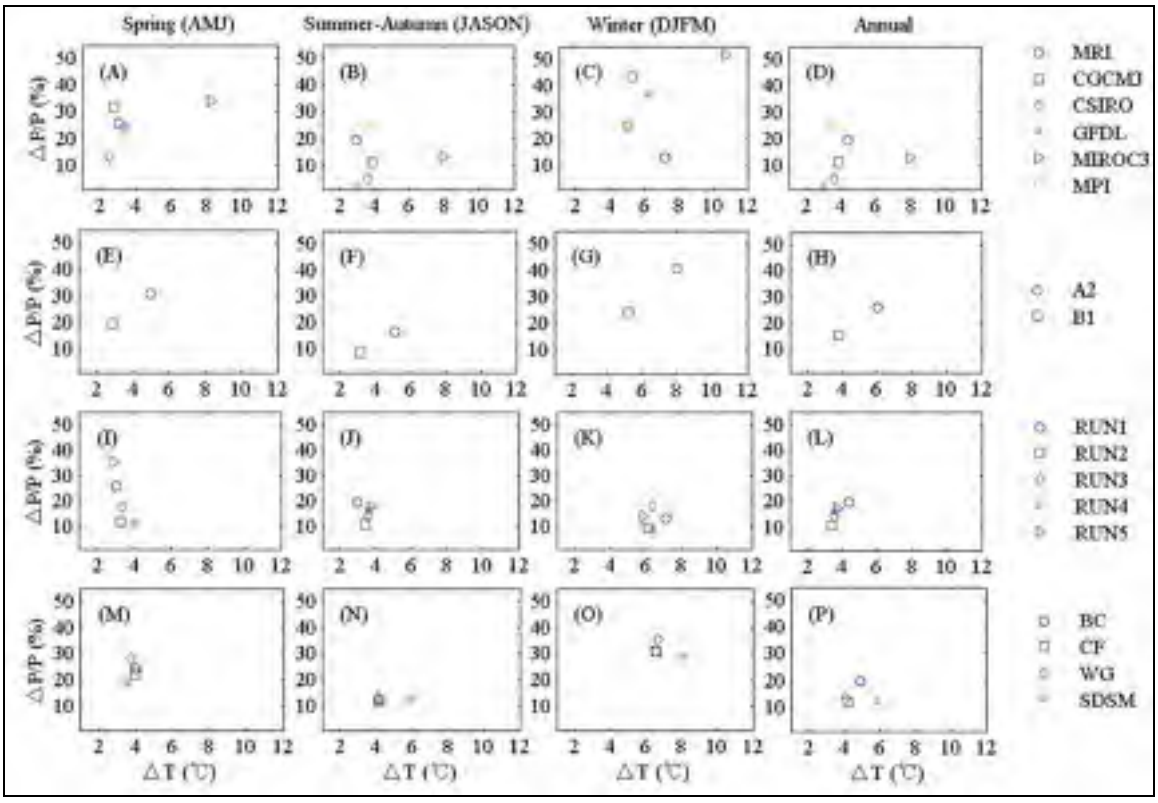

Figure 8.4 Scatter plots of seasonal and annual changes of mean temperature and precipitation for GCMs, GGES, GCM initial conditions and downscaling techniques at the 2081-2100 horizon.

8.5.3 Hydrological impacts

Figure 8.5 presents future average hydrographs simulated by three hydrological models using downscaled climate projections from GCMs, GGES and GCM initial conditions. The mean annual hydrographs are plotted through averaging hydrological projections by the different sources, respectively. The annual mean hydrograph for the reference period (1971-1990) is also plotted for comparison. To avoid any bias resulting from the hydrological modeling process, the hydrograph for the reference period is represented by the average of the simulations of the three hydrological models chosen for the reference period, and not by observations. The results show streamflow increases during winter (November - April) and a decrease in summer (June - October) in most cases. The snowmelt peak discharges are lower than those of the reference period, with the exception of those predicted by the GFDL and

MPI models (figure 8.5a), and from the models downscaled with the WG-based method (figure 8.5d). These observations are consistent with other Nordic watershed studies, and testify to more frequent winter snowmelt episodes and lessened snowpack due to increasing temperatures. For all hydrographs, peak discharges for the future horizon are observed earlier than for the reference period. Lags vary from 8 to 25 days. The uncertainty related to GCM structure is the largest, but all other sources (with the exception of hydrological model parameters) also contribute to large uncertainties. For example, downscaling methods have a comparable uncertainty to GCMs in predicting spring discharges. The MIROC3 model (figure 8.5a) and the SDSM method (figure 8.5d) contribute the largest parts to GCM and downscaling uncertainty, respectively. In order to look at uncertainty in more detail, the global uncertainty of hydrological impacts under climate change is further compared using the nine criteria mentioned earlier.

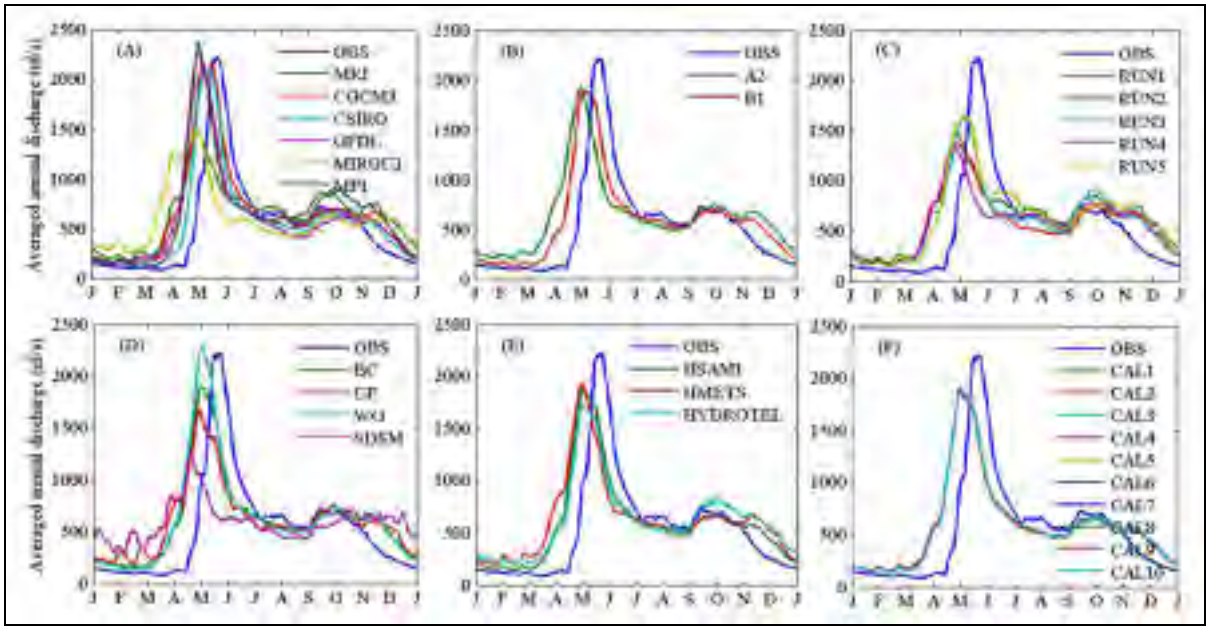

Figure 8.5 Average annual hydrographs for the future (2081-2100) and reference (1971-1990) periods at the Manicouagan 5 river basin. OBS = observed data simulated discharge; CAL1-CAL2 = the set of hydrological model parameters; A=GCMs; B=GGES; C=initial conditions; D=Downscaling methods; E=Hydrology models and F=Hydrology model parameters.

8.5.3.1 The uncertainty of a climate model structure

The relative changes in values between the future and reference periods ((Fut-Ref) / Ref × 100%) for the simulated values of the nine criteria of table 8.4 are presented in table 8.5. All GCMs suggest a statistically significant increase in annual discharge ranging between 5.7% (CSIRO) and 21.7% (MPI) at the P=0.05 level for the 2081-2100 horizon. The paired t-tests show that six GCMs are significantly classified into four groups at P=0.05. Within each group, there is no significant difference among mean annual discharges. Two climate models (MIROC3 and MRI) suggest decreases in spring (AMJ) discharges, but the results are not statistically significant. The response for summer-autumn (JASON) discharge is not clear (three models predict increases and three suggest decreases), but all six GCMs predict statistically significant increases in winter (DJFM) discharge. All GCMs suggest an increase in low flow, ranging between 34.0% (CSIRO) and 199.1% (MIROC3), but the peak discharge has a different pattern. Two GCMs predict slight increases while four GCMs suggest decreases with two models (MIROC3 and MRI) largely contributing to the uncertainty. All GCMs suggest earlier flood season and peak discharge. The end of flood would also come earlier. Specifically, the flood season would move earlier, from 12 days up to 42 days earlier, but the end of flood would be earlier by only 6 to 22 days, indicating that the flood season would be longer.

8.5.3.2 Uncertainty of greenhouse gas emission scenarios

Table 8.6 presents results with respect to GGES. Future changes in discharge are statistically significant. The paired t-tests show that the annual and seasonal discharges predicted by the A2 scenario are consistently greater than those suggested by the B1 scenario. Similarly to the results observed for GCMs, the time to the beginning of flood, time to peak discharge and time to the end of flood for the 2081-2100 horizon are observed earlier than for the reference period, and the flood season will be longer.

Table 8.5 Statistics of simulated discharge for the reference period (1971-1990) and relative changes ((Fut-Ref) / Ref × 100%) between the future (2081-2100) and reference periods

Criterion ID	1	2	3	4	5	6	7	8	9
Reference	543.4	1025.6	579.8	134.8	97.7	2220.8	1 May	24 May	13 Jun
CGCM3	21.4*a	24.2*a	5.6*a	91.7*a	78.2	-2.7	11 Apr (20)	16 May (8)	7 Jun (6)
CSIRO	5.7*b	8.1*b	-2.6b	37.5*b	34.0	-5.3	19 Apr (12)	11 May (13)	3 Jun (10)
GFDL	11.0*c	18.6*a	-7.9*c	70.2*c	68.4	2.6	9 Apr (22)	1 May (23)	31 May (13)
MIROC3	11.9*d	-6.2c	-8.7*c	227.6*d	199.1	-33.1	20 Mar (42)	29 Apr (25)	22 May (22)
MPI	21.7*a	13.7*d	22.1*d	64.4*c	45.9	7.2	13 Apr (18)	1 May (23)	25 May (19)
MRI	19.4*a	-2.6c	20.8*d	137.3*e	97.7	-33.9	1 Apr (30)	30 Apr (24)	31 May (13)

* denotes a significant difference of modeled discharges between the future and reference periods at the P=0.05 level. Data from two emission scenarios, three downscaling methods and three hydrological models (n=18) for each GCM were tested against the mean discharge at the reference period using a t-test. Different letters in each column indicate a statistically significant difference (P=0.05) for a paired t-test.

The last three statistics are the Julian days of average time of occurrence rather than relative changes; the number in parenthesis indicates how much earlier the occurrence is (in days) when compared to the reference period.

8.5.3.3 Uncertainty of GCM initial conditions

Ensemble runs are only available for the MRI model. Ensemble runs result from running the same GCM with different initial conditions. These runs represent a natural variability as seen by a climate model. Five runs of MRI under either A2 or B1 scenarios were downscaled by three methods (bias correction, CF and WG-based methods) to obtained climate projections. Hydrographs simulated by three hydrological models are then averaged. The results show

that all ensemble runs suggest statistically significant (P=0.05) increases in annual discharge between 5.7% and 19.8% (table 8.7). Four runs suggest a decrease in spring discharge while one predicts an increase. The paired t-tests show that there are significant differences among all the runs, except for the spring discharges between run1 and run3. All runs show statistically significant increases in summer-autumn and winter discharges, which are classified into three groups by paired t-tests at the P=0.05 level. Compared to the reference period, low flows would increase by 77.1% to 110.8% while peak discharges would decrease by 25.5% to 40.2%. Run1 contributes largely to low flow uncertainty. In addition, all runs suggest an earlier snowmelt, shorter time to peak discharge, and a longer flood season. The changing range of the time to the end flood (4 to 22 days) was greater than that of the time to the beginning of flood (23 to 32 days).

Table 8.6 Statistics of simulated discharge for the reference period (1971-1990) and relative changes ((Fut-Ref) / Ref × 100%) between the future (2081-2100) and the reference periods

Criterion ID	**1**	**2**	**3**	**4**	**5**	**6**	**7**	**8**	**9**
Reference	543.4	1025.6	579.8	134.8	97.7	2220.8	1 May	24 May	13 Jun
A2	19.5*a	9.6*a	6.6*a	146.9*a	128.3	-12.5	2 Apr (29)	1 May (23)	29 May (15)
B1	7.9*b	9.0*b	3.2*b	62.7*b	55.8	-14.8	14 Apr (17)	9 May (15)	3 Jun (10)

* denotes a significant difference of modeled discharges between the future and reference periods at the P=0.05 level. Data from six GCMS, three downscaling methods and three hydrological models (n=54) for each GGES were tested against the mean discharge at the reference period using a t-test. Different letters in each column indicate a statistically significant difference (P=0.05) for a paired t-test.

The last three statistics are the Julian days of average time of occurrence rather than relative changes; the number in parenthesis indicates how much earlier the occurrence is (in days) when compared to the reference period.

Table 8.7 Statistics of simulated discharge for the reference period (1971-1990) and relative changes ((Fut-Ref) / Ref × 100%) between the future (2081-2100) and the reference periods

Criterion ID	**1**	**2**	**3**	**4**	**5**	**6**	**7**	**8**	**9**
Reference	543.4	1025.6	579.8	134.8	97.7	2220.8	1 May	24 May	13 Jun
RUN1	19.5*a	-2.6a	21.3*a	136.5*a	110.8	-33.8	1 Apr (30)	30 Apr (24)	31 May (13)
RUN2	5.7*b	-8.1*b	2.4b	102.1*b	74.2	-38.3	30 Mar (32)	30 Apr (24)	5 Jun (8)
RUN3	13.6*c	-1.5a	13.0*c	103.4*b	76.7	-25.5	6 Apr (25)	9 May (15)	2 Jun (11)
RUN4	9.0*d	-14.1*c	13.8*c	114.9*c	87.0	-40.2	30 Mar (32)	26 Apr (28)	22 May (22)
RUN5	19.8*a	6.3d	19.0*a	101.6*b	77.1	-26.5	8 Apr (23)	13 May (11)	9 Jun (4)

* denotes significant difference of modeled discharges between future and reference period at the P=0.05 level. Data from 2 GGES, three downscaling methods and three hydrological models (n=18) for each run were tested against the mean discharge at the reference period using a t-test. Different letters in each column indicate a statistically significant difference (P=0.05) for a paired t-test.

The last three statistics are the Julian days of average time of occurrence rather than relative changes; the number in parenthesis indicates how earlier the occurrence is (in days) when compared to the reference period, Mar=March, Apr=April and Jun=June.

8.5.3.4 Uncertainty of downscaling techniques

Compared to the reference period, the average annual discharge for the 2081-2100 horizon shows a statistically significant increase (9.0% to 17.1%) for every downscaling method ($P<0.05$) (table 8.8). Moreover, the paired t-tests show significant differences between each paired group. The bias correction and WG-based methods predict a statistically significant increase in spring discharge while the SDSM predicts a sharp decrease. All of the downscaling methods suggest statistically significant increases in summer-autumn and winter

discharges, and increases in low flow. The SDSM predicts the largest increase in winter temperatures, resulting in the largest increase in winter discharge and the largest decrease in peak flood discharge. Similarly to other uncertainty sources, the time to the beginning and the end of flood, and the time to peak discharge would be earlier and the flood season would last longer.

Table 8.8 Statistics of simulated discharge for the reference period (1971-1990) and relative changes ((Fut-Ref) / Ref × 100%) between the future (2081-2100) and the reference periods

Criterion ID	**1**	**2**	**3**	**4**	**5**	**6**	**7**	**8**	**9**
Reference	543.4	1025.6	579.8	134.8	97.7	2220.8	1 May	24 May	13 Jun
BC	14.4*a	9.8*a	5.2*a	90.3*a	78.8	-14.4	10 Apr (21)	2 May (22)	2 Jun (11)
CF	13.0*b	0.8b	2.1*b	141.9*b	123.1	-24.4	3 Apr (28)	1 May (23)	3 Jun (10)
WG	17.1*c	19.5*c	3.1*c	79.9*c	54.5	3.0	9 Apr (22)	5 May (19)	31 May (13)
SDSM	9.0	-23.2	-3.4	260.4	252.3	-44.1	25 Mar (37)	20 Apr (34)	27 May (17)

* denotes a significant difference of modeled discharges between the future and the reference periods at the P=0.05 level. Data from six GCMS, two GGES and three hydrological models (n=36) for bias correction (BC), CF and WG-based downscaling methods were tested against the mean discharge at the reference period using a t-test. The results of the SDSM were not included. Different letters in each column indicate a statistically significant difference (P=0.05) for a paired t-test.

The last three statistics are the Julian days of average time of occurrence rather than relative changes; the number in parenthesis indicates how much earlier the occurrence is (in days) when compared to the reference period.

8.5.3.5 Uncertainty of hydrological model structure

All hydrological models suggest statistically significant increases in annual (9.7% to 17.1%) and winter discharge (69.9% to 136.6%), respectively, at the P=0.05 level (table 8.9). The

paired t-tests show significant differences between the hydrological models in predicting annual, summer-autumn and winter discharge. There are no consistent differences between the two lumped models and the distributed physically-based model. Overall the trends are the same as previously discussed.

Table 8.9 Statistics of simulated discharge for the reference period (1971-1990) and relative changes ((Fut-Ref) / Ref × 100%) between the future (2081-2100) and the reference periods

Criterion ID	**1**	**2**	**3**	**4**	**5**	**6**	**7**	**8**	**9**
Reference	543.4	1025.6	579.8	134.8	97.7	2220.8	1 May	24 May	13 Jun
HSAMI	9.7 *a	11.0*a	-2.7a	69.9*a	58.2	-14.8	10 Apr (21)	2 May (22)	5 Jun (8)
HMETS	17.1*b	9.9*a	2.7b	136.6*b	119.3	-12.8	3 Apr (28)	2 May (22)	30 May (14)
HYDROTEL	15.4*c	2.3b	9.6*c	121.6*c	123.6	-21.4	12 Apr (19)	1 May (23)	3 Jun (10)

* denotes a significant difference of modeled discharges between the future and the reference periods at the P=0.05 level. Data from six GCMS, two GGES and three downscaling methods (n=36) for each hydrological model were tested against the mean discharge at the reference period using a t-test. Different letters in each column indicate a statistically significant difference (P=0.05) for a paired t-test.

The last three statistics are the Julian days of average time of occurrence rather than relative changes; the number in parenthesis indicates how much earlier the occurrence is (in days) when compared to the reference period.

8.5.3.6 Uncertainty of hydrological model parameters

The observed future trends are the same as discussed above. Table 8.10 clearly shows that the uncertainty linked to the choice of model parameters is very low compared to the other sources discussed above.

8.6 Discussion and conclusions

The past decade has seen a rapidly increasing number of climate change impact studies, with a large number of these focusing on water resources. With the growing availability of GCMs outputs, the results display a larger uncertainty, especially for a more distant future. Earlier studies took a relatively narrow view of uncertainty sources, often with GCM structure and GGES as the only two sources considered. Wilby and Harris (2006) were the first to propose a framework for quantifying uncertainties in climate change on river low flows. To our knowledge, this is still the most thorough uncertainty study in the literature. The proposed framework was solid, but the case application was not fully exhaustive, as mentioned earlier.

This research assessed the integrated impacts of climate change uncertainty on various hydrological variables, under an equal-weighted scheme. The uncertainty envelopes combine results from an ensemble of six GCMs, two GGES, five GCM initial conditions, four downscaling techniques, three hydrological model structures and 10 sets of hydrological model parameters. Since the uncertainties of dynamical and statistical downscaling were specifically investigated by a previous study (Chen et al., 2011c), only four statistical downscaling techniques are used in this research.

The results show that all of the GCMs, GGES, GCM initial conditions and downscaling techniques suggest increases in seasonal and annual precipitations and mean temperatures for the 2081-2100 horizon. GCMs and GGES are consistently major contributors to uncertainty, while GCM initial conditions and downscaling methods show less uncertainty at the seasonal and yearly scales. The GCM initial conditions are critical for spring precipitation, but are much less important for other seasons and at the yearly scale. Compared to the other sources, the uncertainty of downscaling methods was less important in predicting seasonal and annual precipitation and mean temperature. The SDSM predicts the largest increase in annual mean temperatures and makes a considerable contribution to the uncertainty of downscaling methods.

Table 8.10 Statistics of simulated discharge for the reference period (1971-1990) and relative changes ((Fut-Ref) / Ref × 100%) between the future (2081-2100) and the reference periods

Criterion ID	**1**	**2**	**3**	**4**	**5**	**6**	**7**	**8**	**9**
Reference	543.4	1025.6	579.8	134.8	97.7	2220.8	1 May	24 May	13 Jun
CAL1	9.7*	11.0*	-2.7*	69.9*	58.2	-14.8	10 Apr (21)	2 May (22)	5 Jun (8)
CAL2	9.9*	11.8*	-4.1*	75.9*	64.8	-14.1	9 Apr (22)	2 May (22)	5 Jun (8)
CAL3	10.6*	11.7*	-2.6*	75.1*	63.9	-14.3	9 Apr (22)	2 May (22)	5 Jun (8)
CAL4	9.4*	11.9*	-5.0*	73.2*	61.2	-14.1	9 Apr (22)	3 May (21)	5 Jun (8)
CAL5	9.6*	11.8*	-4.5*	74.2*	62.9	-14.3	9 Apr (22)	3 May (21)	5 Jun (8)
CAL6	9.8*	11.1*	-4.2*	79.0*	67.6	-15.1	9 Apr (22)	2 May (22)	5 Jun (8)
CAL7	9.5*	11.1*	-3.1*	68.9*	59.5	-14.4	10 Apr (21)	2 May (22)	5 Jun (8)
CAL8	9.4*	10.0*	-3.6*	76.4*	68.0	-15.7	9 Apr (22)	2 May (22)	5 Jun (8)
CAL9	10.1*	10.5*	-2.6*	76.8*	68.1	-15.5	9 Apr (22)	2 May (22)	5 Jun (8)
CAL10	10.3*	11.3*	-2.2*	73.4*	61.6	-15.0	10 Apr (21)	2 May (22)	5 Jun (8)

* denotes a significant difference of modeled discharges between the future and the reference periods at the P=0.05 level. Data from six GCMS, two GGES and three downscaling methods (n=36) for each set of hydrological model parameter were tested against the mean discharge at the reference period using a t-test.

The last three statistics are the Julian day of average time of occurrence rather than relative changes; the number in parenthesis indicates how much earlier the occurrence is (in days) when compared to the reference period.

Climate projections (precipitation and temperatures) were then transferred to watershed streamflows using hydrological models. Compared to the reference period, there is a consistent increase in winter streamflows (November - April) and a decrease in summer (June - October) discharge. The snowmelt peak discharges are diminished, with the exception of those predicted by the GFDL and the MPI GCMs, and by the WG-based downscaling method. Peak snowmelt discharges for the future horizon are observed earlier than for the reference period. The MIROC3 GCM and the SDSM downscaling method contribute largely to their uncertainty envelopes, because their behaviors are markedly different in several instances.

In order to outline global uncertainty in more detail, table 8.11 ranks all six uncertainty sources in order of importance; each hydrological variable based on its relative change ((Fut-Ref) / Ref × 100%) or range [Min, Max] for the 2081-2100 horizon. As outlined by several previous studies, GCMs are consistently major contributors to uncertainty and ranks either as the first or the second most important source for all nine of the studied hydrological variables. Downscaling methods are the next most important source of uncertainty and rank first in importance for three hydrological variables and second for two others. GCM initial conditions are the third largest source of uncertainty and rank first or second for four variables. Surprisingly perhaps, GGES are only the fourth largest source of uncertainty, with a contribution similar to that of hydrological model structure. Both these sources rank either third, fourth or sixth, for all hydrological variables. The results for GGES and hydrological model structure may partly be influenced by the smaller sample size that may underestimate the true uncertainty envelope. However, the two chosen GGES are really opposites and represent optimistic and pessimistic scenarios, and should adequately cover the range of uncertainty. The same can be said about the choice of very different hydrological model structures. The least important source of uncertainty is by far the one linked to the choice of hydrological model calibration parameters. A similar conclusion was drawn by Poulin et al. (2011) when they investigated the contributions of model structure and parameter choice to the uncertainty related to hydrological modeling in climate change impact studies.

Overall, this research underlines some of the dangers arising from climate change impact studies based on a single GCM and/or downscaling method and/or impact model. Using two carefully selected models and/or methods may also be insufficient, because the process by which climate projections become hydrologic variables is non-linear. A good example relates to downscaling uncertainty. The uncertainty of downscaling methods is less important in predicting seasonal and annual changes of precipitation and mean temperature (figure 8.3). In particular, the CF and bias correction methods used in this study are very similar; but they are markedly different in predicting streamflows.

The uncertainty cascade considered in this work is not exhaustive. GGES and GCM runs were limited by the availability of model outputs for using a SDSM and looking at GCM initial condition. Only the CGCM3 output was downscaled by the SDSM and five runs of MRI were used to assess the GCM initial conditions. In addition, all climate projections and hydrological models were equally weighted to predict the hydrology on the watershed. Some authors have recommended assigning unequal weights to GCMs and hydrological models based on their performances at the reference period. For example, GCMs can be weighted according to their relative ability to reproduce present climate variables, and hydrological models can be weighted by their performance at reproducing flow series (Wilby and Harris, 2006). However, assigning unequal weights to GCMs and/or hydrological models is still a controversial topic in climate change impact studies (Stainforth et al., 2007; Brekke et al, 2008). The main reasons are that (1) the interpretation of the output range as a formal uncertainty estimate basically depends on the spread of results from a small number of climate models and/or hydrological models, and (2) the performances of models for present and future periods are probably different. Since this study focuses on outlining the global uncertainty from a range of sources, the simple equal-weighted scheme may be more appropriate.

Results from this work outline several of the pitfalls of climate change impact studies, and also show that it will be extremely difficult to suggest a universal simplified approach to uncertainty studies. Major sources of uncertainty depend on the variable under study and may

also likely depend on the basin under study. In certain cases, some sources of uncertainty may hide within others. For example, if one source of uncertainty is consistently larger than another, it may be unnecessary to take the latter one into account. This research averaged all projections for each uncertainty source, and could not extract such information from the major uncertainty contributors. This would be an area for future research.

Table 8.11The relative change ((Fut-Ref) / Ref × 100%) range (in square brackets) of each statistic (hydrological variable) between future (2081-2100) and reference periods for all sources of uncertainty, and the descending ranking of all sources of uncertainty for each variable (in parentheses). For the last three statistics, differences are expressed in days and not in terms of relative difference. SD=downscaling techniques, HM=hydrological model, HMP=hydrological model parameters

Criterion ID	**1**	**2**	**3**	**4**	**5**	**6**	**7**	**8**	**9**
GCM	[5.7, 21.7] (1)	[-6.2, 24,2] (2)	[-8.7, 22.1] (1)	[37.5, 227.6] (1)	[34.0, 199.1] (2)	[-33.8, 7.2] (2)	[12, 42] (1)	[8, 25] (1)	[6, 22] (2)
GGES	[10.8, 19.5] (3)	[9.0, 9.6] (6)	[3.2, 6.6] (5)	[62.7, 146.9] (3)	[55.8, 128.3] (3)	[-14.8, -12.5] (5)	[17, 29] (3)	[15, 23] (4)	[10, 15] (5)
RUN	[5.7, 19.8] (2)	[-14.1, 6.3] (3)	[2.4, 21.3] (2)	[101.6, 136.5] (5)	[74.2, 110.8] (5)	[-40.2, -25.5] (3)	[23, 32] (4)	[11, 28] (1)	[4, 22] (1)
SD	[9.0, 17.1] (4)	[-23.2, 19.5] (1)	[-3.4, 5.2] (4)	[79.9, 260.4] (2)	[54.5, 252.3] (1)	[-44.1, 3.0] (1)	[21, 37] (2)	[19, 34] (3)	[10, 17] (4)
HM	[9.7, 17.1] (5)	[2.3, 11.0] (4)	[-2.7, 9.6] (3)	[69.9, 136.6] (4)	[58.2, 123.6] (4)	[-21.4, -12.8] (4)	[19, 28] (4)	[22, 23] (5)	[8, 14] (3)
HMP	[9.4, 10.6] (6)	[10.0, 11.9] (5)	[-5.0, -2.2] (6)	[68.9, 79.0] (6)	[58.2, 68.1] (6)	[-15.7, -14.1] (6)	[21, 22] (6)	[21, 22] (5)	[8, 8] (6)

CONCLUSION

The IPCC (2007) has stated that the average global surface temperature will very likely increase on the order of a few degrees by the end of this century, and that consequently, global hydrological cycles will intensify. To assess the hydrological impacts of climate changes, high quality and high resolution future climate projections will be needed. However, the current available dynamical and statistical downscaling techniques have their strengths and limitations, resulting in different climate projections. It is not an easy task to select one over the other. This research coupled climate models and statistical downscaling methods, merging a stochastic weather generator with the climate models to quantify the hydrologic impacts of climate change for a Canadian river basin (Quebec Province). The performances of weather generators were first improved. A statistical downscaling approach combining the attributes of the weather generator and CF methods was then developed to downscale precipitation, Tmax and Tmin from the CRCM scale (45km) to catchment scale to quantify the hydrologic impacts of climate change. To accomplish this, several aspects of statistical downscaling were also examined. A range of downscaling approaches result in different future climate projections, which means that the choice of a downscaling method adds uncertainties to quantify the impacts of climate change on hydrology. Moreover, the uncertainty comes not only from downscaling methods but also from other sources, such as GCMs, GGES, GCM initial conditions, hydrological model structures and parameters. The downscaling uncertainty and the global uncertainty were investigated in terms of quantifying the hydrologic impacts of climate change. The main conclusions are summarized using the same five sections described in the introduction.

1) Weather generator improvements:

A spectral correction method resulted in a weather generator that can accurately reproduce the low-frequency variability of precipitation and temperatures, as well as accurately preserve autocorrelations of annual precipitation and temperatures. Moreover, the auto- and cross-correlations of and between Tmax and Tmin were also significantly improved by using an integration scheme derived from using the strong points of two weather generators,

WGEN and CLIGEN. The improved weather generator is able to accurately generate precipitation, Tmax and Tmin time series of unlimited length for studying the impact of rare occurrences of meteorological variables. Furthermore, by perturbing weather generator parameters according to the relative change projected by a climate model, it can be used as a downscaling tool for climate change studies.

2) Statistical downscaling:

The downscaling of daily precipitation occurrence was unsuccessful with the SDSM-like method and the discriminant analysis-based method, while the discriminant analysis-based method was much better than the SDSM-like method. In particular, the results were consistently improved as the resolution of the climate model got finer. For downscaling from NCEP, 45-km CRCM and 15-km CRCM scale to station scale, the success rate of dry days changed from 75.4% (NCEP) to 77.7% (45-km CRCM) and finally to 82.0% (15-km CRCM). For the prediction of the NCEP precipitation amount using NCEP predictors, the average explained variances were consistently lower than 40%. The explained variance was much improved for the prediction of 45-km CRCM precipitation amount using 45-km CRCM predictors. However, going to the CRCM at a 15-km scale did not yield spectacular improvements. The average explained variance was still less than 85% for both calibration and validation. The explained variance was very low when downscaling from NCEP to station scale. Using CRCM variables at both the 45-km and 15-km scales improved the results but not dramatically, as the percentages of explained variance was still less than 50%. Going to an even finer scale such as 5km or 1km scale would probably improve the results even more. However, it should be noted that such smaller scales would basically transform the direct outputs of climate models into impact models, thus negating the need for statistical downscaling approaches. Perhaps even more disappointing is the fact that the weather typing approach was not better at downscaling precipitation than approaches without classification, despite the added complexity.

3) Downscaling of weather generator parameters:

A new statistical downscaling method combining the attributes of stochastic weather

generator and CF methods is presented. This method takes into account relative changes of precipitation occurrence and the variance of all variables projected by a climate model. In addition, time series of any length can be generated for the studies of extremes. It was compared with the CF method for quantifying the hydrological impacts. The results showed that both downscaling methods suggest increases in annual and seasonal discharges for the 2025-2084 period. The weather generator-based method predicted more increases in spring (AMJ) discharge, and smaller increases in summer-autumn (JASON) and winter (DJFM) discharges than the CF method. Peak discharges for the 2025-2085 period were predicted by two downscaling methods to be earlier than was observed at the reference period (1971-1990). Both downscaling methods showed increases in mean annual and seasonal low flow, but there were considerable differences between them.

4) Downscaling uncertainty:

All of the downscaling methods suggested temperature increases over the basin for the 2071-2099 horizon. The regression-based statistical methods predicted a larger increase in autumn and winter temperatures. Predicted changes in precipitation were not as univocal as those of temperatures and they varied depending on the downscaling methods and seasons. There was a general increase in winter discharge (November - April) and decreases in summer discharge were predicted by most methods. Consistently with the large predicted increases in autumn and winter temperature, regression-based statistical methods showed severe increases in winter flows and considerable reductions in peak discharge. Across all variables, a large uncertainty envelope was found to be associated with the choice of a downscaling method. This envelope was compared to the envelope originating from the choice of 28 climate change projections from a combination of 7 GCMs and 3 GGES. Both uncertainty envelopes were similar, although the latter was slightly larger. The regression-based statistical downscaling methods contributed significantly to the uncertainty envelope.

5) Global uncertainty of hydrologic impacts:

GCMs were consistently the largest major contributor to uncertainty in quantifying the hydrological impacts of climate change. However, other sources of uncertainty, such as

downscaling methods and GCM initial conditions were also important, especially for some criteria. For example, the choice of downscaling method dominates the uncertainty for spring discharge, annual low flow and peak discharge, while GCM initial conditions offered the largest source of uncertainty with respect to the time to peak discharge and time to the end of flood. Uncertainties linked to GGES and hydrological model structure were somewhat less than those related to GCMs and downscaling methods, but much more than those from hydrological model parameters which were little important for all considered variables.

Overall, the improvement of weather generator is the first innovation of this work. The weather generator was used as a downscaling tool for climate change studies. This downscaling method is straightforward and easy to apply. Taking into account the change of precipitation occurrence and variance of all variable is the major advantage of this method over the CF method. The assessment of statistical downscaling approach highlighted the possibility of using this widely used downscaling method. This will be a benchmark, even a landmark research on the reliability of statistical downscaling as a tool for climate change impacts studies. The outline of downscaling uncertainty and global uncertainty underlined some of the dangers arising from climate change impacts studies based on a single GCM and /or downscaling method and /or impact model. It is important of consider all sources of uncertainty.

RECOMMENDATIONS

This part outlines the limitations of this work and the recommendations for further research. They are extracted from the articles of Chapters 1-8 and summarized for each of the five sections of the thesis.

1) Weather generator improvements:

The low-frequency variability corrections for the weather generator model were conducted at the monthly and yearly scale for precipitation and at the yearly scale for temperatures. The other scales' variability, for example, seasonal variability, was also significantly improved, but not reproduced as well as that of the monthly and yearly scales. Therefore, it may be useful to add the seasonal scale for precipitation and both monthly and seasonal scales for temperatures into the correction scheme. However, when correcting for both monthly and seasonal variability of Tmax and Tmin, the perturbation scheme may result in too many cases where Tmin is greater than Tmax for a given day. In addition, the proposed approach keeps the precipitation occurrence process constant. Ongoing work indicates that transition probabilities also display inter-annual variability, and are partly correlated with annual precipitation. Even though the proposed spectral correction approach significantly improved the simulation of water discharge, further improvements may be required so that occurrence variability is specifically taken into account. Moreover, this research only used a commonly used distribution (gamma distribution) to generate daily precipitation, which is inadequate at reproducing the extreme of precipitation, because it not heavy-tailed. Thus, a modeling of extreme precipitation events through the use of well adapted heavy-tailed frequency distribution such as mix exponential distribution or Frechet distribution may be necessary for future work.

2) Statistical downscaling:

Regression-based statistical downscaling approaches did not work well for precipitation with the very low explained variances. In this sense, the statistical downscaling approach seems to have hit a dead-end for precipitation. However, it probably still has advantages in uncertainty

studies, since RCM data is scarce and difficult to obtain. Data is rarely available from more than one RCM (driven by one GCM) over a given area while GCM data is now abundant with global coverage. With regards to the uncertain future, it is essentially impossible to adequately cover the major source of uncertainty (climate models) at the regional scale. Consequently, downscaling techniques from GCM data will continue to be a productive avenue of research.

3) Downscaling of weather generator parameters:

Similarly to the CF method, weather generator-based methods considers relative changes projected by climate models, thus, long time series', including climate change information, are required to calculate the relative changes. Therefore, it is impossible to robustly verify this method using present climate data. However, there are still a few options for validating this method in future studies. The first option is to compare its performance in predicting hydrology with that of the finer RCM data (for example, at the 15-km scale), with a specific hydrology model calibration. Secondly, it can be validated by comparing the performance of hydrological prediction with the constructed outflow using RCM variables. Last but not least, it can be verified by comparing its results with other robustly-validated downscaling methods, for example Zhang's method (2005), which has been verified with very good performances in the US.

4) Downscaling uncertainty:

This work indicated that the choice of a downscaling method is critical for any climate change impact study on hydrology. Even if several downscaling methods are provided, it is difficult to say which one is most appropriate for a given situation. Thus, additional research is needed. However, it can be argued that regression-based methods should be used with caution due to their distinctive behavior compared to other downscaling methods; their downscaled future temperatures are very high, especially when compared to the direct outputs from regional climate models (which exhibit relatively small biases in the current climate). In particular, they did not perform very well for downscaling precipitation when assessing was done with the linear regression-based downscaling method.

5) Global uncertainty of hydrological impacts:

All climate projections, as well as hydrological models, were equally weighted to predict the hydrology on the watershed for this research. Some authors have recommended assigning unequal weights to GCMs and hydrological models based on their performances at the reference period. For example, GCMs can be weighted according to their relative ability to reproduce present climate variables, and hydrological models can be weighted by their performance at reproducing flow series (Wilby and Harris, 2006). However, assigning unequal weights to GCMs and/or hydrological models is still a controversial topic in climate change impact studies (Stainforth et al., 2007; Brekke et al, 2008). The main reasons are that (1) the interpretation of the output range as a formal uncertainty estimate basically depends on the spread of the results from a small number of climate models and/or hydrological models, and (2) the performances of models for present and future periods are probably different. Since this study focuses on outlining the global uncertainty from a range of sources, the simple equal-weighted scheme was more appropriate. However, it will likely be worthwhile to compare these results with an unequally-weighted scheme in future research. Major sources of uncertainty depend on the variable under study and may also depend on the basin under study.

Similarly to previous studies, GCM is the largest contributor of uncertainty for quantifying the hydrological impacts of climate change. Thus, it may be necessary to take in account GCM uncertainty for any impact study. GGES is important for this study, while not so much impartant for other studies such as the study of Wilby and Harris (2006). Definitely, it will be more important for advanced future. However, hydrological model parameters uncertainty is consistently less than others. So it may be ignored for further studies. Finally, only outlining the importance of each uncertainty component is not enough for global uncertainty study. In certain cases, some sources of uncertainty may be hidden within others. For example, if one source of uncertainty is consistently larger than another, it may be unnecessary to take the latter one into account. This research averaged all projections for each uncertainty source, and could not extract such detailed information from the major uncertainty contributors.

Extracting the hidden uncertainty information (defines the overlap between uncertainty sources) and specify how many uncertainty components have to be considered require additional work.

Overall, even though several innovations were obtained by this work, there remain a significant number of opportunities for further study. It is hoped that the contributions presented in this thesis will be a solid basis to build upon.

APPENDIX I

DOWNSCALING OF WEATHER GENERATOR PARAMETERS USING ATMOSPHERIC CIRCULATION INDICES, GCM AND RCM VARIABLES AS PREDICTORS

Statistical downscaling poorly produces the low-frequency variation of precipitation (Wilby et al., 1998). This may be because the applied predictors did not accurately explain the local climate variability. Precipitation occurrences and quantity are controlled by synoptic-scale atmospheric circulation. Linking weather generator parameters with low-frequency predictors, such as the North Atlantic Oscillation (NAO) and El Nino Southern Oscillation (ENSO), may present advantages in preserving the low-frequency variability. However, the prerequisite is that strong correlations must exist between low-frequency predictors and weather generator parameters. Since precipitation is much more difficult to downscale than temperature, correlations between four precipitation parameters including P01, P11, unconditional probability of daily precipitation occurrence (PI), and seasonal precipitation (SP), and atmospheric circulation indices were calculated for 16 stations dispersed across North America, in addition to correlations between precipitation parameters and several GCM and/or RCM predictors. The locations of the 16 selected stations are presented in Figure A.1.

A I-1 Correlations between precipitation parameters and atmospheric circulation indices

Sixteen meteorological stations dispersed across North America were used to investigate the correlations between atmospheric circulation indices and SP, P01, P11 and PI. Table A.1 presents the number of stations (out of 16) that have significant correlations ($p<0.05$) to the 12 atmospheric circulation indices and SP, P01, P11 and PI for the period 1970-1999. The results showed that correlations between atmospheric circulation indices and precipitation parameters were not statistically significant at the $P=0.05$ level for most stations. The correlation was stronger in the autumn and winter than in the other seasons. However, the largest number of correlations was only six out of 16 stations, in between winter for P01 and

with the East Pacific/North Pacific pattern. For spring and summer, there were zero or only one station out of the 16 with significant correlation at P=0.05. This indicates that precipitation is controlled by complicated factors, and not only by global atmospheric circulation. For example, local details such as topography play very important roles in precipitation. Wilby et al. (2002b) explored the use of the North Atlantic Oscillation (NAO) and Sea Surface Temperature (SST) patterns to downscale seasonal precipitation variability. That study showed somewhat positive results in monthly rainfall statistics, mostly because they had carefully selected only two stations in the British Isles, stations which had strong correlations between NAO or SST and precipitation parameters. For most of other stations, there were no strong correlations (Wilby et al, 2002b).

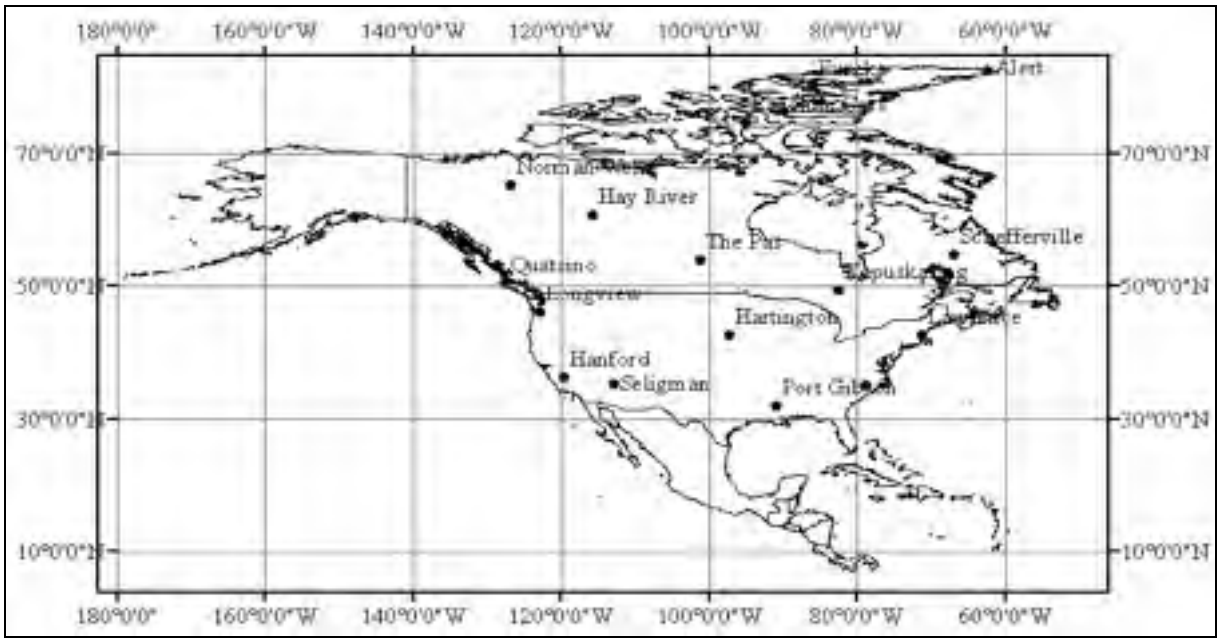

Figure-A I-1 Sixteen selected study stations in North America.

A I-2 Correlations between precipitation parameters and GCM predictors

The correlation coefficients between precipitation parameters (SP, P01, P11 and PI) and 25 CGCM3 predictors were calculated for 16 stations dispersed across North America (Table A.2). There were stronger correlations between SP and CGCM3 predictors, as well as between PI and CGCM3 predictors, than between transition probabilities of precipitation

occurrence (P01 and P11) and CGCM3 predictors at the P=0.05 level. However, there were consistently fewer than eight stations that had significant correlations at P=0.05. Moreover, these correlations were not consistent for all seasons. For example, winter SP was correlated to mean sea level pressure (mslpna), while summer SP was not. Therefore, for most stations, it was impossible to accurately downscale precipitation using GCM variables.

Table-A I-1 The number of sites with significant correlations ($p<0.05$) between four precipitation parameters (SP=seasonal total precipitation, P01=a wet day following a dry day, P11= a wet day following a wet day and PI= unconditional probability of daily precipitation occurrence) and 12 atmospheric circulation variables or patterns (NAO=North Atlantic Oscillation, EA= East Atlantic Pattern, WP=West Pacific Pattern, EP/NP=East Pacific/North Pacific Pattern, PNA=Pacific/North American Pattern, EA/WR=East Atlantic/West Russia Pattern, SCA=Scandinavia Pattern, ENSO=El Niño-Southern Oscillation, SST=Sea Surface Temperature, PDO=Pacific Decadal Oscillation, AMO=Atlantic Multidecadal Oscillation, SLP=Sea Level Pressure), stratified by season from 1970 to 1999. Sample size, n=16, (S1=spring, S2=summer, A=autumn and W=winter)

Variable	**SP**				**P01**				**P11**				**PI**			
	S1	**S2**	**A**	**W**	**S1**	**S2**	**A**	**W**	**S1**	**S2**	**A**	**W**	**S1**	**S1**	**A**	**W**
NAO	0	1	2	2	1	1	1	1	0	0	1	4	0	1	2	3
EA	1	0	0	0	1	0	0	1	1	0	1	0	1	0	1	1
WP	1	1	1	0	0	0	1	1	2	1	1	0	0	0	1	1
EP/NP	0	1	1	3	0	0	1	6	0	0	0	0	1	0	2	4
PNA	0	0	2	2	1	0	3	1	0	0	3	1	1	0	2	2
EA/WR	1	1	1	1	2	0	1	4	1	1	0	2	1	0	1	4
SCA	0	0	1	1	1	1	3	1	0	0	2	2	0	1	4	2
ENSO	0	1	0	1	1	3	1	2	2	1	0	3	1	1	0	3
SST	1	0	0	2	2	1	0	1	1	1	2	0	2	1	0	2
PDO	0	1	2	1	1	1	2	3	2	1	3	1	0	1	2	2
AMO	1	1	2	1	3	1	2	1	0	1	1	1	1	1	3	3
SLP	0	1	0	1	1	3	0	2	3	1	0	4	1	1	0	3

Table-A I-2 The number of sites with significant correlations (P<0.05) between four precipitation parameters (SP=seasonal total precipitation, P01=a wet day following a dry day, P11= a wet day following a wet day and PI= unconditional probability of daily precipitation occurrence) and 25 CGCM predictors, stratified by season from 1970 to 1999. Sample size, n=16, (S1=spring, S2=summer, A=autumn and W=winter)

GCM	**SP**				**P01**				**P11**				**PI**			
Variable	**S1**	**S2**	**A**	**W**	**S1**	**S2**	**A**	**W**	**S1**	**S2**	**A**	**W**	**S1**	**S2**	**A**	**W**
mslpna	2	1	1	3	1	2	2	3	0	1	1	1	1	2	2	4
p500na	0	1	1	1	1	2	0	2	1	1	2	2	1	1	0	3
p5thna	1	1	1	1	1	0	0	1	3	3	0	3	1	1	0	3
p5zhna	1	3	4	5	2	3	4	3	1	1	3	3	0	5	4	5
p5_fna	0	1	0	3	0	1	1	1	2	2	0	3	1	2	0	4
p5_una	1	2	0	3	0	1	1	2	2	0	1	4	0	2	0	4
p5_vna	0	2	4	6	1	1	2	4	1	1	2	2	2	1	3	5
p5_zna	0	2	0	3	1	2	2	3	1	1	1	2	0	2	0	3
p850na	1	0	0	4	0	1	1	4	0	1	2	0	1	1	1	4
p8thna	0	1	1	4	0	1	1	2	1	2	0	2	0	1	1	3
p8zhna	1	4	2	5	4	2	2	6	1	1	4	2	2	4	5	5
p8_fna	0	0	0	2	0	1	1	3	1	1	2	3	0	1	0	3
p8_una	0	1	2	6	0	0	2	2	3	0	1	3	0	0	1	5
p8_vna	3	0	2	5	4	1	1	6	1	1	1	3	6	1	3	7
p8_zna	1	1	1	3	1	0	2	3	2	0	1	2	1	0	1	3
p_thna	0	0	1	3	1	0	0	3	3	4	0	3	1	0	0	3
p_zhna	1	1	2	1	4	2	1	1	2	0	2	2	2	1	3	4
p__fna	1	0	0	5	2	1	1	2	1	1	1	0	0	1	1	3
p__una	2	1	0	6	1	1	1	1	2	1	1	1	2	2	0	4
p__vna	0	3	1	4	3	0	1	4	1	1	1	3	3	2	2	5
p__zna	2	1	3	7	2	2	3	3	4	0	0	2	1	2	3	5
s500na	0	0	1	3	2	0	1	4	1	2	1	0	2	0	1	3
s850na	3	0	2	4	4	1	0	4	1	3	0	4	3	2	0	5

GCM Variable	SP				P01				P11				PI			
	S1	S2	A	W	S1	S2	A	W	S1	S2	A	W	S1	S2	A	W
shumna	3	1	2	3	2	1	0	3	1	2	2	4	3	2	2	4
tempna	1	2	2	2	2	0	0	3	0	1	1	3	1	0	2	2

A I-3 Correlations between precipitation parameters and RCM predictors

Table A.3 presents the number of stations which had significant correlations between 25 CRCM predictors and precipitation parameters (SP, P01, P11 and PI). Compared with CGCM3 predictors, CRCM variables were more strongly correlated with precipitation parameters, because more local details were taken into account when increasing the resolution. In particular, more RCM predictors were significantly correlated to winter precipitation parameters at the P=0.05 level. However, the correlations for other seasons were not nearly as good, indicating that winter precipitation was controlled by large-scale atmospheric circulation to a greater degree than other precipitations. Even if the precipitation parameters for some stations were significantly correlated to CRCM variables at the P=0.05 level, the small correlation coefficients nevertheless result in a small percentage of explained variances for the transfer functions established between precipitation parameters and RCM predictors. Therefore, downscaling of weather generator parameters based on GCM or RCM predictors is still problematic for precipitation.

Table-A I-3 The number of sites with significant correlations ($p<0.05$) between four precipitation parameters (SP=seasonal total precipitation, P01=a wet day following a dry day, P11= a wet day following a wet day and PI= unconditional probability of daily precipitation occurrence) and 25 CRCM predictors, stratified by season from 1970 to 1999. Sample size, n=16, (S1=spring, S2=summer, A=autumn and W=winter)

RCM	**SP**				**P01**				**P11**				**PI**			
Variable	**S1**	**S2**	**A**	**W**	**S1**	**S2**	**A**	**W**	**S1**	**S2**	**A**	**W**	**S1**	**S2**	**A**	**W**
cld500	2	3	1	7	3	3	1	8	2	1	0	4	3	1	2	9
cld700	1	2	2	7	2	1	1	7	2	2	0	3	2	2	1	8
cld850	2	1	2	7	2	1	1	6	2	1	1	2	3	2	3	8
phi500	0	0	1	2	2	3	0	4	2	1	1	3	0	2	0	3
phi700	0	0	0	3	1	2	0	3	1	1	1	1	0	3	0	6
phi850	0	1	1	6	1	1	1	6	0	1	1	2	1	2	1	7
rhum500	2	1	2	5	4	1	0	6	1	1	0	2	3	2	0	7
rhum700	0	0	2	6	3	0	2	8	3	2	1	4	4	0	2	8
rhum850	1	1	2	8	3	1	2	8	2	1	2	2	3	1	4	10
u500	1	2	3	5	0	1	1	2	2	1	1	3	0	2	1	4
u700	0	1	2	4	0	0	1	2	4	0	0	2	0	0	0	5
u850	1	1	2	3	1	1	1	5	4	0	1	3	1	1	0	5
v500	1	0	4	5	2	1	1	3	2	1	1	2	2	3	2	4
v700	0	2	4	5	2	1	1	5	2	1	2	4	1	1	4	4
v850	1	2	2	3	3	1	2	4	1	0	1	3	3	0	4	4
w500	1	1	1	8	1	1	0	6	2	0	1	7	1	1	1	10
w700	1	1	1	9	0	0	2	7	2	1	1	7	1	1	1	10
w850	0	0	2	6	1	1	2	7	1	0	1	5	1	1	3	9
pnm	1	3	2	4	1	1	1	4	1	1	1	2	1	2	1	5
sq	1	0	1	2	2	1	0	3	3	0	0	2	4	1	0	5
stmn	1	1	2	3	2	0	0	2	2	1	2	4	2	1	3	2
stmx	1	2	2	1	4	3	1	1	1	1	0	2	2	4	0	1
su	0	3	1	4	3	4	1	4	3	3	3	2	6	4	2	5

RCM Variable	SP				P01				P11				PI			
	S1	**S2**	**A**	**W**	**S1**	**S2**	**A**	**W**	**S1**	**S2**	**A**	**W**	**S1**	**S2**	**A**	**W**
sv	1	0	2	4	5	1	0	4	2	1	0	2	3	1	1	3
pcp	2	3	2	12	3	2	0	11	2	0	1	7	4	4	0	10

LIST OF REFERENCES

Arnell, Nigel W. 1992. « Factors controlling the effects of climate change on river flow regimes in a humid temperate environment ». Journal of Hydrology, vol. 132, n° 1-4, p. 321–42.

Baffault, Claire, Mark A. Nearing and Arlin D. Nicks. 1996. «Impact of CLIGEN parameters on WEPP−predicted average annual soil loss». Transactions of the ASAE, vol. 39, n°2, p. 447-457.

Bardossy, Andras and Erich J. Plate. 1992. «Space time model for daily rainfall using atmospheric circulation patterns». Water Resources Research, vol. 28, n° 5, p. 1247-1259.

Bardossy, Andras, H. Muster, L. Duckstein and I. Bogardi, 1994. «Knowledge based classification of circulation patterns for stochastic precipitation modelling». In Stochastic and statistical methods in hydrology and environmental engineering, eds. by Hipel, K.W., A.W. McLeod , U.S. Panu, and V.P. Sing, p. 19-26. Dordrecht: Kluwer.

Bardossy, Andras, Lucien Duckstein and Istvan Bogardi. 1995. «Fuzzy rule-based classification of atmospheric circulation patterns». International Journal of Climatology, vol. 15, n° 10, p.1087-1097.

Bathurst, J.C., and P.E. O'Connell. 1992. «Future of distributed parameter modeling: the Système Hydrologique Européen». Hydrological Processes, vol. 6, p. 265–277.

Beersman, Jules, Migil Kaas, David Viner and Mike Hulme. 2000. «Climate scenarios for water-related and coastal impacts». In Proceedings of the EU concerted action initiative ECLAT-2 workshop 3. (KNMI, Netherlands, May 10-12th 2000), 140p, Norwich: Climate Research Unit.

Bengtsson, Lennart. 1996. «The climate response to the changing greenhouse gas concentration in the atmosphere». In: Decadal Climate Variability, Dynamics And Variability, eds. by Anderson, David L.T. and Jurgen Willebrand, p. 293-326. Berlin: Springer.

Beven, Keith. 1989. «Change ideas in hydrology – the case of physically based models». Journal of Hydrology, vol. 105, n° 1-2, p.157–172.

Booj, M.J. 2005. «Impact of climate change on river flooding assessed with different spatial model resolutions». Journal of Hydrology, vol. 303, n° 1-4, p. 176-198.

Brekke Levi D., Michael D. Dettinger, Edwin P. Maurer and Michael Anderson. 2008.

«Significance of model credibility in estimating climate projection distributions for regional hydroclimatological risk assessments». Climate change, vol. 89, n° 3-4, p. 371-394.

Brissette, Francois. 2010. Hydrology model Ecole de Technologie Supérieure—HMETS. User Manual, 10 p.

Buishand, T. A. 1978. «Some remarks on the use of daily rainfall models». Journal of Hydrology, vol. 36, n° 3-4, p 295-308.

Busuioc, Aristita, Filippo Giorgi, Xunqiang Bi and Monica Ionita. 2006. «Comparison of regional climate model and statistical downscaling simulations of different winter precipitation change scenarios over Romania». Theoretical and Applied Climatology, vol. 86, n° 1-4, p. 101-123.

Caron Annie. 2006. «Étalonnage et validation d'un générateur de climat dans le contexte des changements climatiques». MSc thesis, p134.

Caya, Daniel and Laprise Rene. 1999. «A Semi-Implicit Semi-Lagrangian Regional Climate Model: The Canadian RCM». Monthly Weather Review, vol. 127, n° 3, p. 341-362.

Chapman, Tom. 1994. «Stochastic Models for Daily Rainfall». In Water Down Under 94: Surface Hydrology and Water Resources Papers, National conference. (Institution of Engineers, Australia, 1994), p. 7-12. Barton: Preprints of Papers. ACT.

Chapman, Tom. 1998. «Stochastic modelling of daily rainfall: the impact of adjoining wet days on the distribution of rainfall amounts ». Environmental Modelling & Software, vol. 13, n° 3-4, p. 317-323.

Chen ,Jie, Francois Brissette and Robert Leconte. 2011a. «Coupling statistical and dynamical methods for spatial downscaling of precipitation». Climatic Change. (Under review).

Chen, Jie, Francois Brissette and Robert Leconte. 2010. «A daily stochastic weather generator for preserving low-frequency of climate variability». Journal of hydrology, vol. 388, n°3-4, p. 480-490.

Chen, Jie, Francois Brissette and Robert Leconte. 2011c. «Uncertainty of downscaling method in quantifying the impact of climate change on hydrology». Journal of Hydrology, doi:10.1016/j.jhydrol.2011.02.020.

Chen, Jie, Francois Brissette, Robert Leconte and Annie Caron. 2011b. «WeaGETS - a weather generator with a multi-option for generating precipitation and temperatures». Environmental modelling & software. (Under review) .

Chen, Jie, Xunchang Zhang, Wenzhao Liu and Zhi Li. 2008. «Assessment and Improvement

of CLIGEN Non-Precipitation Parameters for the Loess Plateau of China». Transactions of the ASABE, vol. 51, n° 3, p. 901-913.

Chen, Jie, Xunchang Zhang, Wenzhao Liu and Zhi Li. 2009. «Evaluating and extending CLIGEN precipitation generation for the Loess Plateau of China». Journal of the American Water Resources Association, vol. 45, n° 2, p. 378-396.

Chen, Y. D., X. Chen, C. Y. Xu, and Q. Shao. 2006. «Downscaling of daily precipitation with a stochastic weather generator for the subtropical region in South China». Hydrology and Earth System Sciences Discussion, vol. 3 n° 1-39, p. 1145–1183.

Chin, Edwin H. 1977. «Modeling daily precipitation occurrence process with Markov chain». Water Resources Research, vol. 13, n° 3, p. 949-956.

Christensen, Nadia S, Dennis P. Lettenmaier. 2007. «A multimodel ensemble approach to assessment of climate change impacts on the hydrology and water resources of the Colorado River basin». Hydrology and Earth System Sciences, vol. 11, n° 4, p. 1417–1434.

Coe, R. and R.D. Stern. 1982. «Fitting models to rainfall data». Journal of Applied Meteorology and Climatology, vol. 21, n° 7, p. 1024–1031.

Conover, W.J. 1999. Practical Nonparametric Statistics. Third edition. Wiley, New York, 596 p.

Conway, D. and P.D. Jones. 1998. «The use of weather types and air flow indices for GCM downscaling». Journal of Hydrology , vol. 212-213, n° 1-4, p. 348-361.

Conway, D., and P. D. Jones, 1996. «POPSICLE-Production of Precipitation Scenarios for ClimateImpacts in Europe». In final report, Environment Research Programme (EV5V-CT-94-0510), 50 p. Norwich: Climatic Research Unit, University of East Anglia.

Corte-Real, Joao, Hong Xu and Budong Qian. 1999. «A weather generator for obtaining daily precipitation scenarios based on circulation patterns». Climate Research, vol. 13, p. 61–75.

DAI CGCM3 Predictors, 2008. «Sets of Predictor Variables Derived From CGCM3 T47 and NCEP/NCAR Reanalysis». version 1.1, April 2008, Montreal, QC, Canada, 15 pp.

Déqué, M., and A. L. Gibelin, 2002. «High versus variable resolution in climate modelling». In Research Activities in Atmospheric and Oceanic Modelling, ed. by Ritchie, H. p. 74–75, World Meteorological Organization, Geneva.

Diaz-Nieto, Jacqueline and Rober L. Wilby. 2005. «A comparison statistical downscaling

and climate change factor methods: impacts on low flows in the river Thanes, United Kingdom». Climatic Change, vol. 69, n° 2-3, p. 245-268.

Duan, Qingyun, Soroosh Sorooshian and Vijai K. Gupta. 1992. «Optimal use of the SCE-UA global optimization method for calibrating watershed models». Journal of Hydrology, vol. 158, n° 3-4, p. 265-284.

Duan, Qingyun. 2003. Calibration of watershed models, vol. 6. Eds. by Duan, Qingyun and H. Gupta, A.N. Sorooshian, Water science and application, Washington D.C., 345 p.

Dubrovsky, Martin, Josef Buchteke and Zdenek Zalud, 2004. «High-frequency and low-frequency variability in stochastic daily weather generator and its effect on agricultural and hydrologic modeling». Climatic Change, vol. 63, n° 1-2, p. 145–179.

Duffy, P.B., B. Govindasamy, J.P. Iorio, J. Milovich, K.P. Sperber, K.E. Taylor, M.F. Wehner and S.L. Thompson. 2003. «High-resolution simulations of global climate, part 1: Present climate». Climate Dynamics, vol. 21, n° 5-6, p. 371–390.

Elshamy, M. Elshamy, Howard S. Wheater, Nicola Gedney and Chris Huntingford. 2006. «Evaluation of the rainfall component of a weather generator for climate impact studies». Journal of Hydrology, vol. 326, p. 1–24.

Fassnacht, S. R. 2006. «Upper versus lower Colorado river sub-basin streamflow: characteristics, runoff estimation and model simulation». Hydrological Process, vol. 20, n° 10, p. 2187-2205.

Fortin, Jean-Pierre , Richard Turcotte, Serge Massicotte, Roger Moussa, Josée Fitzback and Jean-Pierre Villeneuve. 2001. «Distributed watershed model compatible with remote sensing and GIS data. I: Description of the model». Journal of hydrologic engineering, vol. 6, n° 2, p. 91-99.

Fortin, Jean-Pierre, Roger Moussa, Claude Bocquillon and Jean-Pierre Villeneuve. 1995. «Hydrotel, un modèle hydrologique distribué pouvant bénéficier des données fournies par la télédétection et les systèmes d'information géographique». Revue des sciences de l'eau, vol. 8, n° 1, p. 97-124.

Fortin, Jean-Pierre, S. Duchesne, M. Bernier, Kim H. Huang and Jean-Pierre Villeneuve. 2007. «HYDROTEL, un modèle hydrologique distribué pouvant générer des informations spatialisées détaillées très utiles pour la gestion de bassins versants de tailles diverses». Actes des Journées Scientifiques Inter-Réseaux de l'Agence Universitaire de la Francophonie, Hanoi, Viet Nam, November 6-7.

Fortin, Vincent. 2000. Le modèle météo-apport HSAMI: historique, théorie et application. Varennes: Institut de Recherche d'Hydro-Québec, p 68.

Foufoula-Georgiou, Efi, Dennis Lettenmeier. 1987. «A Markov renewal model for rainfall occurrence». Water Resources Research, vol. 23, n° 5, p. 875–884.

Gates, P. and H. Tong, 1976. «On Markov chain modeling to some weather data». Journal of Applied Meteorology, vol. 15, p. 1145-1151.

Gleick, Peter H. 1986. «Methods for evaluating the regional hydrologic impacts of global climatic changes». Journal of Hydrology, vol. 88, n° 88, p. 97–116.

Goodspeed, M. J., and C. L. Pierrehumbert. 1975. Synthetic input data time series for catchment model testing. In: Prediction in Catchment Hydrology. T.G.Chapman and F.X.Dunin (Eds.), Aust. Acad. of Sci., Canberra, p. 359–370.

Graham L. Phil. Stefan Hageman, Simon Jaun and Martin Beniston. 2007b. «On interpreting hydrological change from regional climate models». Climatic Change, vol. 81, n° 1, p. 97–122.

Graham, L. Phil, J. Andreasson and B. Carlsson. 2007a. «Assessing climate change impacts on hydrology from an ensemble of regional climate models, model scales and linking methods - a case study on the Lule River basin». Climatic Change vol. 81, p. 293–307.

Green, J. R. 1964. «A model for rainfall occurrence». Journal of Royal Statistical Society, B26, 345–353.

Gregory, J. M., T. M. L. Wigley and P.D. Jones. 1993. «Application of Markov models to area-average daily precipitation series and interannual variability in seasonal totals». Climate Dynamics, vol. 8, n° 6, p. 299-310.

Guttorp, Petter. 1995. Stochastic Modeling of Scientific Data. Chapman and Hall, London, 372 p.

Gyalistras, Dimitrios, Hans von Storch, Andresas Fischlin and Martin Beniston. 1994. «Linking GCM-simulated climatic changes to ecosystem models: case studies of statistical downscaling in the Alps». Climate Research, vol. 4, n° 6, p. 167-89.

Hamlet, Alan F. and Dennis P. Lettenmaier. 1999. «Effects of climate change on hydrology and water resources in the Columbia River Basin». Journal of the American Water Resources Association, vol. 35, n° 6, p. 1597–1623.

Hansen, James W. and Theodpros Mavromatis. 2001. «Correcting low-frequency variability bias in stochastic weather generators». Agricultural and Forest Meteorology, vol. 109, n° 4, p. 297–310

Hanson, C. L., K. A. Cumming, D. A. Woolhiser and C. W. Richardson. 1994. Microcomputer program for daily weather simulations in the contiguous United

States. USDA−ARS, Publ. ARS−114, Washington D.C.

Hay, Lauren E., Robert L. Wilby and George H. Leavesly. 2000. «A comparison of delta change and downscaled GCM scenarios for three mountainous basins in the United States». Journal of the American Water Resources Association, vol. 36 n° 2, p. 387–397.

Hayhoe, Henry N. 2000. «Improvements of stochastic weather data generators for diverse climates». Climate Research, vol. 14, n° 3, p.75–87.

Headrick, M. G., and B. N. Wilson. 1997. «An evaluation of stochastic weather parameters for Minnesota and their impact on WEPP». ASAE Paper No. 972230. St. Joseph, Mich.: ASAE.

Henson, Robert. 2008. The rough guide to climate change. Rough Guides Ltd, London, 374 p.

Hostetler, S.W. 1994. «Hydrologic and atmospheric models. The (continuing) problem of discordant scales. An editorial comment». Climatic Change, vol. 27, n° 4, p. 345-350.

Hutchinson, Michael F. 1987. «Methods of generation of weather sequences». In Agricultural Environments, Characterisation, Clasification and Mapping, ed. by Bunting A.H., p. 149–157. CAB International, Wallingford, UK.

Hutchinson, Michael F., C.W. Richardson, P. T. Dykes. 1993. «Normalisation of rainfall across different time steps». In Management of Irrigation and Drainage Systems, (Park City, UT, 21-23 July 1993), p. 432–439. Irrigation and Drainage Division, ASCE, US Department of Agriculture.

Hutchinson, Michael F., Dan W. McKenney, Kevin Lawrence, John H. Pedlar, Ron F. Hopkinson, Milewska Ewa and Papadopol Pia. 2009. «Development and testing of Canada-wide interpolated spatial models of daily minimum-maximum temperature and precipitation for 1961-2003». Journal of Applied Meteorology and Climatology, vol. 48, p. 725-741.

IPCC, Intergovernmental Panel on Climate Change. 2007. Fourth Assessment Report: Climate Change.

Jenkins, Geoff and Jason Lowe. 2003. «Handling uncertainties in the UKCIP02 scenarios of climate change». In Hadley Centre Technical Note 44, 15p. Met Office, Exeter, UK.

Johnson, Gregory L., Clayton L. Hanson, Stuart P. Hardegree and Edward B. Ballard. 1996. «Stochastic Weather Simulation: Overview and Analysis of two Commonly Used Models». Journal of Applied Meteorology, vol. 35, n°10, p.1878-1896.

Jones, J. W., R. E. Colwick and E. D. Threadgill. 1972. «A simulated environmental model

of temperature, evaporation, rainfall and soil moisture». Transaction of ASAE, vol. 15, p. 366–372.

Jones, P.D., M. Hulme and K.R. Briffa. 1993. «A comparison of Lamb circulation types with an objective classification scheme». International Journal of Climatology, vol. 13, p. 655-63.

Kalnay, E., M. Kanamitsu, R. Kistler, W. Collins, D. Deaven, L. Gandin, M. Iredell, S. Saha, G. White, J. Woollen, Y. Zhu, M. Chelliah, W. Ebisuzaki, W. Higgins, J. Janowiak, K. C. Mo, C. Ropelewski, J. Wang, A. Leetmaa, R. Reynolds, R. Jenne and D. Joseph. 1996. «The NCEP/NCAR 40-year reanalysis project». Bulletin American Meteorological Society, vol. 77, n° 3, p. 437-471.

Katz, Richard W. 1977. «An application of chain-dependent processes to meteorology». Journal of Applied Probability, vol. 14, p. 598-603.

Katz, Richard W. and Marc B. Parlange. 1993. «Effects of an index of atmospheric circulation on stochastic properties of precipitation». Water Resources Research, vol. 29, n° 7, p. 2335-2344.

Katz, Richard W. and Marc B. Parlange. 1998. «Overdispersion phenomenon in stochastic modeling of precipitation». Journal of Climate, vol. 11, n° 4, p. 591-601.

Kay, A.L., H.N. Davies, V.A. Bell and Jones, R.G., 2009. «Comparison of uncertainty sources for climate change impacts: flood frequency in England». Climatic Change, vol. 92, n° 1-2, p. 41–63.

Kevin, McKague, Rudra Ramesh, Ogilvie John, Ahmed Imran and Gharabaghi Bahram. 2005. «Evaluation of weather generator ClimGen for southern Ontario». Canadian Water Resources Journal, vol. 30, n° 4, p. 315-330.

Kidson, John W. and Craig S. Thompson . 1998. «A comparison of statistical and model-based downscaling techniques for estimating local climate variations». Journal of Climate, vol. 11, n° 4, p. 735–753.

Kilsby, C.G., P.D. Jones, A. Burton, A.C. Ford, H.J. Fowler, C. Harpham, P. James, A. Smith and R.L. Wilby. 2007. «A daily weather generator for use in climate change studies». Environmental Modelling and Software, vol. 22, n° 12, p. 1705-1719.

Kou,Xiaojun, Jiangping Ge, Yi Wang and Cunjie Zhang. 2007. «Validation of the weather generator CLIGEN with daily precipitation data from the Loess Plateau, China». Journal of Hydrology, vol. 347, n° 3-4, p. 347– 35.

Koutsoyiannis, Demetris. 2001. «Coupling stochastic models of different time scales». Water Resources Research, vol. 37, n° 2, p. 379-392.

Koutsoyiannis, Demetris. 2003. «Rainfall disaggregation methods: Theory and applications». In Proceedings, Workshop on Statistical and Mathematical Methods for Hydrological Analysis, (Rome, 1-23, May, 2003), p. 1-23. Universita degli Studi di Roma ‘‘La Sapienza.

Lamb, H.H. 1972. «British Isles weather types and a register of daily sequence of circulation patterns, 1861-1971». In Geophysical Memoir, p. 116. London: HMSO.

Leavesley, George. H. 1994. «Modeling the effects of climate change on water resources - a review». Climatic Change, vol. 28, n° 1-2, p. 159-177.

Martin, E., B. Timbal and E. Brun. 1997. «Downscaling of general circulation model outputs simulation of the snow climatology of the French Alps and sensitivity to climate change». Climate Dynamics, vol. 13, n° 1, p. 45-56.

Maurer E. P. and H. G. Hidalgo. 2008. «Utility of daily vs. monthly large-scale climate data: an intercomparison of two statistical downscaling methods». Hydrology Earth System Sciences, vol. 12, n° 2, p. 551–563.

May, W. and E. Roeckner. 2001. «A time-slice experiment with the ECHAM4 AGCM at high resolution: The impact of horizontal resolution on annual mean climate change». Climate Dynamics, vol. 17, n° 8, p. 407–420.

Mearns, L.O., I. Bogardi, F. Giorgi, I. Matyasovszky and M. Palecki. 1999a. « Comparison of climate change scenarios generated from regional climate model experiments and statistical downscaling». Journal of Geophysical Research, vol. 104, n° D6, p. 6603–6621.

Mearns, L.O., T. Mavromatis, E.Tsvetsinskaya, C. Hays, and W. Easterling. 1999b. «Comparative responses of EPIC and CERES crop models to high and low spatial resolution climate change scenarios». Journal of Geophysical Research, vol. 104, n° D6, p. 6623–6646.

Minville, Marie, Francois Brissette and Robert Leconte. 2008. «Uncertainty of the impact of climate change on the hydrology of a nordic watershed». Journal of Hydrology, vol. 358, n° 1-2, p. 70-83.

Minville, Marie, Francois Brissette, Stephane Krau and Robert Leconte. 2009. «Adaptation to Climate Change in the Management of a Canadian Water-Resources System Exploited for Hydropower». Water Resources Manage, vol. 23, n° 14, p. 2965–2986.

Murphy, James. 1999. «An evaluation of statistical and dynamical techniques for downscaling local climate». Journal of Climate, vol. 12, n° 8, p. 2256-2284.

Music, Biljana and Daniel Caya. 2007. «Evaluation of the Hydrological Cycle over the Mississippi River Basin as Simulated by the Canadian Regional Climate Model (CRCM) ». Journal of Hydrometeorology, vol. 8, p. 969–988.

Music, Biljana and Daniel Caya. 2009. «Investigation of the Sensitivity of Water Cycle Components Simulated by the Canadian Regional Climate Model to the Land Surface Parameterization, the Lateral Boundary Data, and the Internal Variability». Journal of Hydrometeorology, vol. 10, p. 3–21.

Muzik, I. 2001. «Sensitivity of hydrologic systems to climate change». Canadian Water Resources Journal, vol. 26 n° 2, p. 233–253.

Nicks, A. D., L. J. Lane, and G. A. Gander, 1995. «Weather generator». In Ch. 2. USDA−Water Erosion Prediction Project: Hillslope Profile and Watershed Model Documentation, eds. By Flanagan D. C. and M. A. Nearing. NSERL Report No. 10, p. 2.1-2.22. West Lafayette, Ind.: USDA−ARS−NSERL.

Nicks, A.D., Lane L.J., 1989. «Weather Generator». In Chapter 2. USDA-Water Erosion Prediction Project: Hillslope Profile Version, eds. by Lane L.J. and M.A. Nearing. NSERL Report No. 2, p. 2.1-2.22. USDA-ARS National Soil Erosion Research Laboratory, West Lafayette, Indiana.

Orlanski I. 1975. «A rational subdivision of scales for atmospheric processes». Bulletin of the American Meteorological Society, vol. 56, p. 527-530.

Poulin Annie, Francois Brissette, Robert Leconte, Richard Arsenault and Jean-Stephane Malo. 2010. «Uncertainty of hydrological modelling in climate change impact studies». Journal of Hydrology. (In press)

Prudhomme, Christel and Helen Davies. 2009. «Assessing uncertainties in climate change impact analyses on the river flow regimes in the UK. Part 2: future climate». Climatic Change, vol. 93, n° 1-2, p. 197–222.

Pruski, F.F. and M.A. Nearing. 2002. «Climate-induced changes in erosion during the 21st century for eight U.S. locations». Water Resources Research, vol. 38, n° 12, p. 341-3411.

Qian, Budong, Henry Hayhoe and Sam Gameda. 2005. «Evaluation of the stochastic weather generators LARS-WG and AAFC-WG for climate change impact studies». Climate Research, vol. 29, p. 3-21.

Qian, Budong, Sam Gameda, Henry Hayhoe, Reinder D. Jong and Andy Bootsma. 2002. «Comparison of LARS-WG and AAFC-WG stochastic weather generators for diverse Canadian climates». Climate Research, vol. 26, no 6, p. 175–191.

Qian, Budong, Sam Gameda, Reinder D. Jong, Peter Fallon and Jemma Gornall. 2010. «Comparing scenarios of Canadian daily climate extremes derived using a weather generator». Climate research , vol. 41, no 2, p. 131-149.

Quebec Government. 2004. L'énergie au Québec. Québec: Ministère des resources naturelles et de la faune. 128 p.

Quintana Segui, P., A. Ribes, E. Martin, F. Habets, J. Boé. 2010. «Comparison of three downscaling methods in simulating the impact of climate change on the hydrology of Mediterranean basins». Journal of Hydrology, vol. 383, n° 10, p. 111–124.

Racsko, P., L. Szeidl and M. Semenov. 1991. «A serial approach to local stochastic weather models». Ecological Modelling vol. 57, n° 1-2, p. 27-41.

Richardson, Clarence W. 1981. «Stochastic simulation of daily precipitation, temperature, and solar radiation». Water Resources Research, vol. 17, n° 1, p. 182-190.

Richardson, Clarence W. and D. A. Wright, 1984. «WGEN: A model for generating daily weather variables». U.S. Depart. Agr, Agricultural Research Service. Publ. ARS-8, 84 p.

Risbey, James S. and Dara Entekhabi. 1996. «Observed Sacremento Basin streamflow response to precipitation and temperature changes and its relevance to climate impact studies». Journal of Hydrology, vol. 184, no 3-4, p. 209–223.

Roldan, Jose and David A. Woolhiser. 1982. «Stochastic daily precipitation models, 1. A comparison of occurrence processes». Water Resources Research, vol. 18, n° 5, p. 1451–1459.

Rowell, David P. 2006. «A demonstration of the uncertainty in projections of UK climate change resulting from regional model formulation». Climatic Change, vol. 79, no 3-4, p. 243–257.

Running, Steven W. and Ramarkrishna R. Nemani. 1991. «Regional hydrologic carbon balance responses of forests resulting from potential climate change». Climatic Change, vol. 19, n° 4, p. 349–68.

Sailor, David J. and Xiangshuang Li. 1999. «A semiempirical downscaling approach for predicting regional temperature impacts associated with climatic change». Journal of Climate, vol. 12, n° 1, p. 103–114.

Salathe Jr, Eric P., 2003. «Comparison of various precipitation downscaling methods for the simulation of streamflow in a Rainshadow River Basin». International Journal of Climatology, vlo. 23, p. 887-901.

Schmidli. Jurg, Christopn Frei and Pier L. Vidale. 2006. «Downscaling from GCM precipitation: a benchmark for dynamical and statistical downscaling methods». International Journal of Climatology, vol. 26, n° 5, p. 679–689.

Schoof, Justin T., S. C. Pryor. 2001. «Downscaling temperature and precipitation: a comparison of regression-based methods and artificial neural networks». International Journal of Climatology, vol. 21, p. 773–790.

Semenov Mikhail A. and Elaine M. Barrow 2002. LARS-WG, A Stochastic Weather Generator for Use in Climate Impact Studies, User Manual, 28p.

Semenov, Mikhail A. and Elaine M. Barrow. 1997. «Use of a stochastic weather generator in the development of climate change scenarios». Climatic Change, vol. 35, n° 4, p. 397-414.

Semenov, Mikhail A., J.R. Porter. 1995. «Climatic variability and the modelling of crop yields». Agricultural and Forest Meteorology, vol. 73, n° 3-4, p. 265-283.

Semenov, Mikhail A., Roger J. Brooks, Elaibe M. Barrow and Clarence W. Richardson. 1998. «Comparison of the WGEN and LARS-WG stochastic weather generators for diverse climates». Climate Research, vol. 10, n° 8, p. 95–107.

Smith, James A. 1987. «Statistical model of daily rainfall occurrences». Water Resources Research, vol. 23, n° 5, p. 885–893.

Solman, S. and M. Nunez. 1999. «Local estimates of global climate change: a statistical downscaling approach». International Journal of Climatology, vol. 19, n° 8, p. 835–861.

Srikanthan, R. and T.A. McMahon. 2001. «Stochastic generation of annual, monthly and daily climate data: a review». Hydrology and Earth Systems Sciences, vol. 5, n° 4, p. 653–670.

Stainforth, D.A., M.R. Allen, E.R. Tredger and L.A. Smith. 2007. «Confidence, uncertainty and decision-support relevance in climate predictions». Philosophical transactions of the royal society A, vol. 365, n° 12, p. 2145-2161.

Stern, R.D. and R. Coe. 1984. «A model fitting analysis of daily rainfall data». Journal of the Royal Statistical Society A, vol. 147, n° part 1, p. 1-34.

Stockle, Claudio O., Gaylon S. Campbell and Roger Nelson. 1999. «ClimGen Manual». Biological Systems Engineering Department, Washington State University, Pullman, WA.

Timbal, B., E., Fernandez and Z. Li, 2009. «Generalization of a statistical downscaling

model to provide local climate change projections for Australia». Environmental Modelling & Software, vol. 24, p. 341-358.

Todorovic, P. and D.A. Woolhiser. 1974. «Stochastic model of daily rainfall» In Proceeding of the Symposium on Statistical Hydrology, Misc. Publ. 1275, p. 223-246. U.S. Dep. of Agric., Washington, D. C.

Trigo, Ricardo M. and Jean P. Palutikof. 2001. «Precipitation scenario over Iberia: a comparison between direct GCM output and different downscaling techniques». Journal of Climate, vol. 14, n° 23, p. 4422–4446.

Turcotte, Richard, Louis-Guillaume Fortin, Vincent Fortin and Jean-Pierre Villeneuve. 2007. Operational analysis of the spatial distribution and the temporal evolution of the snowpack water equivalent in southern Quebec, Canada. Nordic Hydrology, vol. 38 no 3, p. 211-234.

von Stoch , Hans, Eduardo Zorita and Ulrich Cubasch. 1993. «Downscaling of global climate change estimates to regional scales: An application to Iberian rainfall in wintertime». Journal of Climate, vol. 6, n° 6, p. 1161-1171.

von Storch, H., Hewitson, B., Mearns, L., 2000. «Review of empirical downscaling techniques». In Regional climate development under clobal warming. General Technical Report no. 4. Conf. Proceedings RegClim Spring Meeting Jevnaker, eds. by T. Iversen and B.A.K. Hioskar, (Torbjornrud, Norway, May 8–9, 2000), p. 29–46.

Wang, Q. J. and R.J. Nathan. 2007. «A method for coupling daily and monthly time scales in stochastic generation of rainfall series». Journal of Hydrology, vol. 346, n° 3-4, p. 122-130.

Wetterhall F., S. Halldin and C.Y. Xu. 2007. «Seasonality properties of four statistical-downscaling methods in central Sweden». Theoretical and Applied Climatology, vol. 87, n° 1-4, p. 123–137.

White, Dale, Michael Richman and Brent Yamal. 1991. «Climate regionalization and rotation of principal components». International Journal of Climatology, vol. 11, p. 1-25.

Whitfield, P. H. and A. J. Cannon. 2000. «Recent variation in climate and hydrology in Canada». Canadian Water Resources Journal, vol. 25, n° 1, p. 19–65.

Widmann Martin, Christopher S. Bretherton and Eric P. Salathé Jr, 2003. «Statistical precipitation downscaling over the Northwestern United States using numerically simulated precipitation as a predictor». Journal of Climate, vol. 16, n° 5, p. 799-816.

Wilby, Robert L. 1994. «Stochastic weather type simulation for regional climate change

impact assessment». Water Resources Research , vol. 30, n° 12, p. 3395-403.

Wilby, Robert L. 1997. «Non-stationarity in daily precipitation series: implications for GCM downscaling using atmospheric circulation indices». International Journal of Climatology, vol. 17, n° 4, p. 439-454.

Wilby, Robert L. and C.W. Dawson. 2007. SDSM4.2 – A decision support tool for the assessment of regional climate impacts. User Manual, 94p.

Wilby, Robert L. and I. Harris. 2006. «A framework for assessing uncertainties in climate change impacts: Low-flow scenarios for the River Thames, UK». Water Resources Research, vol. 42, W02419, doi:10.1029/2005WR004065.

Wilby, Robert L. and T.M.L. Wigley. 1997. «Downscaling general circulation model output: A review of methods and limitations». Progress in physical geography, vol. 214, n° 4, p. 530–548.

Wilby, Robert L., Larren E. Hay, William J. Gutowski Jr, Raymond W. Arritt, Eugene S. Takle, Zaitao Pan, Geoge H. Leavesley and Martyn P. Clark. 2000. «Hydrological responses to dynamically and statistically downscaled climate model output». Geophysical Research Letters, vol. 27, no 8, p. 1199-1202.

Wilby, Robert L., C.W. Dawson, E.M. Barrow. 2002a. «SDSM-A decision support tool for the assessment of regional climate change impacts». Environmental Modelling & Software 17, 145–157.

Wilby, Robert L., D. Conway and P. D. Jones. 2002b. «Prospects for downscaling seasonal precipitation variability using conditioned weather generator parameters». Hydrological Process, vol. 16, n° 6, p. 1215-1234.

Wilby, Robert L., Hany Hassan and Keisuke Hanaki. 1998a. «Statistical downscaling of hydrometeorological variables using general circulation model output». Journal of Hydrology, vol. 205, n° 1-2, p. 1-19.

Wilby, Robert L., Larren E. Hay and Geoge H. Leavesley. 1999. «A comparison of downscaled and raw GCM output: implications for climate change scenarios in the San Juan River Basin, Colorado». Journal of Hydrology, vol. 225, n° 1-2, p. 67–91.

Wilby, Robert L., T. M. L. Wigley, D. Conway, P. D. Jones, B. C. Hewitson, J. Main and D. S. Wilks. 1998b. «Statistical downscaling of general circulation model output: A comparison of methods». Water Resources Research, vol. 34, n° 11, p. 2995-3008.

Wilks, Daniel S. 1989. «Conditioning stochastic daily precipitation models on total monthly precipitation». Water Resources Research, vol. 25, n° 6, p. 1429-1439.

Wilks, Daniel S. 1992. «Adapting stochastic weather generation algorithms for climate change studies». Climatic Change, vol. 22, n° 1, p. 67-84.

Wilks, Daniel S. 1995. Statistical methods in the atmospheric science. Academic Press: California, 648 p.

Wilks, Daniel S. 1999a. «Multisite downscaling of daily precipitation with a stochastic weather generator». Climate Research, vol. 11, p. 125–136.

Wilks, Daniel S. 1999b. «Interannual variability and extreme-value characteristics of several stochastic daily precipitation models». Agricultural and Forest Meteorology, vol. 93, n° 3, p. 153-169.

Wilks, Daniel S. 2010. «Use of stochastic weather generator for precipitation downscaling». Climte Change, vol. n° 1, p. 898-907.

Woolhiser, David A. and G.G.S. Pegram, 1979. «Maximum likelihood estimation of Fourier coefficients to describe seasonal variation of parameters in stochastic daily precipitation models». Journal of Applied Meteorology and Climatology, vol. 18, n° 1, p. 34–42.

Woolhiser, David A. and Jose Roldan. 1982. «Stochastic daily precipitation models, 2. A comparison of distribution of amounts». Water Resources Research, vol. 18, n° 5, p. 1461–1468.

Woolhiser, David A. and Jose Roldan. 1986. «Seasonal and regional variability of parameters for stochastic daily precipitation models». Water Resources Research, vol. 22, n° 6, p. 965–978.

Xu, Chongyu and V.P. Singh. 2004. «Review on regional water resources assessment models under stationary and changing climate». Water Resources Management, vol. 18, n° 6, p. 591–612.

Xu, Chongyu. 1999. «From GCMs to river flow: a review of downscaling methods and hydrologic modeling approaches». Progress in Physical Geography, vol. 23, n° 2, p. 229-249.

Yevjevich, Vujica and T.G.J. Dyer. 1983. «Basic structure of daily precipitation series». Journal of Hydrology, vol. 64, n° 1-4, p. 49–67.

Zhang Xunchang, M.A. Nearing, J.D. Garbrecht and J.L. Steiner. 2004. «Downscaling monthly forecasts to simulate impacts of climate change on soil erosion and wheat production». Soil Science Society American Journal, vol. 68, p. 1376–1385.

Zhang, Xunchang and Jurgen D. Garbrecht. 2003. «Evaluation of CLIGEN precipitation

parameters and their implication on WEPP runoff and erosion prediction». Transactions of the ASAE, vol. 46, n° 2, p. 311-320.

Zhang, Xunchang and Wenzhao Liu. 2005. «Simulating potential response of hydrology, soil erosion, and crop productivity to climate change in Changwu tableland region on the Loess Plateau of China». Agricultural and Forest Meteorology, vol. 131, n° 3-4, p. 127-142.

Zhang, Xunchang. 2004. «CLIGEN non-precipitation parameters and their impact on WEPP crop simulation». Transactions of the ASAE, vol. 20, n° 4, p. 447-454.

Zhang, Xunchang. 2005. «Spatial downscaling of global climate model output for site-specific assessment of crop production and soil erosion». Agricultural and Forest Meteorology, vol. 135, p. 215–229

Zhang, Yan, Baoyuan Liu, Zhiqiang Wang and Qingke Zhu. 2007. «Evaluation of CLIGEN for storm generation on the semiarid Loess Plateau in China». Catena, vol. 73, p. 1-9.